Studies on the Effect of Various Polyphenols and Polyols on Structure and Aggregation of Recombinant Human γ-Synuclein

Thesis submitted to the Jawaharlal Nehru University in partial fulfilment for the award of the degree of

DOCTOR OF PHILOSOPHY

in

BIOTECHNOLOGY

By

Sneha Roy

School of Biotechnology
Jawaharlal Nehru University
New Delhi 110067
India

JULY 2018

School of Biotechnology
Jawaharlal Nehru University
New Delhi, India

CERTIFICATE

This is to certify that the present work entitled **"Studies on the Effect of Various Polyphenols and Polyols on Structure and Aggregation of Recombinant Human γ-Synuclein"** submitted to the Jawaharlal Nehru University, New Delhi in partial fulfilment of the requirement for the award of the degree of Doctor of Philosophy, embodies original work carried out in School of Biotechnology, Jawaharlal Nehru University, New Delhi. This work is original and has not been submitted so far, in part, or full, for any other degree or diploma of any other university.

Ms. Sneha Roy
(PhD Candidate)
Biophysical Chemistry Laboratory
School of Biotechnology
Jawaharlal Nehru University
New Delhi-110067
INDIA

19/07/2018

Prof. Rajiv Bhat
(Supervisor)
School of Biotechnology
Jawaharlal Nehru University
New Delhi-110067
INDIA

Prof. Pawan Dhar
(Dean)
School of Biotechnology
Jawaharlal Nehru University
New Delhi-110067
INDIA

Scanned with CamScanner

INTRODUCTION

Proteins are linear and unbranched chains of amino acids and after water are the most abundant biological molecules that are involved in plethora of biological processes. One of the remarkable characteristics of living entities is the self assembly of the most of the intricate components with precision and accuracy. Protein folding is the most fundamental example of self –assembly where the linear polypeptide chain of amino acids folds into a functional three dimensional state. Important insights into the mechanism of protein folding emphasising on the structural, kinetic and thermodynamic analyses of various intermediate as well as transition states, from information gained by experiments, theory and simulation studies have now emerged. While the puzzle of protein folding still remains unsolved, the misfolding of proteins into aggregates increases the load on the cellular machineries that are evolved to avoid aggregation and prevent the underlying aggregate borne diseases, making it inevitable to find the missing links of protein folding and to fully understand factors that are responsible for the deviation from protein folding pathways.

An Overview of Protein Folding

Historically, Anfinsen's Nobel Prize winning experiment on "scrambled RNase" demonstrated that the proteins fold spontaneously and that all the information needed for a polypeptide chain to fold into a three-dimensional conformation is encoded in its amino acid sequence (Anfinsen, 1973). The denaturation of RNase A enzyme in the presence of a denaturant, i.e. Urea rendered the enzyme inactive with the mixture of several isomeric forms of the reduced disulfide bonds which when subjected to renaturation in the presence of mercaptoethanol underwent disulfide interchange giving rise to a homogenous product indistinguishable from the native state. This led to the emergence of the "Thermodynamic Hypothesis". According to this hypothesis, a protein under denaturing conditions or in an unfolded state posses astronomical conformations which under folding conditions are spontaneously driven to optimize their intramolecular as well as solvent-protein interactions (intermolecular) to attain a lowest minimum free energy, that correspond to its native state. Anfinsen suggested that the retention of the memory of the native structure is one of the factors that lead to the correct folding of the protein to its

three-dimensional state. He further suggested that cooperative interactions are essential for the stability of the proteins and proposed that the ability of the denatured protein to fold back to its native state is governed solely by the internal residues that comprise the hydrophobic core of the protein than the residues exposed to the solvent and thus only those residues are required to be conserved that allow natural selection and high degree of mutation of other residues occurring during evolution (Anfinsen, 1973).

Cyrus Levinthal made the argument that is famously known as "Levinthal's paradox" that under denaturing conditions the number of possible conformations would take a sizeable amount of time to find the native conformation and attain the functional three-dimensional structure in microsecond to millisecond time-scale within which most proteins fold (Rose et al., 2006) and thus suggested that achieving the global minimum and that too quickly are two mutually exclusive events, which are defined as thermodynamic and kinetic control, respectively. While thermodynamic control is a slow process that is determined by the final native condition irrespective of the denatured state and independent of any pathway, the kinetic control is quick as it is pathway dependent and the final structure could vary depending on the denatured state from which the folding was initiated (Ken A Dill and Hue Sun Chan, 1997). Thus according to Levinthal the native state of a protein is attained by a directed search, but how it is attained remained unexplained, leaving it a paradox.

The argument led to the quest for protein folding pathways and gave rise to the 'new-view' that sees folding as "diffusion-like process" (Karplus and Weaver, 1976) where the unfolded polypeptide instead of going through a single route to the native state resembles a multi-dimensional landscape where each conformation with varying degrees of freedom undergo conformational fluctuations that follows myriad of pathways to finally attain the native state (Wolynes et al., 1995; Ken A. Dill and Hue Sun Chan, 1997). A typical protein energy landscape is shown in Figure 1, which is characterized by a tapered end indicating limited population of low energy, native-like conformations and wide open surface at the top that describes the multiple unfolded ensembles that tread their way downhill to the native state (Dill and MacCallum, 2012). Wolynes and colleagues suggested that for a protein to be kinetically foldable there must exist sufficient slope in the energy landscape to go downhill in the funnel to attain global energy minimum and attain the native state

with minimum frustrations because the native-like interactions favoured by natural selection are more stable than the non-native states, thus resulting in a smoother funnel (Wolynes et al., 1995). Computer simulation studies have revealed that the folding funnels that appear smoother on a global scale may be rugged on local scales (Dill and MacCallum, 2012) indicating the inherent fluctuations between the unfolded and folded conformations that bring the highly separated amino acids closer and attains the lower energy native state by trial and error (Dobson, 2003b). Since the energy landscape is encoded by the amino acid sequence, the shape of the folding funnel also depends on the sequence of each protein where the folding chain proceeds towards lower intra-chain energy by undergoing hydrophobic collapse, salt-bridge formation, intra-chain hydrogen bonding etc. until the conformational possibilities of the chain narrows (Ken A. Dill and Hue Sun Chan, 1997; Dobson et al., 1998; Rose et al., 2006). Proteins are believed to fold by nucleation events comprising of 'key residues' in the structure that form folding nucleus with native-like topology in parts of the polypeptide chain and are characterized by self-dependent units of secondary structures such as helices and turns which act as stepping stones for the successive folding of the polypeptide (Wolynes et al., 1995; Dobson, 2003b; Jahn and Radford, 2005; Dill and MacCallum, 2012). The small single domain proteins (<100 residues) involve a two –state folding populated with only two kinds of species, unfolded and native resulting in a smoother energy landscape, while large proteins (> 100 residues) have a rough energy surface and form folding intermediates *en-route* to the native state (Jahn and Radford, 2005). The funnel illustrates that the folding is slowed by a thermodynamic bottleneck which comprises of the transition state reflecting multiple pathways of protein folding giving rise to formation of high energy intermediate structures through which the molecules must pass to attain the native state (Wolynes et al., 1995; Dobson, 2003b; Onuchic and Wolynes, 2004; Brockwell and Radford, 2007). These intermediate states are kinetic traps of misfolded conformers which can act two-way by accelerating protein folding (on-pathway) or become kinetic dead ends that in turn may give rise to off-pathway events, such as protein aggregation, thus becoming rate limiting for protein folding reactions (Brockwell and Radford, 2007; Jahn and Radford, 2008).

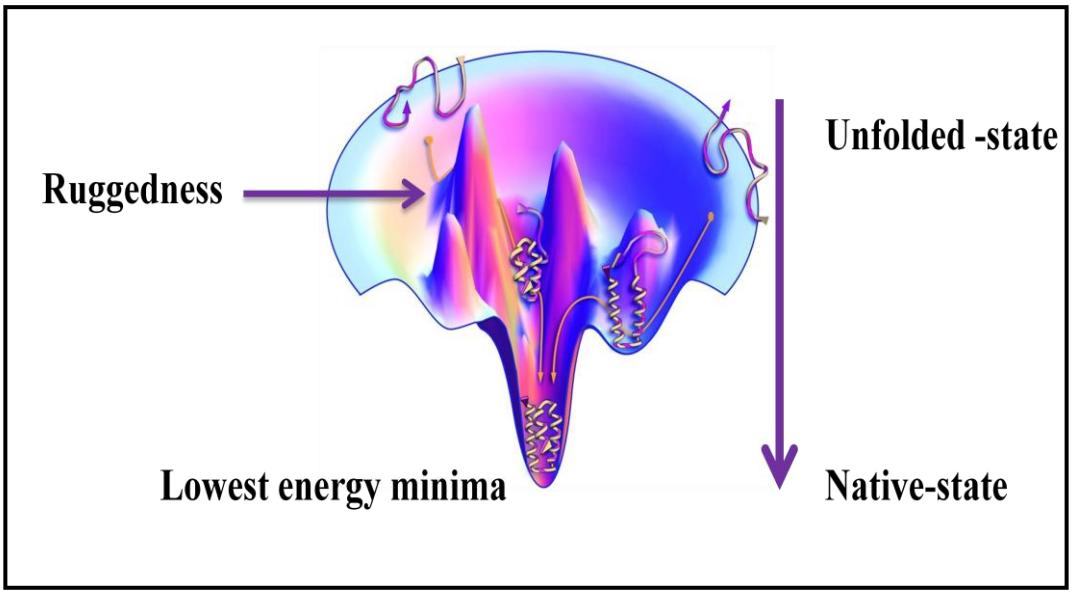

Figure 1. **Funnel-energy landscape of protein folding.** The funnel shows multiple high energy conformations wending downhill to attain limited number of low energy conformations. Folding occurs via alternative multiple trajectories. Recreated and reused with permission (Dill and MacCallum, 2012).

Protein Misfolding and Aggregation

The transiently trapped intermediate species formed during process of protein folding can accumulate under various conditions and favour intermolecular interactions giving rise to aggregates, thus leading to misfolding of protein. These intermediate non-native states have solvent exposed hydrophobic residues and unstructured segments of peptide backbone which tend to self-associate into disordered aggregates in a concentration-dependent manner where their associations are driven by hydrophobic and interchain hydrogen bonding interactions (Horwich, 2002; Dobson, 2003a; Barral et al., 2004; Jahn and Radford, 2005; Ecroyd and Carver, 2008; Y. E. Kim et al., 2013). The advancements in the experimental methods capable of measuring protein folding at a very short time-scale (μs time-scale) such as ultra-rapid mixing, or detection of transient species by using techniques like FRET, NMR spectroscopy or fluorescence correlation spectroscopy (FCS) have revealed the presence of partially folded intermediates in the folding process of even the simplest proteins. The state-of-the-art techniques like NMR relaxation dispersion measurements are capable of detecting the scarcely populated (as low as 1%) non-native protein conformations and also provide residue specific

knowledge of the kinetic and thermodynamic properties of the species (Jahn and Radford, 2008).

Protein folding *in vivo* is a much complex process due to the challenges posed by the crowded cellular milieu which the nascent polypeptide chain encounters (Ellis, 2001a, b; Dobson, 2003b; Barral et al., 2004; Stefani, 2008). The extremely high concentration of macromolecules inside the cells, approximately in the range of 300-400 g l^{-1} is referred to as macromolecular crowding, where the macromolecules occupy around 20-30% of the total cellular volume. Crowding effect is also termed as 'excluded-volume' effect, emphasising that it is a physical non-specific effect which originates from steric repulsion. A highly crowded environment means that the effective concentration and thermodynamic activity of each molecule is greater than its actual concentration and the volume freely available to a macromolecule is reduced due to the excluded-volume effect. Such an effect is expected to promote self-association and enhance protein folding by either collapsing the unfolded polypeptide chain into compact state or lead to the association of partially folded intermediates into off-pathway (non-functional) aggregates (Ellis, 2001a, b). The exposed hydrophobic residues on the nascent polypeptide chain during translation and translocation as well as assembled oligomeric complexes of the polypeptide further present obstacles in proper folding of the polypeptide into functional three-dimensional native state (Thomas et al., 1995).

In order to ensure correct folding, the cellular machinery has evolved molecular chaperones and folding catalysts which counteract the non-native interactions and facilitate proper folding under cellular conditions (Thomas et al., 1995; Fink, 1999; Dobson, 2003b). Molecular chaperones are defined as proteins that increase the overall efficiency of protein folding by interacting, stabilizing and assisting the nascent polypeptide to acquire correct folding by reducing the probability of non-native, competing interactions, particularly aggregation (Dobson, 2003b; Hartl and Hayer-Hartl, 2009). The chaperones play multiple roles such as *de novo* protein folding, refolding of stress-denatured protein, intracellular protein transport as well as degradation of misfolded proteins. The class of chaperones that are predominantly involved in protein biogenesis are heat-shock proteins (Hsp) - 70 family and chaperonins (Hsp 60s) that recognize the exposed hydrophobic amino acid side chains in the non-native conformations and promote their correct folding through ATP-dependent cycles of association and dissociation (Hartl and Hayer-Hartl,

2009). Apart from the chaperone-assisted folding of proteins, the folding catalysts comprise of important enzymes such as protein disulphide isomerase and peptidylprolyl isomerase that enhance the rate of formation and reorganization of disulphide bonds and accelerate the potentially slow steps of protein folding by increasing the rate of *cis-trans* isomerisation of peptide bonds including proline residues respectively (Fink, 1999).

The cells are also equipped with sophisticated quality control system that examines if the proteins are correctly folded and target the misfolded proteins for degradation by generating 'unfolded protein response' (UPR) which involves ubiquitin-proteasome pathway where ubiquitin binds to the target proteins marking them for destruction (Dobson, 2003a; Goldberg, 2003; Stefani and Dobson, 2003). Additionally under evolutionary pressure to avoid aggregation, the functional proteins have developed sequences that are less prone to aggregation, such as presence of proline residues in the membrane α-helices (Jahn and Radford, 2008) and negative designs present in β-sheet containing proteins that prevent the edge-to-edge aggregation (Richardson and Richardson, 2002). The protective role of evolution against aggregation is also explained by the finding that significant part of eukaryotic genome codes for natively unfolded proteins which are characterised by low surface hydrophobicity and high net charge (due to uncompensated charge) that remain unfolded under physiological conditions. Such proteins are collectively defined as natively unfolded proteins or intrinsically disordered proteins (Uversky, 2002a). Even though the cells are evolved to tightly regulate and assist the correct folding of the nascent polypeptide, due to the marginal stability of the native state relative to the denatured state (Jahn and Radford, 2005), the aggregation can be triggered by factors such as mutations (Chiti, Taddei, et al., 2002; Chiti et al., 2003a), changes in the folding environment, chemical modifications (oxidation, proteolysis) reducing conformational stability, aberrant interactions with metal ions, faulty chaperones and defects in the protein control machineries (Stefani and Dobson, 2003; Stefani, 2004; Hipp et al., 2014).

Since protein folding plays the central role in biological processes, it is inevitable that malfunctioned protein will give rise to plethora of diseases which are collectively called as conformational diseases or misfolding diseases (Kopito and Ron, 2000; Zˇerovnik, 2002). Protein misfolding predominantly gives rise to highly organized cross β-sheet containing extracellular fibrillar aggregates called

'Amyloids' which contribute majorly to the protein misfolding diseases causing wide range of neurodegenerative diseases such as Creutzfeldt-Jacob's disease, Parkinson's disease, Alzheimer's disease, etc. and some form of cancer (Yang-Hartwich et al., 2015) broadly defined as 'Amyloidoses'(Koo et al., 1999; Selkoe, 2003; Stefani and Dobson, 2003).

❖ ***Amyloidogenesis***

'Amyloid' term was first coined by Virchow in 1853 to define waxy, eosinophilic tissue deposits that were assumed to be composed of carbohydrates and within ten years of their nomenclature they were identified to be deposits of proteins by Fredrich and Kekule. In 1959 the EM studies revealed the deposits to be fibrillar in nature which were observed to be rigid and unbranched species with characteristic tinctorial properties such as binding to Congo red dye (Horwich, 2002). The wide variety of proteins and peptides associated with the amyloidogenic diseases share no sequence or structural similarity and yet the fibrils formed by such proteins share a strikingly similar morphological as well as structural characteristics (Stefani and Dobson, 2003; Dobson, 2004). The X-ray diffraction studies in 1968 revealed that amyloids exhibit cross β-signature and the β-sheet comprises the strongest repeating unit of the fibril that runs parallel to the fibrillar axis with their strands aligned perpendicular to this axis (Nelson et al., 2005).

The amyloids share common characteristics which include formation of fibrils with elongated and unbranched morphology with a diameter of 70-120Å (Sunde et al., 1997; Jahn and Radford, 2008), binding to dye such as Congo red and thioflavin T, resulting in characteristic green-yellow birefringence of Congo red and increased fluorescence with ThT, lag-time dependent rate limiting kinetics with cooperative binding and self-seeding properties which exhibit unusual stability (Nelson et al., 2005). These fibrils are extremely stable species and are resistant to degradation by proteases and denaturants, making them stubborn for elimination by the cell regulatory machinery (Ecroyd and Carver, 2008). The fibrils also usually consist of 2 to 6 protofibrils, which are approximately 2 nm in diameter that are twisted around each other and appear like supercoiled rope-like structures (Serpell et al., 2000). A detailed investigation on the mechanism of cross β-sheet formation in amyloid fibrils studied by X-ray diffraction studies revealed three levels of organization within the fibrils. First, involves the alignment of the protein molecules in a β-sheet form which

is followed by the self-complementation of the two sheets forming the sheet pairs containing a dry interface. Dry interface with an absence of any water molecule other than those hydrating the carboxylate ion at the ends of polypeptide chain facilitate tight interdigitation of the same amino acids of the mating sheets giving a 'steric-zipper'- like appearance that involves van der Waals interactions and are stronger than the other protein interface. The third level draws in the interaction between the sheet structures to form fibrils by the non-covalent forces which are relatively weaker than the forces involved in the first two steps. The second level explains the lag phase of fibrillation since the amide side chains take longer to acquire proper orientation required for interdigitation of the mating sheets and stacking of amide hydrogen bonds in the dry interface. The decrease in entropy gives rise to the kinetic barrier of fibril formation and thus is energetically an unfavourable reaction (Nelson et al., 2005). Although till date a fully objective atomic model for common spine structure has not been available, an array of sophisticated biophysical techniques like solid-state NMR (ss NMR), cryo-electron microscopy, X-ray fiber diffraction and powder diffraction are continuing to provide in-depth insights about the core structure of amyloids (Nelson et al., 2005), such as understanding amyloid polymorphism (Close et al., 2018).

The amyloid formation predominantly occurs by 'nucleation –dependent polymerization' mechanism where the protein monomer at nucleation stage, undergoes structural rearrangements and associations giving rise to a thermodynamically unfavourable and rate-limiting step where it is converted into ordered oligomeric nucleus followed by an exponential or growth phase where the nucleus grows rapidly by further addition of competent monomeric/oligomeric species forming the intermediate species such as protofibrils and finally the saturation or steady-state which marks the formation of mature amyloid fibrils where the fibrils and monomer population are in equilibrium with each other (Harper and Lansbury Jr, 1997). An amyloid fibril formation has been characterized by a sigmoidal growth curve that represents the nucleation –dependent polymerization model (Naiki and Gejyo, 1999) as depicted in Figure 2. The characteristic features that identifies such a model are, (a) aggregation only above critical concentration of the protein present, (b) even slightly above critical concentration, lag phase is observed before polymerization and (c) amelioration of lag phase upon addition of seeds, which are the pre-formed fibrillar species containing amyloid forming

characteristics (Harper and Lansbury Jr, 1997). Whilst most of the proteins form amyloids by nucleation –dependent phenomena, fibrils have also been reported to form by nucleation-independent kinetics (Gosal et al., 2005; Ecroyd et al., 2008).

The formation of amyloids is now believed to be a generic property of the polypeptides. Contrary to earlier hypothesis that amyloids are only formed by disease related proteins, in 1998 it was accidentally observed that proteins unrelated to any disease also forms amyloid fibrils similar to those formed by the pathogenic proteins. Later on it was established that by changing the solution conditions (such as low pH, high temperature, lack of interacting partners, presence of salts and co-solvents etc.) proteins can be deliberately pushed towards amyloid formations such that their native structures are partially or completely disrupted with retention of hydrogen-bonding capacity (Stefani and Dobson, 2003). It has also been observed that short peptides of 4 to 6 residues can form well –defined fibrils with all the characteristics of the fibrils formed by longer (>100 residues) proteins (Manuela López de la Paz et al., 2002). Therefore it is established that the amyloid formation is governed by the inherent physico-chemical property of the polypeptide main chain rather than amino-acid side chains and in the light of this, the generic property of polypeptides to form amyloids with common structural features is well explained as the peptide backbone irrespective of proteins remains unchanged (Stefani and Dobson, 2003). The amino acid side chains however have been observed to govern the fibrillation propensities of polypeptides (Azriel and Gazit, 2001; Chiti, Calamai, et al., 2002; Chiti et al., 2003b; Manuela Lopez de la Paz and Serrano, 2004) and the solvent conditions that affect the ionization states of amino acids, such as changes in pH are reported to form fibrillar species with altered morphology (Gosal et al., 2005). A collective view establishes the fact that native proteins are evolved to contain amino acid sequences and structural adaptations that alleviate aggregation and favour folding of protein into compact states which are dictated primarily by the amino acid side chain interactions that differ for each polypeptide chain. However, factors such as enhanced β-sheet propensity, increased hydrophobicity and decreased overall charge could divert the pathway towards aggregation and amyloid formation from protein folding pathways (Stefani and Dobson, 2003). The observations lead to the consensus that protein folding and aggregation are two distinct yet competing pathways where a polypeptide can undergo aggregation or folding depending on the environmental conditions (Stefani, 2008).

The different mechanisms of protein aggregation are illustrated in Figure 3. Destabilization of the native state is a prerequisite for amyloid formation. While destabilizing conditions such as addition of denaturant, high temperature, low pH, mutation or truncation lead to accumulation of partially unfolded intermediates with exposed hydrophobic residues (Jahn and Radford, 2008), a partial folding of the intrinsically disordered proteins to form the molten globule state is key step towards fibrillogenesis (Uversky, 2008). Formation of aggregates by mechanism such as domain swapping (ds), edge-to edge association (ee), strand association (sa) and β-strand stacking (bs) has been proposed to be responsible for amyloid formation (Jahn and Radford, 2008). An early formation of disordered or amorphous aggregate has been observed in the initial stages of fibrillation which reorganize in the exponential phase and later adopt the characteristic cross β-structure of the amyloids (Plakoutsi et al., 2005).

Apart from the pathogenic implications of amyloid formation, recent studies have shown evidence that many of these amyloids have functional properties in many eukaryotic and prokaryotic organisms (Greenwald and Riek, 2010). Several examples of functional amyloids have been observed such as formation of amyloids by curlin protein in *E. coli* that enables bacteria to colonize by forming biofilms, aggregation of Ure 2p protein in the yeast *S. cerevisae* that helps in adapting to nitrogen deprived conditions etc. (Theillet et al., 2014). The role of functional amyloids in mammalian cells has also been reported. Disordered Pmel17 protein is reported to form fibrillar species in melanosomes that protects the cells from UV and oxidative damage (Fowler et al., 2007).

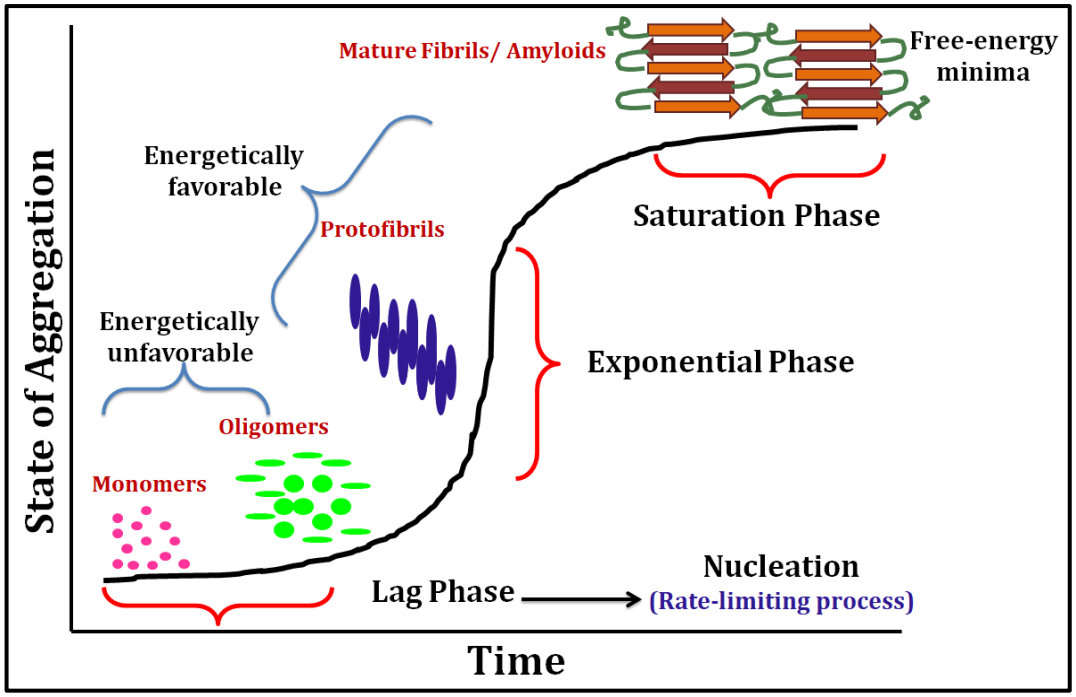

Figure 2. Representative sigmoidal curve depicting nucleation –dependent polymerization model of amyloid formation. The figure shows sequential steps of fibril polymerization and different aggregation states of a protein formed at different stages of fibrillation.

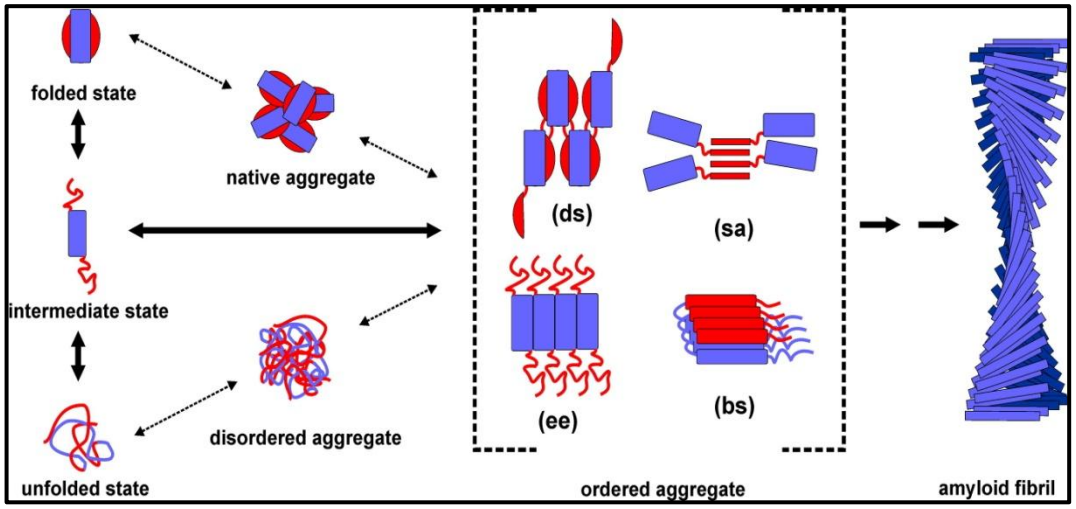

Figure 3. Proposed mechanisms of protein aggregation. The schematic depicts the possible structural rearrangements of a polypeptide which in its different states undergo and form amyloid fibrils. The four main mechanisms shown are domain-swapping (ds), strand association (sa), edge-edge-association (ee) or β-strand stacking (bs) respectively. Reused with permission (Jahn and Radford, 2008).

❖ ***Folding and Aggregation: two competing pathways***

Several studies have demonstrated that the partially unfolded intermediates that predominantly resemble a molten globule state exhibit significant fraction of native-contacts along with non-native contacts and that the intrinsic properties of amino acid side chains that govern the structural preferences such as high hydrophobicity, secondary structure propensity and high net charge are equally important in determining the aggregation propensity (Jahn and Radford, 2008; Mezzenga and Adamcik, 2018). Under crowded cellular milieu, competition between the intramolecular and intermolecular interactions exists, that results in a dramatic increase in the ruggedness of the energy landscape (Jahn and Radford, 2008) . A combined energy landscape of folding and aggregation is illustrated in Figure 4. The evidence for kinetic partitioning between folding and aggregation was also provided by Chiti and co-workers and it was established that the regions on the α/β acylphosphatase (AcP) protein which determine the rate of aggregation are distinct from those that determine the rate of protein folding. It is seen that while the mutations in the highly structured regions in the transition states largely affect the rate of folding, little consequence is observed on rate of aggregation. The study thus established that the AcP residues involved in major interaction in the folding nucleus do not play role in the rate-limiting steps of aggregation (Chiti, Taddei, et al., 2002).

Although the entire polypeptide chain is involved in fibril formation, the detailed investigation on the intrinsic properties of the natively unfolded proteins, i.e. Aβ-42, α-Synuclein and tau which readily forms amyloid have revealed that the polypeptide sequences contain two sensitive regions which are categorised as ‘aggregation-prone’ and ‘aggregation-sensitive region’ defined as P- and S- region respectively (Pawar et al., 2005). While the P-regions comprise the local regions with high aggregation propensity and promote the aggregation of the entire polypeptide sequence, the S-region is the susceptible region likely to be the part of the amyloid core only upon mutation (Pawar et al., 2005). A similar observation of kinetic partitioning was also made in the case of highly aggregation prone protein Transthyretin (TTR). It was demonstrated that the reassembly of TTR to functional homotetrameric form depends on the concentration of the folded TTR monomer which partitions itself between the reassembly and the aggregation pathway. The reassembly pathway is observed to compete with the aggregation pathway for the TTR monomer but upon accumulation of large amount of aggregates the partitioning

tilts towards the aggregation pathway (Wiseman et al., 2005). Further using techniques such as positional scanning mutagenesis, it has been revealed that there is a presence of tolerant and restrictive mutation sequences on amyloid sequence of a protein and fibril formation is a fine balance between the specific side chain interactions and electrostatic interactions within the sequence of the protein (Manuela Lopez de la Paz and Serrano, 2004). The kinetics observed for fibril formation unlike first order kinetics of protein folding involves competition between unimolecular concentration-dependent intrachain interaction and multimolecular interchain interaction that dominates with an increasing protein concentration (Horwich, 2002). The energy landscape of aggregation as shown in Figure 4 depicts the complexity of the protein folding and aggregation and includes the formation of wide range of conformational variants and multitude of pathways that is presented to the polypeptide as it skirts around the landscape. The energy minima on the aggregation side of the landscape is poorly defined due to the heterogeneity and high dynamicity of the intermediate oligomeric species formed in the pathway but the energy minima for the protofibrils and fibrils, which are stable rigid structures are expected to be well-defined in the landscape. Thus, in the view of the energy landscape theory, the fact that virtually any protein can form amyloids subjected to appropriate conditions suggest that amyloid fibril is the universal global free-energy minima of all polypeptides that may assemble by common mechanisms governed by the physico-chemical properties of the polypeptide chain (Jahn and Radford, 2008).

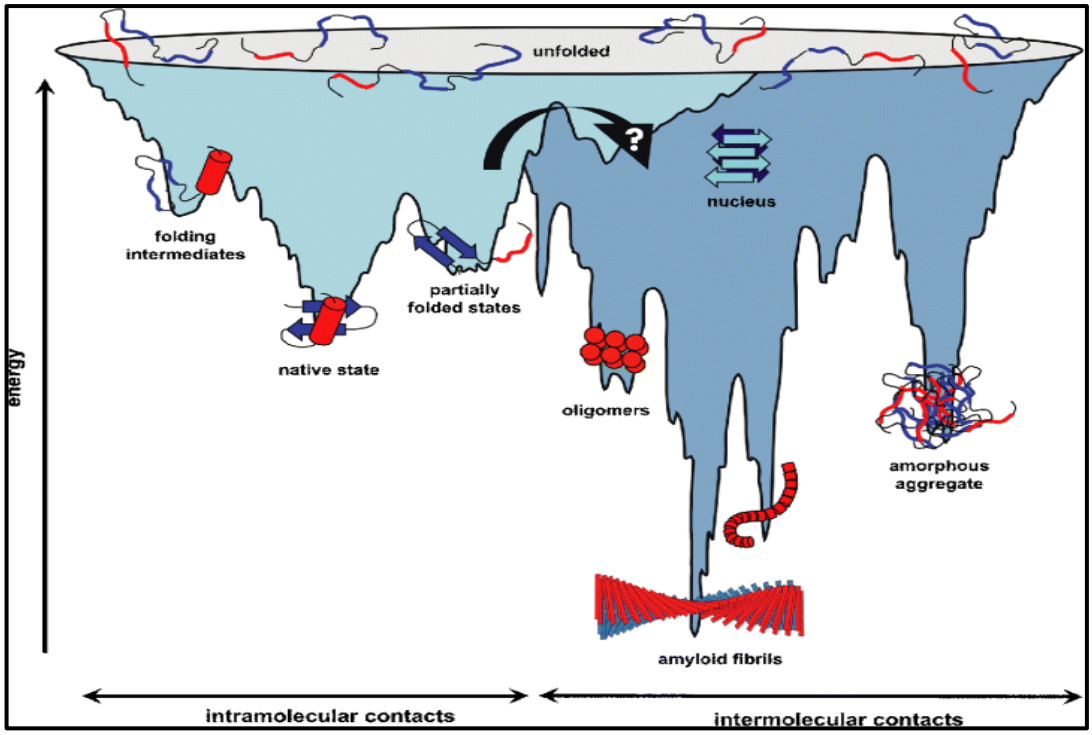

Figure 4. A schematic representation showing partitioning between the energy landscape of protein folding and aggregation. The landscape illustrates a simple folding funnel (*light blue*) for a conformational search of single polypeptide chain to its native state. A highly rugged energy landscape due to intermolecular protein interactions is shown for the aggregation pathway (*dark blue*). Reused with permission (Jahn and Radford, 2005).

❖ ***Amyloid toxicity and Diseases***

Amyloids and Neurodegeneration

The accumulation of protein aggregates in the form of amyloid plaques in the brain are the key characteristics of wide range of neurodegenerative diseases such as Alzheimer's disease (AD), Parkinson's disease (PD), Huntington's disease (HD), amyotrophic lateral sclerosis (ALS) etc. (Koo et al., 1999; Caughey and Lansbury Jr, 2003; Forman et al., 2004; Ross and Poirier, 2004) and the wide range of amyloidogenic diseases are summarized in Table I. There is a growing evidence that the early aggregates formed as intermediates in the amyloidogenic pathway comprising the soluble oligomeric species, protofibrillar species and amorphous aggregates are more toxic than the mature fibrils and play an important role in cellular dysfunction and death (Caughey and Lansbury Jr, 2003). The lack of correlation between the clinical symptoms and the extent of accumulated fibrils suggests the role of early oligomeric species in the pathogenesis. In the case of

neurodegenerative diseases such as AD, an absence of any direct relationship between the amyloid plaque and AD related dementia suggested that the toxic effects of non-fibrillar Aβ42 deposits occur before the plaques are formed and dementia is observed. Also, administration of Aβ oligomers to the live animals resulted in deficits in long-term potentiation and memory loss. On the other hand PD is characterized by the amyloid aggregates of α-Synuclein, called Lewy bodies and out of many mutational variants of α-Syn that gain toxic function, A30P forms spherical protofibrils by slowing aggregation and binds to the membrane with a greater affinity than the mature fibrils or the monomers, establishing that the early oligomers are more pathogenic than the mature fibrils (Caughey and Lansbury Jr, 2003). The increasing experimental evidences have demonstrated the toxic effects of oligomeric species of several amyloidogenic proteins such as Aβ-peptide (Stine et al., 2003; S. J. C. Lee et al., 2017), α-Synuclein (Danzer et al., 2007; Winner et al., 2011), IAPP (Meier et al., 2006; Haataja et al., 2008; Zraika et al., 2010), tau oligomers (Ward et al., 2012) etc. Although the majority of reports demonstrate the cytotoxic effects of amyloid oligomers, the toxic effects of mature fibrils could not be ruled out (Novitskaya et al., 2006). The finding that species formed early in the aggregation of two small globular proteins PI3- SH3 (SH3 domain of phosphatidyl-inositol-3′-kinase) and HypF-N which are not related to any amyloid diseases further suggest that amyloid forming is a general phenomena which is not restricted only to the disease causing proteins. Also, it was proposed that the amyloid oligomers of proteins irrespective of their relatedness to a disease share common structural features as well as common mechanisms of toxicity (Bucciantini et al., 2002). In another study, the binding of the micellar Aβ-specific antibody to amyloid oligomers of various amyloidogenic peptides further supported that the amyloid oligomers share common structural characteristics (Kayed et al., 2003). It was observed that HypF-N protein under fibrillating conditions formed two types of oligomers with similar morphology but the packing of hydrophobic interactions among the protein molecules differed from each other which in turn governed their toxic characteristics. The oligomers with the higher exposed hydrophobic residues with lower packing were observed to have higher cell penetrating ability and thus high toxicity (Campioni et al., 2010), establishing the role of hydrophobic exposure in oligomer toxicity. Although, the structural characterization of amyloid oligomers although is challenging due to their transient and dynamic nature, most of the toxic

amyloid oligomers are reported to contain β-sheet structures (Apetri et al., 2006; Lasagna-Reeves et al., 2010; Illes-Toth et al., 2015), and possess seeding capabilities (Farmer et al., 2017) as well as prion like self propagating properties (Lasagna-Reeves et al., 2012).

The presence of aggregates both inside and outside the cell has been observed to induce apoptosis and thus is toxic and causes cell death. The increasing experimental evidences majorly suggest that membrane permeabilization by amyloid oligomers leading to the dysregulation of Ca^{2+} homeostasis is the underlying cause of amyloid-mediated toxicity (Mattson et al., 1992; Demuro et al., 2005; Glabe, 2006). It is suggested that upon exposure to toxic amyloid aggregates the intracellular reactive oxygen species (ROS) elevates due to the influx of Ca^{2+} ions which is followed by the up-regulation of the oxidative metabolism aimed at generating ATP which in turn is required by the membrane pumps for the clearance of excess Ca^{2+} ions from the vicinity. Elevated ROS leads to the oxidation of the proteins which are involved in the ion transfer as well as other downstream signalling required for the clearance of excess Ca^{2+} ions, thus leading to depletion of ATP and accumulation of Ca^{2+} ions inside the cells. The depletion of ATP and accumulation of toxic aggregates is much evident in the old age due to which most of the amyloid-borne diseases are a group of chronic diseases that become prevalent with aging (Stefani and Dobson, 2003). The amyloidogenic proteins have been reported to interact with lipid membranes and form pores or single channels on the membrane surface that led to the concept of 'Channel Hypothesis'(Glabe, 2006). The interaction of misfolded species with membrane is reported to occur by two-step mechanism which involves the electrostatic interaction between the positively charged side chain residues and negatively charged or polar head groups of membrane followed by the burial of hydrophobic residues into the hydrophobic interior of the membrane (Stefani and Dobson, 2003). A recent study on the underlying effect of α-Synuclein oligomer toxicity shows an increased swelling and permeability of mitochondrial membrane by selective oxidation of the ATP synthase β subunit that leads to mitochondrial peroxidation and thus cell death (Ludtmann et al., 2018). Together, it is established that the oxidative stress due to accumulated ROS could further amplify the damaging effects by causing the impairment of ion pumps as well as permeabilization of mitochondrial membrane which in turn could lead to the activation of various apoptotic events, thus causing cell death.

Amyloids and Cancer

Apart from their pronounced effects seen in neurodegenerative diseases, the abnormal accumulation of proteins is also associated with various forms of cancer. The aggregates of the wild-type and mutant p53 protein which is the most important tumour suppressor protein and is also regarded as the gate-keeper of cell growth and division, has been reported to form aggregates of its conformational variants that impair the proapoptotic functions of p53, leading to rise of malignancy. Several cancers such as neuroblastoma, breast cancer, retinoblastoma, colon cancer (Stefani, 2004), ovarian cancer (Yang-Hartwich et al., 2015) etc. are reported to occur due to such aggregates of p53. Additionally, the mutant variant of p53 showed a prion-like behaviour where a dominant negative effect was observed as the protofibrils and oligomeric species of mutant p53 sequester the wild-type p53 into inactive conformations that promote massive aggregation (Stefani, 2004; Bom et al., 2012). The wild-type and mutant p53 have also been reported to associate into tetramers that irreversibly aggregate to form amyloids (Higashimoto et al., 2006). Additionally, the aggregated p53 is also considered to be a marker for chemoresistance, indicating the deleterious effects of aggregated p53 in cancer (Yang-Hartwich et al., 2015).

Table I. Amyloidogenic proteins and the associated diseases

Diseases	**Proteins Involved**
Parkinson's disease	α-Synuclein
Alzheimer's disease	Aβ-peptide
Huntington's disease	Huntingtin
Systemic amyloidoses	Immunoglobulin light chain
Amyotropic Lateral Sclerosis (ALS)	Superoxide dismutase
Transmissible spongiform encephalopathy	PrP^{SC}
Familial amyloid polyneuropathy	Transthyretin
Hereditary non-neuropathic systemic amyloidoses	Lysozyme
Cerebral amyloid angiopathy	β-amyloid
Atherosclerosis	Apolipoprotein A1

❖ ***Therapeutic Strategies Against Amyloidogenesis***

The diverse etiology underlying the amyloidogenic diseases suggest broad range of therapeutic strategies which are grouped into four main categories, such as stabilization of the native states by use of structural analogues, reducing the aggregation-prone species, inhibition of the nucleus formation or growth of aggregates and enhancement of housekeeping mechanisms by using chaperones (Dobson, 2003a). A large part of amyloid research now attempts to design and use wide range of inhibitors that bring inhibition by one or all of the above mentioned strategies. The use of synthetically designed peptides such as β-sheet breakers, a five residue peptide has been reported to prevent Aβ fibrillogenesis and also disassemble preformed fibrils and reduce cytotoxicity (Soto et al., 1998). A recent study has reported the use of a novel β-breaker peptide NABi, which inhibits Aβ fibril formation both in vitro and in vivo and prevents neuronal cell death, a hallmark in AD (Jang et al., 2018). The uses of vitamins have also been reported to affect fibrillation of amyloidogenic proteins, such as a concentration dependent inhibition of hen egg white lysozyme (HEWL) and Aβ- peptide fibrillation as well as reduced cytotoxicity is observed in the presence of vitamin K3(Alam et al., 2016). Similarly vitamin B12 is observed to impart neuronal cell protection by inhibiting Aβ fibrillogenesis (Alam et al., 2017).

Chaperones which are the controllers of protein folding machinery have also been observed to inhibit amyloid formation in various proteins. Hsp 70 prevents Aβ oligomer formation and reduces cytotoxicity (Rivera et al., 2018), Hsp 104 targets multiple intermediates of the Aβ fibrillation pathway and strongly suppresses Aβ fibrillation in an ATP independent manner by abolishing Aβ fibrils seeding capacity (Arimon et al., 2008), DJ-1 having structural analogy to the chaperone Hsp 31 is an oxidative stress-induced chaperone that prevents α-Synuclein fibrillogenesis (W. Zhou et al., 2006). Recently, HspB1 and Hsc 70 chaperones have been demonstrated to bind to the microtubule binding repeat region of tau protein with different affinities. While HspB1 chaperone delays fibrillation by interacting weakly with the early species of tau protein, the Hsc 70 strongly interacts with amyloidogenic regions to prevent elongation by capping the ends of tau fibrils (Baughman et al., 2018). A new class of inhibitors which are structural analogues of apomorphine have also previously been reported to inhibit Aβ fibrillation by affecting its polymerization and deposition (Lashuel et al., 2002). Apart from these many small

molecule inhibitors such as use of polyphenols (Ngoungoure et al., 2015; Zaidi and Bhat, 2018), cyclic peptides (Jinghui and Pieter, 2014), metal-ion chelators (Cherny et al., 2001) and neurotransmitters (Jain and Bhat, 2014) have been reported to modulate the fibrillation pathways of wide range of amyloidogenic proteins.

Cellular Stress and Osmolytes

Among the various factors that lead to misfolding and aggregation of proteins, the sudden encounters of biological systems ranging from prokaryotic to eukaryotic organisms to extreme environmental conditions such as water stress, salt stress, extreme temperature, extreme pressure etc. could also lead to a catastrophe for the living organisms. Nature has evolved strategies to maintain the cellular homeostasis under such conditions of stress and it is seen that organisms that adapt to such extreme environmental conditions naturally engineer their metabolic cycles to accumulate low molecular weight organic solutes, which are collectively called as Osmolytes (Yancey et al., 1982; Viña, 2002; Yancey, 2005). The osmolytes are broadly divided into the following categories that include polyhydric alcohols (polyols), small sugars (e.g. sucrose), amino acids (e.g. proline) and derivatives (e.g.ectoine), methylamines (e.g. TMAO) and methylsulfonium solutes (Yancey, 2005).

The pioneering work by Timasheff and colleagues established that the protective osmolytes maintain the tertiary structure of the globular proteins by excluding themselves from the vicinity of both the folded (native) and unfolded (denatured) state of the protein, by a principle called 'preferential-exclusion' (Gekko and Timasheff, 1981; J. C. Lee and Timasheff, 1981; Timasheff, 1995). Later on, Bolen and co-workers estimated the transfer Gibbs free energy of amino acid and peptide backbone from water to osmolytes and proposed that the protective osmolytes exclude themselves from the protein vicinity due to the unfavourable interactions between the peptide backbone and the solvent components that raises the free energy of the unfolded state and pushes the equilibrium towards folded state despite the presence of denaturing conditions, a mechanism of unfavourable interactions that was defined by them as Osmophobic effect (Bolen and Baskakov, 2001). Apart from the presence of protective osmolytes in nature, there also exists destabilizing osmolytes, such as urea, that by the mechanism of 'preferential-interaction' are

reported to interact with the peptide backbone leading to unfolding of the tertiary structure of protein thus leading to protein denaturation (Gekko and Timasheff, 1981; J. C. Lee and Timasheff, 1981; Arakawa and Timasheff, 1983; Street et al., 2006; Lim et al., 2009).

The protective effect of osmolytes on the structure, stability and folding of globular proteins have been extensively studied and is well established (Santoro et al., 1992; Street et al., 2006; Kumar, 2009). A group of osmolytes including amino acids, carbohydrates and polyols have been observed to correct the misfolded mutant CFTR (cystic fibrosis transmembrane conductance regulator) protein (Welch and Brown, 1996). Trehalose, a naturally occurring sugar osmolyte has been reported to increase the thermal stability of proteins and also retain biological function such as enzymatic activity under high temperatures (Kaushik and Bhat, 2003). Trehalose is also reported to inhibit aggregation of denatured protein and stabilize them in partially folded conformation facilitating correct folding by the molecular chaperones (Singer and Lindquist, 1998). Osmolytes like proline, heparin and glycerol are reported to inhibit aggregation of creatine kinase and facilitate the regain of its native activity (F.-G. Meng et al., 2001).

While the effect of osmolytes on globular protein is well established, their consequences with respect to intrinsically disordered proteins (IDPs) pertaining to their structure, stability and aggregation are still confusing.

By using both experimental and simulation studies, previous reports have demonstrated that IDPs collapse to form a compact state in the presence of osmolytes (Qu et al., 1998; Morar et al., 2001; Tran et al., 2008). The random coil ensemble of the denatured carboxyamidated ribonuclease A (RCAM RNase) was reported to collapse in the presence of protective osmolytes and expand in the presence of destabilizing osmolyte, urea (Qu et al., 1998), α-Synuclein, which is an IDP and the acid denatured cytochrome-c were similarly observed to collapse in the presence of glycerol (Morar et al., 2001). A previous study on the folding kinetics of the bacterial P protein has been reported to follow a sequential three-state mechanism of folding in the presence of TMAO that leads to the formation of intermediate states during the pathway of protein folding (Chang and Oas, 2010).

Although it is accepted that the IDPs collapse in the presence of osmolytes (Bai et al., 2017), the downstream effects of such a collapse on their aggregation and

fibrillation tendencies are largely varied. The combined use of osmolytes such as TMAO, urea, and betaine on the fibrillation pathway of the natively unfolded islet amyloid polypeptide (IAPP) has revealed that while TMAO delays the fibril elongation without affecting the lag phase, urea prolongs the lag phase in a concentration-dependent manner. Also, the delayed lag phase is completely revived when TMAO is added along with urea (Seeliger et al., 2013). On the other hand, the dehydrins which are the natively unfolded plant proteins remain unfolded both in the presence of compatible solutes as well as molecular crowders like Ficoll and dextran (Mouillon et al., 2008). The studies on the effect of these osmolytes on aggregation have revealed wide range of outcomes, for example, TMAO is reported to induce oligomerization of Aβ-peptide, while promote fibrillation of tau protein (Scaramozzino et al., 2006), increased fibrillation of Aβ 40 and Aβ 42 in the presence of galactose and mannose, inhibition of Aβ 40 aggregation by trehalose etc.(Macchi et al., 2012).

The diverse effects of the osmolytes on the conformational ensembles and the fibrillation states of the IDPs suggest that the osmolyte mediated regulation of IDPs involves greater complexities that need to be investigated. The schematic representation demonstrating the diverse effects of osmolytes on globular and intrinsically disordered proteins is shown in Figure 5.

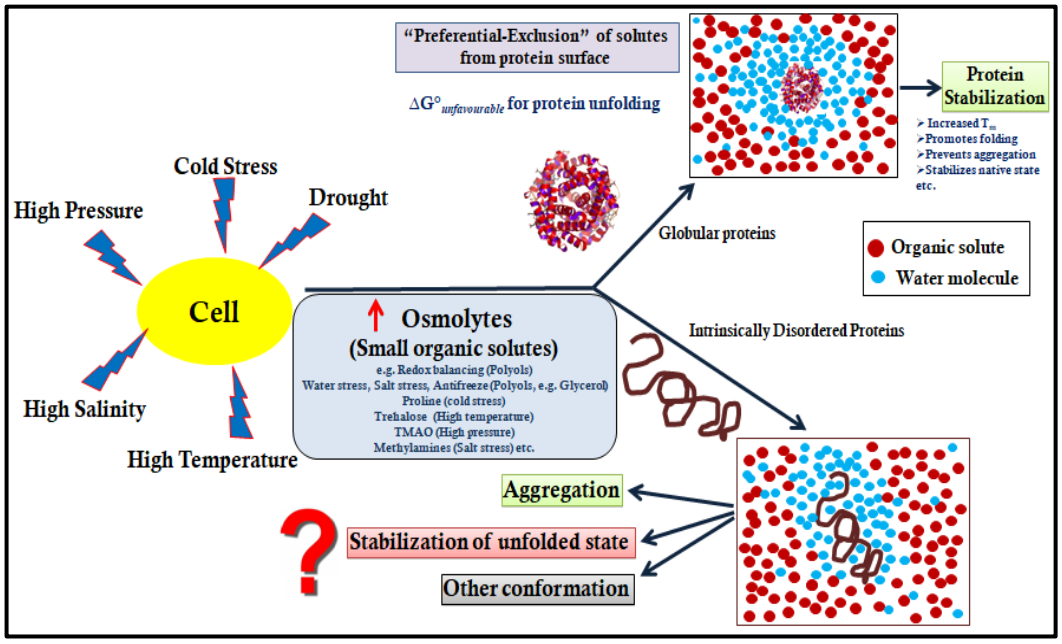

Figure 5. Schematic representation showing osmolyte effects on globular and intrinsically disordered proteins. Osmolytes stabilize the globular proteins by a

mechanism of preferential exclusion but the consequences of their presence in the vicinity of IDPs and the mechanisms involved are still unknown.

Intrinsically Disordered Proteins (IDPs)

Intrinsically disordered proteins are a group of natively unfolded proteins that are flexible, essentially non-compact and lack a well-folded secondary structure under physiological conditions (Uversky, 2002b). It is now established that approximately 30% of mammalian proteome comprises as a full-length disordered protein and 75% as extended disordered regions in signalling proteins (Theillet et al., 2014). Disordered sequences are also found in the structured and ordered domains of well-folded proteins which are termed as intrinsically disordered regions (IDRs) (Dyson, 2016). These proteins have sequence peculiarities where they are characterized by uncompensated charge groups, i.e. they have high net charge in neutral pH and have reduced hydrophobic amino acid residues. In other words, IDPs are enriched in disorder promoting amino acids (Pro, Arg, Gly, Gln, Ser, Glu, Lys and Ala) and are scarce in order-promoting amino acids (Cys, Trp, Tyr, Phe, Ile, Leu, val and Asn). It has been established that the low mean hydrophobicity and high net charge are the prerequisites for a protein to remain unfolded under physiological conditions, thus generating intrinsically disordered proteins (Uversky, 2002a, b; Dyson and Wright, 2005; Uversky, 2016).

The IDPs possess a structural continuum ranging from tightly folded single domains to multidomain proteins containing flexible or disordered regions, to compact yet disordered molten globules and finally highly extended or random heterogeneous states (Dyson and Wright, 2005). The structure-function paradigm was replaced by the ‘Protein Trinity’ model according to which a native cellular protein can occur in the form of ordered, random coil and molten globule states where the biological function can arise from any of these conformations or the transition between them and any of these states could represent the native state of protein (Dunker et al., 2001). The trinity model was later extended to the ‘Protein Quartet’ model where pre-molten globule state was also proposed to be one of the conformational and functional states of the protein (Uversky, 2002a). It is suggested that natively unfolded polypeptide in aqueous solutions, splits into two structurally different groups where one group remains in a random coil state with no ordered

secondary structure and the other is more compact and is in pre-molten globule state that is, it is less compact than the folded and molten globule state but more compact than a random coil protein (Uversky, 2002a). The IDPs are characterized by larger hydrodynamic dimensions as compared to a globular protein corresponding to same molecular mass, lack of ordered secondary structure and high intramolecular flexibility (Uversky, 2002a). Several experiments suggest that the conformational states of IDPs are largely governed by the solvent conditions which can promote either collapse of the unfolded state such as at low pH and high temperature conditions or maintain the unfolded conformation in the presence of denaturants such as GdmCl and Urea (Uversky, 2002b, 2009; Jain et al., 2018). Due to the lack of a 3D structure in IDPs and the susceptibility of the IDPs to various environmental conditions, a given segment of protein molecule can have varying conformationsat different time points. Thus, the IDPs are also called '4D proteins' since their structure is defined by both time and space and a particular structure in an IDP can be observed at a given time only, making it a complex ensemble of structures to be characterized (Uversky, 2016). The techniques such as gel filtration chromatography, SAXS, FTIR, far-UV CD and NMR spectroscopy, light scattering, sedimentation studies have been used for studying the hydrodynamic properties of the intrinsically disordered proteins (Dyson and Wright, 2005). The functional importance of the disordered proteins have been extensively investigated and it is suggested that the conformational plasticity of the IDPs is an important prerequisite for process of molecular recognition (Uversky, 2002a). The various functions of IDPs include the cellular signal transduction, storage of small molecules, chaperoning, regulation of transcription and translation, protein phosphorylation, cell-cycle regulation, scaffolding and the regulation of the self-assembly of multiprotein complexes such as the bacterial flagellum and the ribosome. Several chaperones and RNA binding proteins are reported to possess unfolded regions that bind to the misfolded proteins and RNA molecules, acting as recognition elements and/or assist the unfolding of the kinetically trapped intermediate (Dyson and Wright, 2005; Mollica et al., 2016). One of the remarkable characteristics of IDPs is to undergo 'disorder-to – order' transition and form more ordered states or fold into secondary or tertiary structure upon binding with their targets or interacting partners (Dyson and Wright, 2005; Mittag et al., 2010). IDPs are also observed to form 'fuzzy complexes' where the IDPs retain high degree of disorder even in bound

states (Mollica et al., 2016; Uversky, 2016). Broadly two mechanisms are observed to be the limiting cases of IDP binding which are, (a) conformational selection, where folding in the IDP occurs before binding and (b) induced fit, where IDP gains structure after binding. However, complex binding mechanisms involving different combinations of these two have also been envisaged (Mollica et al., 2016).

The folding and binding of IDPs/IDRs accomplish interaction with their targets by high specificity and low binding affinity, which may facilitate specific ligand binding interactions for the signalling cascades while dissociating when signalling is completed. It is suggested that binding of an IDP due to the loss of conformational entropy gives rise to an unfavourable entropic contribution to binding and uncouples binding strength from specificity, thus facilitating high specificity with a low binding affinity (Dyson and Wright, 2005; H.-X. Zhou, 2012; Babu, 2016; Mollica et al., 2016). Among the other advantages of the specific qualities of IDPs and IDRs that facilitate efficient interaction and regulation are, assembly of complexes due to open access of binding site to an IDP and lack of steric hindrance, susceptibility to modifying enzymes such as kinases, e.g. post-translational modifications of linker region as well as other IDRs (Bah and Forman-Kay, 2016), formation of extended binding interfaces which facilitate even high affinity binding, multiple binding partners or promiscuity due to conformational plasticity and high turnover rate of IDPs that facilitate signalling (Mollica et al., 2016). Due to large heterogeneity of the IDPs and massive mechanistic repertoire that involves diverse functionalities, defining the binding interactions of IDPs by a uniform or a generic mechanism is a challenge. The use of advanced techniques such as NMR spectroscopy, molecular simulations and transient kinetic studies are paving way for better understanding of mechanisms of IDP interactions. A recent study has also demonstrated the functional roles of IDPs in providing desiccation tolerance to a microscopic organism called tardigrades by forming glassy amorphous aggregates, a process called vitrification (Boothby et al., 2017).

While the functional versatilities of IDPs in cellular complexities are now increasingly being appreciated, the importance of IDPs in many diseases is also prevalent.The recent studies on IDPs have raised enormous interest due to their increased fibril forming or amyloidogenic proteins that play role in majority of neurodegenerative diseases as well as cancer (Uversky et al., 2008; Babu et al., 2011). As the IDPs lack a well folded tertiary structure, unlike globular proteins

where partial unfolding is required for fibril formation, the IDPs undergo partial folding and attain a molten-globule state, which is a prerequisite for fibrillation (Uversky, 2008). Stabilization of a partially folded conformation both in a globular as well an IDP is must for fibrillation that facilitates the important intermolecular interactions including electrostatic interaction, hydrogen bonding and hydrophobic interactions required for self-association and oligomerization (Uversky, 2008).

Synuclein Family

Synucleins are a class of intrinsically disordered proteins, comprising of three genes α, β, and γ-synuclein which are small, soluble, highly conserved vertebrate proteins expressed predominantly in neurons (George, 2001; Uversky et al., 2002; Sung and Eliezer, 2007; Ducas and Rhoades, 2014) and are mapped to human chromosome 4q21, 5q35 and 10q23 respectively (Clayton and George, 1998). The α, β, and γ-syn are composed of 140, 134 and 127 amino acid residues, respectively corresponding to a molecular weight of ~14 kDa (Jain et al., 2018). The members of this family share a great level of sequence homology. The synucleins are characterised by a highly conserved N-terminal domain, hydrophobic NAC domain and a least conserved acidic stretch in the –COOH terminal domain. The N-terminal domain is implicated as α- helical lipid binding motif sharing similarity to the class - A_2 lipid-binding domain. Within the N-terminal region, lies the NAC domain marked by a repetitive, degenerative amino acid motif KTKEGV with conserved periodicity of 11 amino acid repeats imparting hydrophobicity variations among the proteins (Uversky et al., 2002; Sung and Eliezer, 2007). The α and β-Syn are predominantly localized in the presynaptic nerve terminals, while γ-Syn is abundant in peripheral nervous systems, i.e. spinal cord and sensory ganglia, both primary sensory and sympathetic neurons. γ- Syn among the other members is most widely distributed within neuronal cytoplasm being present throughout the cell bodies and axons, as well as expressed in wide range of tissues such as olfactory epithelium, breast and ovarian tumours (George, 2001; Uversky et al., 2002; Sung and Eliezer, 2007).

Among all the synucleins, α-Syn remains most widely studied due to its increased amyloid forming propensity which is predominantly linked to the etiology of Parkinson's disease (PD). The pathognomonic fibrillar deposits of α-Syn are most abundant components of Lewy bodies (LB) or Lewy neuritis (LN) which is a

hallmark of PD, characterised by lesions which are the aggregates of proteins and lipids (Cookson, 2005; Auluck et al., 2010). The fibrillar deposits of α-Syn in the form of LB have also been reported to be causative agents for other neurodegenerative diseases such Alzheimer's disease (AD), dementia with Lewy bodies (DLB) and multiple system atrophy (MSA), thus establishing their prevalent role in neurodegenerative diseases, which are collectively termed as 'Synucleopathies' (Murray et al., 2001; Bennett, 2005). A recent study has also established the similarities between prion protein and α-Syn, suggesting a prion like propagation of synucleopathies (Tamgüney and Korczyn, 2017).

Although the three synucleins share high sequence similarities, the subtle differences in their sequences, such as lack of the NAC domain (11-residues stretch) in β-Syn and a shorter or slightly less negative C-terminal in γ-Syn have been observed to impart differences in their fibrillation and secondary structure propensities, and conformational dynamics (Uversky et al., 2002; Marsh et al., 2006; Sung and Eliezer, 2007; Ducas and Rhoades, 2014). The fibrillation propensities of the synucleins are in the following order α-Syn > γ-Syn > β-Syn (Biere et al., 2000; Jain et al., 2018). The absence of the NAC domain in β-Syn is responsible for its negligible fibrillation propensity (Uversky et al., 2002), however, under conditions such as low pH, β-Syn is observed to form fibrils (Jain et al., 2018). β-Syn at high molar concentration is reported to inhibit both α-, and γ-Syn fibrillation (Jain et al., 2018) and the chaperoning effects of β-Syn has been well established previously (Park and Lansbury, 2003; D. Lee et al., 2004; Tsigelny et al., 2007). A recent study, by the use of techniques like single molecule fluorescence spectroscopy and cell-free protein expression systems has demonstrated that β-Syn preferentially incorporates into the smaller oligomers of α-Syn and strongly inhibits fibrillation of A30P and G51D variants compared to E46K, H50Q and A53T, which are the other pathogenic mutants of α-Syn (Leitao et al., 2018). Although the direct involvement of β-Syn in neurodegenerative diseases, is still not evident, the SNPs (single nucleotide polymorphs) of β-Syn have been related to the onset of PD upon aging (Brighina et al., 2007; Brockhaus et al., 2018).

γ-Synuclein

γ-Synuclein is the third and the least studied member of the synuclein family which lacks the tyrosine rich C-terminal signature domain of α- and β-Syn, containing a single tyrosine residue at 39 position and shares approximately 60% sequence similarity with α-Syn (Uversky et al., 2002). A recent phylogenetic analysis on the relatedness of three synucleins suggest that both α and β-Syn share their parental lineage from γ-Syn, and that γ-Syn has a long evolutionary history, thus being distantly related to the other two synucleins (Jain et al., 2018). γ-Syn is most intriguing in the sense that unlike the other two synucleins it is widely involved in causing both neurodegeneration (Ninkina et al., 2009) and cancer (M. Ahmad et al., 2007), suggesting a connecting link between the progression of these two diseases by complex interplay of the protein that is yet to be deciphered.

γ-Syn or SNCG, also called "Persyn" was originally referred to as Breast Cancer Specific Gene-1 (BSG-1) due to its overexpression in late stages of breast cancer (Jia et al., 1999). Till date, disease causing variants of γ-Syn are not evidenced, however, a common polymorphism of γ-Syn (V110E) was reported previously (Ducas and Rhoades, 2014) and is used in this study. The pathogenic effects of γ-Syn are attributed to its overexpression and elevated levels of γ-Syn in many late stages of cancer are considered a prognostic marker for metastasis (M. Ahmad et al., 2007). Several undesirable and cancer promoting effects of over expressed γ-Syn are as follows: over expressed γ-Syn confers antibiotic resistance against microtubule targeted drugs like paclitaxel, a widely used chemotherapeutic agent in cancer cells and promotes association and polymerization of microtubule proteins (Zhang et al., 2011), enhances malignancy by promoting perineural invasion or distant metastasis (Hibi et al., 2009), chaperoning the estrogen receptor (ER-α) to maintain high ligand binding affinity and stimulating hormone responsive mammary tumorigenecity (Jiang et al., 2004), influence cell cycle by co- localizing in the centrosome and spindle pole of mitotic cells thus affecting signalling transduction (Surguchov et al., 2001), wards off the cancer cells from apoptosis by interacting with various MAPKs (Mitogen Activated Protein Kinases) and imparts resistance to chemotherapeutic drugs thus promoting survival of tumour cells (Pan et al., 2002), interacts with myocilin and thus has a possible role in pathology of glaucoma (Surgucheva et al., 2005), enhances resistance to radiation in breast cancer cells (Tian et al., 2018), etc. The other damaging effects of over expressed γ-Syn is the death of motor neurons due to the formation of aggregates at a higher concentration, the effects collectively

termed as 'γ-Synucleopathies'(Ninkina et al., 2009), and are summarized in Figure 5.

Structural characterization studies reveal that the functional disparities between γ-Syn and α-Syn arises due to their structural differences in the C-terminal tail (Sung and Eliezer, 2007; Manivel et al., 2011), which is more dynamic in γ-Syn than other two synucleins (Ducas and Rhoades, 2014) and adopts a coil-like structure in γ-Syn, while in α-Syn it remains uncoiled and unfolded. Additionally, the C-terminal tail of γ-Syn is reported to be highly exposed to the solvent environment and that the interactions of γ-Syn are also mediated through the C-terminal domain (Manivel et al., 2011). In a previous study, the investigation on the effects of sequence differences and the fibrillation propensities between α- and γ-Syn revealed that the amyloid forming region in γ-Syn has an increased α-helical propensity compared to α-Syn, which in turn imparts lower fibrillation propensity to γ-Syn (Marsh et al., 2006).

From available evidences present in literature for γ-Syn, it is established that γ-Syn is the moderately fibrillogenic but highly oligomeric member of the synuclein family, where it is monomeric at low concentration but associates to form oligomers when concentration increases (Uversky et al., 2002). Biophysical characterization of γ-Syn in terms of its secondary structure, fibrillation propensity as well as hydrodynamic properties reveals that γ-Syn has a smaller hydrodynamic dimension than both the α- and β-syncleins and attains globularity as well as β-sheet propensity at concentrations above or equal to 70μM (Uversky et al., 2002). The severity of γ-Syn in causing neurodegenerative diseases and cancer lies in its tendency to form annular oligomers either on oxidation or at higher concentration, which not only are capable of getting transmitted from one cell to another but are believed to have seeding effect on other intracellular proteins, such as α-Syn, which is a hallmark in PD (Surgucheva et al., 2012). Nevertheless, γ-Syn deposits have also been traced in Lewy bodies in conjunction with the fibrillar deposits of α-Syn (Galvin et al., 1999). Therefore the factors such as high concentration (Uversky et al., 2002), oxidation (Surgucheva et al., 2012) and dissociation of γ-Syn from its interaction partners (Golebiewska et al., 2014) are reported to facilitate oligomerization.

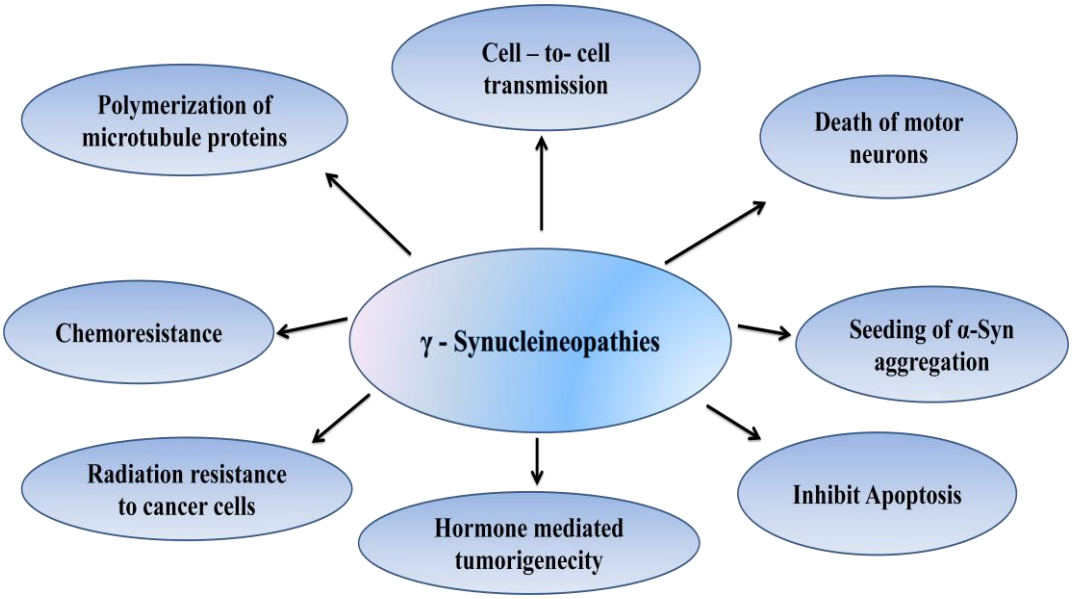

Figure 6. Schematic diagram summarizing the involvement of γ-Synuclein in pathogenesis

In the light of the current scenario and the established evidences on potentially toxic oligomeric intermediates in the fibrillation pathway of γ-Syn, it is important to employ a strategy for regulating the toxicity of these resultant oligomeric species and investigate the effects of various therapeutic modulators on fibrillation pathway of γ-Syn. Despite the evidence of the vast range of pathogenic implications of γ-Syn, no intervention strategies for the modulation of the fibrillation pathway or oligomerization tendency of γ-Syn have been attempted.

In this study we have employed three different polyphenols, namely epigallocatechin-3-gallate (EGCG), quercetin and silibinin and a series of polyols to investigate their effects on the structure and aggregation of human γ-Syn. In the next sections, the advantages of polyphenols, their characteristics and their use as antiamyloidogenic agents are described as well as the diverse effects of polyols on the stability and aggregation behaviour of IDPs, and the underlying mechanisms and their importance in living systems are discussed.

Polyphenols

One of the most promising candidates emerging as effective therapeutics against amyloidogenic diseases are the naturally occurring small molecule phytochemical called polyphenols, which are abundant in plant resources and are characterized by

one or more aromatic phenolic rings in their structure. The natural polyphenols are richly supplemented in wine, tea, nuts, berries, whole grains, and chocolates and in many other plants. The naturally occurring polyphenols are classified based on their source of origin, biological function and chemical structure and some of the major categories are: vitamins (e.g., b-carotene and α-tocopherol), flavonoid (e.g., flavanone and isoflavone), phenolic acids (e.g., benzoic acid and phenylacetic acid), and other miscellaneous polyphenols (resveratrol, curcumin, rosmarinic acid etc.) (Porat et al., 2006; Tsao, 2010). The polyphenolic compounds are reported to have many pharmacological properties such as antioxidative, anticarcinogenic, neuroprotective, anti-inflammatory etc. (Ngoungoure et al., 2015). While the antiamyloidogenic effects of many polyphenols have been investigated, a universal mechanism of polyphenol mediated inhibition of fibrillation does not exist. It is observed that different polyphenols can interact with different amyloidogenic species formed in the pathway such as monomeric, oligomeric or pre-fibrillar form as well as different modes of inhibition and modulation has also been observed. One of the mechanisms by which naturally occurring polyphenols are speculated to inhibit amyloidogenesis is by the process of aromatic stacking where the aromatic rings present in the structure interact with the aromatic residues present in the amyloidogenic protein, thus inhibiting self-assembly process in amyloid formation (Porat et al., 2006; Wu et al., 2006).

Due to the growing evidence of amyloid oligomer toxicity in amyloidogenic diseases, attempts are made to use polyphenols in arresting, modulating or rendering the oligomers less toxic with the use of polyphenols. Epigallocatechin-3-gallate (EGCG) is one of the most widely used polyphenol that is reported to affect oligomerization of both α-Syn and Aβ-peptide, modulating them to form off-pathway, non-toxic species (Ehrnhoefer et al., 2008; del Amo et al., 2012). A similar effect of the polyphenol Baicalein on α-Syn and Aβ-peptide is also reported (Lu et al., 2011). The other examples of antiamyloidogenic effects of polyphenols, involving different modes of inhibition are, stabilization of early aggregates of human lysozyme by red wine polyphenol, resveratrol (Zaidi and Bhat, 2018), fibrillation inhibition and disaggregation of preformed fibrils by polyphenol Baicalein (Zhu et al., 2004; Lu et al., 2011), increased reconfiguration rate of α-Syn leading to inhibition of fibrillation by curcumin (B. Ahmad and Lapidus, 2012), etc. The effects of various polyphenols on different proteins and their mode of actions

are consolidated and well documented in a number of reviews (Cheng et al., 2013; Ngoungoure et al., 2015).

While an enormous amount of evidence for the use of polyphenols as antiamyloidogenic agents for some proteins are available, no such effect of polyphenols on γ-Syn fibrillation has been investigated.

Polyol Osmolytes

As the name suggests, polyols or polyhydric alcohols have 2 or more hydroxyl (-OH) groups in their structures and are naturally produced in organisms under stress (Yancey, 2005). The polyols increase the water retention in cells and are dominantly produced in organisms that tolerate cold stress (Yancey et al., 1982; Yancey, 2005). A linear correlation with the increasing chain length in polyols with their increasing effect on protein stability has been previously established (Gerlsma, 1968). It has been previously observed that the polyols facilitate protein folding by strengthening the hydrophobic interactions in the protein (Gekko, 1981; Gekko and Ito, 1990).

The group of polyols including cyclic polyols like inositol to linear polyols such as ethylene glycol, have been demonstrated to linearly increase the thermal stability of lyozyme protein at pH 2, with their increasing concentrations as well as increasing number of –OH groups (Fujita et al., 1982). Similar correlations between increasing –OH groups in the polyols with increasing stability of hexokinase A (Tiwari and Bhat, 2006) and the stabilization of native-like conformations of the hexokinase A protein by cooperative folding in the presence of polyols have also been established (Devaraneni et al., 2012). Polyols have also been demonstrated to promote refolding and inhibit aggregation of a highly aggregation- prone protein citrate synthase (Mishra et al., 2005). The inhibitory effects of the polyols on the aggregation have been established in wide range of studies (Pérez and Griebenow, 2001; Singh and Singh, 2003; Vagenende et al., 2009; Abbas et al., 2012).

While a correlation with the increasing chain length of polyols with increased stability of globular proteins is well established, no such evidence of linearity has been reported for the IDPs till date. Thus, the fact that the IDPs are prone to aggregation and are largely involved in the generation of amyloids that give rise to amyloidogenic diseases, the investigations on the effects of polyols on the fibrillation tendencies of γ-Syn, which is an IDP is intriguing and would lead to a

better understanding of the parallel regulation of the polyol mediated effects on globular and intrinsically disordered proteins.

Outline of the present study

The involvement of γ-Syn in plethora of diseases ranging from neurodegeneration and cancer led to the commencement of this study with two broad aims. The first aim was to investigate the effects of small molecule modulators called Polyphenols, which are now increasingly being used as therapeutics against amyloidogenic diseases, on the structure and aggregation of γ-Syn. The increased tendency of γ-Syn to self associate and form toxic oligomers despite being moderately fibrillogenic as compared to its fibrillogenic counterpart α-Syn, makes it an important target for small molecule mediated inhibition or modulation. The knowledge of the effects of such modulators on the oligomeric as well as fibrillogenic tendency of γ-Syn, which is yet unknown, is expected to lead to a better understanding of the propagation of the underlying synuclein related diseases. Due to the lack of understanding and unavailability of evidence on the small molecule mediated modulation of γ-Syn fibrillation pathway, this study investigates the effect of three different classes of polyphenols, epigallocatechin-3-gallate (EGCG), quercetin and silibinin on the fibrillation pathway of γ-Syn. The study provides the first report on the detailed mechanism on the polyphenol mediated modulation of the γ-Syn fibrillation pathway by investigating the effect of these polyphenols on the fibrillogenic as well as oligomeric tendency of γ-Syn, by studying in detail their effects on γ-Syn structure, the mode of binding interactions between polyphenols and γ-Syn and most importantly assessing their cytotoxic effects on two different cell lines, breast cancer (MCF-7) and neuroblastoma (SH-SY5Y) cells.

The second aim of the study was to investigate the effect of protective osmolytes called Polyols on the structure, stability and aggregation of γ-Syn. The stabilizing effects of the polyol osmolytes which are naturally found in organisms under stress are well established for the globular proteins but with the prevalence of intrinsically disordered proteins in the eukaryotic as well as prokaryotic genome a very important and fundamental question arises as how cellular homeostasis is maintained in the presence of polyols under stress with the coexistence of globular and IDPs? The previous reports have demonstrated a linear relationship between the increasing numbers of –OH groups in the polyols with increased protein stability. Thus, understanding the effect of these polyols on the structure and aggregation of γ-Syn, which is an IDP, was of interest to be investigated. The study uses a series of polyols

comprising ethylene glycol, glycerol, erythritol, xylitol and sorbitol with increasing number of –OH group ranging from 2 to 6, respectively. By employing various biophysical techniques the variable effect of polyols on the fibrillation propensity and structure of γ-Syn has been observed and discussed. The study gives an important insight into the possible modulatory effect of osmolytes for an IDP, like γ-Syn that may help in understanding the simultaneous regulation of globular as well as intrinsically disordered proteins in cellular systems under stress.

Chapter 2

Materials and Methods

Materials

The following chemicals used for the purification of γ-Syn including di-hydrogen potassium phosphate (NaH_2PO_4), di-potassium hydrogen phosphate (Na_2HPO_4), ammonium sulphate, ammonium acetate, glacial acetic acid, sodium azide and sodium chloride were purchased from Sisco Research Laboratory (SRL), India. Ethanol and streptomycin sulphate was purchased from Sigma-Aldrich, USA. All the three polyphenols, epigallocatechin-3-gallate (EGCG), quercetin and silibinin, polyols (ethylene glycol, glycerol, erythritol, xylitol and sorbitol), pH standards, fluorescent probes 1-anilino-8-napthalene sulfonic acid (ANS) and thioflavin T (ThT) were also purchased from Sigma-Aldrich, USA. The chemicals used were of highest purity and were used for the studies without further purification. For size-exclusion chromatography, the BioSep S-2000 column (300 x 7.8 mm) was purchased from Phenomenex, CA, USA. The 50µl loading syringe for HPLC was purchased from Hamilton, USA. Methanol used for washing and storing the column was of HPLC grade quality and was purchased from Fischer Scientific, USA. The gel filtration standards and protein molecular weight markers were purchased from Bio-Rad Laboratories, USA. All the cell culture media components were purchased from Gibco, ThermoFischer Scientific, USA. The plasmid isolation kit was purchased from Qiagen, Germany. All the buffers and the reagents were prepared in extra pure water (Milli Q) obtained from Millipore water purification unit.

Methodology

1. Protein Expression and Purification:

The expression and purification of recombinant human γ-Syn was carried out according to the protocol reported previously (Volles and Lansbury, 2007). The recombinant human γ-Syn was cloned in BL-21 (DE3) strain of *E.coli* in a pET 29a vector containing the antibiotic resistance gene for kanamycin. The culture was grown in 100 ml Luria broth containing kanamycin (50µg/ml) at 37 ºC, 200 rpm, to an A_{600} of 0.6-1.0 and induced with 1mM IPTG for 4h for optimum expression. After 4h the culture was centrifuged at 6500×g for 20 min, pelleted, resuspended in 0.75ml of buffer [50mM Tris, (pH 8.0), 10 mM EDTA, 150mM NaCl] per 100 ml of culture. The pellet was repeatedly vortexed and mixed for the homogenization of the

pellet and stored at -80 ºC for further use. γ-Syn was purified by a non-chromatographic method (Volles and Lansbury, 2007) and a boiling protocol was employed considering the thermal stability of Synucleins (Jakes et al., 1994). The purification protocol was optimised for a large scale culture (8-10L) for an increased yield of the protein. The pelleted protein was directly placed in boiling water bath for approximately 10 min and centrifuged at a speed of 6500×g for 20 min to remove the debris. The volume of the supernatant was measured and transferred to a fresh tube and to the supernatant streptomycin sulphate (136µl of 10% solution/ ml of supernatant) and glacial acetic acid (228µl/ ml of supernatant) was added followed by a centrifugation at 13000×g for 30 min. The supernatant was precipitated by adding ammonium sulphate [saturated ammonium sulphate at 4ºC, 1:1(v/v)] and centrifuged at 13000×g for 30 min. The pellet was washed with 10ml (per litre culture) of ammonium sulphate solution [4ºC, 1:1 (v/v) and water]. The pellet obtained was resuspended in 9ml of 100 mM ammonium acetate and precipitated by adding equal volume of ethanol (20ºC) and pellet was again collected by centrifugation. The precipitation step was repeated twice and finally the pellet was dissolved in 10mM phosphate buffer maintained at pH 7.4.

The purified γ-Syn was further concentrated using a 10kDa and 100kDa centrikon filters using swinging bucket rotor at 2000×g for 15 min and 1200×g for 40 min respectively. The purity of the protein was confirmed by SDS-PAGE analysis and the intact mass of the protein was determined by ESI-MS analysis. The purified protein was distributed in equal aliquots of 1 ml and stored at -20ºC until further use.

2. Electro-spray Ionization Mass Spectrometry (ESI-MS)

Purified γ-Syn was diluted in a 50:50 mixture of acetonitrile and 0.1% formic acid and was analysed by direct infusion at a flow rate of 15 µl/ min on a positive ion mode with a capillary voltage of 3 kV. The following instrumental parameters were used: cone voltage 30 V; source temperature 100°C; travelling wave height 8–40 V; travelling wave speed 300 m/s; IMS gas flow 85 ml/min. Data were acquired over the range m/z 500–2000. Data were processed by using MassLynx v4.1 software supplied with the mass spectrometer. The ESI-MS spectrum of purified γ-Syn is given below:

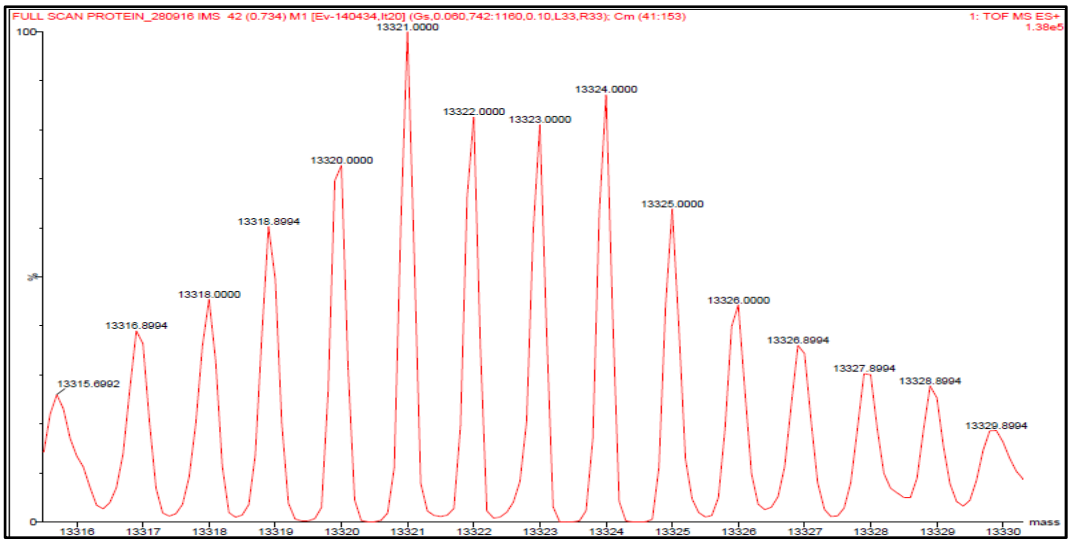

Figure 1. Mass spectrometry analysis of purified γ-Syn by ESI-MS. The mass spectrum of purified γ-Syn shows a molecular weight of 13,321 Da.

3. Plasmid isolation and confirmation of sequence of γ-Syn

The plasmid was isolated by using the QIAprep Spin Miniprep Kit (Qiagen, Germany) and the plasmid quality was checked by running on 1.2% agarose after restriction digestion with NdeI and XhoI restriction enzymes (Thermoscientific, MA, USA). The sequencing was carried out at Xcelris Lab Pvt. Ltd. (India) and was confirmed to be the natural variant of human γ-Syn with a V110E in the sequence. (Figure 2).

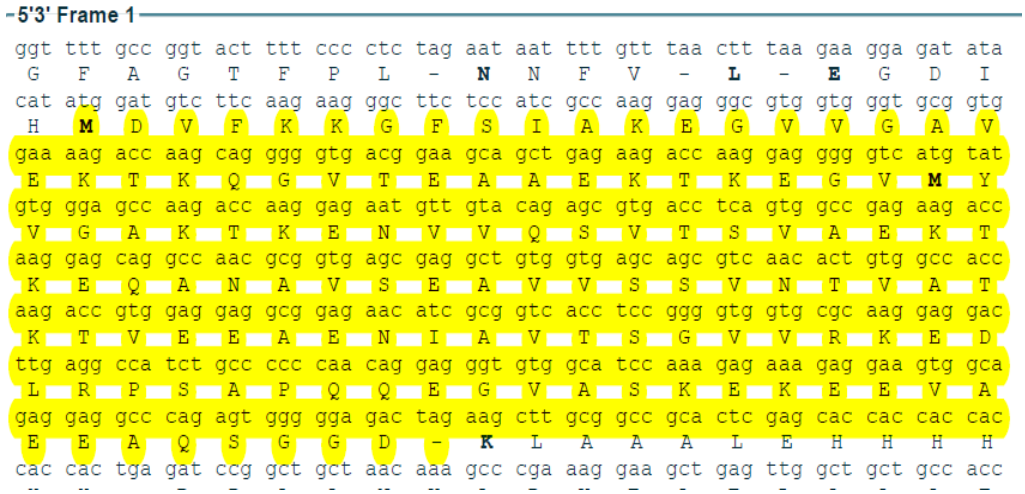

Figure 2. Sequence of full length purified γ-Syn. The highlighted part reads the full sequence of γ-Syn.

4. SDS-PAGE Analysis

Polyacrylamide gel electrophoresis under denaturing conditions was carried out in the presence of 10% SDS. The concentrations of the separating and the stacking gel were kept 15 and 4 % respectively. The compositions of the gels are given in table below and the SDS-PAGE showing purity of γ-Syn is shown in Figure 3:

Components	Separating Gel (10%)	Stacking Gel (4%)
H_2O	1.8 ml	3 ml
30% Polyacrylamide stock	4 ml	670 µl
1.5M Tris (pH 8.8)	2 ml	-
1.0M Tris (pH 6.8)	-	1.25 ml
10% SDS	80 µl	50 µl
10% APS	80 µl	50 µl
TEMED	8 µl	5 µl

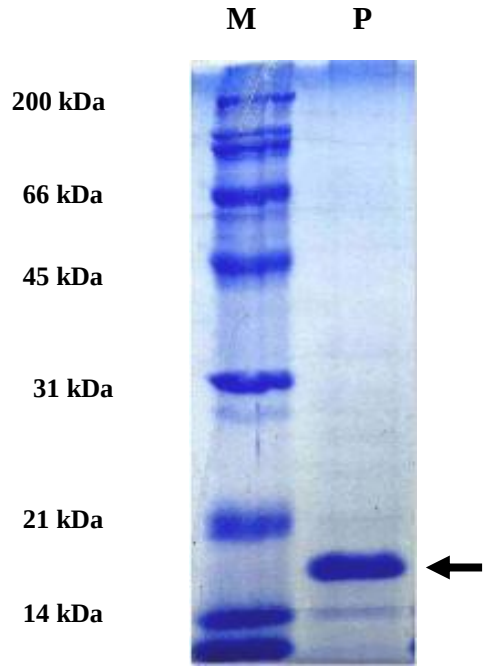

Figure 3. SDS-PAGE showing purity of γ-Syn. Broad range molecular weight protein ladder is denoted by M. The lane P shows the pure band of purified γ-Syn (*black arrow*) with an apparent molecular weight of 19 kDa.

5. Native-PAGE

For native conditions, similar composition was followed except for the addition of SDS into the solutions**.**

6. UV- Vis Spectroscopy

UV-Vis measurements were made using Cary Varian 100 UV-Vis spectrophotometer. The protein concentration was measured using a molar extinction co-efficient of 1400 M^{-1} cm^{-1} at 275 nm and molecular weight of 13,321Da. The concentration of the fluorescent probes, thioflavin T (ThT) and 8-Anilinonaphthalene-1-sulfonic acid (ANS) dye was measured using their molar extinction coefficient of 35000$M^{-1}cm^{-1}$ at 270 nm and 7800 $M^{-1}cm^{-1}$ at 375 nm in 10 mM phosphate buffer, pH 7.4, respectively. The pH of all the solutions was measured using PHM 220 Lab pH meter (Radiometer Analytical SAS, France).

The concentration of polyphenols, EGCG, Quercetin and Silibinin were measured using a molar extinction co-efficient of 11920 $M^{-1}cm^{-1}$ at 270 nm, 27641 $M^{-1}cm^{-1}$ at 378 nm and 4000 $M^{-1}cm^{-1}$ at 336 nm in 10 mM phosphate buffer, pH 7.4 for EGCG and in DMSO for quercetin and silibinin, respectively. All the measurements were made using a quartz cuvette of 1 cm path length.

7. Thioflavin T Assay

Thioflavin T (ThT) is a benzothiazole dye that fluoresces strongly upon binding with the cross-β sheet structures which are a signature of the amyloid fibrils (Ban et al., 2003). The ThT assay was performed to study the fibrillation kinetics of γ-Syn in the presence of polyphenols and polyols. Thioflavin T and EGCG were dissolved in fibrillation buffer containing 20 mM phosphate, 0.1M NaCl, 0.02% NaN_3 at pH 7.4.

7.1 Fibrillation Kinetics of γ-Syn

To monitor the fibrillation kinetics of γ-Syn in the absence and presence of polyphenols and polyols, γ-Syn (1mg/ml; 75 μM) was incubated at 37 ºC, 200 rpm with an increasing concentration of polyphenols (EGCG, Quercetin and Silibinin) and polyols containing 20 μM of ThT dissolved in 20 mM phosphate buffer with 100 mM NaCl at pH 7.4. The measurements were recorded at regular intervals during fibrillation at 480 nm with an excitation of 445 nm, keeping both the

excitation and emission slit widths of 5 nm in a Cary Eclipse Fluorescence Spectrophotometer. Each sample was run in triplicates and the data were averaged before plotting ThT fluorescence with respect to time.

The kinetic parameters of fibrillation that is the lag time and apparent rate of fibrillation was calculated by fitting the fibrillation kinetics into a sigmoidal curve using the empirical formula reported previously (Uversky et al., 2001) and is mentioned below:

$$Y = (y_i + m_i x) + \frac{v_f + m_f x}{1 + e^{\frac{x - x_0}{\tau}}} \quad (1)$$

Where, Y is the fluorescence intensity and x_o is the time to reach 50% of maximal fluorescence. The initial base line during the lag phase is described by $y_i + m_i x$. The final base line at saturation is described by $v_f + m_f x$. The apparent first-order rate constant (k_{app}) for the growth of fibrils is calculated as 1/t, and the lag time is calculated as $x_o - 2\tau$.

7.2 Time-point Addition of Polyphenols and Disaggregation Assay

To investigate the effects of polyphenols on the different stages of γ-Syn fibrillation, the polyphenols, EGCG and quercetin (50 μM) was added at 8, 24 and 48h that correspond to late lag, log and saturation phase of γ-Syn fibrillation under conditions used. The ThT was measured at regular intervals as mentioned above. The dilution effect upon addition of polyphenols was balanced by addition of equal volume of buffer in the control samples.

7.3 Seeding Experiment

The *on-/off-* pathway nature of the γ-Syn species formed in the presence of polyphenols were investigated by seeding studies. The preformed γ-Syn fibrils formed in the absence and presence of the polyphenols were used as a seed for γ-Syn fibrillation. The seeds were prepared by incubating γ-Syn (75 μM) both in the absence and presence of polyphenols (50μM) at 37 ºC, 200 rpm for 48h. The unbound polyphenols and soluble aggregates were removed by centrifugation at 14,000×g for 30 min and the fibrillar pellet was washed twice with the buffer. The seeds were resuspended in the fibrillation buffer and various seed concentrations

(%v/v) were added into the monomeric γ-Syn solution containing 20 μM ThT. The fibrillation kinetics were monitored by recording ThT fluorescence at 480 nm with an excitation wavelength of 445 nm in a 96-well plate using a Varioskan microplate reader (Thermofischer, MA, USA) at a regular interval of 30 min at 280 rpm and a diameter of 8 nm. Additionally, in the case of EGCG, the seeding studies were also carried out with addition of EGCG (50μM) to the preformed γ-Syn seeds and fibrillation was monitored by recording ThT fluorescence at regular intervals of fibrillation.

8. Rayleigh Light Scattering

Polyphenols are known to interfere with the ThT fluorescence (Hudson et al., 2009) and therefore to monitor the effect of polyphenols on the aggregation propensity of γ-Syn, the samples containing γ-Syn in the presence of increasing concentrations of polyphenols were incubated under fibrillating conditions at 37 °C, 200 rpm and the samples were withdrawn at regular time intervals of fibrillation. The Rayleigh scattering of the samples withdrawn at different time points were recorded with synchronous scanning using a 1cm path length cuvette at $\lambda_{ex}= \lambda_{em}$ = 350 nm with excitation and emission slit widths of 2.5 nm and 5 nm, respectively in a Cary Eclipse Fluorescence Spectrophotometer.

9. Dynamic Light Scattering

Dynamic light scattering of polyphenol treated γ-Syn species were carried out in a SpectroSize^{TM} 300 Xtal Concept DLS/SLS equipment. For DLS studies, the samples prepared for Rayleigh scattering were further centrifuged at 14,000×g for 30 min and the supernatant was used for the analysis of the soluble γ-Syn species. The measurements were carried out using quartz precision cell of 1.50 mm path length (Hellma Analytics) at 25ºC. For each sample, 5 acquisitions were collected with single measurement duration of 20s. Each sample was analyzed in triplicates.

10. Transmission Electron Microscopy

The morphology of the γ-Syn fibrils formed in the presence and absence of polyphenols was visualized by transmission electron microscopy (TEM). TEM images were collected using a JEOL TEM 2100 microscope operating with an accelerating voltage of 200 kV. Samples were deposited on carbon coated 200 mesh

copper grid and negatively stained with 1% uranyl acetate. The grids were then dipped in drops of double distilled water to remove any excess stain and tapped onto the filter paper for drying the excess water. The grids were then placed onto the filter paper and allowed to dry overnight before the samples were examined using TEM with images captured using a CCD camera.

11. Atomic Force Microscopy

Freshly cleaved mica sheet was glued on a microscopic slide and the mica surface was exfoliated twice immediately before the addition of the sample onto the mica surface. 10 µl of sample was adsorbed on the mica surface and was allowed to dry for 20 minutes. The unbound sample and remaining salts were further removed by gently washing the mica surface with de-ionized water and again allowed to dry overnight. The AFM measurements were made on a WiTech Alpha 300 RA instrument (WITECH Instrument Co., Ltd., Seoul, Korea) in a non-contact mode. Cantilevers with resonance frequency of 75 kHz and force constant of 40 N/m were used.

12. Size-Exclusion Chromatography

To investigate the effect of polyphenols on the population heterogeneity of γ-Syn species during fibrillation and to understand the modulation of γ-Syn fibrillation pathway in the presence of polyphenols, SEC-HPLC was carried out. The soluble aggregates of γ-Syn formed in the presence and absence of the polyphenols were investigated in order to investigate the effects on the oligomerization properties of γ-Syn. Aliquot of γ-Syn in presence of EGCG, Quercetin and Silibinin (50 µM) was withdrawn at different time intervals of fibrillation and the larger aggregates or the insoluble material was removed by centrifugation for 30 min at 14,000×g. For disaggregation studies, the monomeric solution of γ-Syn (75 µM) was incubated with polyphenols (50 µM) added at three different time intervals 8h, 24h and 48h marking the three stages of fibrillation, i.e. late lag, log and saturation phase of fibrillation, respectively and the soluble aggregates were collected by centrifugation as mentioned above. The supernatant was further filtered through 0.22 µm filter and 20 µl of supernatant was eluted through BioSep SEC-S 2000 column (300 x 7.8 mm), from Phenomenex in 20 mM phosphate buffer containing 0.1 M NaCl, pH 7.4 using a Waters 2489 UV/Vis separations module attached with Waters 515 HPLC

pumps. The HPLC system was operated and the data were collected and analyzed by Empower software supplied with the HPLC system. The column was eluted at a flow rate of 0.5 ml/min at 25 ºC and the absorbance of the mobile phase was measured at 275 nm for γ-Syn. In order to investigate the binding affinity of polyphenols (EGCG and Quercetin) to the different species of γ-Syn, the absorbance was monitored at 270 nm and 378 nm respectively corresponding to absorbance of EGCG and quercetin respectively. The column was calibrated using the following standards obtained from Bio-Rad: Thyroglobulin (670 kDa), γ-globulin (158 kDa), ovalbumin (44 kDa), myoglobin (17 kDa) and vitamin B_{12} (1.3 kDa). The hydrodynamic properties of the species were calculated using the empirical formula as previously reported (Uversky et al., 2002). The monomer and oligomers formed during the fibrillation were quantified by calculating area under the peak using Origin software.

13. Circular Dichroism (CD) Spectroscopy

The effect of polyphenols and the polyols on the secondary structure of γ-Syn was studied by far-UV CD spectroscopy. Far-UV CD spectra were collected using a JASCO-815 CD spectrophotometer equipped with a peltier device. The spectra were collected from a wavelength of 195-260 nm at a step size of 0.1 nm, bandwidth of 1nm and scanning speed of 20nm/ min at 25 °C. Total of 3 accumulations were collected and averaged.

In the presence of increasing concentrations of EGCG (10, 30 and 50 μM), the far-UV CD spectra of γ-Syn (0.5mg/ml) under native conditions were carried out in 20 mM phosphate buffer (without salt), pH 7.4. For fibrillation conditions, γ-Syn (1mg/ml) was incubated with varying concentrations of EGCG (10, 30 and 50 μM) in 20 mM phosphate buffer containing 100 mM NaCl, pH-7.4 at 37 ºC, and 200 rpm in triplicates. For analysis, the incubation samples were dissolved in a 20 mM phosphate buffer with no salt, bringing the final concentration of γ-Syn to 0.3mg/ml and reducing NaCl concentration to 33.3 mM. The spectra of appropriate buffers were simultaneously subtracted. The measurements were carried out using a cuvette of 1mm path length. To monitor the far-UV CD spectra of the γ-Syn oligomers, the fibrillation samples withdrawn after 48h of fibrillation were centrifuged at 14,000×g for 30 min to remove the insoluble aggregates. The far-UV scans were measured using a cuvette of 0.1 mm path length to reduce interference by 100 mM NaCl

present in the fibrillation buffer and the data were normalized with reference to the initial concentration. The far-UV CD studies in the presence of Quercetin and Silibinin under native conditions was carried out using 0.3 mg/ml of γ-Syn in the presence of increasing concentrations of Quercetin (10, 30 and 50 μM) and Silibinin (30 and 50 μM) using a cuvette of 1 mm path length. For the analysis under fibrillation conditions, similar protocol was used, as mentioned above for EGCG. The buffer used for the analysis was supplemented with 0.1% DMSO for maintaining the solubility of the polyphenols.

The far-UV CD data of γ-Syn in the presence of increasing concentration of polyols, under native conditions dissolved in 20 mM phosphate buffer, pH 7.4, were collected using a 0.1mm path length cuvette with a wavelength range of 195-250 nm at a step size of 0.1 nm, bandwidth of 2nm, scanning speed 20 nm/min at 25 °C. Total of 3 accumulations were collected. To record the far-UV CD spectra under fibrillation conditions, γ-Syn (1mg/ml) was incubated with equimolar concentrations (2M of polyols in 20mM phosphate buffer containing 100 mM NaCl, pH 7.4 and the spectra were collected using a cuvette of 1mm path length with similar parameters as used for the native conditions. The bandwidth of 2nm was reduced to 1nm. For analysis, the incubation samples were withdrawn at regular time intervals during fibrillation (0h, 8h, 24h and 48h) and diluted in a similar way as mentioned for polyphenols. The spectra of appropriate buffers were simultaneously subtracted. All the data were normalized as mean residue ellipticity units expressed as degree cm^2 $dmol^{-1}$ using the following equation:

$$[\theta] = \frac{\text{CD (mdeg)}}{[\text{Peptide}] \times 10 \times \text{l} \times \text{n}} \qquad (2)$$

where, [θ] is mean residue ellipticity, CD (mdeg), is the negative ellipticity, [peptide] is the concentration of protein in M, l is path length of cuvette in cm and n is the number of amino acids in the protein.

14. ANS (8-Anilinonaphthalene-1-sulfonic acid) Binding Assay

ANS binding assay was carried out to investigate the extent of exposed surface hydrophobicity of γ-Syn in the presence and absence of polyphenols and polyols both under native and fibrillation conditions. ANS is an amphiphilic dye that

fluoresces strongly with a characteristic blue shift emission upon binding with the hydrophobic patches (Bolognesi et al., 2010). The incubation samples were withdrawn at different time intervals during fibrillation and ANS spectra was recorded from 400-600 nm with an excitation at 375 nm at 25 °C and slit widths of 5 nm were used for both excitation and emission. The samples withdrawn were diluted in fibrillation buffer making a final concentration of 0.3 mg/ml keeping final ratio of ANS to protein concentration equal to 5.

15. Steady-State Fluorescence

The binding of polyphenols to γ-Syn (22.5 μM) was studied by continuously titrating γ-Syn with an increasing concentration of polyphenols (2 μM to 30 μM) at different temperatures and the binding was ascertained by the quenching of tyrosine fluorescence upon titration with polyphenols. The association constant K_a was calculated using the Modified Stern-volmer quenching equation:

$$F_0 / F = 1 + K_{sv}[Q] \qquad (3)$$

$$\log [F_0\text{-}F / F_0] = n \log[Q] + \log K_a \qquad (4)$$

where, K_{sv} is Stern-volmer constant for static quenching, F_o and F is fluorescence intensity in the absence and presence of quencher respectively, K_a is the association constant, n is number of binding sites and Q denotes the quencher concentration (Lackowicz, 1983).

16. Time-Resolved Fluorescence

Time-resolved fluorescence intensity was measured by the time-correlated single photon counting (TCSPC) method using a model F900 fluorescence lifetime spectrometer (Edinburgh Instruments, UK). The lifetime of the single tyrosine present in γ-Syn was recorded with 75 μM γ-Syn in presence of increasing concentrations of EGCG (5-25 μM) , excited at 284 nm wavelength using a Nano LED pulsed laser. The emission was recorded at emission maxima (λ_{max}) of 342 nm as determined from the steady state fluorescence spectra. The instrument response factor (IRF) was typically 1.5 ns (fwhm) as recorded by scattering a dilute

suspension of colloidal silica (Ludox). To determine the decay constants, a peak count of 3000 was collected for total decay duration of 50ns. The data were recorded into 4096 channels at a timing resolution of 0.012 ns /channel.

Data Analysis and Curve Fitting: The resulting data were analyzed by using the FAST software provided with the instrument. Non-linear least squares method was employed which assumes the fluorescence decays to be the sum of discrete exponential components expressed by the equation as reported (Neyroz et al., 2006; Nath et al., 2010; Sahay et al., 2014).

$$I(t) = \sum_i^n \alpha_i \exp(-t/\tau_i) \qquad (5)$$

Where *n* is number of discrete exponentials, *i* is the index, and α_i and τ_i are the amplitudes and lifetimes respectively. The average of fluorescence lifetime was calculated as:

$$\tau_m = \sum \alpha_i \tau_i \qquad (6)$$

The goodness of the fit was decided by the reduced χ^2 and from the randomness of the weighted residuals distributions.

17. Isothermal Titration Calorimetry

The ITC experiments for defining the thermodynamic parameters of polyphenol binding to γ-Syn were carried out on VP-ITC model from Microcal, LLC, USA at 25 ºC, pH-7.4.

The γ-Syn samples were centrifuged at 14,000 ×g for 20 min to remove any high order suspended particles and the supernatant was filtered through 0.22 μm filter. All the samples before loading into the calorimeter cell were degassed for 10 min using the Thermo Vac degassing unit supplied by Microcal to ensure that no bubbles were formed.

Parameters for EGCG:

Sample cell containing γ-Syn (0.22 mM) was continuously titrated with 9 μL of EGCG (6.6 mM) with a uniform interval of 800s with a rotating syringe at 329 rpm. Corresponding control experiments for determining the heat of dilution of EGCG was performed by titrating EGCG into the buffer under identical conditions. The

heat associated with the EGCG-buffer reaction was subtracted from EGCG- γ-Syn reaction to obtain the actual heat of interaction.

Parameters for quercetin:

The binding interaction between quercetin and γ-Syn was monitored at 37°C, by loading the sample cell with γ-Syn (10.4μM) and using a 10-fold higher concentration of quercetin (104 μM) dissolved in 1% DMSO into the syringe. γ-Syn was continuously titrated with 4μl of quercetin at a regular interval of 420s and a uniform stirring at 329 rpm. To avoid heat of dilution effects due to differences in the concentration of DMSO, quercetin and γ-Syn were diluted in the same buffer (10mM phosphate buffer, pH7.4) containing 1% DMSO.

Parameters for silibinin:

To investigate the binding interactions between γ-Syn and silibinin, γ-Syn was titrated with a 20-fold higher concentration (4.25mM) of silibinin, dissolved in 10mM phosphate buffer, pH7.4, containing 1% DMSO. γ-Syn was titrated with a first injection of 2μl and successive injections of 10μl at a regular spacing of 540s to attain equilibrium. The mixing was maintained by constant stirring at 329 rpm and the binding interaction was carried out at 25°C.

All data were analyzed using Origin7 software provided by Microcal.

18. MTT Assay

MTT assay is an *in vitro* assay routinely used for measuring the metabolic activity of cells. MTT contains a yellow coloured tetrazolium component that in the presence of mitochondrial dehydrogenases of the live cells gets reduced to a violet colour formazan product which is solubilised in DMSO and the absorbance is read at 570 nm. The change in the colour is calculated as % MTT reduction which provides an indication of the metabolic conditions of the cells (Amijee et al., 2012). The cytotoxic effect of the polyphenol modulated γ-Syn species were investigated on breast cancer (MCF-7) and neuroblastoma (SH-SY5Y) cells by MTT assay. Both the cells were cultured in DMEM except the media was supplemented with 10% L-glutamine for growing SH-SY5Y cells.

MTT assay with EGCG:

γ-Syn fibrils were formed by incubating γ-Syn (75 μM) in the absence and presence of EGCG (50 μM) in fibrillation buffer at 37 ºC with shaking at 200 rpm for 24h.

The cytotoxicity of the disaggregated fibrils and the resultant oligomeric species formed in the presence of EGCG were also investigated. The fibrillation samples for the disaggregation studies, were prepared by incubating γ-Syn (75 μM) at 37 ºC with shaking at 200 rpm and EGCG (50 μM) was added at 8, 24 and 48h of fibrillation. At the end of the fibrillation reaction (72h), the samples were divided into two groups where one group was centrifuged at 14,000 ×g for 30 min to remove the insoluble aggregates, leaving only the soluble disaggregated oligomers and another was used as such without centrifugation containing the whole of soluble and insoluble disaggregated species. The buffer without protein and with or without EGCG was maintained as controls. The incubation samples were withdrawn at 24h of incubation for assessing the toxicity of EGCG generated oligomers and at the end of fibrillation for assessing toxicity of disaggregated oligomers as well as fibrils formed at different stages upon EGG addition.

MTT assay with quercetin and silibinin:

The cytotoxic effects of quercetin and silibinin treated γ-Syn species on MCF-7 and SH-SY5Y cells were also investigated using MTT assay. For both quercetin and silibinin, γ-Syn was separately incubated with the increasing concentrations (10, 30 and 50 μM) of both the polyphenols at 37°C, 200 rpm and the fibrillation samples were withdrawn at regular intervals of fibrillation (0, 24 and 48h) to assess the toxicity of the various γ-Syn species formed in the presence of respective polyphenols. Additionally, the cytotoxic effects of the quercetin – mediated disaggregated γ-Syn species were investigated on neuroblastoma (SH-SY5Y) cells. The fibrillation samples were prepared by incubating γ-Syn (75μM) 37°C, 200 rpm and quercetin was added at different stages (8, 24 and 48h) of fibrillation as in the case of EGCG, except the fibrillation samples were not centrifuged before the treatment and the cytotoxic effects of the whole species were investigated.

MTT protocol:

For all the assays, a 7-fold dilution of the incubation samples were applied to human breast cancer (MCF-7) and neuroblastoma (SH-SY5Y) cells respectively. Cells were plated at a density of 20,000 cells/well on 96-well plates in 200μL of media. The cells were grown for 24 h at 37ºC to allow the cells to reach the exponential phase. After 24 h the protein aggregates were added and the cells were kept for incubation

for 2 days at 37 ºC. Cytotoxicity was measured by using 3-[4, 5-dimethylthiazol-2-yl]-2, 5-diphenyltetra-zolium bromide (MTT) toxicity assay. 20 µL of MTT (5 mg/ml) was added to each well containing 200 µL of media. MTT addition was done under dark and the plates after MTT addition were incubated for 4h in the incubator. After completion of 4 h, the MTT crystals formed were dissolved using 200 µL of 100% DMSO and the readings were immediately recorded at 570 nm and background was corrected for 650 nm. The assays were performed in three independent reactions. The statistical analysis for assessing the toxicity of EGCG-generated γ-Syn oligomeric species, was done using unpaired t-test and for assessing the toxicity of disaggregated oligomers and fibrils formed in the presence of EGCG, quercetin and silibinin generated γ-Syn species, and quercetin mediated disaggregated γ-Syn species, one-way ANOVA was employed.

19. LDH (Lactate Dehydrogenase) Assay

The LDH cytotoxicity assay measures the non-viable or dead cells by monitoring the extent of release of cytoplasmic LDH into the culture medium upon cell death due to damage of the plasma membrane. An increase in absorbance of a red formazan product at 490 nm directly indicates an increased LDH activity which in turn corresponds to the number of lysed cells. For LDH assay the fibrils were formed by incubating γ-Syn (150 µM) in presence and absence of EGCG (100 µM), keeping the ratio of γ-Syn: EGCG (1:0.6) as used in MTT-assay and the incubation samples for the assay were then similarly prepared as for the MTT assay. MCF-7 and SH-SY5Y cells were plated out at a density of 50,000 cells per well in a 200 µl of media in a 96- well plate. The cytotoxicity of γ-Syn species formed in the presence and absence of EGCG was quantified using Pierce™ LDH Cytotoxicity Assay Kit (Thermo Fischer Scientific) and the % cytotoxicity was calculated using the manufacturer's protocol.

Chapter 3

Effect of Polyphenols on the Structure and Aggregation of γ-Synuclein

Chapter 3.1

Effect of Epigallocatechin-3-gallate (EGCG) on the Structure and Aggregation of γ-Synuclein

1. Background

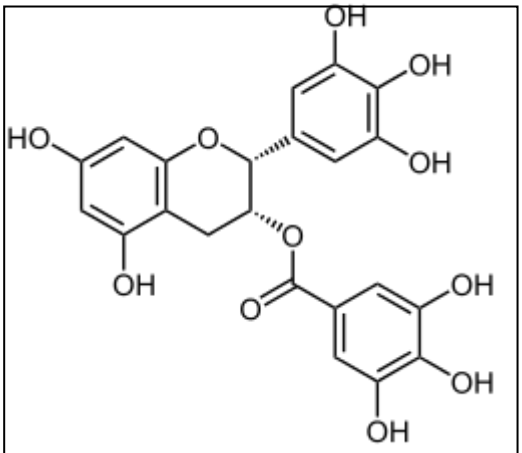

Chemical structure of EGCG

Epigallocatechin-3-gallate (EGCG), the primary catechin present in green tea belonging to the family of flavonones has a well established neuroprotective (Pervin et al., 2018) as well as anticancer properties (Azam et al., 2004). EGCG has been reported to inhibit the fibrillation of a wide range of amyloidogenic proteins like α-Syn, Aβ peptide, Huntingtin (Ehrnhoefer et al., 2006; Ehrnhoefer et al., 2008), wild type apolipoprotein A-I (apo A-I) (Townsend et al., 2018), etc. The most prevalent characteristic of EGCG inhibited fibrillation pathway is the formation of non-toxic, stable oligomeric species or benign protein aggregates which do not further participate in the polymerization process thus rendering them off-pathway (Bieschke et al., 2010; Palhano et al., 2013). Cross-linking of amyloid fibrils by oxidized EGCG (Palhano et al., 2013), covalent modification with the sulfhydryl groups on the protein (Ishii et al., 2008), interference with the aromatic core of amyloidogenic protein like Aβ resulting in the formation of structured non-toxic aggregates (del Amo et al., 2012), immobilization of the C-terminal region of α-Syn leading to the reduced degree of oligomer binding to the membrane (Lorenzen et al., 2014) and formation of a molecular zipper by EGCG to facilitate the assembly of EGCG-containing oligomers (Ehrnhoefer et al., 2008) are the proposed mechanisms of EGCG mediated inhibition and altered oligomer as well as amyloid toxicity. By using techniques like ion-mobility mass spectrometry, it has also been revealed that EGCG alters the oligomerization and fibrillation assembly of hIAPP protein by binding to the specific conformers among the dynamic ensembles of the protein (Young et al., 2013). The antiamyloidogenic property of EGCG also imparts it an antimicrobial activity which is demonstrated by the EGCG mediated remodelling of the Fap fibrils, required for the quorum sensing in pathogenic organisms like *P. aeruginosa* (Stenvang et al., 2016).

In the light of the above background, in this study the effect of EGCG on the structure and aggregation of γ-Syn has been investigated. The study demonstrates

that EGCG retards nucleus formation leading to deceleration of fibril polymerization and mediates its inhibitory effect by modulating the on-going fibrillation pathway to form two separate populations of SDS- resistant higher- ordered γ-Syn oligomers (~ 4 and 10 mer), that are conformationally restrained and gain an α-helical propensity during fibrillation. It is demonstrated that the EGCG generated oligomers act as partial templates for γ-Syn polymerization and the kinetic characteristics suggest that they are on-pathway but are kinetically retarded species (increased lag time) that fail to build-up into mature fibrils during polymerization. Investigations on the mode of binding interaction between EGCG and γ-Syn, reveal that the effect of EGCG binding is mediated by weak, non-covalent interactions (K_d ~ mM), that points to the importance of weak binding interactions in modulating the γ-Syn fibrillation pathway. The study also establishes that EGCG attenuates the protofibrillar stages of the pathway and disaggregates protofibrils as well as the mature fibrils into similar kind of SDS-resistant oligomers. Interestingly, the EGCG-generated oligomers are observed to be differentially toxic to the breast cancer (MCF-7) and neuroblastoma (SH-SY5Y) cells, where they completely rescue the MCF-7 cells from γ-Syn toxicity but are more toxic than the untreated γ-Syn oligomers for the SH-SY5Y cells. This indicates the critical role of γ-Syn and complexities it may impart in the treatment of amyloidogenic diseases. The investigation on the cytotoxic effects of the disaggregated γ-Syn oligomers reveal a high toxicity of MCF-7 cells relative to the disaggregated γ-Syn fibrils that highlights an early gain of toxic characteristics by species of γ-Syn which is governed by the morphology of the species formed. The observations made in this study suggest that the modulators that could inhibit the early stages of γ-Syn fibrillation without leading to disaggregation may prove to be potential candidates for preventing synucleopathies. Additionally, the study observes differences in the mechanism of EGCG-mediated modulation of γ-Syn fibrillation from that previously reported for α-Syn, which indicates a critical role of γ-Syn in underlying pathogenesis and suggest that an in-depth investigation on the effects of such modulators on γ-Syn fibrillation will help to better understand the events leading to the onset of synucleopathies and help in the development of effective intervention strategies.

2. Results

2.1 Effect of EGCG on the fibrillation kinetics of γ-Syn:

2.1.1 Thioflavin T assay

The effect of EGCG on the kinetics of γ-Syn fibrillation was analyzed by Thioflavin T binding assay. ThT is a benzothiazole dye that fluoresces strongly upon binding with the cross β-sheet structures which are a signature for amyloid fibrils (Ban et al., 2003). The ThT fluorescence was found to decrease by almost 8-fold in magnitude upon binding with γ-Syn fibrils formed in the presence of EGCG and an apparent fibrillation rate (k_{app}) of untreated γ-Syn was found to be 0.36 ± 0.02 h^{-1}. Incubation of γ-Syn in the presence of increasing concentration of EGCG (5-50 μM) resulted in a concentration-dependent decrease in ThT fluorescence (Figure 1A and 1B) with negligible rise in ThT fluorescence recorded in the presence of EGCG at higher concentrations (>30 μM). The decrease in the apparent fibrillation rate (k_{app}) of γ-Syn with respect to EGCG is shown in Figure 1C.

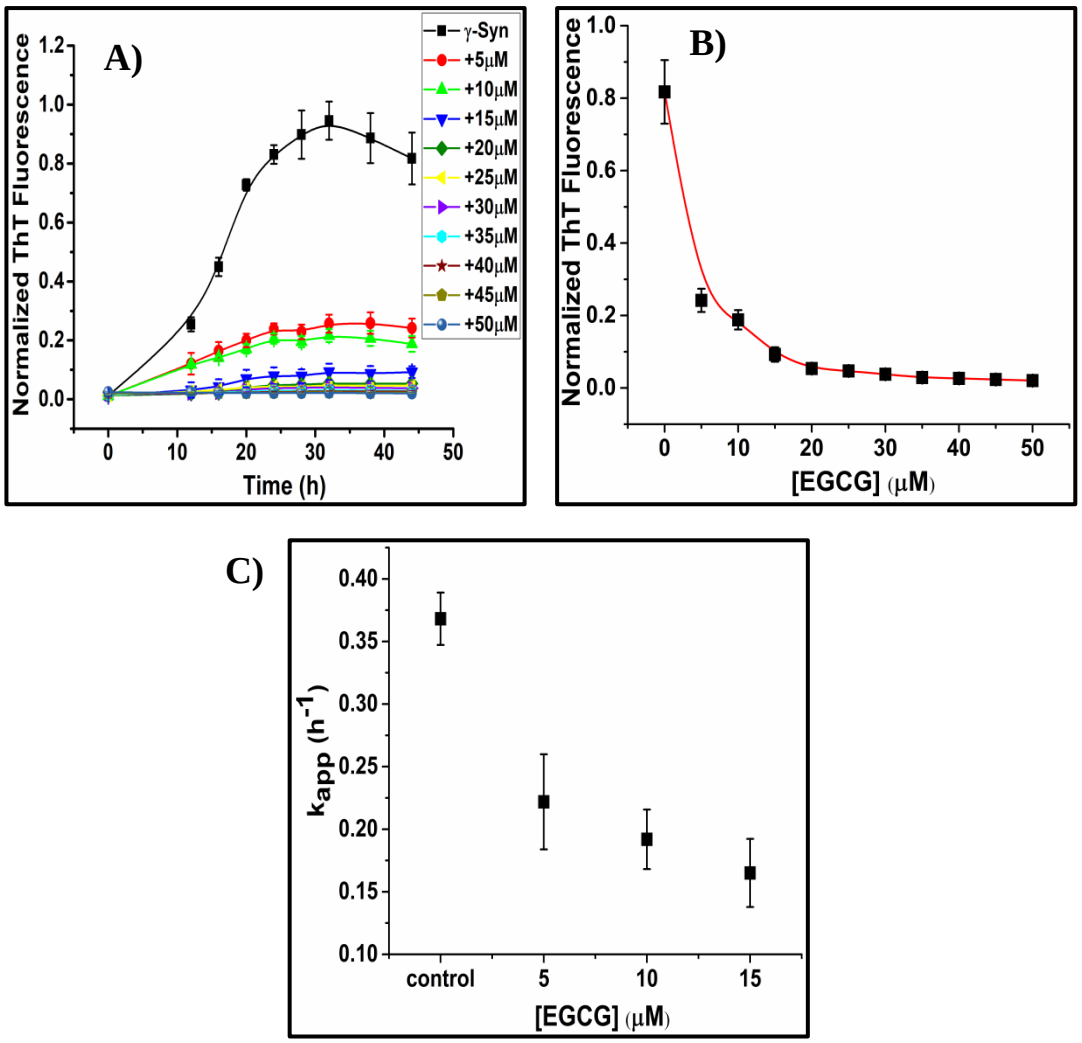

Figure 1. Fibrillation kinetics of γ-Syn in the presence of increasing concentration of EGCG investigated by Thioflavin T assay. Monomeric γ-Syn was incubated in the presence of increasing concentration of EGCG (5- 50μM) under fibrillating conditions and the ThT fluorescence was recorded at regular interval of time during fibrillation. The concentration - dependent decrease in the ThT fluorescence in the presence of EGCG, (A) with respect to time and (B) with respect to EGCG concentration shows inhibition of fibrillation. (C) The decrease in the apparent rate of fibrillation (k_{app}) with respect to increasing concentration of EGCG shows retardation of fibrillation. The error bars represent the ±SD (n=3).

2.1.2 Light scattering by γ-Syn species formed during fibrillation in the presence of EGCG.

The effect of EGCG on the aggregation propensity of γ-Syn was also validated by Rayleigh scattering since ThT does not bind to the amorphous aggregates and is also reported to be interfered by the presence of exogenous compounds (Hudson et al.,

2009). γ-Syn was incubated under fibrillating conditions in the presence of an increasing concentration of EGCG and the scattering intensity was recorded at regular intervals during fibrillation. During the initial stages of γ-Syn fibrillation an early rise in the scattering intensity in the presence of 50μM EGCG was observed, indicating the formation of higher ordered oligomers by EGCG. The overall scattering was however reduced in the presence of EGCG, suggesting inhibition of γ-Syn aggregation by EGCG (Figure 2A). To further confirm the formation of higher order oligomers by EGCG, the scattering intensity of the soluble γ-Syn species formed in the presence of EGCG, obtained after centrifugation was monitored. A concentration dependent increase in the scattering intensity by the soluble γ-Syn species formed in the presence of EGCG was observed, further suggesting the formation of higher order oligomers by EGCG (Figure 2B).

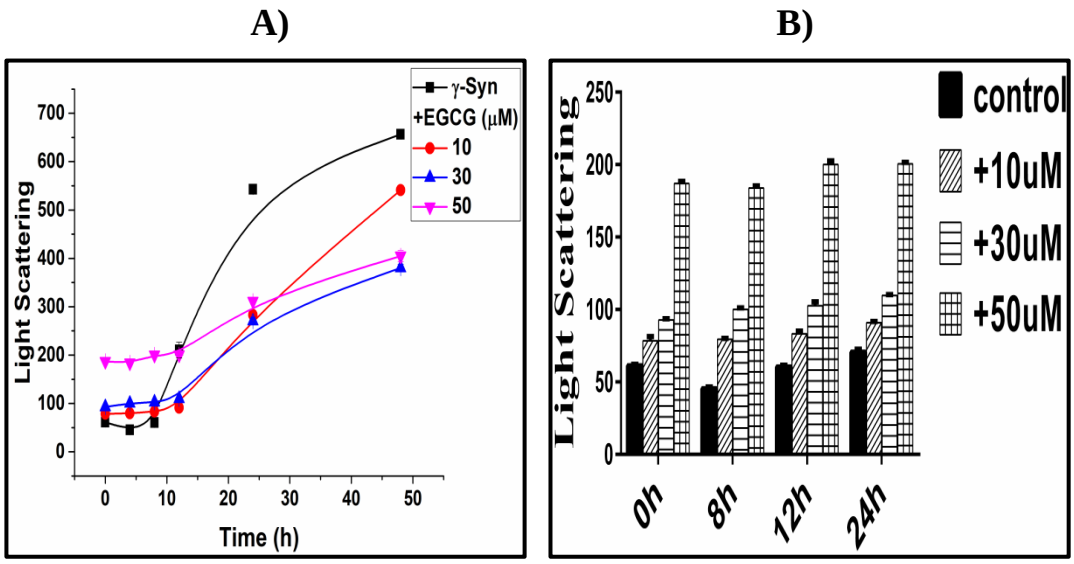

Figure 2. Light scattering by γ-Syn species formed in the presence of an increasing concentration of EGCG. (A) The concentration-dependent decrease in the scattering intensity shows inhibition of aggregation by EGCG. Early increase in the scattering intensity in the presence of 50 μM EGCG indicates the formation of higher –order oligomers. (B) Light scattering by soluble γ-Syn species formed in the presence of EGCG obtained by centrifugation confirms formation of higher-order oligomers by EGCG. γ-Syn was incubated with increasing concentration of quercetin (10, 30 and 50μM) and incubated at 37 °C, 200 rpm. The scattering intensity was recorded using a quartz cuvette of 1 cm path length at $\lambda_{ex}=\lambda_{em}$ at 350 nm.

2.1.3 Transmission Electron Microscopy of γ-Syn fibrils formed in the presence of EGCG

The effect of EGCG on the morphology of γ-Syn fibrils was studied by negatively stained transmission electron microscopy. Incubation of monomeric γ-Syn with EGCG (5-50 μM) during fibrillation showed a concentration dependent disappearance of the γ-Syn fibrils (Figure 3A) corresponding well with the decrease in ThT fluorescence (Figure 1A). At higher concentrations of EGCG (50 μM), amorphous protein aggregates and some spherical oligomers were also seen which were also confirmed by Rayleigh scattering (Figure 3B). Also, the TEM images of the successive stages of fibril formation showed a time-dependent build-up of γ-Syn monomers into mature fibrils, whereas in presence of EGCG, shorter fragments of γ-Syn were observed (Figure 3B).

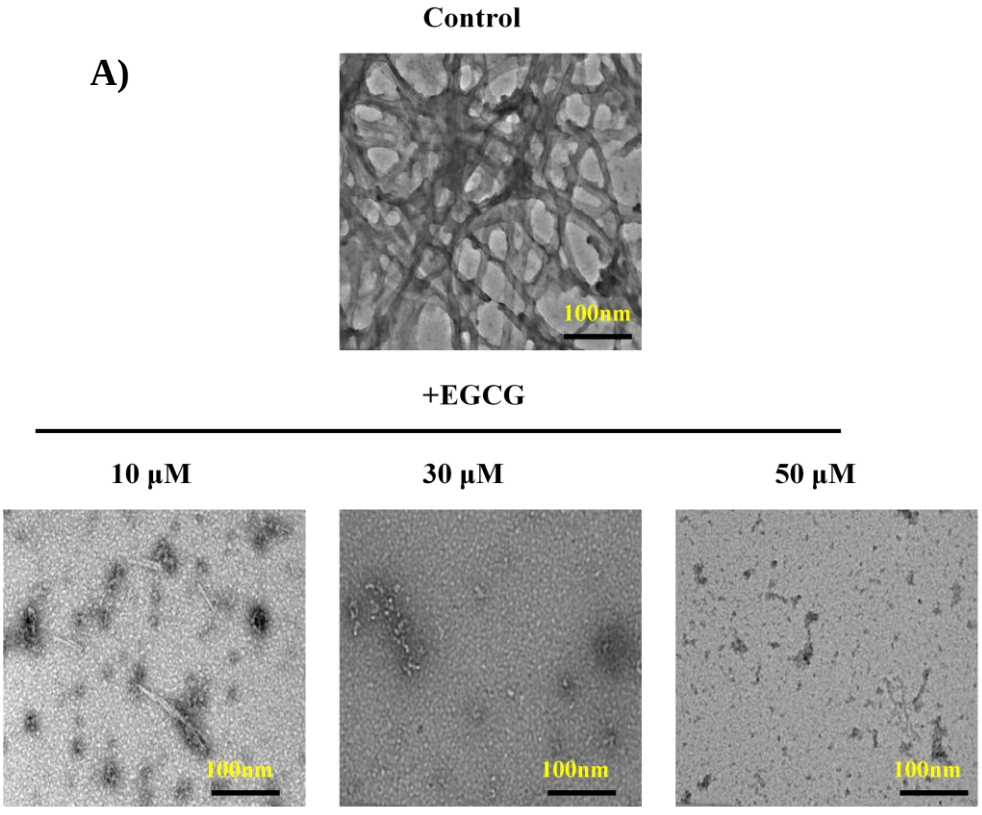

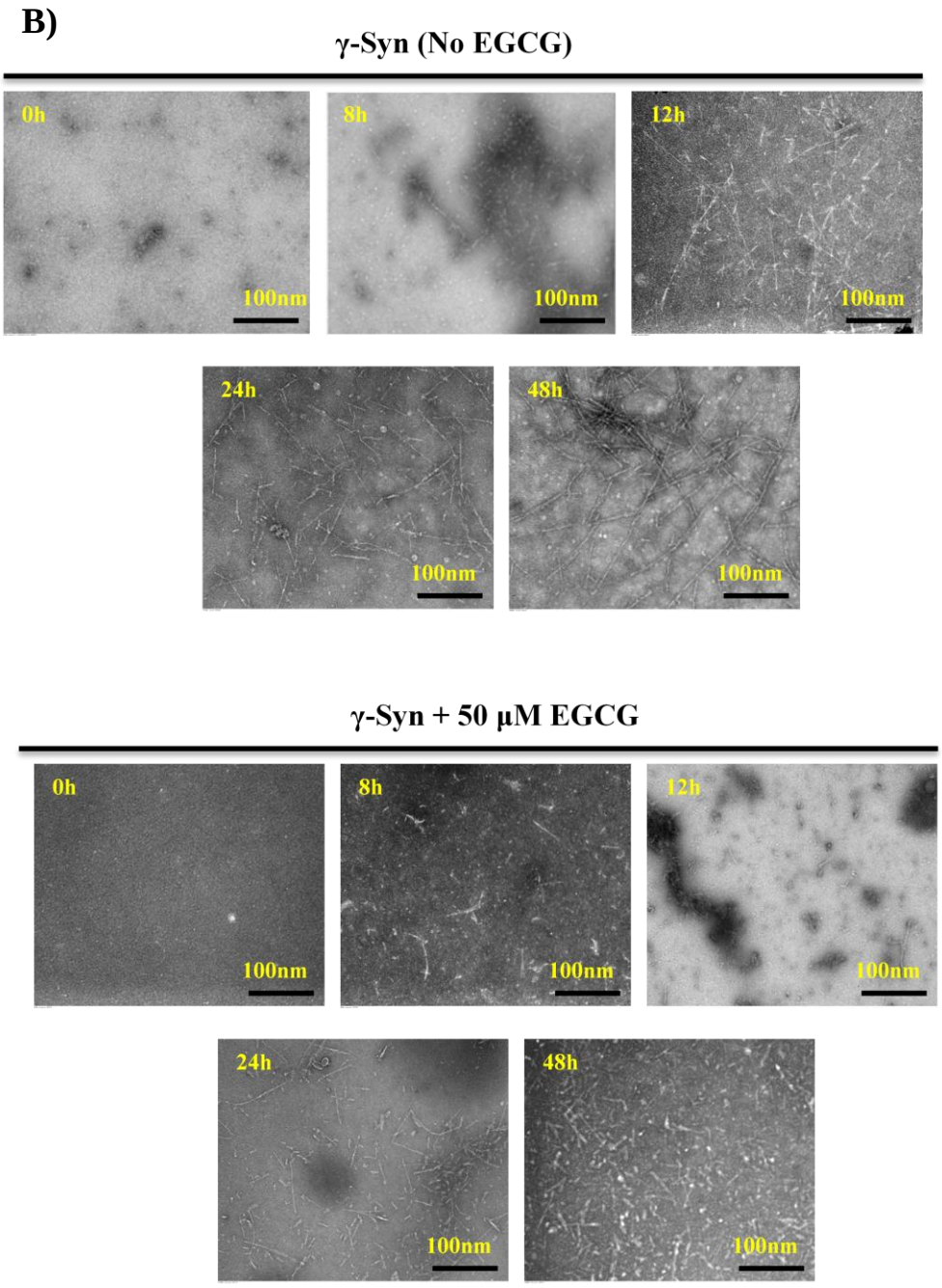

Figure 3. Morphology of γ-Syn fibrils formed in the presence of EGCG visualized by transmission electron microscope. (A) Transmission electron microscopy images of fibrils formed at the end of fibrillation in presence of increasing concentration of EGCG (Scale bars, 100nm). (B) Time- dependent polymerization of monomeric γ-Syn in absence *(upper panels)* and presence *(lower panels)* of EGCG (50µM) at 0h, 8h, 12h, 24h and 48h of fibrillation shows the formation of mature γ-Syn fibrils in absence of EGCG. In presence of EGCG, short and partially polymerized fibrils were seen (Scale bars, 100nm).

2.1.4 Atomic Force Microscopy of γ-Syn species formed in the presence of EGCG

AFM measurements of γ-Syn fibrils formed both in presence and absence of EGCG (50 μM), demonstrated a significant suppression of fibril formation in presence of EGCG. γ-Syn in the absence of EGCG formed mature intertwined fibrils with their average height of ~11 nm. However, in the presence of EGCG no mature fibrils were observed and highly populated large spherical oligomers with an average height of 26.2 nm ± 4.05 nm and sparsely populated smaller oligomers with an average height of 12.28 nm ± 4.23 nm were observed. These oligomers were found to self-associate with each other giving rise to a beaded appearance as shown in Figure 4.

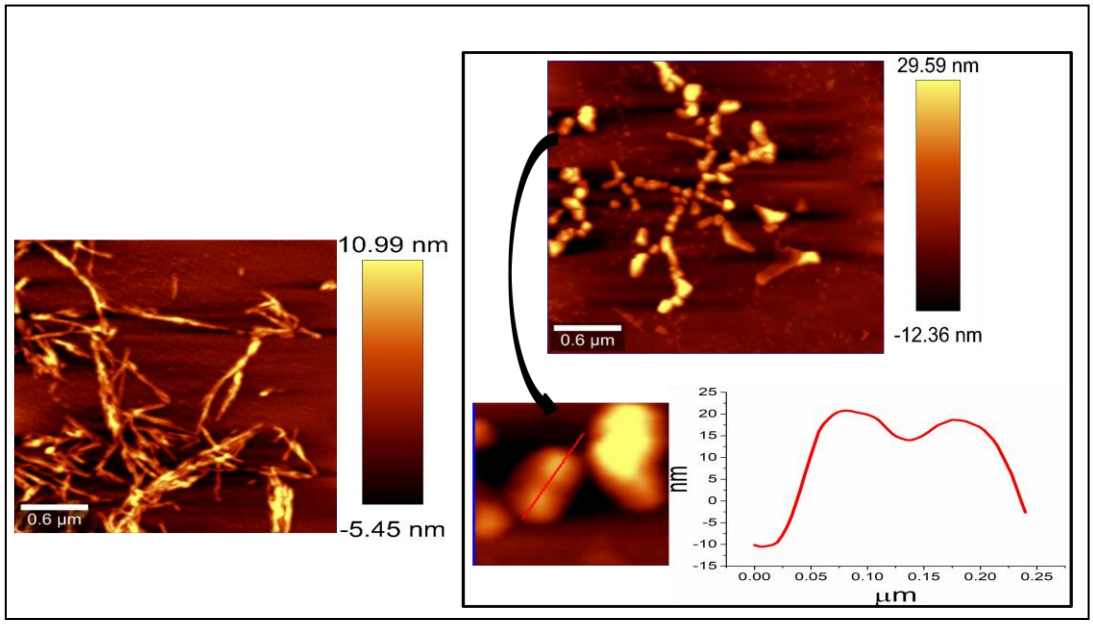

Figure 4. AFM analysis of the γ-Syn species formed in the absence and presence of EGCG (50μM). Atomic force microscopy images shows disappearance of mature γ-Syn fibrils in the presence of EGCG (50 μM). Formation of self-associated large spherical oligomers, are also depicted in the cross section of the oligomers *(right panel; below)*.

2.2 Effect of EGCG on different stages of γ-Syn fibrillation:

2.2.1 Thioflavin T assay

The effect of EGCG on different stages of γ-Syn fibrillation was further probed by adding EGCG (50 μM) at different time intervals (8h, 24h and 48h) which respectively correspond to lag, log and saturation stage of γ-Syn fibrillation under conditions used. The ThT fluorescence was found to decrease substantially at all

time-points when EGCG was added (Figure 5A), indicating attenuation of fibrillation both at nucleation and exponential stages in the presence of EGCG. The decrease in ThT fluorescence upon addition of EGCG on preformed fibrils further indicated disaggregation of γ-Syn fibrils by EGCG (Figure 5B).

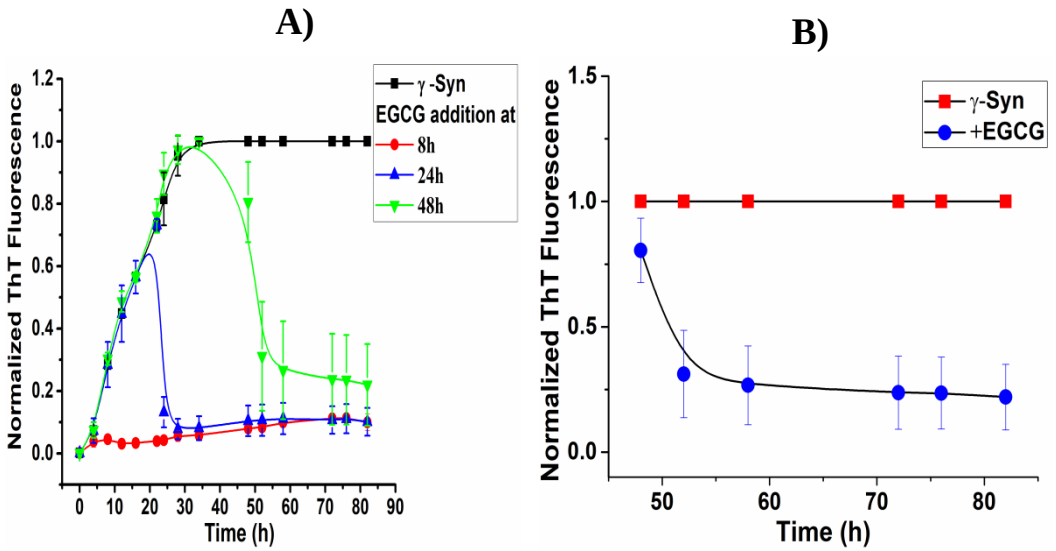

Figure 5. Fibrillation kinetics of γ-Syn upon addition of EGCG at different stages of fibrillation studied by ThT assay. A) Thioflavin T assay showing decrease in ThT fluorescence and inhibition of γ-Syn fibrillation at all three stages upon addition of EGCG at 8h, 24h and 48h. B) EGCG mediated disaggregation of preformed γ-Syn fibrils depicted by a continuous decrease in the ThT fluorescence upon addition of EGCG. The error bars represent ±S.D. (n=3).

2.2.2 TEM images of γ-Syn fibrils formed upon addition of EGCG at different stages of γ-Syn fibrillation

The TEM images of the fibrils, formed upon addition of EGCG at lag, log and saturation phases (8h, 24h and 48h respectively), reveal the presence of shorter and disintegrated fragments indicating the disaggregation of protofibrils and pre-formed γ-Syn fibrils (Figure 6).

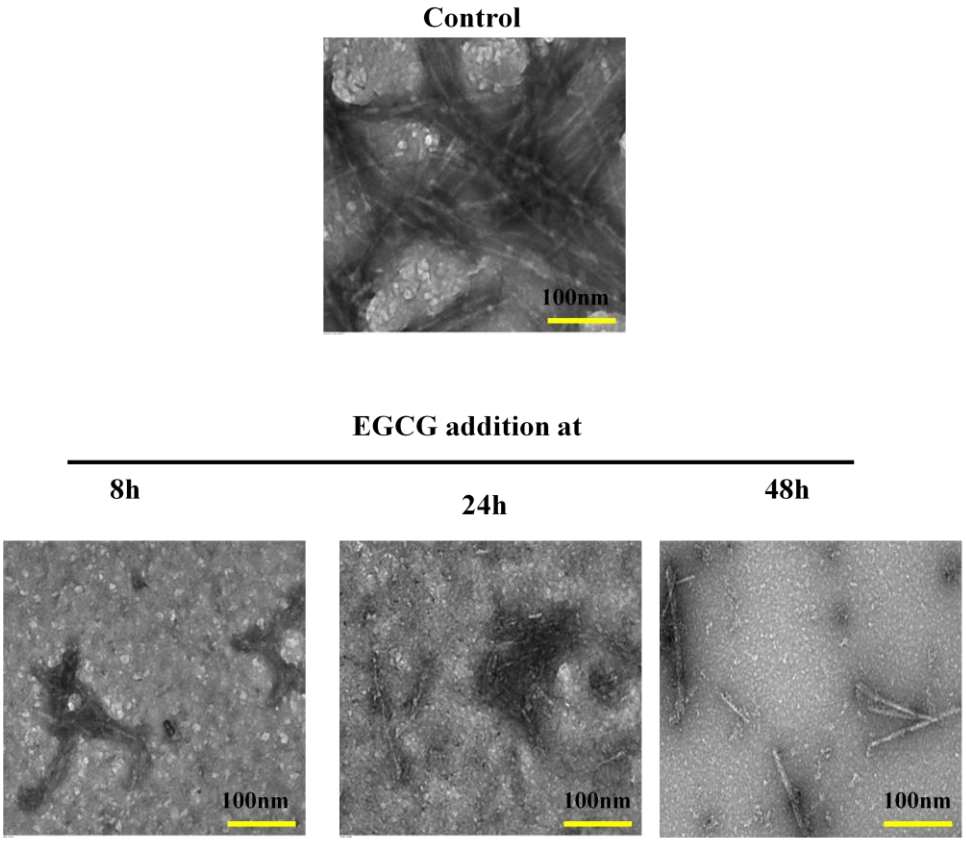

Figure 6. TEM images of γ-Syn species formed upon addition of EGCG (50μM) at different stages of fibrillation. TEM images of γ-Syn fibrils formed at different stages of EGCG mediated inhibition. *(Upper panel)*: Control, *(lower panel)* EGCG added at 8h, 24h and 48h respectively, showing formation of short and disintegrated fibrils indicating fibril disaggregation (Scale bars, 100 nm).

2.2.3 Atomic Force Microscopy (AFM) of γ-Syn fibrils formed in presence of EGCG

The morphology of the γ-Syn fibrils formed upon addition of EGCG at different stages of fibrillation was also analyzed by AFM studies. Addition of EGCG at initial late lag and log phase of fibrillation resulted in the formation of protofibrillar and oligomeric species at 8 and 24h respectively. The average heights of both the oligomeric and protofibrillar species were ~9.5nm. At 48h of EGCG addition, short disaggregated fibrils along with formation of spherical oligomers were observed with an average height of ~12 nm.

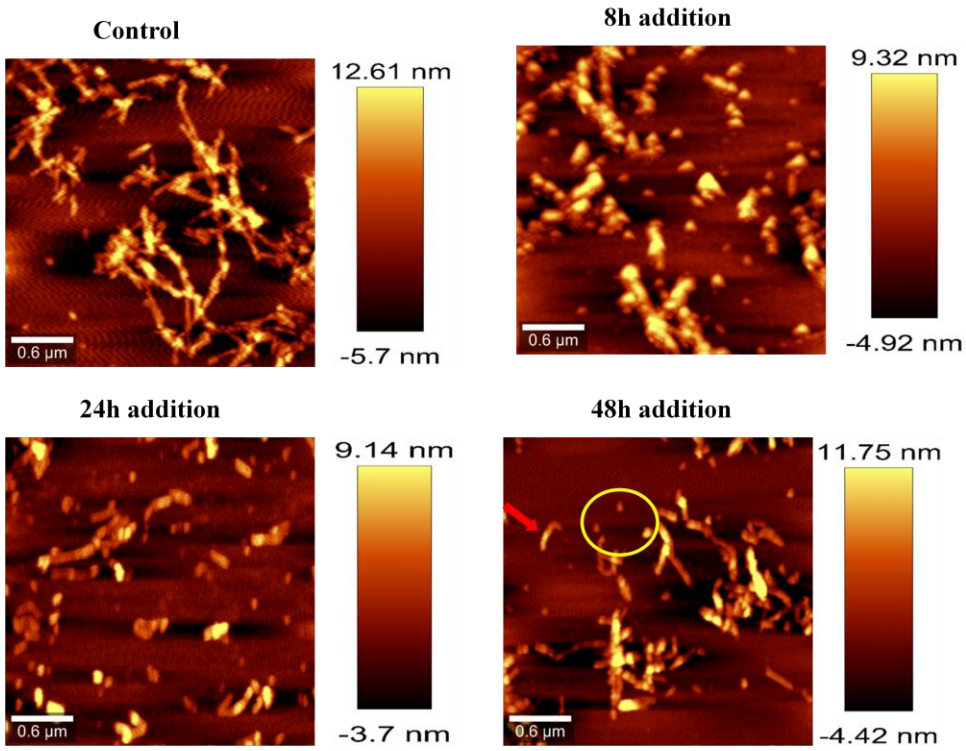

Figure 7. AFM images of γ-Syn fibrils formed upon addition of EGCG at different stages of fibrillation. AFM images showing disaggregation of γ-Syn fibrils upon addition of EGCG at different stages of fibrillation *(Left to Right)* : Control, EGCG added at 8h, 24h and 48h respectively. Addition of EGCG at 48 h shows broken fibrils (r*ed arrow)* and disaggregated spherical oligomers *(yellow encircled).*

2.3 Modulation of γ-Syn fibrillation pathway in the absence and presence of EGCG:

The EGCG mediated inhibition and modulation of γ-Syn fibrillation pathway was further investigated by studying the effect of EGCG on the population of various γ-Syn species formed during aggregation by size-exclusion chromatography and investigating the nature of the species formed by SDS- and Native-PAGE analysis.

2.3.1 Size-exclusion chromatography of γ-Syn fibrils formed in the absence and presence of EGCG

2.3.1.1 Absorbance monitored at 275nm: The γ-Syn species formed both in the absence and presence of EGCG (50 µM) during fibrillation were withdrawn at regular time intervals (0, 24 and 48h) and the soluble fractions obtained after centrifugation were subjected to SEC at an absorbance of 275 nm (Figure 8B).

Untreated γ-Syn solution in the absence of fibrillation eluted with a major monomeric peak at ~15.6 min and a small oligomeric peak at ~10.5 min, corresponding to an apparent molecular weight of ~44 kDa and ~670 kDa (> 10 mer), respectively as calculated from the standard calibration curve (Figure 8A). The SEC profiles of γ-Syn during aggregation showed an increase in the oligomeric peak area during the exponential phase (24h) of fibrillation, whereas during the end of fibrillation (48h) the soluble protein was significantly reduced eluting as monomers with only a negligible trace of oligomers present (Figure 8B). There were appearances of low absorbance multiple peaks eluting immediately after the major monomeric peak (~10.5 min) which disappeared with an increasing time of fibrillation, suggesting the presence of small fractions of various conformations which are getting retarded for a longer period of time in the column. The possibility that these peaks were a resultant of different γ-Syn conformations was further validated by estimating the hydrodynamic radii of γ-Syn using the empirical equations established for calculating the hydrodynamic properties of a protein from the apparent molecular weights obtained from SEC (Uversky et al., 2002). The Stoke's radius (R_s) of the monomeric γ-Syn as calculated using the apparent molecular mass (~44 kDa) was found to be ~28.7Å, which corresponds nearly with the previously reported value for monomeric γ-Syn (Uversky et al., 2002).

Upon addition of EGCG (50 μM), at 0h, an immediate rise in the oligomer peak eluting at ~10.3 min was observed. During the exponential phase of fibrillation (24h), the EGCG treated γ-Syn eluted with the appearance of another significant peak at ~13.4 min corresponding to an apparent molecular weight of ~158 kDa, indicating the formation of second type of oligomer (~ 4mer) in the presence of EGCG which otherwise was absent in the SEC profiles of untreated γ-Syn species. These results indicate EGCG mediated formation of γ-Syn oligomers during fibrillation.

2.3.1.2 Absorbance monitored at 270nm: The binding of EGCG to different species of γ-Syn was further investigated by monitoring absorbance at 270 nm, where EGCG absorbs (Figure 8C). Although, the contribution by the tyrosine present in γ-Syn in this region cannot be ruled out, the area under the curve was calculated to nullify the effect of tyrosine on the absorbance measured. The quantitation of the area under the respective peaks at all time intervals (0, 24 and

48h), showed an increase in the oligomeric peak area as compared to the area covered by the monomeric peak, and thus indicated an increased affinity of EGCG towards oligomers of γ-Syn.

2.3.1.3 SEC of γ-Syn species formed upon addition of EGCG at different stages of fibrillation: In order to investigate the disaggregated products of the protofibrillar and fibrillar species of γ-Syn, the SEC profiles of γ-Syn formed upon addition of EGCG (50 μM) at the lag (8h), log (24h) and exponential phase (48h) of the pathway were subjected to the column and elutions were monitored at 275 nm (Figure 8D). The incubation samples with EGCG added at different time intervals were withdrawn at the end of fibrillation and the samples were similarly centrifuged to analyze the soluble aggregates of the pathway. The SEC profiles clearly demonstrated the formation of γ-Syn oligomers at all the three stages of EGCG addition. The increased oligomeric peak area (Figure 8E) even at 48h of EGCG addition further validated the EGCG - mediated disaggregation of γ-Syn fibrils into higher-ordered oligomers (~158 kDa and 670 kDa.

A)

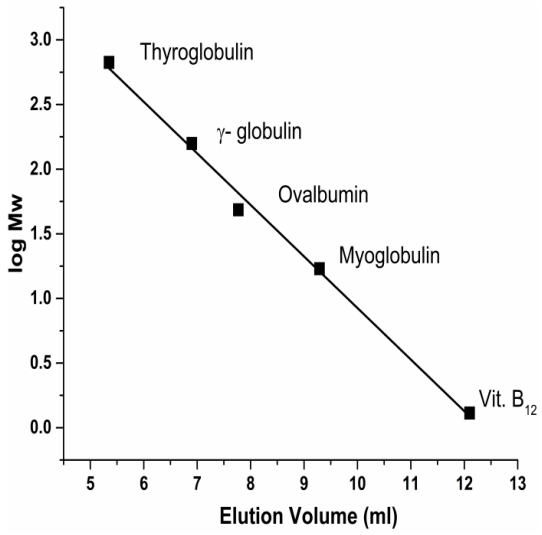

B)

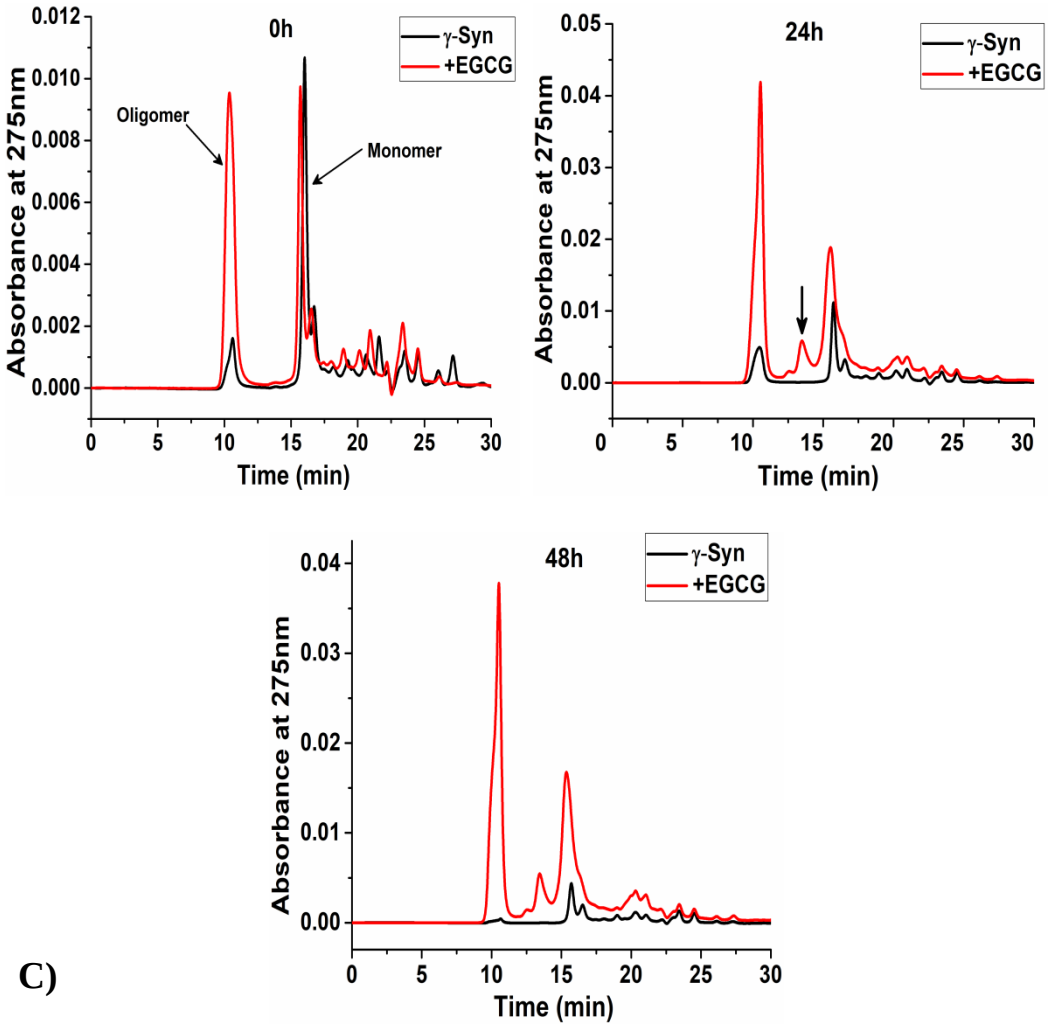
0h
γ-Syn
+EGCG
Oligomer
Monomer
Absorbance at 275nm
Time (min)
24h
γ-Syn
+EGCG
Absorbance at 275nm
Time (min)
48h
γ-Syn
+EGCG
Absorbance at 275nm
Time (min)

C)

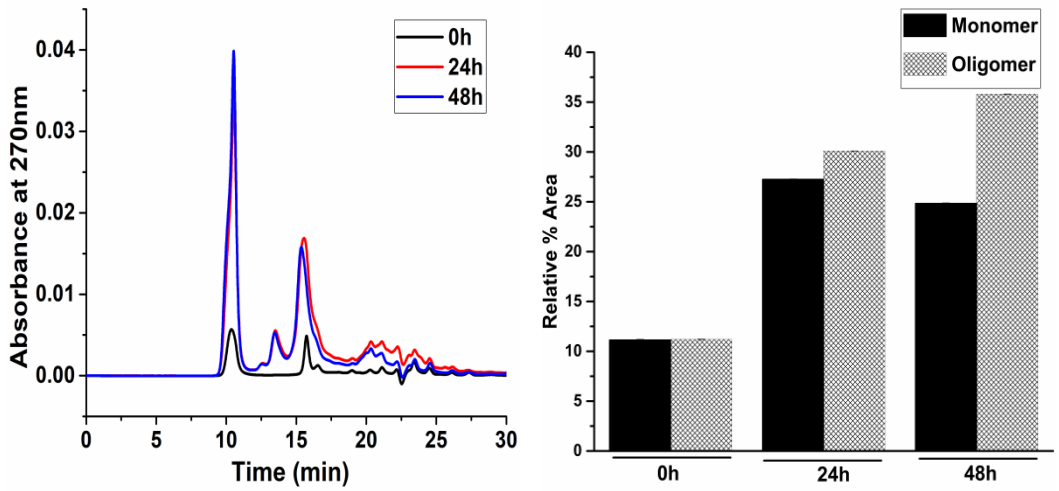
0h
24h
48h
Absorbance at 270nm
Time (min)
Monomer
Oligomer
Relative % Area
0h
24h
48h

D)

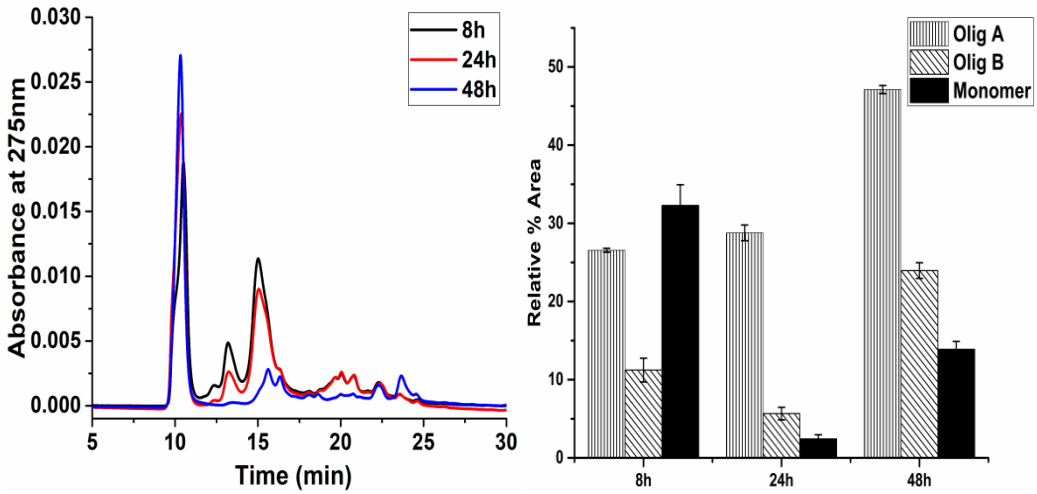

Figure 8. Size-exclusion chromatography of γ-Syn species in the presence of EGCG during fibrillation. A) Calibration curve of protein standards of known molecular weights obtained by size-exclusion chromatography. The protein standards mixture contained Thyroglobulin (670 kDa), γ-globulin (158 kDa), ovalbumin (44 kDa), myoglobulin (17 kDa) and vitamin B_{12} (1.3 kDa). The standard calibration curve was used to determine the apparent molecular weights of γ-Syn species eluting through the column. B) SEC-HPLC of γ-Syn during fibril formation monitored at regular time intervals of 0, 24 and 48h *(left to right)* respectively showing formation of two types of oligomers in the presence of EGCG which are absent in the untreated population. The formation of second type of oligomer at 24h of fibrillation is shown with an *arrow* (⟶). C) The SEC profile at 270 nm indicating preferential binding of EGCG with γ-Syn oligomers *(left panel)* with the relative percent area distribution of the different γ-Syn species depicting the formation of oligomers *(right panel)*. D) SEC-profile *(left panel)* and percent area distribution *(right panel)* of γ-Syn species formed upon addition of EGCG at 8h, 24h and 48h showing disaggregation of pre-existing fibrils of γ-Syn into oligomeric forms, designated in the plot as olig A and olig B corresponding to apparent molecular weights of ~670 kDa and ~158 kDa respectively. The error bars represent ±S.D. from three independent chromatographic runs (n=3).

2.3.2 Native-PAGE analysis

The observations made by SEC were also validated by polyacrylamide gel electrophoresis under native conditions (Figure 9), where bands migrating just below the stacking gel were visualized only in the EGCG treated samples and showed large

intensities with increasing time of fibrillation, thus indicating the formation of higher ordered oligomers by EGCG.

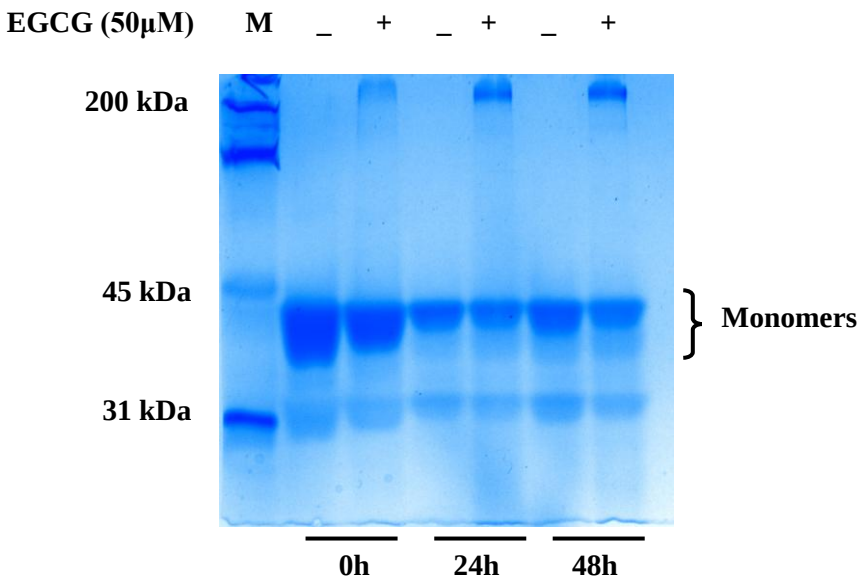

Figure 9. Native-PAGE analysis of γ-Syn species formed at different stages of fibrillation in the presence of EGCG (50µM). The protein molecular weight marker is depicted by lane M. The appearance of bands near ~200 kDa in the presence of EGCG shows formation of higher ordered oligomers.

2.3.3 SDS-PAGE analysis

The nature of the oligomers formed in the presence of EGCG were further investigated by performing electrophoresis under denaturing conditions as shown in Figure 10A. The presence of two discrete bands in EGCG-treated γ-Syn samples depicts the formation of SDS- stable γ-Syn oligomers in the presence of EGCG with an apparent molecular weight of ~200 kDa and above, not seen in the untreated γ-Syn samples. A similar observation was made with the disaggregated species of γ-Syn (Figure 10B), where SDS- stable oligomers were observed to be formed in the presence of EGCG.

A)

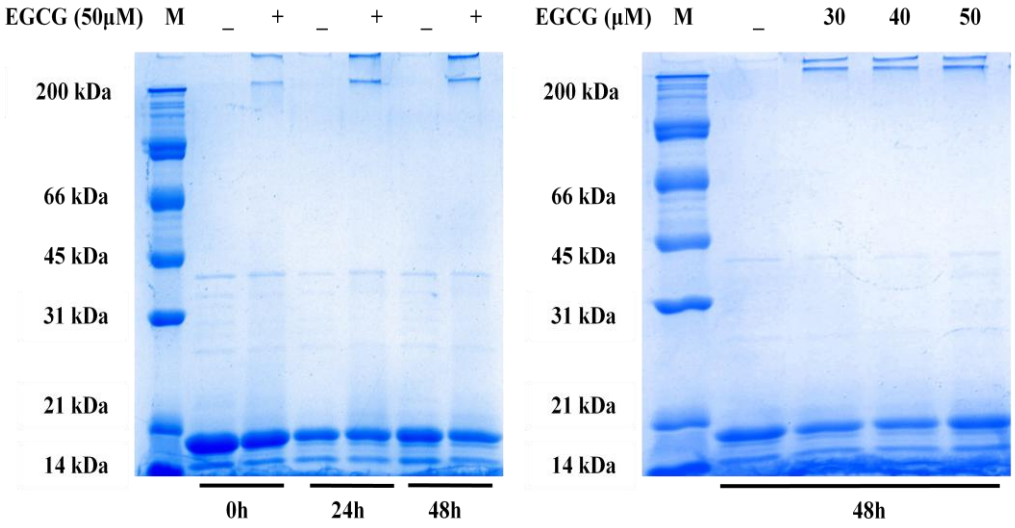

B)

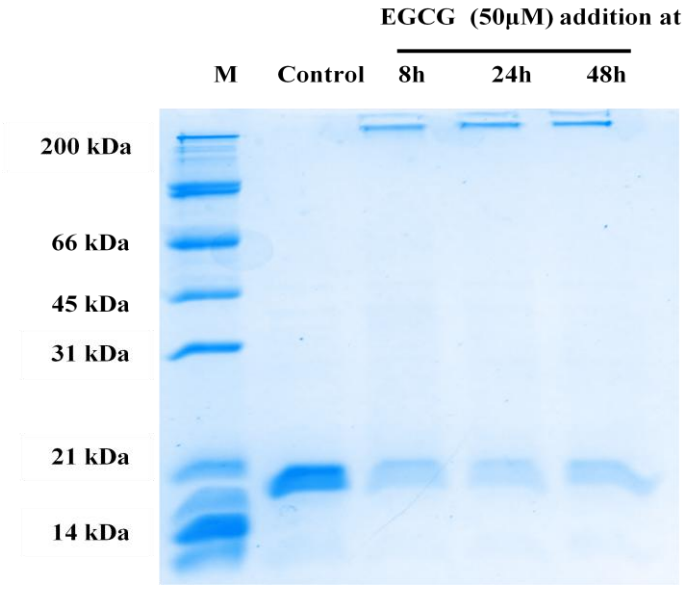

Figure 10. SDS-PAGE analysis of γ-Syn species formed in the presence of EGCG. A) SDS-PAGE at regular intervals of fibrillation *(left panel)* in the presence of EGCG (50 µM) and *(right panel)* in the presence of increasing concentration of EGCG demonstrating the formation of SDS- stable oligomeric species in the presence of EGCG. B) SDS-PAGE of disaggregated oligomers showing EGCG-mediated formation of SDS- resistant oligomers at all stages of EGCG (50 µM) addition. The molecular weight marker lane in all the gels is depicted as M.

2.3.4 Dynamic Light Scattering

The hydrodynamic properties of γ-Syn species formed during aggregation in the presence and the absence of EGCG were also studied by dynamic light scattering. The mean particle size distribution measured at different time intervals during fibrillation are shown in Figure 11. The hydrodynamic radii (R_h) of the γ-Syn oligomers formed both in presence and absence of EGCG were found to be within a range of 50-80 nm, suggesting the formation of higher - ordered oligomers as seen in SEC profiles.

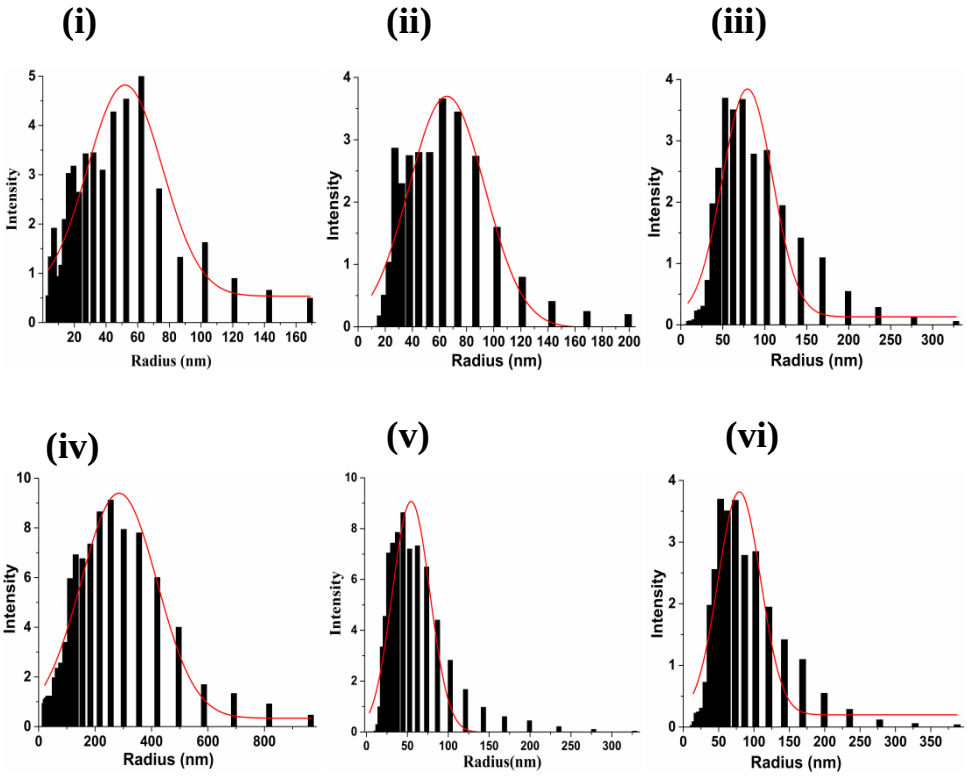

Figure 11. Mean particle size distribution of γ-Syn oligomers formed in presence and absence of EGCG during fibrillation measured by dynamic light scattering. The polydispersity of γ-Syn species during aggregation in absence *(i to iii:* 0h, 24h and 48h respectively) and presence of EGCG *(iv to vi:* 0h, 24h and 48h respectively*)* fitted into a Gaussian distribution of hydrodynamic radii (R_h) shows the formation of γ-Syn oligomers of the hydrodynamic radii ranging between 50-80 nm. The increase in the (R_h) seen upon addition of EGCG at 0h (iv) shows immediate oligomerization of γ-Syn by EGCG.

2.4 Effects of EGCG treated and untreated seeds on γ-Syn fibrillation pathway:

2.4.1 Fibrillation kinetics in the presence of EGCG-treated and untreated γ-Syn seeds by ThT assay

In order to investigate the stage at which EGCG specifically acts and whether the EGCG-generated oligomers act as templates for γ-Syn polymerization, the fibrillation was carried out in the presence of EGCG (50 μM) treated and untreated seeds (20% v/v) incubated for 48h. The fibrillation kinetics was monitored at regular intervals under shaking conditions using ThT fluorescence assay. As shown in Figure 12, the lag time of fibrillation in the presence of γ-Syn seed fibrils was reduced by approximately 10h, compared to the non-seeded γ-Syn fibrillation, whereas the EGCG-treated seeds were found to decrease the lag time by ~6h subsequently delaying fibril elongation. Addition of EGCG (50 μM) to the preformed γ-Syn seeds incubated with the monomeric γ-Syn showed negligible ThT fluorescence, suggesting that EGCG inhibits polymerization of γ-Syn fibrils and that the EGCG-generated oligomers are on-pathway that act as partial templates for γ-Syn polymerization and are thus kinetically retarded in nature.

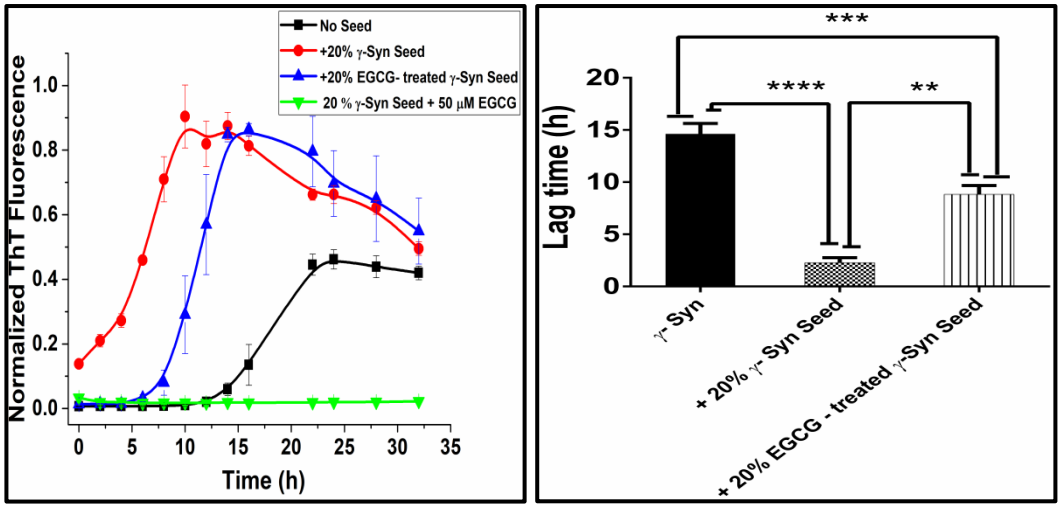

Figure 12. Fibrillation kinetics of γ-Syn in the presence of EGCG treated and untreated seeds studied by ThT assay. Fibrillation kinetics of γ-Syn in presence of EGCG-treated (50 μM) and untreated seeds (20% v/v) (*left panel*) formed after 48h of incubation and bar graph showing the significant difference in the lag time (*right panel*) in the EGCG-

generated seeds as compared to the seeds formed without EGCG (**p < 0.001) and between non-seeded γ-Syn and EGCG-generated γ-Syn seeds (***p < 0.0005). The lag time of fibrillation in the presence of untreated γ-Syn seeds was significantly shorter than the non-seeded kinetics (****p < 0.0001). Negligible ThT fluorescence in the presence of EGCG (50 μM) added to the fibrillation reaction of seeded γ-Syn (*green line*) shows elongation inhibition.

2.4.2 TEM images of γ-Syn species formed in the absence and presence of EGCG treated γ-seeds

The TEM images of the fibrils formed in the presence and absence of EGCG treated seeds (Figure 13A) showed that γ-Syn is capable of self seeding its fibrillation pathway giving rise to thick intertwined mature fibrils whereas only short and partially polymerized fragments were observed in presence of EGCG- treated seeds. This validates the EGCG-mediated formation of unfavourable γ-Syn oligomers that prevent nucleus formation and hence, fibril maturation. Additionally, the formation of short and diffused fibrillar species in the presence of EGCG added to seeded γ-Syn indicated the inhibition of fibril polymerization by EGCG (Figure 13B).

A)

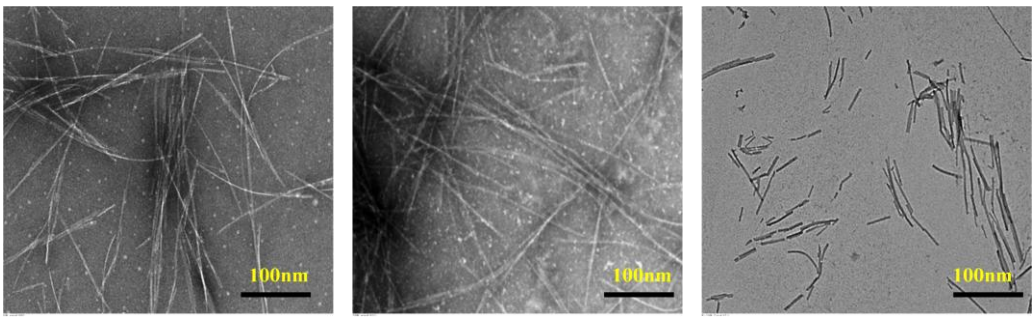

B)

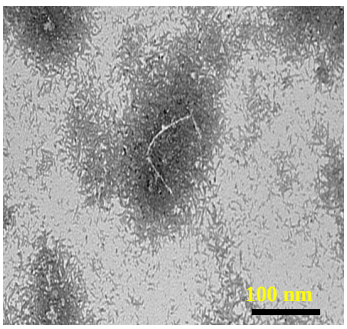

Figure 13. Transmission electron microscopy images of fibrils formed in presence of EGCG-treated and untreated seeds. A) The TEM images showing the morphology of the

fibrils formed (*left to right*: no seed, 20% (v/v) γ-Syn seed and 20% (v/v) EGCG treated γ-Syn seeds respectively). B) TEM image of the species formed upon addition of EGCG (50μM) to preformed γ-Syn fibrils. A magnification of 10,000 was used for all the images. (Scale bars, 100 nm).

2.5 Effect of EGCG on the structure of γ-Syn both under native and fibrillation conditions:

2.5.1 Far-UV circular dichroism (CD) spectroscopy of γ-Syn in the presence of EGCG

2.5.1.1 Far-UV CD studies of γ-Syn under native and fibrillation conditions: To gain insight into the effect of EGCG on the secondary structure of γ-Syn, far-UV CD spectroscopy of the γ-Syn species incubated with an increasing concentration of EGCG (10, 30 and 50 μM) under native and fibrillating conditions was carried out. Monomeric and untreated γ-Syn showed far-UV CD spectra of a typical natively unfolded conformation with a large negative ellipticity at ~200 nm and a small value at ~222 nm, which was also maintained at all the concentrations of EGCG used (Figure 14A). The far-UV CD spectra of γ-Syn, monitored after 24h and 48h of fibrillation (Figure 14B), showed a shift in negative ellipticity to 218 nm, indicating a structural transition from the natively unfolded conformation to a characteristic β-sheet structure. This structural transition was found to be significantly delayed in presence of EGCG in a concentration-dependent manner, with an increase in negative ellipticity at ~208 nm and ~221nm at higher concentration of EGCG (50 μM), indicating the formation of an α-helical like structure by EGCG.

2.5.1.2 Far-UV CD analysis of soluble γ-Syn oligomers formed in the presence and absence of EGCG during fibrillation: The structure of γ-Syn oligomers formed both in the absence and the presence of EGCG were further characterized by far-UV CD spectra measurements of the soluble oligomers obtained after centrifugation of the fibrillating samples carried out as a function of time (Figure 14C). The far-UV CD spectra of soluble γ-Syn oligomers measured at different time intervals, i.e. 0h, 8h, 24h and 48h, showed spectra characteristic of natively unfolded protein, with a negative peak at ~200 nm. The differences in the intensities of the negative ellipticity indicated slight perturbations in the structure. In contrast, the

EGCG generated oligomers during aggregation were found to have increased secondary structure propensity showing a decrease in ellipticity at 200 nm and appearance of negative ellipticity with two minima at 208 nm and 220 nm, indicating increased α-helicity in the conformation. These results indicate an EGCG induced gain in the α-helical propensity in the γ-Syn oligomers which otherwise retain the natively unfolded conformation during fibrillation.

A)

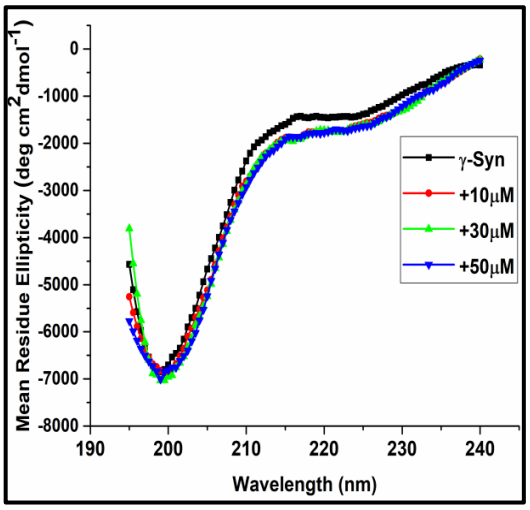

B)

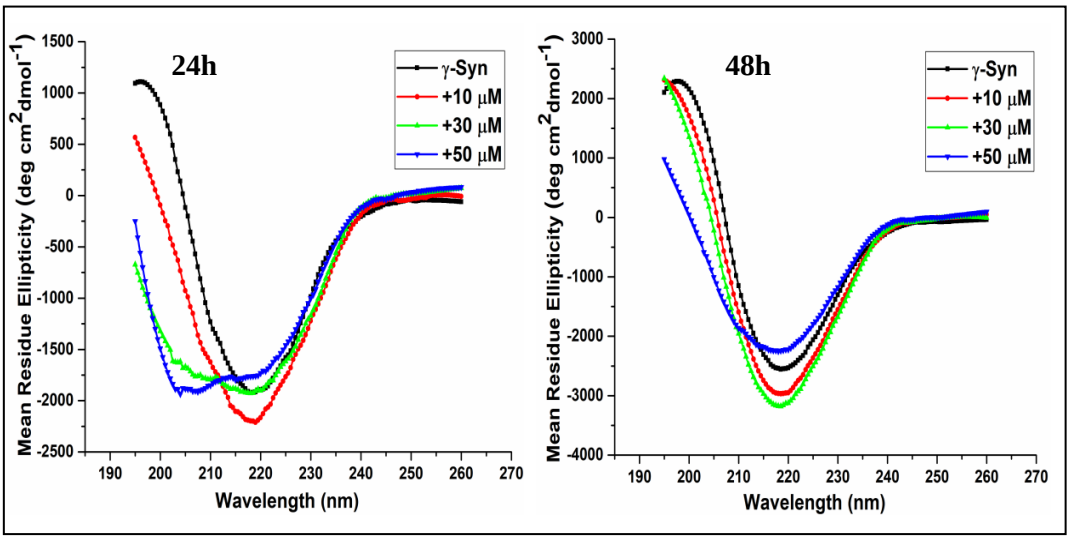

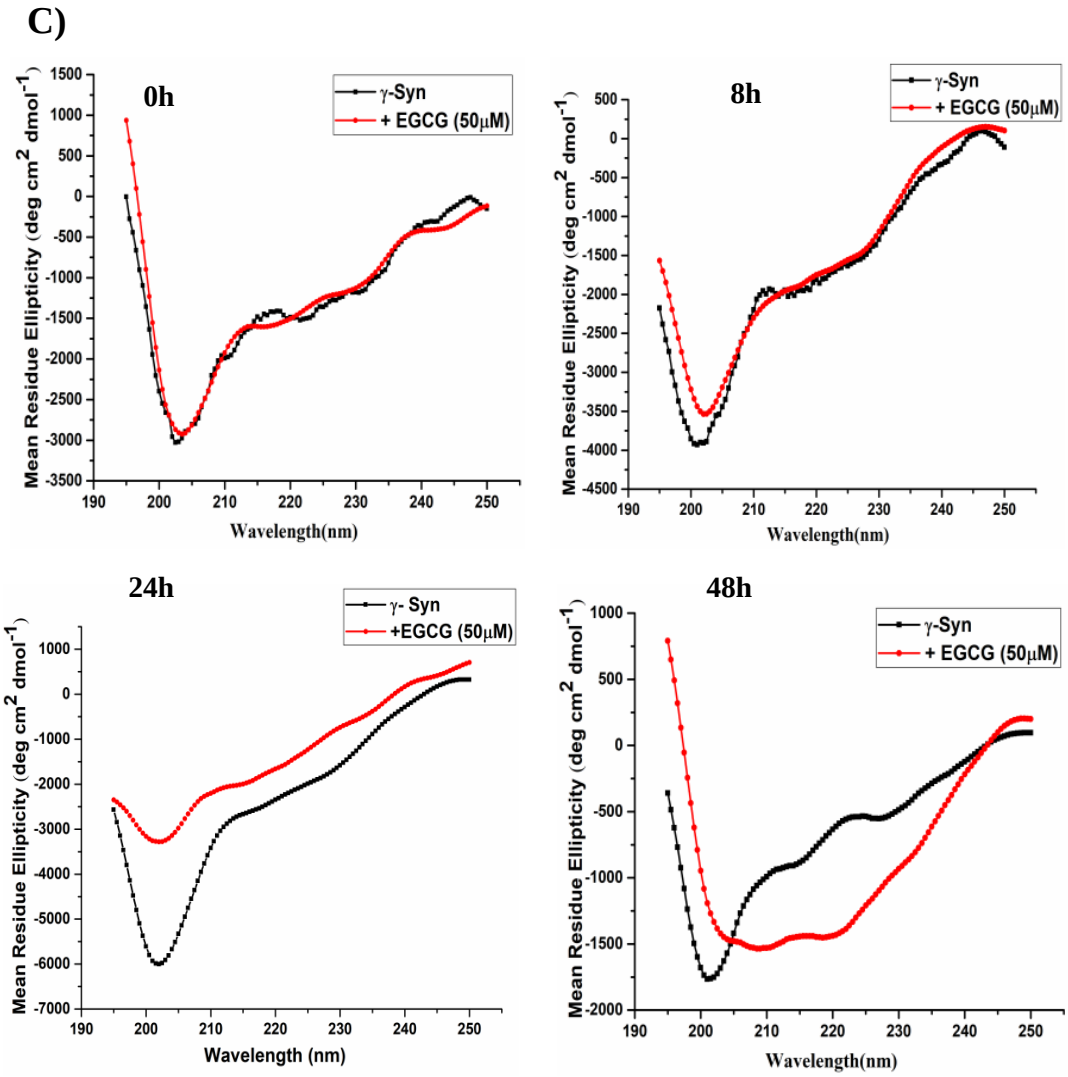

Figure 14. Far-UV CD analysis of γ-Syn in the absence and presence of EGCG under native and fibrillation conditions. A) Far-UV CD spectra of γ-Syn (0.5 mg/ml) dissolved 20 mM phosphate buffer, pH7.4 conditions in the presence of increasing concentration of EGCG (10, 30 and 50μM), monitored under native conditions. B) Far-UV CD spectra of γ-Syn (0.3 mg/ml) in presence of increasing concentrations of EGCG (10, 30 and 50μM) monitored at time- intervals of 24h *(left panel)* and 48h *(right panel)* during fibrillation showing a shift in the negative ellipticity from 200 nm to ~ 218 nm in the untreated γ-Syn, depicting the formation of characteristic β-sheet conformation. The measurements were made using a cuvette of 1mm path length for both native and fibrillation conditions. C) Far-UV CD analysis of γ-Syn oligomers in presence of EGCG (50 μM) during fibrillation (*left to right* : 0h, 8h, 24h and 48h) was carried out at 25 °C using a cuvette of 0.1 mm path length to avoid interference in the measurement by 100 mM NaCl present in the fibrillation

buffer (see Methods). Far-UV spectra of EGCG-treated oligomers at 48h showing double minima at ~208 nm and ~220 nm indicate α-helical structure.

2.5.2 ANS binding assay

The extent of exposed hydrophobic surface area in γ-Syn was assessed by ANS binding assay. ANS (1-anilino-8-naphthalenesulfonic acid), a widely used solvent-sensitive dye is known to fluoresce with a blue-shifted emission upon binding with hydrophobic surroundings (Bolognesi et al., 2010) The ANS fluorescence spectra of monomeric γ-Syn in the presence of increasing concentration of EGCG overlapped with that of the fluorophore in buffer alone, with an emission around 525 nm ± 0.5 nm (Figure 15A). The ANS fluorescence spectra measured at different time intervals (0h, 24h and 48h) during fibrillation (Figure 15B), showed an increase in the fluorescence intensity with a characteristic blue shifted emission (λ_{em} at 480 nm) in the untreated γ-Syn fibrils. The ANS emission spectra obtained in EGCG treated γ-Syn fibrils were also blue shifted but the increments in the intensity were much reduced at all the time-points (Figure 15B). These results demonstrate that the extent of exposed hydrophobic surface area in γ-Syn species increases during aggregation which to a large extent is prevented by EGCG, suggesting that EGCG modulated species maintain an overall low surface hydrophobicity.

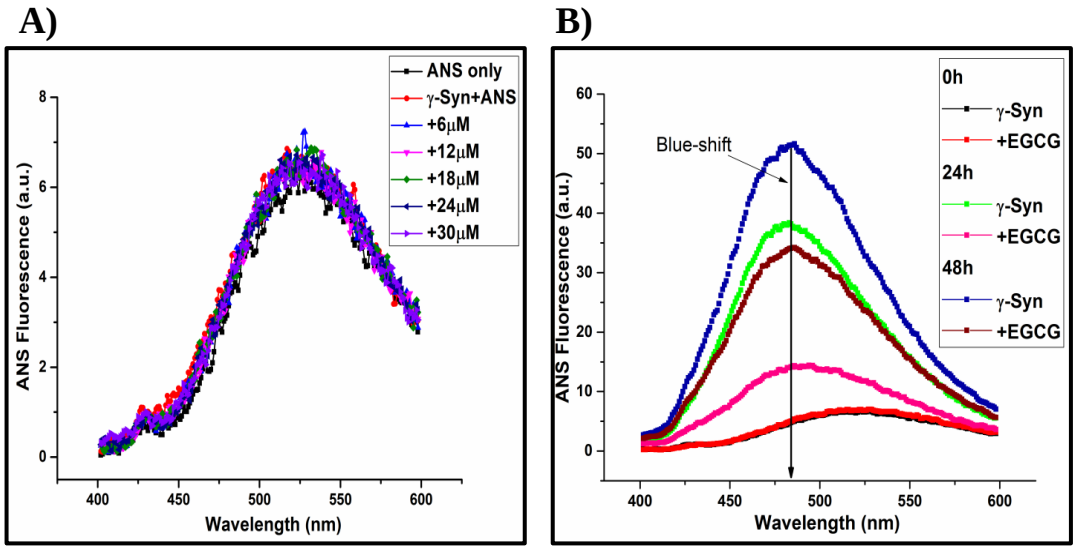

Figure 15. ANS binding to γ-Syn in presence of EGCG shows an overall low surface hydrophobicity. A) Emission spectra of ANS binding to γ-Syn with increasing concentration of EGCG under native conditions. B) ANS binding to aggregating species of γ-Syn in presence and absence of EGCG with a characteristic blue-shift shown at ~480 nm.

2.6 Binding interactions between γ-Syn and EGCG:

The mode of binding interaction between EGCG and γ-Syn was further investigated by using steady-state and time-resolved fluorescence as well as isothermal titration calorimetry (ITC).

2.6.1 Steady-state fluorescence studies: Effect of EGCG on the intrinsic tyrosine fluorescence of γ-Syn

To investigate the accessibility of EGCG to the lone tyrosine present in γ-Syn, tyrosine fluorescence of γ-Syn in the presence of increasing concentration of EGCG (2-30 μM) was monitored upon excitation at 275 nm with emission intensity recorded from 280-400 nm. The single tyrosine in γ-Syn has an emission maximum at 342 nm due to tyrosinate formation upon excitation as also reported for other proteins containing single tyrosine in absence of tryptophan (Szabo et al., 1978; Libertini and Small, 1985). A concentration dependent decrease in tyrosine fluorescence indicated an interaction between γ-Syn and EGCG (Figure 16A). Using the Stern-Volmer quenching equation, the bimolecular quenching constant (k_q) was found to be more than 10^{10} $M^{-1}s^{-1}$ (k_q = $9.6x10^{12}$ $M^{-1}s^{-1}$) (Figure 16B) indicating a static quenching mechanism and a binding interaction between EGCG and γ-Syn.

The binding parameters were evaluated by employing the modified Stern-Volmer equation which resulted in a linear dependence between fluorescence quenching intensity and EGCG concentration from a plot of log (F_o-F/F) *vs.* log (Q) (Figure 16C). γ-Syn was found to bind with EGCG at an approximately equimolar ratio of 1:1. An interaction with a binding constant (K_a) of 6.9×10^3 M^{-1} was obtained suggesting the role of weak non-covalent interactions in EGCG mediated inhibition of γ-Syn fibrillation. In addition, the binding of EGCG to the different species of γ-Syn formed during fibrillation was carried out and the samples of γ-Syn withdrawn at time intervals of 0h, 24h and 48h were similarly titrated with increasing concentrations of EGCG at 25 °C. The modified Stern-Volmer plot showing the binding affinity (K_a) of EGCG to different species of γ-Syn is shown in Figure 16D and Table 1, respectively. EGCG was found to bind with highest affinity with the species formed during exponential phase of fibrillation (24h) validating the increased affinity of EGCG to γ-Syn oligomers as also revealed by SEC.

A)

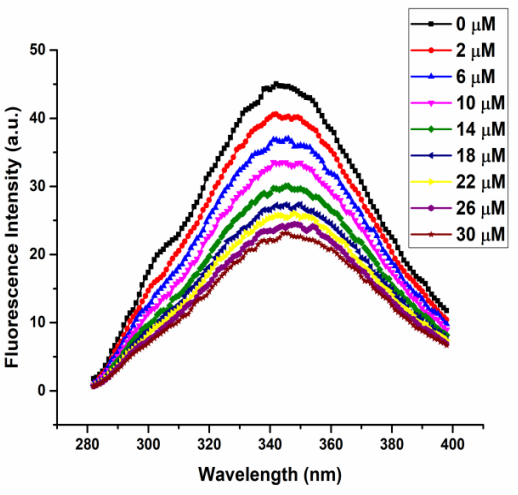
0 μM
2 μM
6 μM
10 μM
14 μM
18 μM
22 μM
26 μM
30 μM
Fluorescence Intensity (a.u.)
Wavelength (nm)

B)

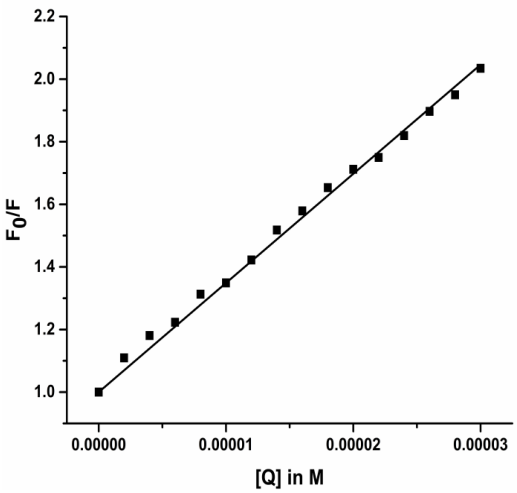
F0/F
[Q] in M

C)

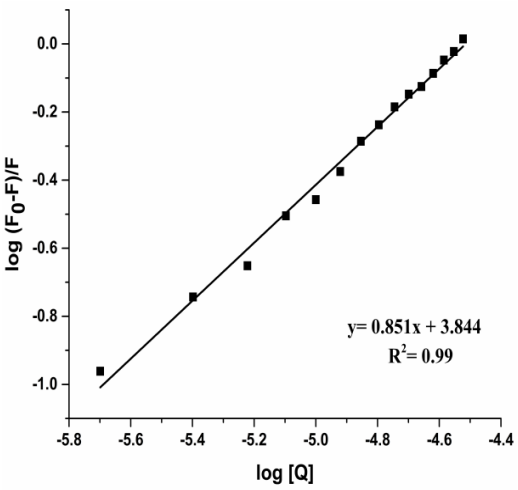
log (F0-F)/F
log [Q]
y= 0.851x + 3.844
R2= 0.99

D)

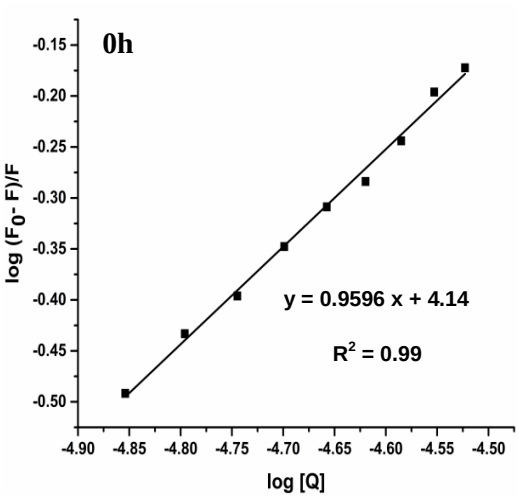
0h
log (F0- F)/F
log [Q]
y = 0.9596 x + 4.14
R2 = 0.99

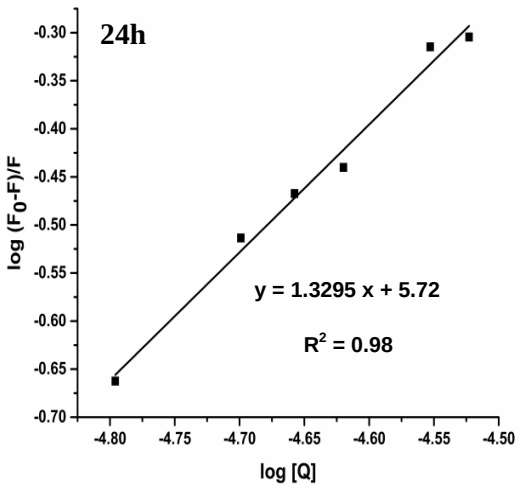
24h
log (F0-F)/F
log [Q]
y = 1.3295 x + 5.72
R2 = 0.98

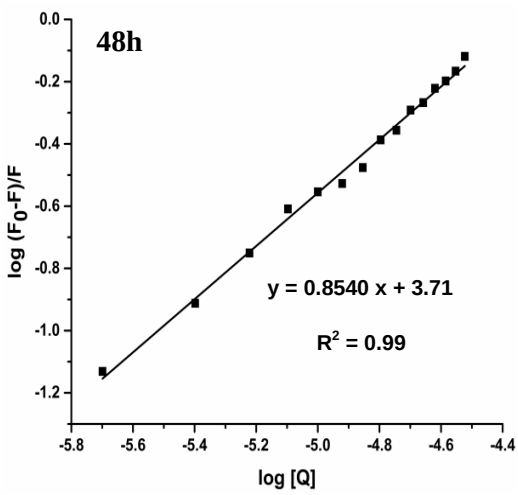

Figure 16. Intrinsic tyrosine fluorescence of γ-Syn in the presence of increasing concentration of EGCG. A) Steady-state fluorescence showing quenching of intrinsic tyrosine fluorescence of γ-Syn (0.3 mg/ml) continuously titrated with an increasing concentration of EGCG (2-30 μM) at 25ºC. B) The bimolecular quenching constant (k_q = $9.6x10^{12}$ $M^{-1}s^{-1}$) at 25ºC indicates a static quenching mechanism between EGCG and γ-Syn. C) Modified Stern-Volmer plot of log $(F_0-F)/F$ vs log [Q] showing weak binding between γ-Syn and EGCG (K_a= $6.9x10^3M^{-1}$). D) Modified Stern-Volmer plots showing binding affinities of EGCG to different aggregating species of γ-Syn. EGCG showed higher affinity (K_a=10^5 M^{-1}) at 24h of fibrillation, indicating increased affinity for oligomeric species of γ-Syn formed during exponential phase of the pathway (24h).

Table 1. Binding of γ-Syn with different aggregating species of γ-Syn.

Time (h)	K_a (Binding Constant)
0	1.4×10^4 M^{-1}
24	5.2×10^5 M^{-1}
48	$5.1 \times 10^3 M^{-1}$

2.6.2 Time-Resolved Fluorescence measurements of γ-Syn in presence of EGCG

2.6.2.1 Fluorescence decay measurements of tyrosine in γ-Syn under native conditions:

The binding mechanism between EGCG and γ-Syn was also investigated by time resolved fluorescence measurements of the single tyrosine present in γ-Syn, carried

out in the presence of increasing concentration of EGCG (5-25 μM). The fluorescence intensity decay curves and the autocorrelation of the weighted residual mean used for deciding the goodness of the fit are shown in Figure 17A and B, respectively. The decay curves both in the presence and absence of EGCG were described by three discrete decay components distributed into shorter lifetime (τ_1 < 0.5ns), intermediate lifetime (τ_2 ~2ns) and longer lifetime (τ_3~ 6ns). The decay lifetimes observed in the presence of EGCG were found to be only marginally less than the average lifetime (τ_m) of native γ-Syn and the decay curves were indistinguishable from each other yielding the ratio of τ_0/τ ~1(Table 2). This indicates that the changes in the fluorescence intensity were brought dominantly due to the changes in the decay amplitudes suggesting the existence of static quenching mechanism and a complex formation between EGCG and γ-Syn, as also observed in the steady-state fluorescence measurements.

2.6.2.2 Conformational dynamics of soluble γ-Syn oligomers formed in the presence of EGCG during aggregation:

The conformational dynamics of γ-Syn oligomers formed both in the presence and absence of EGCG during fibrillation was further assessed by monitoring the lifetime decay of the lone tyrosine in γ-Syn at regular intervals of fibrillation. The samples of soluble oligomeric species of γ-Syn characterized by far-UV CD were also characterized by time-resolved fluorescence spectroscopy and the differences in the lifetimes between the EGCG generated and untreated γ-Syn oligomers were investigated. The fluorescence intensity decay curves at time intervals of 0h, 8h, 24h and 48h and the autocorrelation of the weighted residual mean used for deciding the goodness of the fit are shown in Figure 17C. Time-resolved fluorescence measurements of γ-Syn oligomers both in the presence and absence of EGCG at all the time intervals are appropriately described by three discrete decay components as also observed under native state. The results showing the amplitudes of respective lifetimes along with their mean lifetimes are summarized in Table 3. The data show a faster decay in the EGCG-generated oligomers as compared to the untreated oligomers in the initial stages of fibrillation which become slower during the course of fibrillation, thus indicating a time-dependent collapse in the overall structure in the EGCG-generated oligomers. The untreated γ-Syn oligomers on the other hand show a decreasing fluorescence lifetime with an increase in the time of fibrillation,

much evident during the exponential (24h) and saturation phase (48h), and which indicates a solvent-exposed or an unfolded conformation. The increase in the amplitude (α_1) of the shortest lifetime (τ_1) and a concomitant decrease in the amplitude (α_3) of the longest lifetime (τ_3) in the untreated γ-Syn oligomers and vice-versa in the EGCG-generated oligomers during fibrillation (Figure 17D and E) clearly demonstrate that the unfolded state of the untreated γ-Syn oligomers, when formed in the presence of EGCG, becomes conformationally more restrained and structured upon prolonged incubation. These observations thus further support the results obtained from far-UV CD of the γ-Syn oligomers (Figure 14C).

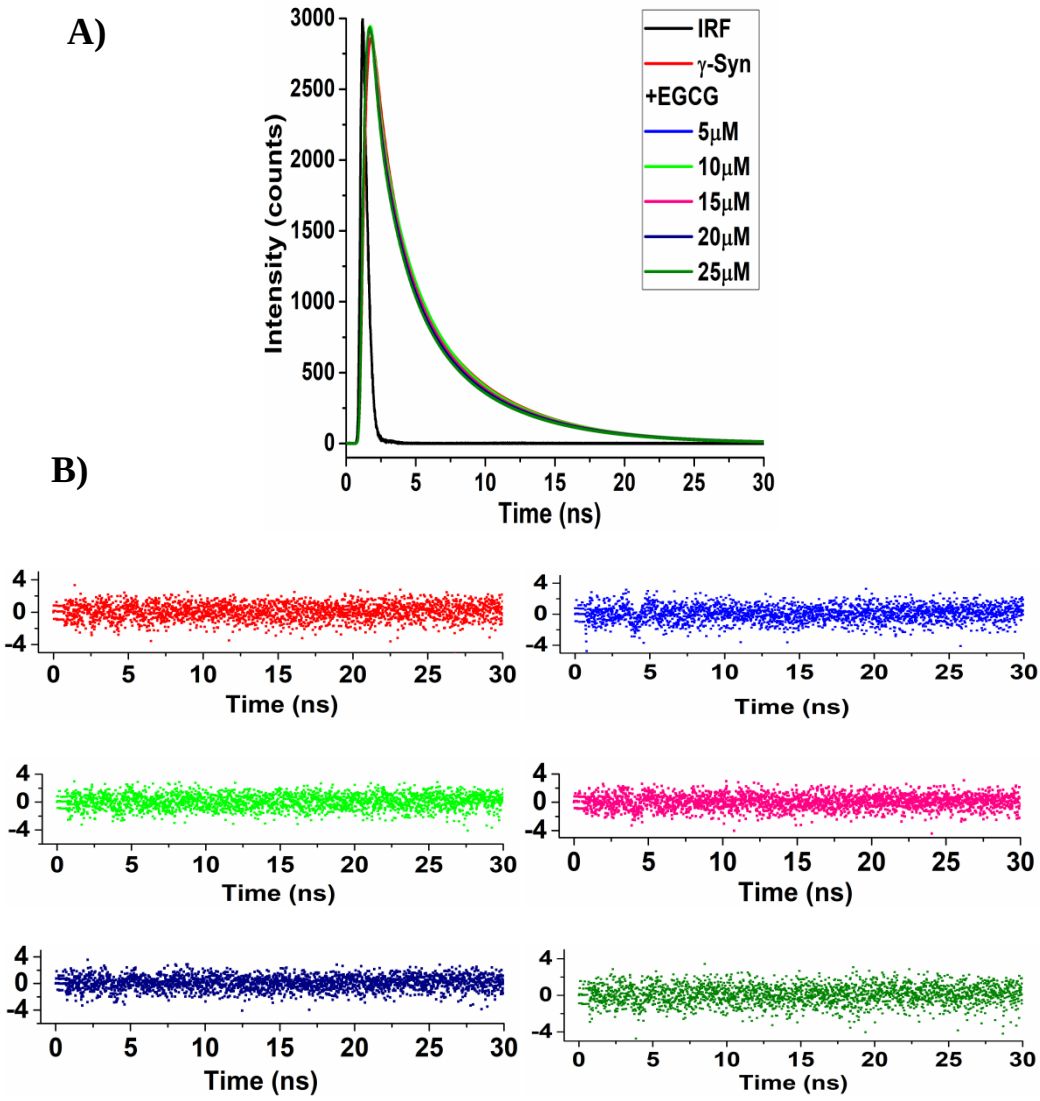

C)

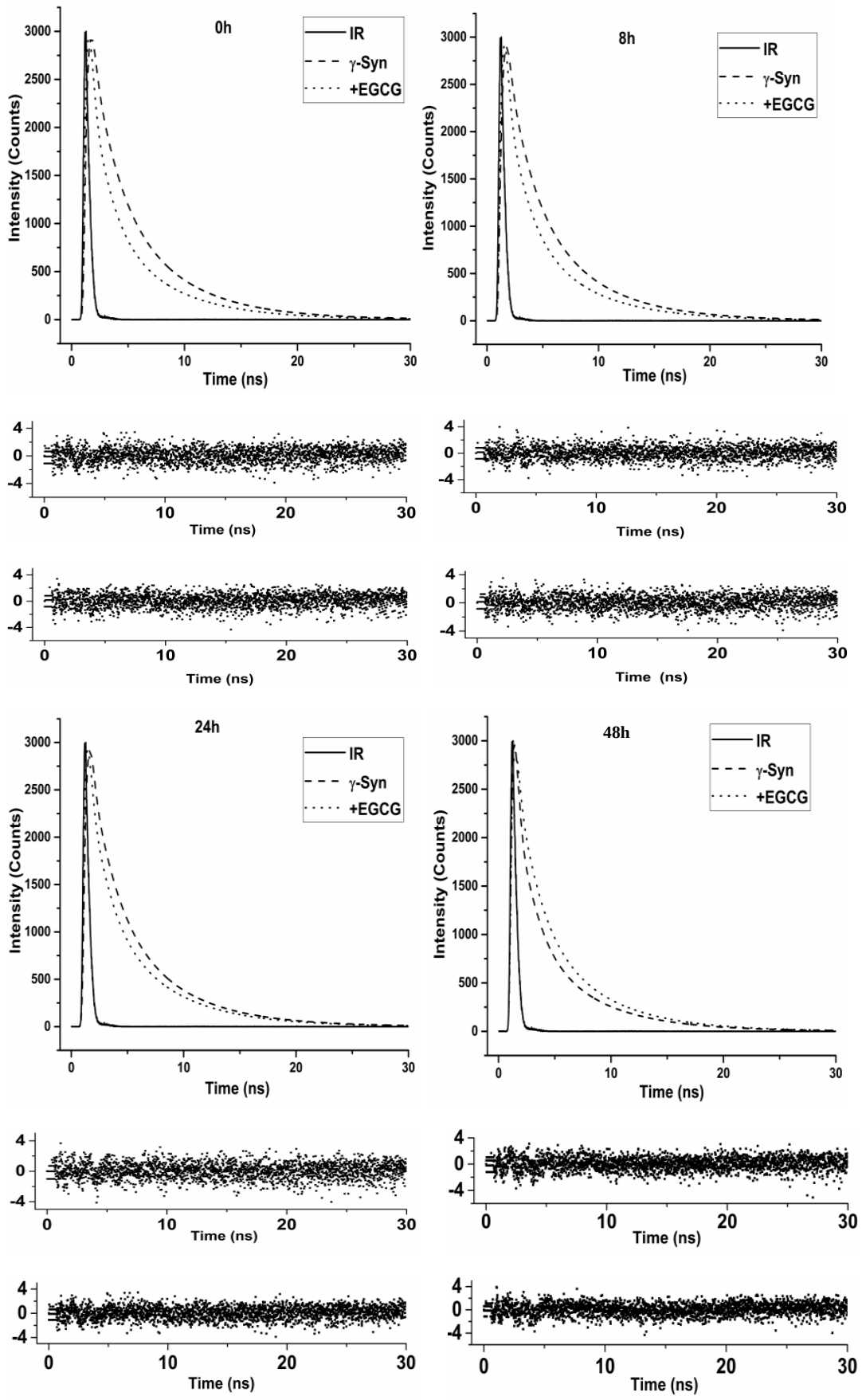

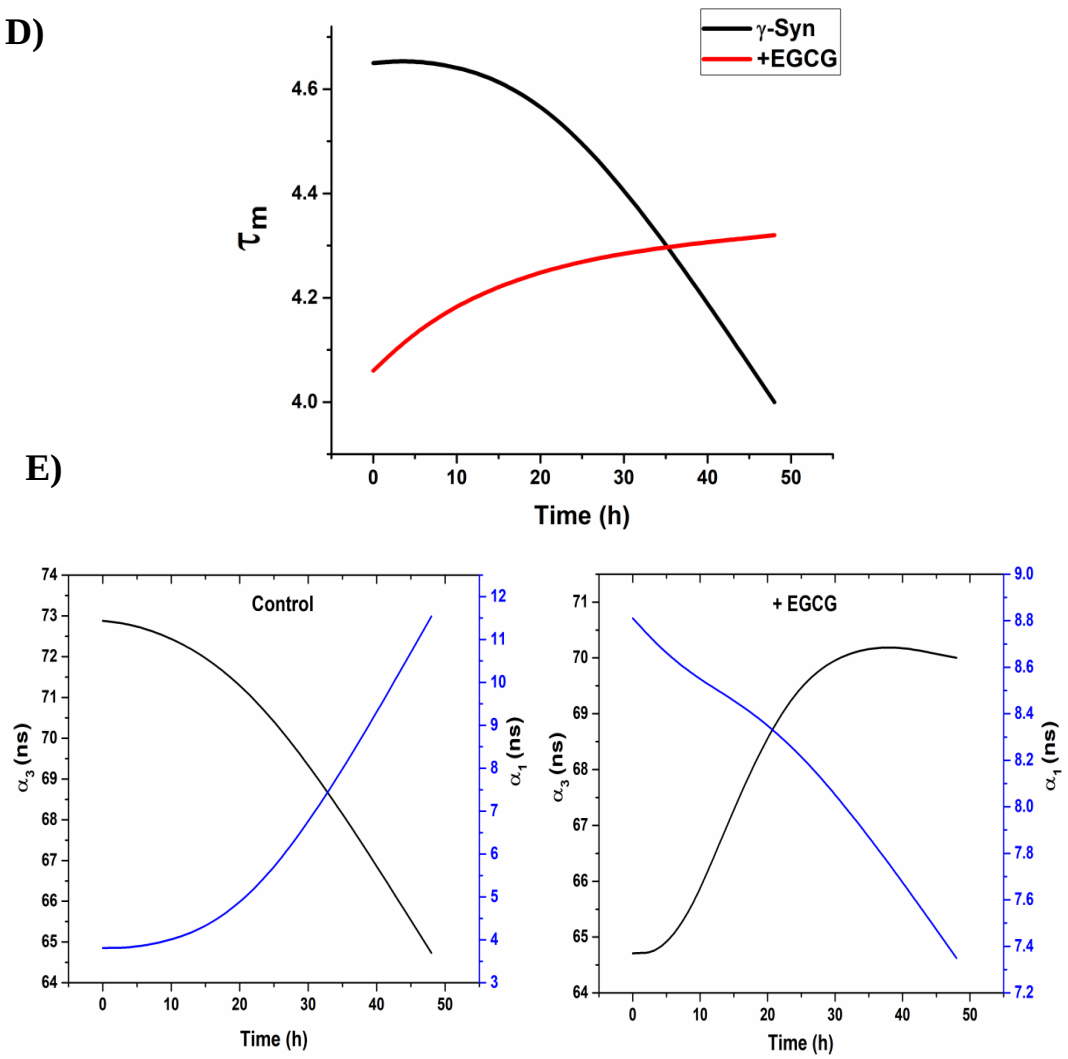

Figure 17. Time-resolved fluorescence measurements of γ-Syn species in the presence and absence of EGCG. A) Time-resolved fluorescence intensity decay of γ-Syn under native conditions in the presence of increasing concentrations of EGCG and B) plots of the autocorrelation function of the weighted residuals used to judge the goodness of the fit (*left to right*: no EGCG, 5, 10, 15, 20 and to 25 μM EGCG respectively) . The fluorescence decay curves were obtained upon excitation at 284 nm and monitoring emission at 342 nm. γ-Syn concentration of 1mg/ ml in 20 mM phosphate buffer, containing 100 mM NaCl at pH 7.4 was used. C) Lifetime decay curves of γ-Syn oligomers formed at 0, 8, 24 and 48h of fibrillation both in the presence and absence of EGCG along with their respective residuals (*left to right*: 0 to 48h ; Residuals, *upper:* γ-Syn, *lower:* with EGCG). D) The plot of average lifetime (τ_m) versus the time of fibrillation demonstrates the difference in the decay kinetics in the EGCG generated and untreated oligomers. E) The relationship between the change in the amplitudes of the fastest (τ_1) and slowest (τ_3) time constants (α_1 and α_3 respectively) with respect to the increasing time of fibrillation in the control and EGCG-treated samples.

Table 2. Lifetime decay parameters of γ-Syn in the absence and presence of EGCG at 25°C.

γ-Syn	τ_1 [ns](α_1)	τ_2[ns](α_2)	τ_3[ns](α_3)	τ_m[ns]	χ^2
γ-Syn (Control)	0.41 (4.29)	2.00 (22.32)	5.83 (73.38)	4.74	1.04
+5μM EGCG	0.35 (4.22)	1.92 (23.08)	5.82 (72.70)	4.68	1.07
+10μM EGCG	0.38 (4.59)	1.93 (21.79)	5.82 (73.61)	4.72	1.09
+15μM EGCG	0.36(4.84)	1.91 (22.97)	5.82 (72.19)	4.66	1.03
+20μM EGCG	0.30 (4.91)	1.80 (23.06)	5.77 (72.03)	4.58	1.07
+25μM EGCG	0.31 (5.62)	1.83 (24.01)	5.78 (70.37)	4.52	1.08

Table 3. Lifetime decay Parameters of γ-Syn oligomers formed in the absence and presence of EGCG at 25 °C.

γ-Syn	τ_1 [ns](α_1)	τ_2[ns](α_2)	τ_3[ns](α_3)	τ_m[ns]	χ^2
γ-Syn (Control)	0.41 (4.29)	2.00 (22.32)	5.83 (73.38)	4.74	1.04
+5μM EGCG	0.35 (4.22)	1.92 (23.08)	5.82 (72.70)	4.68	1.07
+10μM EGCG	0.38 (4.59)	1.93 (21.79)	5.82 (73.61)	4.72	1.09
+15μM EGCG	0.36(4.84)	1.91 (22.97)	5.82 (72.19)	4.66	1.03
+20μM EGCG	0.30 (4.91)	1.80 (23.06)	5.77 (72.03)	4.58	1.07
+25μM EGCG	0.31 (5.62)	1.83 (24.01)	5.78 (70.37)	4.52	1.08

2.6.3 Isothermal Titration Calorimetry of EGCG binding to γ-Syn

The binding of EGCG to γ-Syn was further investigated by ITC analysis. The calorimetric study of the interaction of EGCG with γ-Syn was carried out at 25 °C with a 30 fold molar excess ratio of EGCG over γ-Syn. The representative ITC data are displayed in Figure 18. The dissociation constant (K_d) obtained from the binding isotherm was of weak magnitude and in the mM range (K_d = 2.19 mM, K_a= $0.45\times10^3 M^{-1}$), thereby substantiating the role of weak non-covalent interactions in facilitating the binding of EGCG to γ-Syn. Due to the weak nature of binding interactions, enthalpy and entropy values could not be accurately deduced. ITC results were, however, in accordance with the steady-state fluorescence titration data indicating a weak binding interaction between EGCG and γ-Syn.

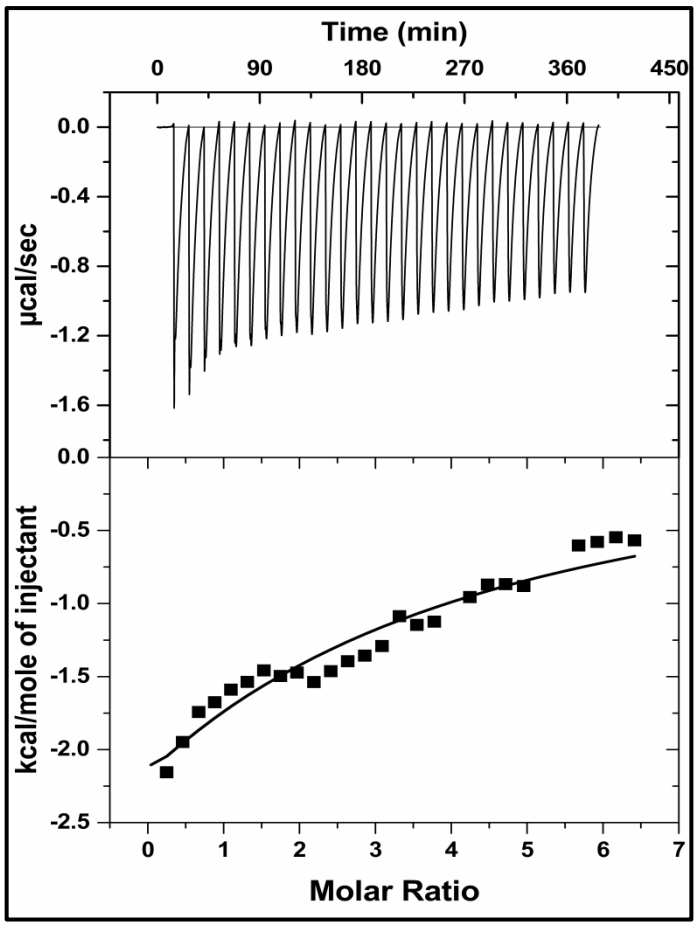

Figure 18. Isothermal titration calorimetry of EGCG interaction with γ-Syn showing a weak binding interaction. The reaction was carried out at 25ºC with a γ-Syn and EGCG ratio of 1:30.*Upper panel:* A raw data plot of heat flow against time for titration of EGCG into γ-Syn and *Lower panel:* Plot of total normalized heat released as a function of ligand concentration for the titration. The solid line shows the one-site fit for the obtained data.

2.7 Cytotoxic effects of EGCG generated γ-Syn species

2.7.1 MTT Assay

Due to the involvement of γ-Syn in both neurodegeneration and cancer, the cytotoxic effects of EGCG generated species monitored by MTT assay were carried out on both breast cancer (MCF-7) and neuroblastoma (SH-SY5Y) cells.

2.7.1.1 MTT assay on MCF-7 cells

γ-Syn was incubated both in the presence and absence of EGCG (50µM) for 24h and the effect of the γ-Syn species on the metabolic activity of the MCF-7 cells were assessed by MTT assay. The treatment of the MCF-7 cells with the protofibrillar and

oligomeric species of γ-Syn generated after 24h of fibrillation, resulted in a decrease in the MTT reduction by approximately 20 % indicating reduced cell viability (Figure 19A). On the other hand, the treatment of cells with the EGCG generated oligomers was found to significantly increase the metabolic activity and thus the cell viability, rescuing the MCF-7 cells almost completely from γ-Syn toxicity.

The cytotoxic effect of EGCG-generated disaggregated γ-Syn species were further investigated on MCF-7cells. The toxicity of the disaggregated oligomers and the whole population of disaggregated γ-Syn fibrils containing various forms of γ-Syn disaggregates, were assessed separately by MTT assay. As the EGCG-diverted γ-Syn oligomers were found to be protective on MCF-7 cells (Figure 19A), it was interesting to compare the cytotoxic effects of the disaggregated oligomers on the same. For the assay, the disaggregated γ-Syn species formed after addition of EGCG (50 μM) at 8h, 24h and 48h (corresponding to lag, log and saturation phase respectively) of fibrillation, were withdrawn at the end of fibrillation (~72 h) and were separated into two groups where in one group only the soluble species obtained after centrifugation were used for the treatment of the cells and in the other group the disaggregated species as a whole were used without centrifugation. The disaggregated oligomers at all the time intervals (8, 24 and 48h) were found to be equally toxic to MCF-7 cells as the untreated γ-Syn oligomers (Figure 19B). On the other hand, the disaggregated fibrils were found to be less toxic than the γ-Syn oligomers. This indicates an early gain of toxic characteristics by γ-Syn which cannot be reversed upon fibril disaggregation by EGCG.

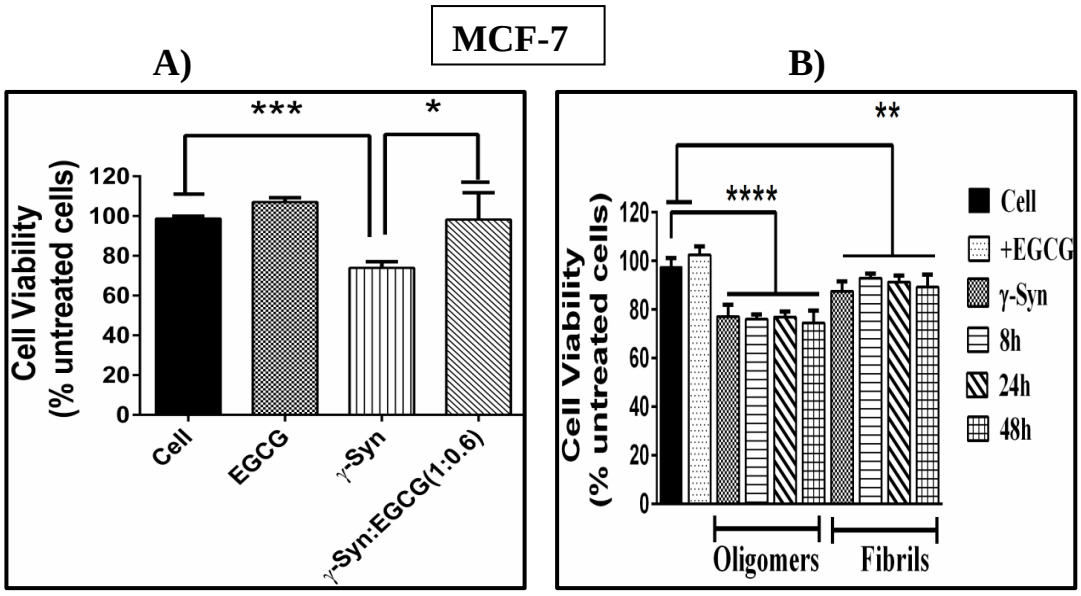

Figure 19. Cytotoxic effects of EGCG treated γ-Syn species on MCF-7 cells by MTT assay. A) MTT assay reveal an increased viability of MCF-7 cells in the presence of EGCG generated oligomers (*$p < 0.01$ and ***$p < 0.0005$, related to the cells treated with γ-Syn oligomers and with respect to the untreated cells respectively). B) MTT assay show the reduction (****$p < 0.0001$) in the MTT absorbance with respect to the controls taken as untreated cells indicate that the disaggregated oligomers are significantly toxic to cells, whereas the whole population of disaggregated fibrils formed upon fragmentation are marginally toxic (**$p < 0.001$) to the untreated cells. The error bars represent ±S.D. ($n = 3$). The statistical analysis was done using one-way ANOVA

2.7.1.2 MTT assay on SH-SY5Y cells

The cytotoxic effects of 24h incubation samples of γ-Syn formed in the presence of EGCG (50μM) were also investigated by MTT assay on neuronal SH-SY5Y cells. A contrasting effect of γ-Syn oligomers on the viability of neuronal cells (SH-SY5Y) was observed. As otherwise observed in MCF-7 cells, the γ-Syn oligomers were found to be only moderately toxic to SH-SY5Y cells (Figure 20) whereas the EGCG generated oligomers were found to reduce viability by almost 30% as compared to the untreated and γ-Syn treated cells. Thus a differential toxicity of EGCG generated oligomers of γ-Syn towards MCF-7 and SH-SY5Y cells were observed.

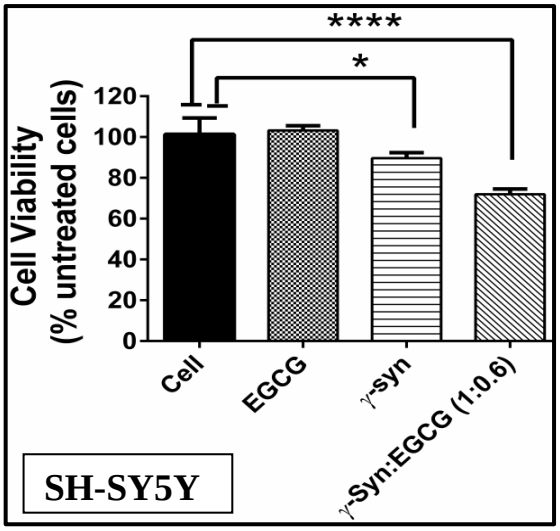

Figure 20. Cytotoxic effects of EGCG treated γ-Syn species on SH-SY5Y cells by MTT assay. MTT assay on SH-SY5Y cells shows a significant reduction in cell viability in the presence of EGCG generated oligomers (****$p < 0.0001$, related to the untreated cells), which reduced only marginally in the presence of untreated γ-Syn oligomers (*$p < 0.01$ with respect to untreated cells).

2.7.2 LDH Assay on MCF-7 and SH-SY5Y cells

The cytotoxic effects of the EGCG generated γ-Syn oligomers on both MCF-7 and SH-SY5Y cells were also validated by investigating the non-viability of the cells by LDH release assay (Figure 21A and B). The treatment of MCF-7 cells by the EGCG generated 24h γ-Syn oligomers increased the viability of MCF-7 cells and contrastingly decreased the viability of SH-SY5Y cells, as also observed in the MTT assay (Figure 19 and 20). The release of LDH into the culture medium is directly related to the extent of cellular damage and thus cell death. Hence, the reduced LDH release in the MCF-7 cells as well as increased LDH release in SH-SY5Y cells upon treatment with the EGCG generated γ-Syn oligomers indicates the contrasting effects of EGCG on these two cell lines, where on one hand it is protective and on the other hand is toxic, respectively. Additionally the cytotoxic effects of the disaggregated γ-Syn oligomers on MCF-7 cells were also validated by the LDH assay. The disaggregated γ-Syn oligomers resulted in an increased release of LDH into the medium as compared to the disaggregated fibrils, thus establishing the membrane permeabilizing and membrane damaging effects of disaggregated γ-Syn oligomers on MCF-7 cells (Figure 21C).

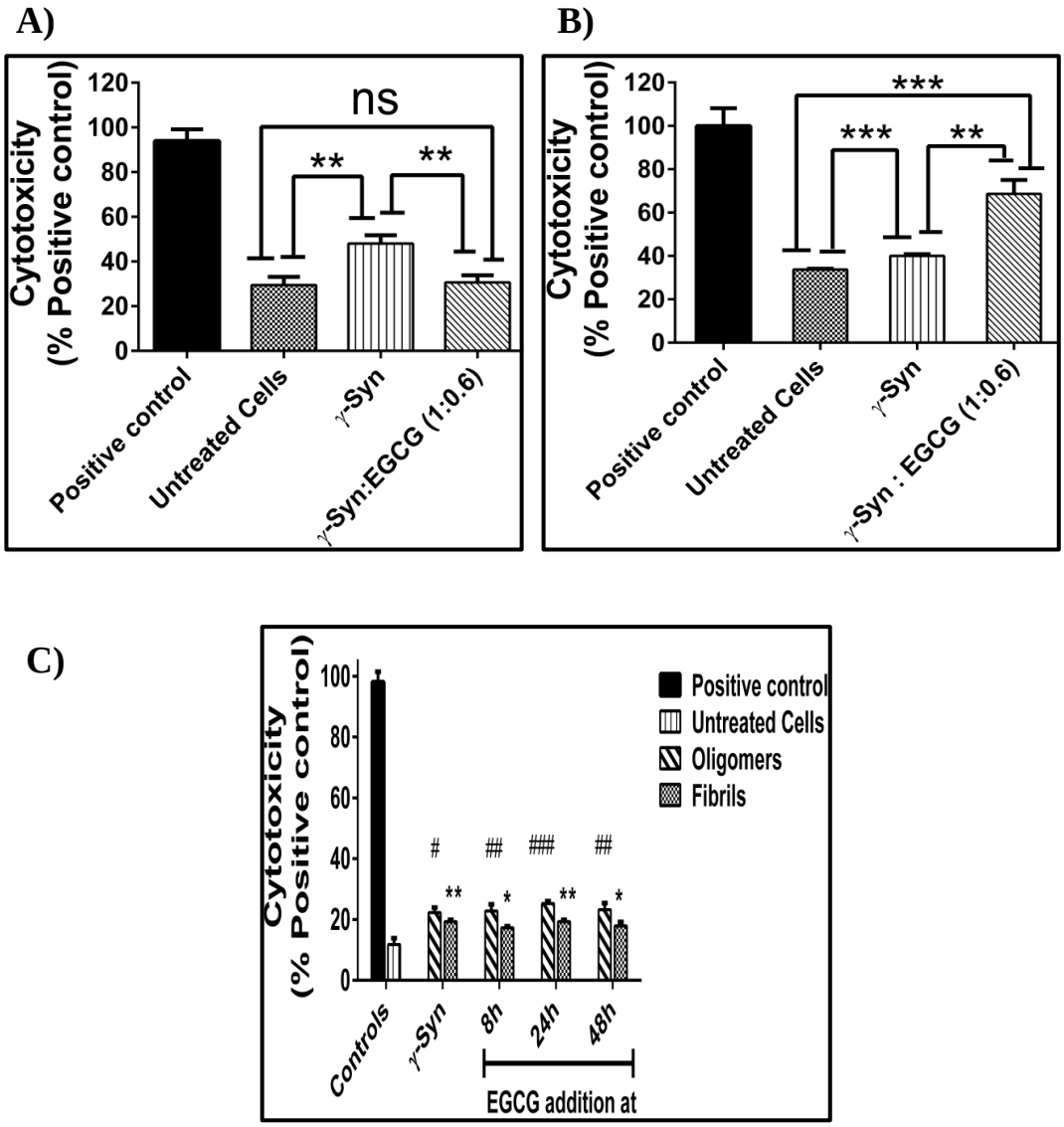

Figure 21. Cytotoxic effects of EGCG treated γ-Syn species on MCF-7 and SH-SY5Y cells monitored by LDH release assay. A) LDH assay on MCF-7 cells show an increased cytotoxicity in presence of γ-Syn oligomers (**p < 0.005 related to the untreated cells) which is completely rescued in the presence of EGCG generated oligomers (**p < 0.005 with respect to the γ-Syn treated cells). B) LDH assay on SH-SY5Y cells shows an increased cell death of SH-SY5Y cells in presence of EGCG-generated oligomers (***p < 0.0005 and **p < 0.005 related to untreated cells and γ-Syn treated cells, respectively). The statistical analysis was done using unpaired t-test. C) The cytotoxic effects of the disaggregated γ-Syn oligomers by LDH assay showing an increased cell death in the presence of EGCG-mediated disaggregated oligomers as compared to disaggregated fibrils (# and * denote the significant difference between the disaggregated oligomers and disaggregated fibrils with respect to untreated cells respectively). The statistical analysis was done using unpaired t-test and the error bars represent ±S.D. (n=3).

3. Discussion

EGCG has previously been reported to inhibit fibrillation of other amyloidogenic proteins such as α-Synuclein and Aβ peptide but at a ratio of 5 to 10-fold molar excess over protein concentration (Ehrnhoefer et al., 2008; Palhano et al., 2013) which in the case of γ-Syn interestingly suppresses 50% of fibrillation at a 15-fold less stoichiometry and a ratio of less than 1:1 is needed to bring complete inhibition (Figure 1A). The strong suppression of γ-Syn fibrillation by a significantly lower concentration of EGCG suggests that it acts on the nucleation phase of the pathway where it interacts with the nucleus or seeds present in low concentration as reported for small molecule mediated inhibition of Aβ fibrillation (Necula et al., 2007).

Size-exclusion chromatography of γ-Syn species formed in the presence of EGCG monitored under fibrillating conditions demonstrate that EGCG diverts the on-going fibrillation pathway and disaggregates the existing fibrils into two similar kinds of SDS-resistant higher ordered oligomers with apparent molecular weights of ~158 kDa and ~670 kDa (Figure 8 and 10), with the formation of larger oligomers (~ 670 kDa) favoured over the smaller ones. The disaggregation of the pre-existing fibrils and protofibrils of γ-Syn into SDS- resistant oligomers by EGCG, without forming amorphous aggregates, has also been reported for polyphenol Baicalein which shows a similar effect on mature fibrils of α-Syn (Zhu et al., 2004). The appearance of short and broken fibrils as observed in the TEM and AFM studies (Figure 6 and 7), further substantiates the attenuation of γ-Syn fibrillation at all the stages in the presence of EGCG as well as indicates EGCG mediated disaggregation. The light scattering results further demonstrate the formation of soluble aggregates as well as higher order oligomers by EGCG (Figure 2 and 11). The apparent molecular weight of monomeric γ-Syn was found to be ~44 kDa, an overestimated value which results from the natively unfolded nature of the intrinsically disordered protein (Golebiewska et al., 2014). The hydrodynamic radius (R_s) of the monomeric γ-Syn under the experimental conditions was found to be 28.7Å which is smaller than that estimated for a completely random coil form indicating compactness in the overall structure which in turn suggests a high self-associating tendency of γ-Syn, reported in previous studies as well (Uversky et al., 2002). The R_s values calculated by using the apparent molecular weight obtained from the SEC differ slightly from the R_s value calculated previously, possibly arising due to the differences in the

protein concentrations used, emphasizing the role of concentration dependent self association of γ-Syn. The gradual build up of γ-Syn oligomers during the exponential phase of the pathway and their subsequent decline by the end of fibrillation in the absence of EGCG (Figure 8B) demonstrates the transient nature of these highly reactive species which possibly remain in a dynamic equilibrium with the monomer and disassemble into unstructured monomers under denaturing conditions unlike the EGCG generated oligomers (Figure 10). Although the exact mechanism of EGCG induced stability of γ-Syn is still unclear, the effect of EGCG could be understood in light of a previous study where it is reported that the hydroxyl rich aromatic structure of EGCG could form stable hydrogen bonds with the unfolded polypeptide such as α-Synuclein and Aβ-peptide, thus establishing that intermolecular interactions facilitate the self assembly of the EGCG stabilised oligomers (Ehrnhoefer et al., 2008).

Seeding studies (Figure 12) reveal that the EGCG-generated γ-Syn oligomers act only as partial templates for monomer addition for fibril polymerization and are intermediates of the γ-Syn fibrillation pathway. The intermediate lag time observed in the presence of EGCG-treated seeds suggests that the EGCG-generated oligomers increase the kinetic barrier for nucleus formation and thus delays overall fibrillation by retarding nucleation. It is interesting to note that EGCG has been previously reported to modulate α-Syn fibrillation pathway into SDS- resistant, higher ordered oligomers which are off-pathway in nature (Ehrnhoefer et al., 2008) unlike the oligomers of γ-Syn, which are observed to be on-pathway in this study. Such contrasting effect of a polyphenol on two closely related members of the same family indicates the involvement of complex modulating mechanisms that needs to be further investigated. The inhibition of fibril polymerization by EGCG and the presence of short or partially polymerized fibrils formed in the presence of EGCG-generated γ-Syn seeds (Figure 12 and 13) further suggests the formation of kinetically retarded species by EGCG. Also, the shortened lag phase of γ-Syn fibrillation in the presence of preformed seeds (Figure 12) indicates a nucleation dependent polymerization mechanism as also seen in α-Syn fibrillation (Uversky et al., 2002).

Since the presence of EGCG shifts the equilibrium towards formation of oligomeric species, it is also suggested that EGCG favours conformations that have less likelihood of being the precursors for γ-Syn fibrillation. Far-UV CD analysis

and ANS binding studies reveal stabilization of natively unfolded conformation in presence of EGCG, depicted by a negative ellipticity at ~198 nm (Figure 14A) and a weak ANS fluorescence intensity (Figure 15A), corresponding to the low mean hydrophobicity of these intrinsically disordered proteins (Uversky, 2011). It is well established that formation of β-sheet is a signature for amyloid fibrils (Klunk et al., 1989; Simmons et al., 1994; Chiti, Taddei, et al., 2002) and an increase in the hydrophobicity is one of the important physicochemical properties that is known to be involved in driving the formation of β-sheet structures leading to the build-up of toxic oligomeric species (Chiti, Taddei, et al., 2002; Pawar et al., 2005; Bolognesi et al., 2010; Campioni et al., 2010). It is observed in this study that the formation of characteristic β-sheet structures in γ-Syn during fibrillation is significantly delayed by an increasing concentration of EGCG which is also accompanied by the gain of an α-helical propensity (negative ellipticity and double minima at ~208 nm and ~221nm) (Figure 14B). Supporting these results, an enhanced ANS fluorescence intensity upon its binding with the aggregating species of γ-Syn indicates the formation of a molten-globule like state, a prerequisite for intrinsically disordered proteins for the formation of fibrils, (Uversky, 2008) which is substantially diminished in the presence of EGCG (Figure 15B). The α-helical propensity of γ-Syn oligomers as observed by far-UV CD studies further highlights the increased structural stability of these oligomers that demonstrates their role in inhibiting the maturation of γ-Syn fibrils (Figure 14C).

Formation of an α-helical structure by small molecule ligands in Aβ-peptide has also been reported to reduce Aβ-oligomer toxicity (Nerelius et al., 2009). The increased tendency of γ-Syn to form α-helical structure in its amyloid forming region, is reported to be an intrinsic property that can be induced under various conditions making it less prone to fibrillation compared to α-Syn which possess a high β-sheet forming propensity in that region (Marsh et al., 2006). The results such as immediate oligomerization upon EGCG addition (Figure 8), also depicted by an early increase in the light scattering intensity (Figure 2), clearly suggests that the EGCG mediated γ-Syn oligomerization occurs spontaneously and is relatively faster than γ-Syn amyloidogenesis alone which agrees with the theory of competitive binding (Gosal et al., 2005; Ehrnhoefer et al., 2008). In the light of this theory, it is proposed that EGCG competes out the self-associating unfolded γ-Syn monomers binding preferentially with the unstructured oligomers, and thereby reducing the

formation of β-sheet containing species and remodelling the pathway to form kinetically retarded α-helix containing oligomeric species majorly divided into two higher-ordered forms.

The binding interaction between EGCG and γ-Syn, using the steady-state and time-resolved fluorescence spectroscopy and further validated by isothermal titration calorimetry reveal the role of weak non-covalent interactions between EGCG and γ-Syn that result in significant modulation of the γ-Syn fibrillation pathway. The lone tyrosine present in γ-Syn shows a characteristic tyrosinate emission at 342nm, as has also been observed for unfolded histone H1 protein containing single tyrosine (Libertini and Small, 1985). The quenching of tyrosine fluorescence in presence of increasing concentration of EGCG at 25 °C (Figure 16A and B), with a bimolecular quenching constant higher than the diffusion controlled value ($k_q > 10^{10}$ M^{-1}) and the lifetime decay profiles of γ-Syn showing negligible change in the presence of EGCG under non-aggregating conditions (Figure 17A and Table 2), establish a static quenching mechanism indicating a complex formation between γ-Syn and EGCG.

Isothermal titration calorimetry of γ-Syn binding to EGCG further reveals a weak binding affinity with a dissociation constant in the mM range. In agreement with this, the association constant (K_a) deduced from the modified Stern-Volmer plot (Figure 16C) obtained from steady-state fluorescence studies also reveals a weak binding affinity between EGCG and γ-Syn, although estimating a ~10-fold higher value than that observed by ITC. This is likely due to the nature of two techniques, wherein fluorescence relies on the single tyrosine probe and ITC is based on measuring global heat changes. The steady-state fluorescence spectra of different aggregating species of γ-Syn in presence of EGCG further reveal a higher affinity of EGCG towards oligomers of γ-Syn (Table 1 and Figure 16C), substantiating the observation made by SEC (Figure 8C). Additionally, the conformational dynamicity of these oligomers as studied by time-resolved fluorescence spectroscopy under fibrillating conditions (Figure 17C) reveals a time-dependent decrease in the overall structural dynamicity in the EGCG-generated γ-Syn oligomers which upon prolonged fibrillation becomes more structured, thus supporting the gain of an α-helical propensity in EGCG-generated oligomers during fibrillation (Figure 14B). The faster decay kinetics of untreated γ-Syn oligomers during fibrillation (Figure 17C), as also supported by the retention of natively unfolded conformation of γ-Syn

oligomers observed by far-UV CD (Figure 14C) suggests the increased structural dynamicity of the oligomers of γ-Syn. This suggest that EGCG promotes the formation of conformationally restrained, α-helical structure by perturbing the local conformations in the natively unfolded γ-Syn to become more solvent exposed during the early stages of fibrillation which is depicted by faster fluorescence decay in the EGCG-generated oligomers during the initial stages of fibrillation.

One of the important aspects of small molecule mediated modulation of fibrillation pathways is to investigate their cytotoxic effects as the oligomers and the protofibrillar intermediates formed during amyloidogenesis have previously been reported to be more toxic than the mature fibrils (Bucciantini et al., 2002; Caughey and Lansbury Jr, 2003; Ferreira et al., 2007). Given the fact that γ-Syn is involved in both cancer and neurodegeneration, the study compares the cytotoxic effects of EGCG-generated γ-Syn oligomers on breast cancer (MCF-7) and neuroblastoma (SH-SY5Y) cells, taken as representatives of the diverse diseases, respectively. The increase in cell viability of MCF-7 cells (Figure 19A and 21A) and a reduction in the viability of SH-SY5Y cells (Figure 20A and 21B) in the presence of EGCG-generated oligomers points toward the cell-specific behaviour of γ-Syn that could possibly play a critical role in the propagation of such diseases. This also highlights the complexities in the use of EGCG and other polyphenols in the prevention of synucleopathies and needs further exploration.

Furthermore, the mature fibrils of several amyloidogenic proteins have also been known to disaggregate under several conditions such as prolonged incubation during fibrillation (Cremades et al., 2012), changes in pH (Picotti et al., 2007) and addition of chemical denaturants (Calamai et al., 2005). The toxic characteristics of the disaggregated oligomers playing a role in pathogenesis has also been observed previously (Cremades et al., 2012). The reduction in the viability of MCF-7 cells in the presence of EGCG-disaggregated species (Figure 19B and 21C) suggests that γ-Syn gains toxic characteristics early during nucleation phase which otherwise in the presence of EGCG at earlier stages fails to form toxic oligomeric intermediates (Figure 19A). Interestingly, significant toxicity of the disaggregated oligomers observed against the partial toxicity of the fragmented fibrils (Figure 19B and 21C) demonstrates the increased membrane permeabilizing ability of γ-Syn oligomers as compared to the disaggregated fibrils, thus imparting cell damaging effects, eventually causing cell death. This observation in turn highlights the critical role of

the length and physical structure of the amyloid species in possibly affecting their cellular permeability and in turn governs their cytotoxicity. A relationship between the fibril length and the amyloid toxicity has also been reported previously for amyloidogenic proteins like β_2m, lysozyme and α-Synuclein where a reduction in the fibril length by fragmentation was associated with increased cytotoxicity (Xue et al., 2009). These results suggest that several factors such as the stage of inhibition, morphology of the aggregating species as well as the cell type together play a role in governing the toxicity of these species. A schematic representation illustrating the EGCG-mediated modulation of γ-Syn fibrillation pathway is shown in Figure 22.

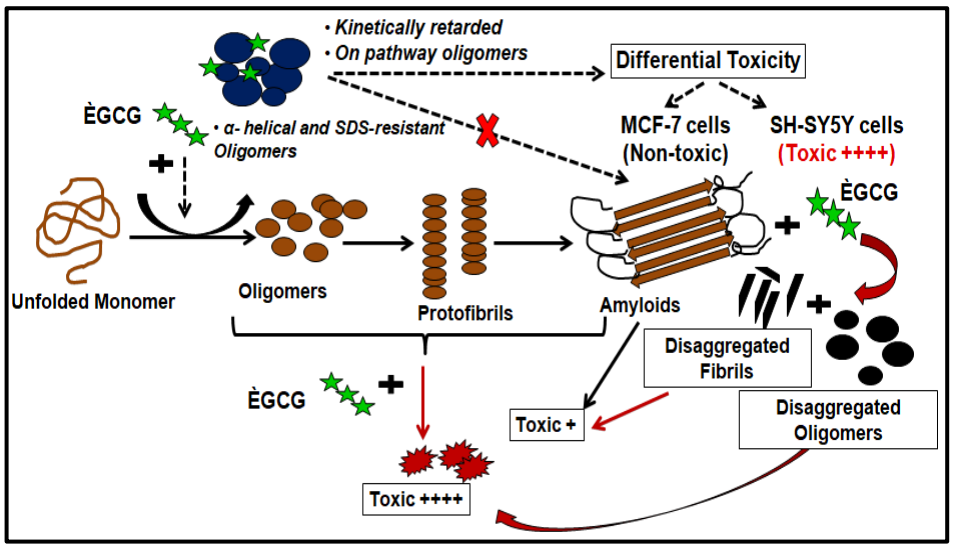

Figure 22. A schematic representation of the mechanism of EGCG–mediated modulation of γ-Syn fibrillation pathway. The figure illustrates the mechanism of EGCG-mediated modulation of γ-Syn fibrillation pathway. The *black arrows* (⟶), represent γ-Syn fibrillation pathway in the absence of EGCG, the *black dashed arrows* (⇢), represent EGCG modulated γ-Syn fibrillation pathway and the *red arrows* (⟶), depict disaggregation pathway of γ-Syn in the presence of EGCG. The cytotoxic effects of both EGCG untreated and treated γ-Syn species are denoted by ++++ and +, for highly toxic and partially toxic effects respectively.

Chapter 3.2

Effect of Quercetin on the Structure and Aggregation of γ-Synuclein

1. Background

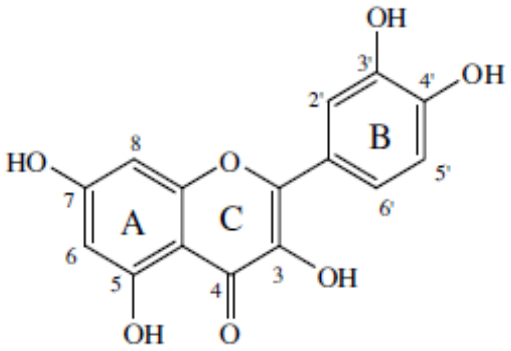

Chemical Structure of Quercetin

Quercetin (3, 3′, 4′, 5, 7-pentahydroxylflavone) is the most widely studied flavonoid that comprises 65-70% of dietary flavonoid and has beneficial effects in wide range of diseases such as cancer therapy, neurodegenerative diseases, cardiovascular diseases, inflammatory diseases etc. (Dajas, 2012; Suganthy et al., 2016). Quercetin was first isolated in the year 1936 by the physiologist Albert Szent-Györgyi de Nagyràpolt, winning the Nobel Prize in the field of physiology and medicine (Suganthy et al., 2016). Quercetin is ubiquitously present in most plants, fruits, vegetables, nuts, grains, phenolic acids and alcohols. Red wine and tea infusions are considered to be the richest sources of quercetin that contain highest concentrations ranging from 4 - 16 and 10 - 25 mg/l respectively (Suganthy et al., 2016).

The chemical structure of quercetin comprising of five hydroxyl groups which includes the 3′,4′ dihydroxy structure in the B-ring and 2,3 double bond in the C-ring with 4-oxo function confers the compound a high antioxidant property (X. Meng et al., 2009) that also is responsible for most of its pharmacokinetic properties. Quercetin has been demonstrated to have both anticancer and neuroprotective properties which are extensively documented in reviews published previously (Ossola et al., 2009; Dajas, 2012). The direct oxygen scavenging role of quercetin has been demonstrated to be responsible that protects neuronal cells from ROS mediated damage and prevent neurodegeneration (Dajas, 2012). Oxidative stress has been indentified to be the major cause of neurodegenerative diseases such as Parkinson's disease, Alzheimer's disease etc., where the accumulation of reactive oxygen species lead to neuronal cell loss and dysfunction (Zhu et al., 2013). Among many neuroprotective effects, quercetin has been reported to protect the neuronal SH-SY5Y cells from the H_2O_2 induced apoptotic damage (Suematsu et al., 2011), reverse the histopathological features of Alzheimer's disease (AD) by ameliorating

the cognitive and emotional impairments in disease mice model (Sabogal-Guáqueta et al., 2015), inhibit fibrillation of many amyloid forming proteins and disaggregate the preformed fibrils of proteins such as α-Synuclein (X. Meng et al., 2010; Zhu et al., 2013), Aβ-peptide (H. Kim et al., 2005; Jiménez-Aliaga et al., 2011), bovine insulin (Wang et al., 2011) etc.

The involvement of γ-Syn in both neurodegeneration and cancer makes it an important target for investigation of the inhibitory effects of quercetin on γ-Syn fibrillation. The study demonstrates a concentration- dependent inhibition of γ-Syn fibrillation as well as disaggregation with absence of complete suppression. Quercetin preferentially binds with the oligomeric species of γ-Syn formed in the exponential phase of the pathway by a strong binding interaction (k_d ~ μM) and modulates the pathway to form SDS-labile species that are less fibrillogenic and off-pathway in nature. It is shown that quercetin does not affect the overall secondary structure of γ-Syn but maintains an overall low surface hydrophobicity of γ-Syn that possibly decelerates fibrillation. Interestingly, the quercetin generated species (fibrils and compact species) although off-pathway in nature were observed to be toxic to both the breast cancer (MCF-7) and neuroblastoma (SH-SY5Y) cells, providing the evidence for the toxic characteristics of the small molecule generated mature fibrils compared to the oligomeric counterparts. The study observes a high cytotoxic effect of lone quercetin on both the cell lines cautioning the use of quercetin as a universal therapeutic against both neurodegeneration as well as cancer. Lastly, the study suggests that the small molecule mediated intervention of fibrillation leading to inhibition may not always be desirable to combat adverse effects of amyloid-borne diseases and cancer.

2. Results

2.1. Effect of Quercetin on the fibrillation kinetics of γ-Syn

2.1.1 Thioflavin T Assay

The fibrillation kinetics of recombinant human γ-Syn in the presence of increasing concentration of quercetin (5-50μM) was monitored using Thioflavin T (ThT) fluorescence. Monomeric γ-Syn was incubated under fibrillating conditions in the presence of quercetin dissolved in 1% DMSO and the ThT fluorescence was measured at regular time intervals during fibrillation. As shown in Figure 1, the ThT

fluorescence was found to decrease in the presence of quercetin in a concentration dependent manner. Although a significant decrease in ThT fluorescence was observed in the presence of quercetin, a complete suppression of fibrillation was not observed at any concentration. Upon saturation, approximately 30% of the amyloid was bound to ThT compared to the amyloid formed by the untreated γ-Syn, indicating ~70% reduction in fibrillation in the presence of 50μM quercetin. These results suggest an inhibitory effect of quercetin on γ-Syn fibrillation.

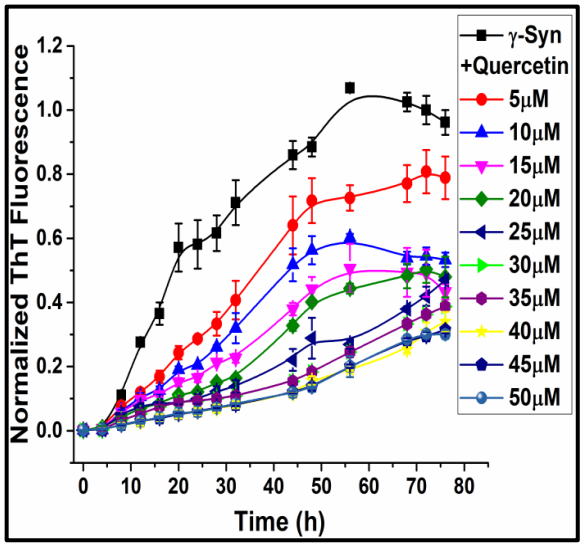

Figure 1. Fibrillation kinetics of γ-Syn in the presence of increasing concentration of Quercetin by Thioflavin T assay. Monomeric γ-Syn was incubated in the presence of increasing concentration of quercetin (5- 50μM) under fibrillating conditions and the ThT fluorescence was recorded at regular interval of time. The concentration dependent decrease in the ThT fluorescence in the presence of quercetin showed fibrillation inhibition. The error bars represent the ±SD (n=3).

2.1.2 Light scattering by γ-Syn species formed during fibrillation in the presence of quercetin

The presence of exogenous compounds such as polyphenols due to their strong absorptive and fluorescent properties are reported to interfere with the ThT fluorescence assay, leading to quenching of ThT fluorescence (Hudson et al., 2009). The effect of quercetin on the fibrillation propensity was thus also validated by Rayleigh scattering. γ-Syn was incubated under fibrillating conditions in the presence of an increasing concentration of quercetin and the scattering intensity was recorded at regular intervals during fibrillation. The concentration dependent

decrease in the scattering intensity as shown in Figure 2, clearly demonstrated inhibition of γ-Syn aggregation by quercetin, however as observed in the ThT assay complete suppression even at 50μM was not observed.

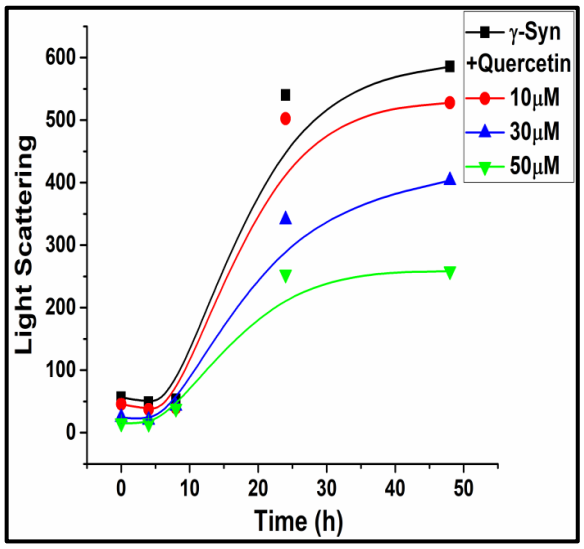

Figure 2. Light scattering by γ-Syn species formed in the presence of an increasing concentration of Quercetin. The concentration-dependent decrease in the scattering intensity shows inhibition of aggregation by quercetin. γ-Syn was incubated with increasing concentration of quercetin (10, 30 and 50μM) and incubated at 37 °C, 200 rpm. The scattering intensity was recorded using a quartz cuvette of 1 cm path length at $\lambda_{ex}=\lambda_{em}$ at 350 nm.

2.1.3 Transmission Electron Microscopy of γ-Syn fibrils formed in the presence of Quercetin

The morphology of the γ-Syn fibrils formed in the absence and presence of quercetin was analyzed by negatively stained images using transmission electron microscopy (TEM). As shown in Figure 3, the untreated γ-Syn formed thick intertwined fibrils upon completion or saturation stage of fibrillation. In the presence of quercetin, a concentration- dependent disappearance of mature γ-Syn fibrils was observed thus indicating inhibition of γ-Syn fibrillation by quercetin.

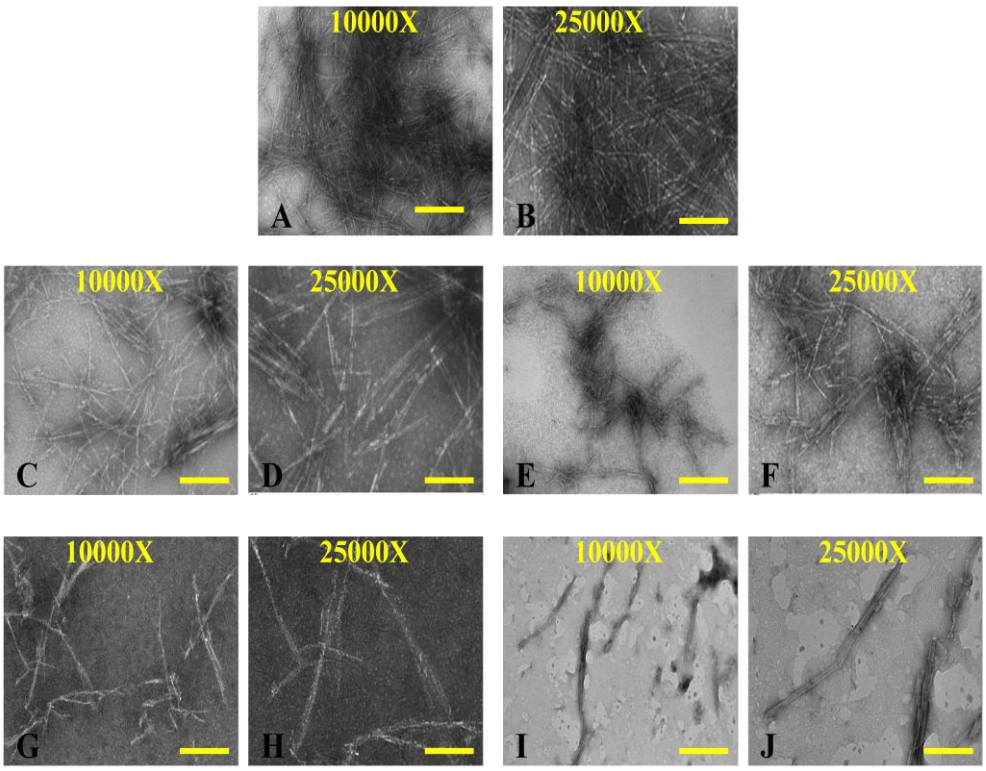

Figure 3. Morphology of γ-Syn fibrils formed in the presence of Quercetin visualized by transmission electron microscopy. TEM images of γ-Syn fibrils formed upon saturation (end of fibrillation) in absence of Quercetin (A, B) and in presence of 5μM (C, D), 30 μM (E, F), 40 μM (G, H) and 50 μM (I, J) Quercetin respectively. Scale bar: 100nm.

2.1.4 Atomic Force Microscopy (AFM) of γ-Syn fibrils formed in presence of Quercetin

The morphology of the γ-Syn fibrils formed in the presence and absence of quercetin was also studied by AFM analysis (Figure 4). The AFM analysis clearly demonstrated the formation of long intertwined fibrils in the untreated γ-Syn (control) with the average height of fibrils ~11 nm. In the presence of quercetin, a concentration dependent disappearance of mature fibrils was observed. At a higher concentration of quercetin (50 μM), the average height of the fibrillar species were reduced to ~7 nm, indicating inhibition of fibrillation. In the presence of 30 μM of quercetin, there were appearances of small spherical as well as fragmented protofibrillar species, resulting in amorphous aggregate formation with an increased height of ~17 nm. These results thus establish the inhibitory effect of quercetin on γ-Synuclein fibrillation.

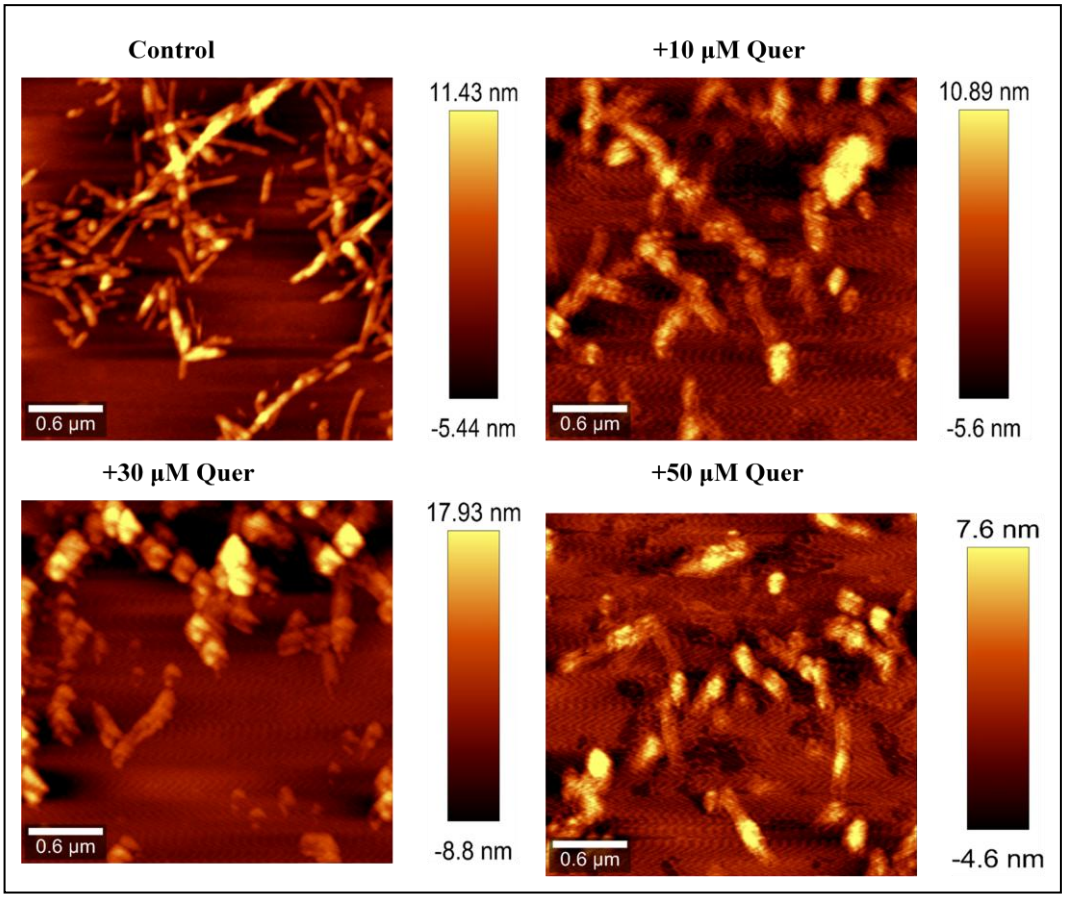

Figure 4. AFM images of the γ-Syn species formed in the presence of an increasing concentration of quercetin. The AFM images showing a concentration-dependent disappearance of mature fibrils in the presence of quercetin (*left to right*: control and in the presence of 10, 30 and 50 µM quercetin respectively).

2.2. Effect of Quercetin on different stages of γ-Syn fibrillation:

2.2.1 Thioflavin T Assay

To investigate the effect of quercetin on different stages of γ-Syn fibrillation, quercetin (50µM) was added to the incubation sample at different time intervals (8, 24 and 48h) which correspond to the lag, log and exponential phase of fibrillation**.** The ThT fluorescence was recorded at regular intervals immediately after adding quercetin at above mentioned time-points. Upon addition of quercetin, an immediate drop in the ThT fluorescence was observed which was followed by an overall decrease in ThT fluorescence during fibrillation (Figure 5). The drop in the ThT fluorescence immediately upon addition of quercetin could be due to the known interference between ThT and coloured polyphenols like quercetin (Hudson et al., 2009). However, the successively reduced ThT fluorescence in the later stages

suggested attenuation of fibril polymerization and disaggregation of mature γ-Syn fibrils by quercetin. The disassembly of the mature γ-Syn fibrils under the effect of quercetin was also further confirmed by the light scattering assay as mentioned below.

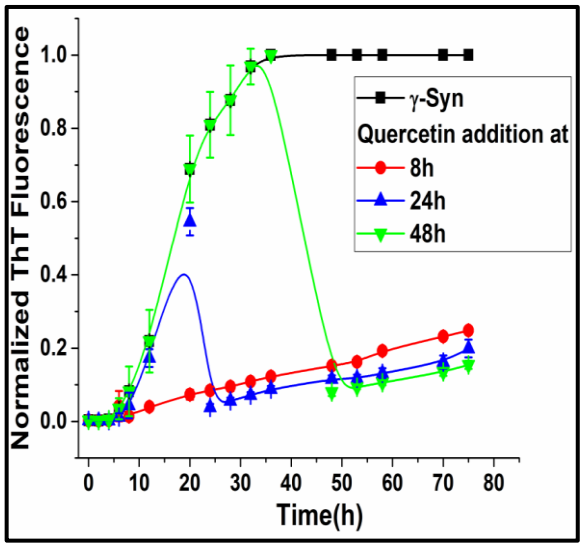

Figure 5. Fibrillation kinetics of γ-Syn upon addition of quercetin at different stages of fibrillation studied by ThT assay. The decrease in the ThT fluorescence upon addition of quercetin (50μM) at lag, log and saturation phase of fibrillation (8, 24 and 48h respectively) suggested attenuation of fibrillation and fibrillar disaggregation by quercetin. The error bars represent ±SD (n=3).

2.2.2 Light scattering by γ-Syn species formed after addition of quercetin at different stages of fibrillation

The fibrillation samples used above for the ThT assay were further analyzed by light scattering assay. The scattering intensities of the fibrils formed at the end of fibrillation with quercetin added at 8, 24 and 48h of fibrillation showed a reduced scattering at all the time points with respect to control suggesting inhibition of protofibrillar polymerization and disaggregation of mature γ-Syn fibrils in the presence of quercetin (Figure 6). Also, the scattering intensity was found to decrease in the order of 8h >24h > 48h of quercetin addition demonstrating pronounced effect of quercetin on the saturation stage of fibrillation leading to disaggregation of mature γ-Syn fibrils into smaller structures.

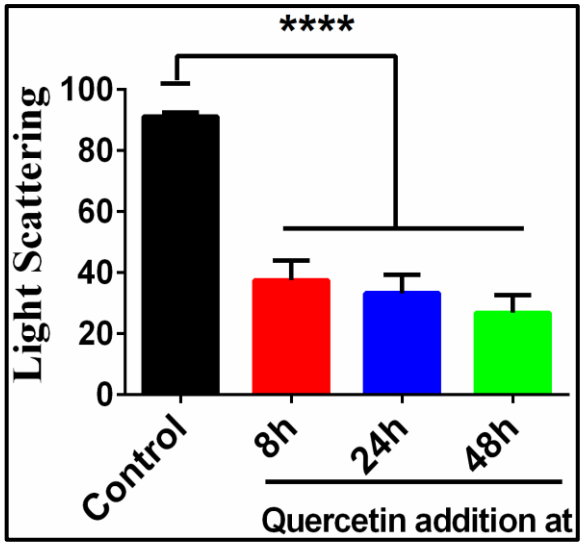

Figure 6. Rayleigh light scattering by γ-Syn species formed after addition of quercetin at different stages of fibrillation. The scattering intensity by the γ-Syn species formed at saturation after addition of quercetin at different stages (8, 24 and 48h) of fibrillation, recorded at an $\lambda_{ex}=\lambda_{em}$ ($\Delta\lambda=0$) using a 1 cm quartz cuvette showed a significant reduction in the scattering intensity at all the time points with respect to control (****$p < 0.0001$), indicating disaggregation pre-formed protofibrils and fibrils by quercetin. The statistical analysis was performed using unpaired t-test. The error bars represent ±SD (n=3).

2.2.3 TEM images of γ-Syn fibrils formed upon addition of quercetin at different stages of γ-Syn fibrillation

The morphology of the γ-Syn species formed upon addition of quercetin at above mentioned time-points of fibrillation were also studied by TEM images (Figure 7). The untreated fibrils of γ-Syn as also observed previously formed dense network of mature fibrils. The γ-Syn fibrils formed upon addition of quercetin at 8 and 24h of fibrillation although showed network of long fibrils, the fibrillar yield with respect to untreated fibrils was found to be much reduced. At 48h of quercetin addition, short and disintegrated fibrillar species were observed with an absence of mature fibrils, thus clearly demonstrating disaggregation of mature γ-Syn fibrils by quercetin.

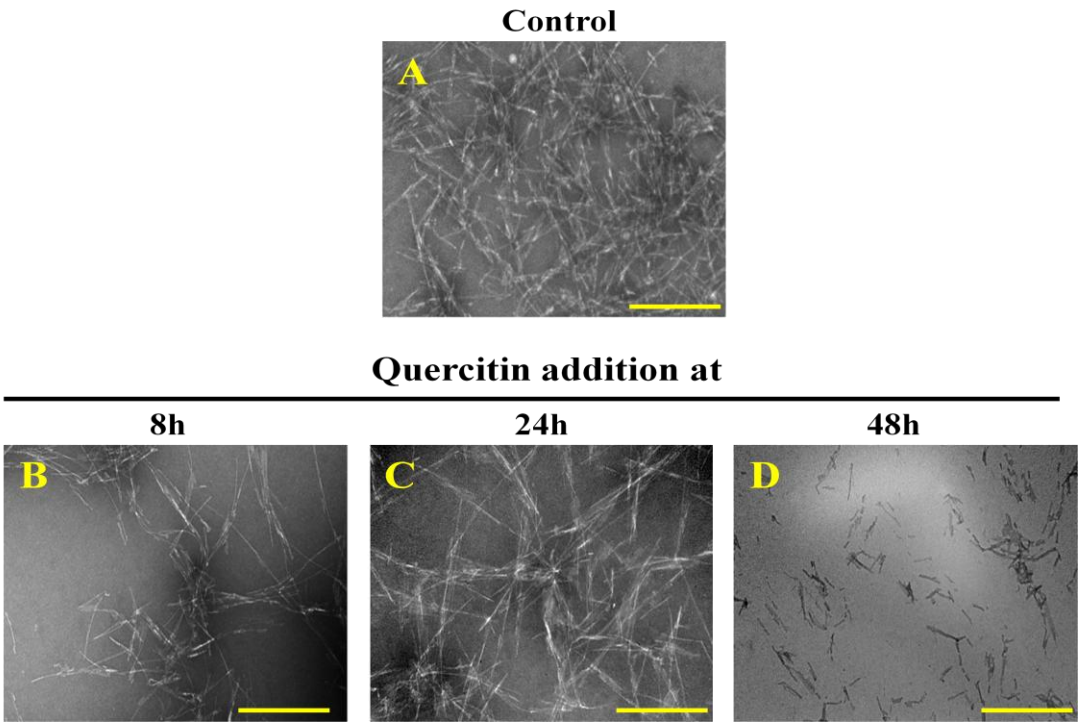

Figure 7. Transmission electron microscopy images of fibrils formed upon addition of quercetin at different stages of fibrillation. Morphology of the fibrils observed in absence of quercetin addition, *(upper panel):* Control and upon addition of quercetin at *(left to right):* 8h, 24h and 48h respectively. Addition of quercetin at all three time-points (8, 24 and 48h) showed diminished fibrils and disaggregation of mature γ-Syn fibrils at 48h of quercetin addition. A 100-nm scale bar is shown for comparison. A magnification of 10,000 X was used for all the images.

2.2.4 AFM analysis of γ-Syn fibrils formed upon addition of quercetin at different stages of fibrillation

The morphology of the fibrils formed upon addition of quercetin at different stages of γ-Syn fibrillation was further studied by AFM analysis (Figure 8). The γ-Syn fibrils formed in the absence of quercetin showed long fibrillar networks with an average height ranging between 12 – 15 nm. Upon addition of quercetin at 8h (lag phase) of fibrillation, there was an appearance of numerous oligomeric and protofibrillar structures with an average height between 9-10 nm. This indicated an attenuation of nucleation and thus fibril polymerization, when quercetin is added in the early stages of γ-Syn fibrillation. Addition of quercetin during the exponential phase of fibrillation (24h) formed isolated fibrils lacking dense networks along with the appearance of short protofibrillar species, indicating inhibition of elongation and

fibril disaggregation. At 48h of quercetin addition, short and disintegrated fibrillar species were observed with a reduced average height ranging between 6-8 nm, demonstrating disassembly and dissolution of mature γ-Syn fibrils in the presence of quercetin. The results clearly demonstrate that quercetin effectively acts on all the stages of γ-Syn fibrillation and leads to inhibition of fibril polymerization at early and mid-stage of fibrillation while disaggregating preformed mature γ-Syn fibrils upon saturation.

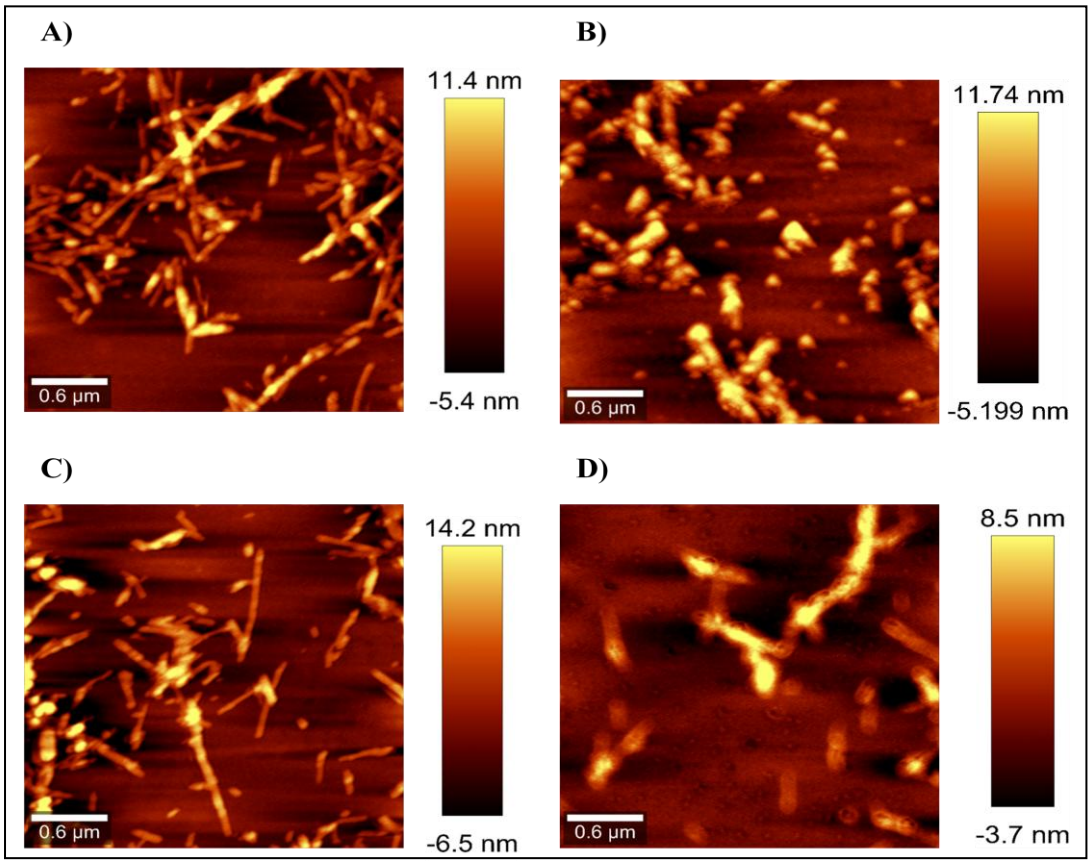

Figure 8. AFM analysis of γ-Syn species formed upon addition of quercetin at different stages of fibrillation. AFM images showing the morphology of the γ-Syn fibrils formed in the absence of quercetin addition (*A*) and disaggregation of γ-Syn fibrils upon addition of quercetin at 8, 24 and 48h of quercetin addition (*B to D,* respectively).

2.3 Modulation of γ-Syn fibrillation pathway in the absence and presence of quercetin:

In order to elucidate the mechanism of inhibition by quercetin, it was important to investigate the effect of quercetin on the population heterogeneity of γ-Syn species

formed during fibrillation and understand how quercetin modulate the fibrillation pathway of γ-Syn to bring inhibition.

2.3.1 Size-exclusion chromatography of γ-Syn fibrils formed in the presence and absence of quercetin

The SEC-HPLC analysis of the soluble fraction of the fibrillation reaction was carried out to investigate the population distribution among various γ-Syn species formed in the absence and presence of quercetin during fibrillation. The analysis was done at an absorption wavelength of 275 nm and 378 nm to record the absorbance of γ-Syn, indicating the heterogeneity of γ-Syn species formed during fibrillation and by recording quercetin absorbance indicating the affinity of quercetin to various species of γ-Syn respectively.

2.3.1.1 Absorbance monitored at 275 nm: The soluble fractions of γ-Syn obtained after centrifugation of the incubated γ-Syn samples during course of aggregation in the presence and absence of quercetin (50μM) were studied at regular time interval (0, 24 and 48h) of γ-Syn fibrillation and the SEC profiles monitored at 275 nm are shown in Figure 9A. The SEC profile of untreated γ-Syn both under native and fibrillating conditions is mentioned previously (Section 2.3.1.1, p.66). In the presence of quercetin (50μM), during exponential phase of the pathway (24h), a gradual rise in the oligomer peak at ~10.5 min along with an increasing peak eluting at ~22min was observed. By the end of fibrillation (48h), the SEC-profile of quercetin treated γ-Syn showed a substantial decrease in the oligomer peak as well as only a trace of monomeric species were present.

2.3.1.2 Absorbance monitored at 378 nm: To investigate the affinity of quercetin to different species of γ-Syn formed during fibrillation, the SEC analysis was carried out by monitoring absorbance at 378 nm, the absorbance wavelength for quercetin (Figure 9B). At 24h of fibrillation, a predominant rise in the oligomer peak was observed with a successive decline at saturation (Figure 9B). At 48h (saturation stage), slight rise in the peak eluting between 20-23 min was observed. This demonstrates that quercetin has a higher affinity toward the oligomeric species of γ-Syn.

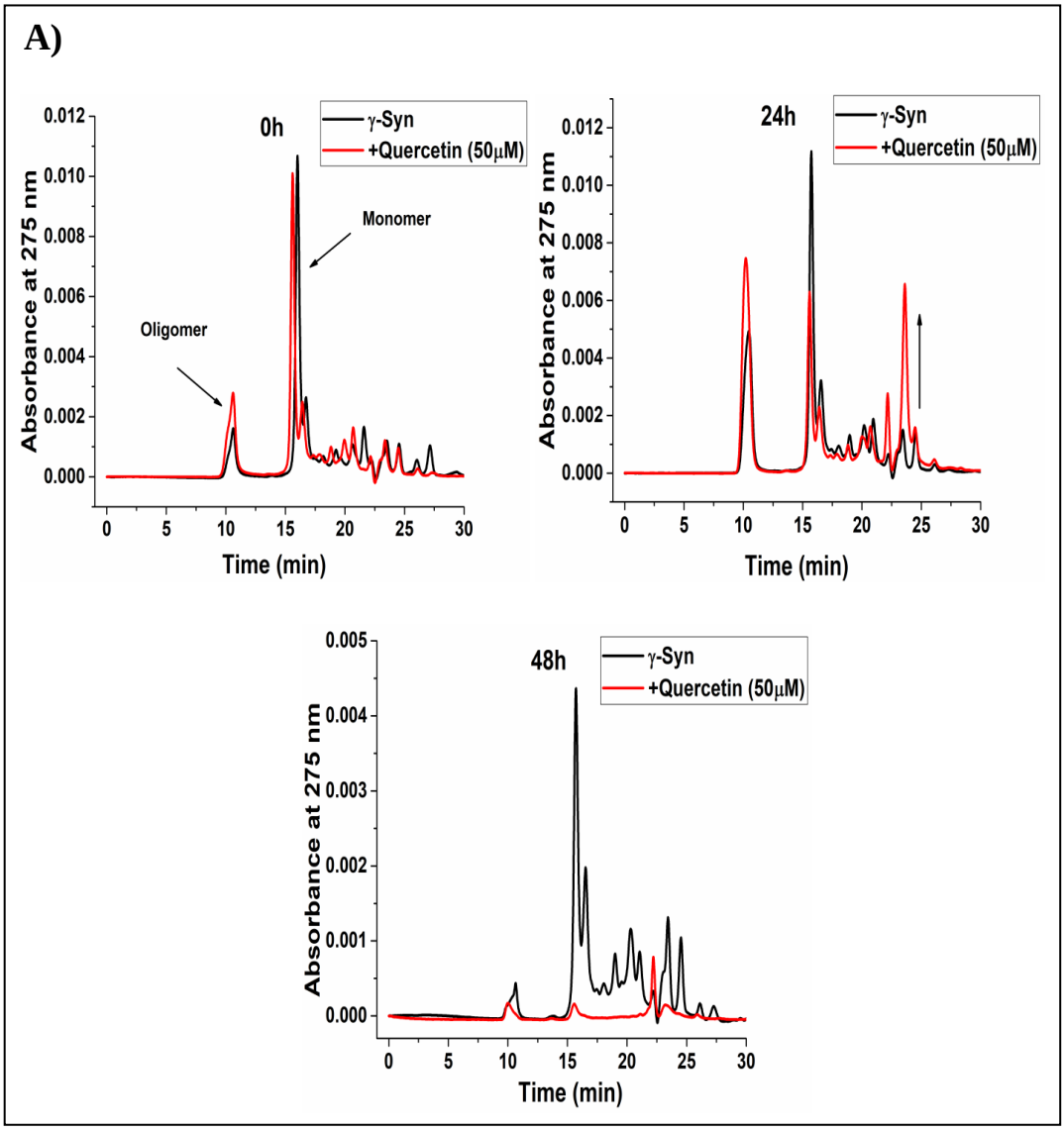
A)
0h
γ-Syn
+Quercetin (50μM)
Monomer
Oligomer
Absorbance at 275 nm
Time (min)
24h
γ-Syn
+Quercetin (50μM)
Absorbance at 275 nm
Time (min)
48h
γ-Syn
+Quercetin (50μM)
Absorbance at 275 nm
Time (min)

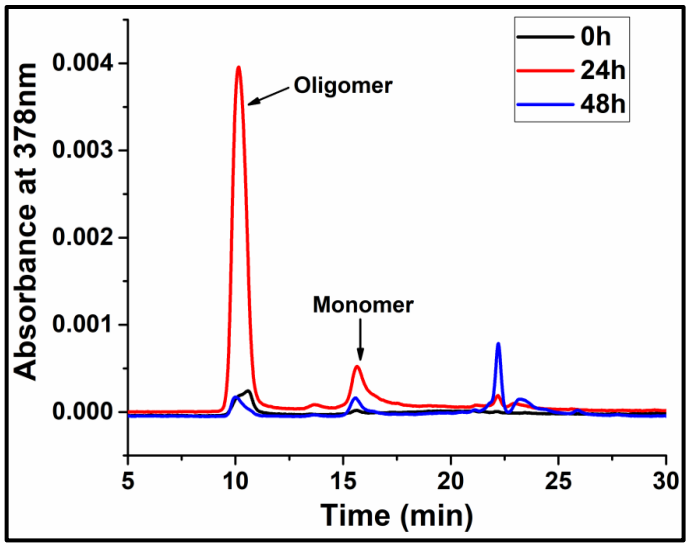
B)
0h
24h
48h
Oligomer
Monomer
Absorbance at 378nm
Time (min)

Figure 9. Size-exclusion chromatography of γ-Syn species formed in the presence and absence of quercetin. A) Size-exclusion profiles of γ-Syn species formed at different intervals (0, 24 and 48h) during fibrillation in the presence and absence of quercetin (50 μM). At 24h of fibrillation, an increase in the peak at ~23 min is shown with an *arrow* (⟶). (B) SEC profiles of quercetin bound γ-Syn species monitored at 378 nm, shows increased affinity of quercetin to oligomeric species of γ-Syn.

2.3.2 SDS - PAGE analysis

To investigate the nature of the γ-Syn species formed in the presence of increasing concentration of quercetin (30 and 50μM), SDS-PAGE analysis of the soluble and insoluble fraction of γ-Syn species formed after 48h of incubation was carried out. The supernatant was obtained after centrifugation at 14,000×g for 30 minutes. In the absence of quercetin, a thick fibrillar pellet band was observed which decreased in the intensity in the presence of increasing concentration of quercetin, indicating that majority of the soluble fraction (monomer and oligomers) of γ-Syn is converted to fibrils in the absence of quercetin. The soluble fraction was indistinguishable in the absence and presence of 30μM quercetin but in the presence of 50μM quercetin, the soluble fraction was not visible along with the reduced intensity in the pellet fraction. Since the SDS-stable species were not observed in the stacking gel in the fibrillar pellet formed in the presence of 50μM quercetin, the reason behind reduction of both soluble and insoluble fraction in the presence of 50μM quercetin needs to be further investigated. Overall, it is demonstrated that γ-Syn forms SDS-labile species both in the absence and presence of quercetin.

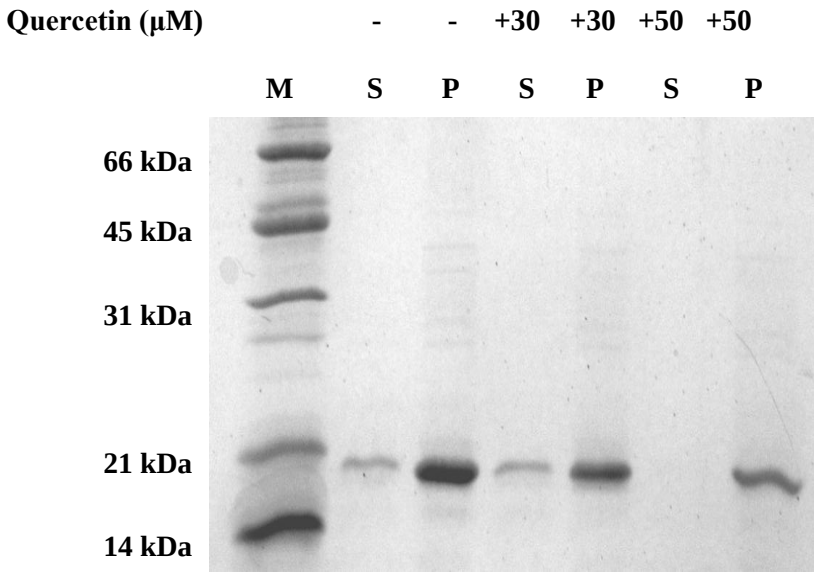

Figure 10. SDS- PAGE analysis of γ-Syn species formed in the absence and presence of increasing concentration (30 and 50 µM) of quercetin at 48h of fibrillation. The molecular weight marker is denoted by M and the soluble (supernatant) and the insoluble (pellet) fractions are denoted by S and P, respectively.

2.3.3 Dynamic light scattering

The soluble aggregates of γ-Syn formed in the presence of quercetin used for SEC-HPLC studies were further used to characterize their hydrodynamic properties by DLS. The summary of the mean particle size distribution of γ-Syn species formed in the presence of increasing concentration of quercetin at different time intervals is given in Table1. The hydrodynamic radii (R_h) of monomeric γ-Syn were measured to be around 28.08nm. On addition of quercitin an overall increase in the R_h of the γ-Syn species were observed.

Table I. Hydrodynamic Radii of γ-Syn Formed in the Presence of Quercetin

Conc. (μM) / Time(h)	0	10	30	50
	Hydrodynamic Radii (nm)			
0	28.08 ± 5.36 24.07 ± 1.50	6.90 ± 1.20 28.85 ± 3.00 17.00 ± 2.03	7.93 ± 1.40	8.31 ± 1.27 6.26 ± 0.70 31.07 ± 7.37
24	25.20 ± 4.46	16.91 ± 1.86	29.78 ± 6.31	33.77 ± 4.25 9.65 ± 1.88
48	29.00 ± 1.68 28.48 ± 1.47 9.02 ± 0.89	43.68 ± 2.67 37.88 ± 5.46 30.35 ± 5.66	39.63 ± 5.51 22.08 ± 4.20 22.87 ± 4.14	67.30 ± 16.03 51.86 ± 9.20 52.42 ± 8.44

2.4 Effects of Quercetin treated and untreated seeds on γ-Syn fibrillation pathway:

2.4.1 Fibrillation kinetics in the presence of quercetin-treated and untreated γ-Syn seeds by ThT assay:

To investigate whether the quercetin generated species act as template for γ-Syn polymerization and to understand the underlying mechanism of inhibition, the seeding studies were carried out. Preformed γ-Syn seeds formed in the absence and presence of quercetin (50 μM) were used to seed the monomeric γ-Syn and the fibrillation kinetics of monomeric γ-Syn in the presence and absence of seeds were monitored by ThT assay. As shown in Figure 11 (A and B), the lag time of fibrillation was significantly reduced in the presence of untreated γ-Syn seeds, a characteristics of nucleation-dependent polymerization mechanism as also mentioned previously (Section 3, p.92). The lag time of fibrillation in the presence of quercetin treated seeds showed a lag time shorter than the non-seeded but longer than the γ-Syn seeded kinetics. Although a difference in the lag time between the quercetin treated and non-seeded fibrillation was observed, it was found to be only

marginally significant (*p < 0.05), indicating that the quercetin generated species do not act as templates for γ-Syn fibrillation. Additionally the apparent rate (k_{app}) of γ-Syn fibrillation in the presence of quercetin- treated seeds and non-seeded fibrillation differed only marginally from each other (Figure 11C), indicating that the overall fibrillation remains unaffected in the presence of quercetin generated species. Thus the results suggest that quercetin-generated species are *off-pathway* in nature.

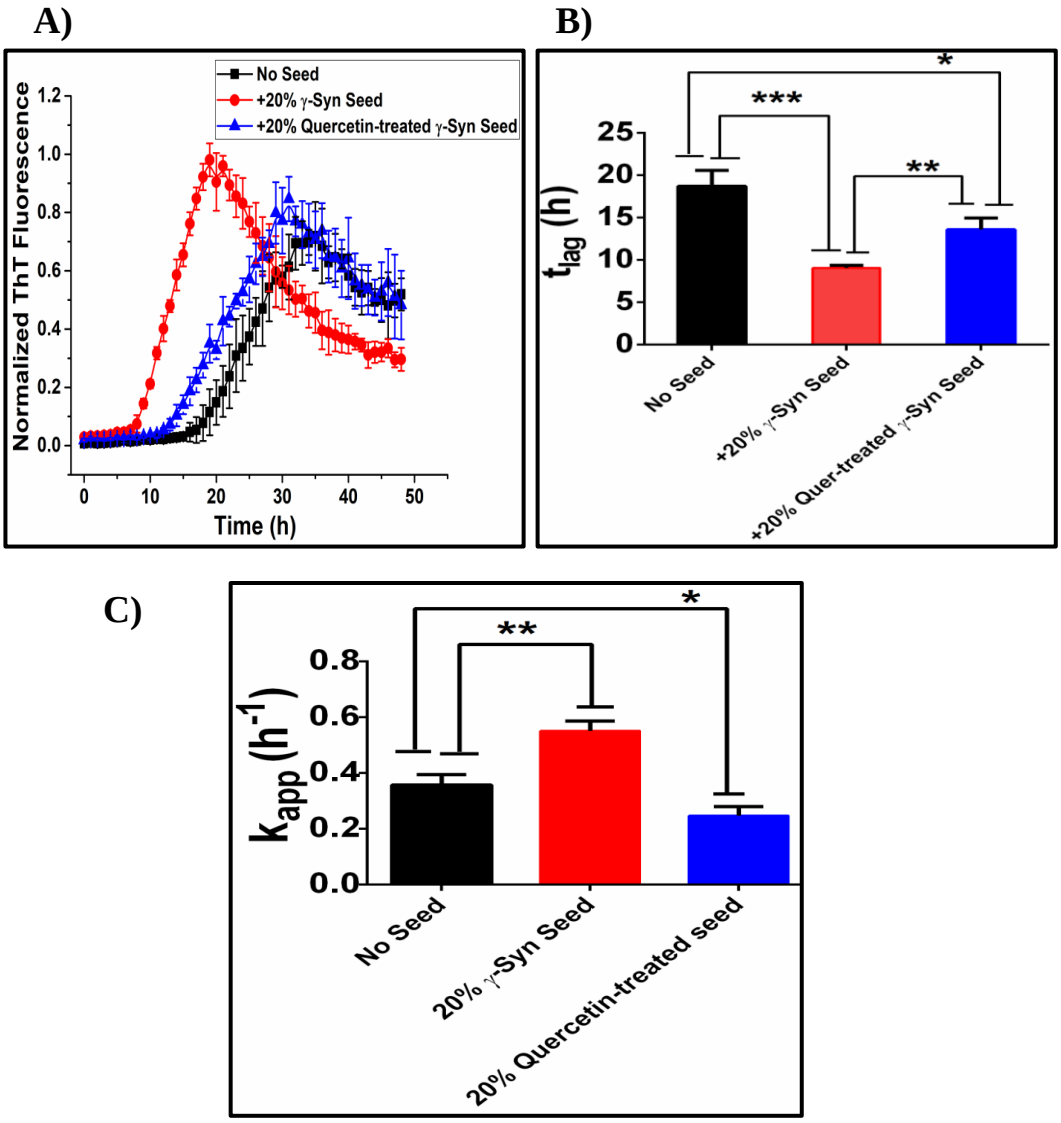

Figure 11. Fibrillation kinetics of γ-Syn in the presence of quercetin treated and untreated seeds studied by ThT assay. A) ThT assay in the presence of quercetin treated and untreated seeds showing a shortened lag time in the presence of untreated γ-Syn seeds (*red circle*) with respect to both non-seeded kinetics (*black square*) and quercetin treated γ-Syn seeds (*blue triangle*). Data shows a marginally reduced lag time of fibrillation in the presence of quercetin treated seeds with respect to non-seeded kinetics. B) Bar graph showing the significance of the difference in the lag time (t_{lag}) of fibrillation. The data shows

that the t_{lag} (h) is significantly reduced in the presence of untreated γ-Syn seeds (***p < 0.001, with respect to non-seeded reaction). The t_{lag} (h) of fibrillation in the presence of quercetin treated seeds is only marginally reduced (*p < 0.05) than the non-seeded fibrillation. C) Bar graph showing the significance of the difference in the apparent rate of fibrillation (k_{app}). The data shows that the rate of fibrillation is increased in the presence of untreated γ-Syn seeds as compared to non-seeded reaction (**p < 0.005), whereas the difference in the (k_{app}) (h^{-1}) between the quercetin –treated and non-seeded reaction was only marginally different (* p < 0.05), indicating that quercetin generated species are off-pathway in nature. The statistical analysis was performed using unpaired t-test and the error bars represent ±SD (n=3).

2.4.2 TEM images of γ-Syn species formed in the absence and presence of quercetin treated γ-seeds

The morphology of the γ-Syn species formed in the presence and absence of quercetin generated seeds was further was visualized by TEM studies (Figure 12). In the presence of untreated γ-Syn seeds, thick fibrils with well-defined boundaries were observed, whereas in the presence of the non-seeded γ-Syn, long and thinner fibrils were observed with reduced yield as compared to the seeded fibrils. In the presence of quercetin-generated seeds, significant reduction in the fibrillar yield was further observed with respect to both seeded and non-seeded γ-Syn. Thus, the formation of mature fibrils in the presence of quercetin-treated seeds suggest that quercetin inhibited species are *off-pathway* in nature.

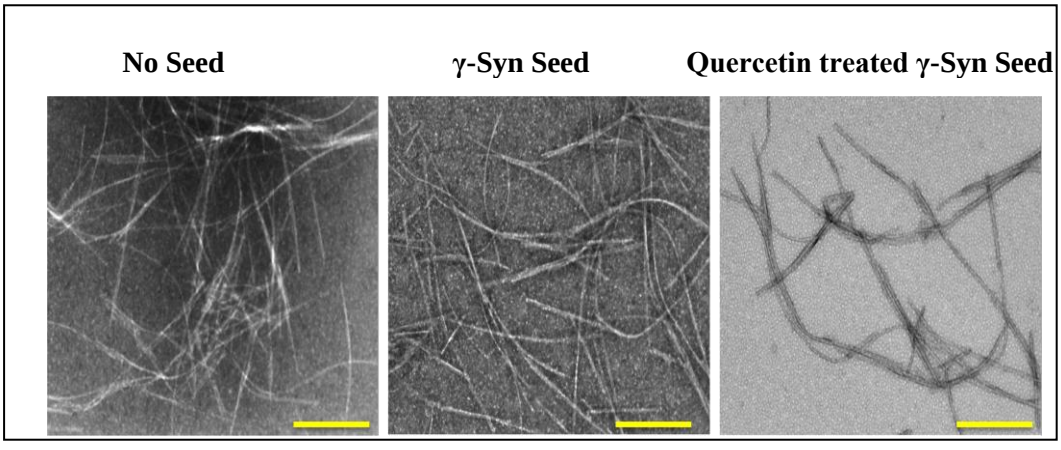

Figure 12. Transmission electron microscopy images of fibrils formed in presence of Quercetin-treated and untreated seeds. The TEM images showing the morphology of the fibrils formed (*left to right*: no seed, 20% (v/v) γ-Syn seed and 20% (v/v) Quercetin treated

γ-Syn seeds respectively) A magnification of 10,000 was used for all the images. (Scale bars, 100 nm).

2.5 Effect of quercetin on the structure of γ-Syn under both native and fibrillation conditions:

2.5.1 Far-UV CD analysis of γ-Syn in the presence of quercetin

To gain insight into the effect of quercetin on γ-Syn structure and fibrillation, circular dichroism spectroscopy of the γ-Syn species incubated with an increasing concentration of quercetin (10, 30 and 50 μM) under native and fibrillating conditions was carried out. Untreated and freshly prepared solutions of γ-Syn showed far-UV CD spectra of a typical natively unfolded conformation with a large negative ellipticity at ~200 nm and a small value at ~222 nm, which was also maintained at all the concentrations of quercetin used (Figure 13A). However, in the presence of higher concentration of quercetin (30 and 50 μM), a decrease in the negative ellipticity at ~200 nm was observed indicating a gain of secondary structure along with a decrease in the natively unfolded conformation in γ-Syn. The far-UV CD spectra of γ-Syn both in the absence and presence of quercetin, monitored after 24h and 48h of fibrillation (Figure 13B), showed a shift in negative ellipticity to 218 nm, indicating a structural transition from the natively unfolded conformation to a characteristic β-sheet structure.

A)

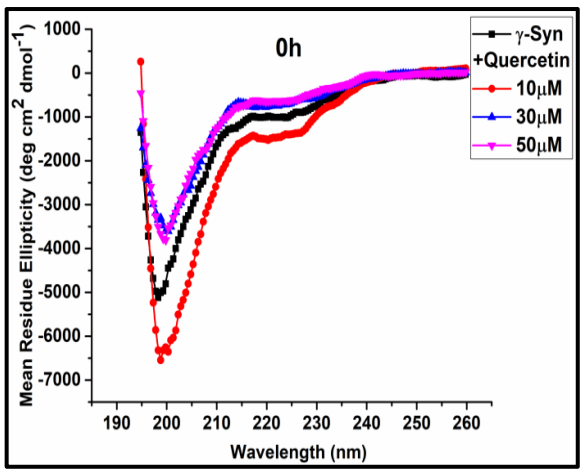

B)

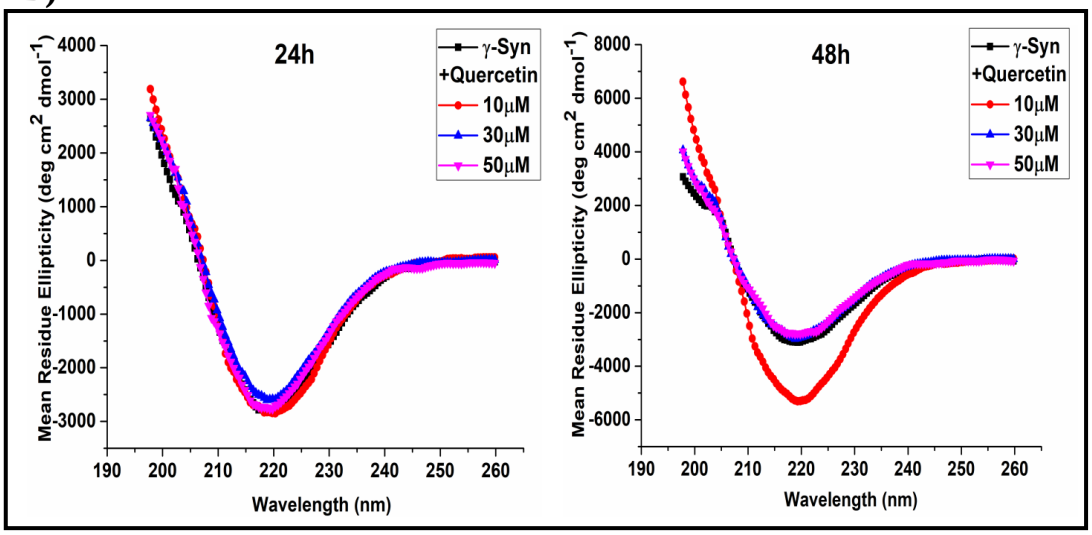

Figure 13. Far-UV CD spectra of γ-Syn in the presence of quercetin both native and fibrillating conditions. (A-B) The far-UV CD of γ-Syn in the presence and absence of quercetin under both native and fibrillating conditions respectively were monitored at 25 °C using a cuvette of 1mm path length. A) Far-UV CD spectra of γ-Syn (0.3 mg/ml) dissolved 20 mM phosphate buffer, pH-7.4 conditions in the presence of increasing concentration of quercetin (10, 30 and 50μM), monitored under native conditions. B) Far-UV CD spectra of γ-Syn (0.3 mg/ml) in presence of increasing concentrations of quercetin (10, 30 and 50μM) monitored at time- intervals of 24h *(left panel)* and 48h *(right panel)* during fibrillation showing a shift in the negative ellipticity from 200 nm to ~ 218 nm both in the absence and presence of quercetin, depicting the formation of characteristic β-sheet conformation.

2.5.2 ANS binding assay

The effect of quercetin on the exposed surface hydrophobicity of γ-Syn was further assessed by ANS binding assay. ANS fluoresces strongly with a blue shifted emission upon binding with the hydrophobic patches in a protein. Binding of ANS to γ-Syn under native conditions showed a concomitant decrease in the ANS fluorescence intensity the presence of increasing concentration of quercetin (Figure 14A). This indicates a competitive binding between ANS and quercetin on γ-Syn leading to displacement of bound ANS at higher concentrations of quercetin (Figure 14A). ANS fluorescence measured at regular time intervals during γ-Syn fibrillation (Figure 14B to E) in the absence of quercetin showed an increase in the ANS fluorescence intensity with a characteristic blue shifted emission at ~480 nm. On the other hand, the increments in the ANS intensity in the presence of quercetin were significantly reduced during aggregation. It is to be noted that at 8h of fibrillation

(Figure 14B), an overlapping spectra of ANS bound with the protein both in the absence and presence of quercetin was observed, indicating the conformational changes in the protein that minimizes the interference between ANS and quercetin. During the later stages of fibrillation (24 and 48h) (Figure 14C and D), the significant decrease in the ANS intensity in the presence of quercetin indicated an overall low hydrophobicity in the γ-Syn species formed by quercetin. Changes in the ANS fluorescence intensity at emission maxima of 480 nm, with an increasing concentration of quercetin at regular time intervals during fibrillation is shown in Figure 14 E.

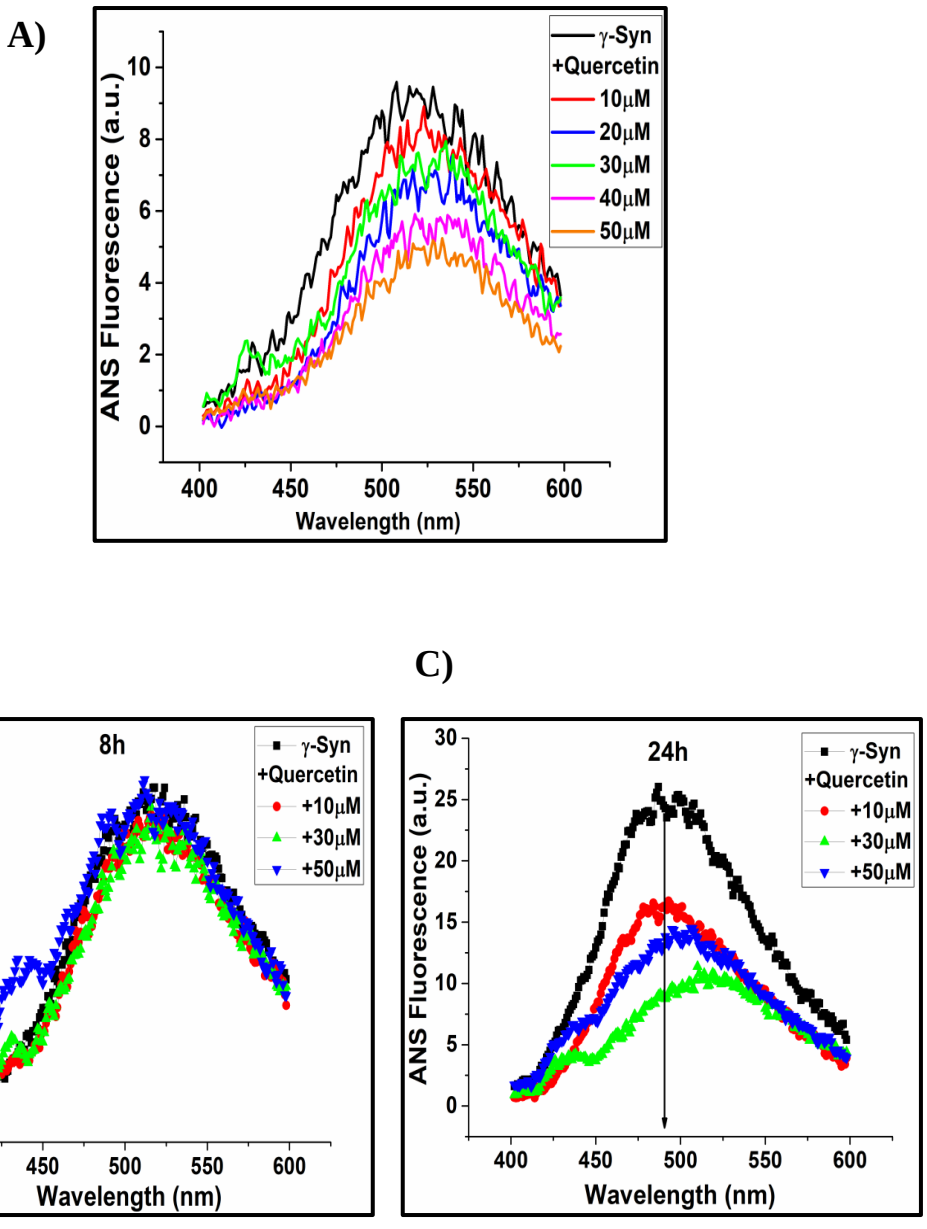

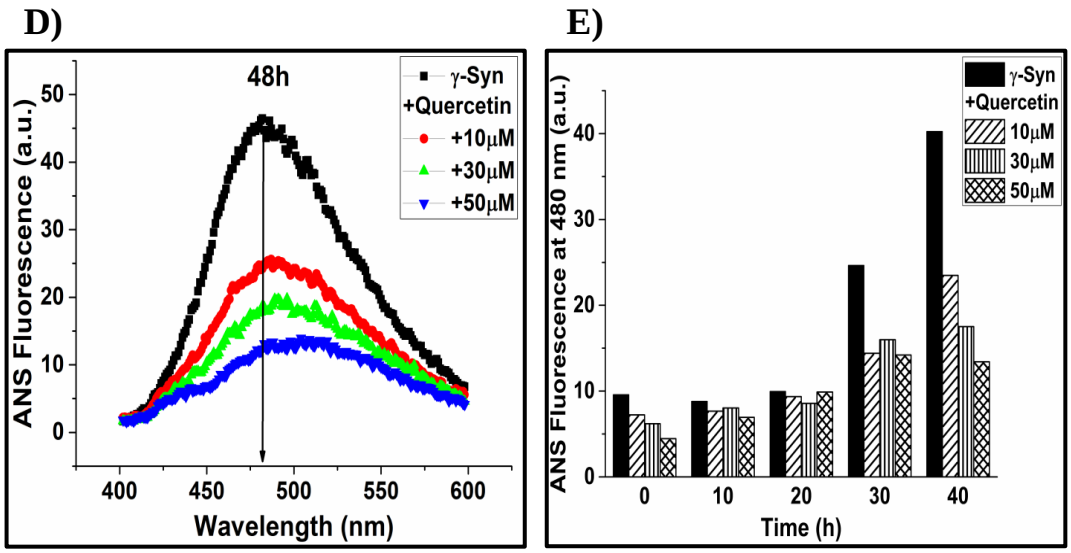

Figure 14. ANS binding analysis of γ-Syn in the absence and presence of quercetin. A) Emission spectra of ANS binding to γ-Syn under native conditions in the presence of increasing concentration of quercetin. B to D) ANS binding to aggregating species of γ-Syn formed in the presence of increasing concentration of quercetin showing blue shifted emission at ~480 nm. E) Bar showing the difference in the ANS fluorescence intensities at an emission maximum of 480 nm at regular intervals of fibrillation in the presence of quercetin.

2.6 Binding interactions between γ-Syn and quercetin:

The mode of binding interaction between quercetin and γ-Syn was further investigated using steady- state fluorescence and isothermal titration calorimetry (ITC) to gain an in-depth understanding of the mechanism underlying the quercetin mediated inhibition of the γ-Syn fibrillation pathway.

2.6.1 Effect of quercetin on intrinsic tyrosine fluorescence of γ-Synuclein

To investigate the mode of binding interaction between quercetin and γ-Syn and probe the accessibility of quercetin to the single tyrosine present in γ-Syn, the changes in the tyrosine fluorescence intensity in the presence of increasing concentration of quercetin (2-30μM) were monitored at different temperatures. As shown in Figure 15A, continuous titration of γ-Syn with an increasing concentration of quercetin at 25°C, showed a concentration dependent decrease in the tyrosine fluorescence. The quenching of tyrosine fluorescence in the presence of quercetin thus indicated an interaction between γ-Syn and quercetin. Using the Stern-Volmer

equation, the bimolecular quenching constant (k_q) was calculated to be more than $10^{10}M^{-1}s^{-1}$ (k_q = $1.95\times10^{13}M^{-1}s^{-1}$) (Figure 15B) indicating a static quenching mechanism and complex formation between γ-Syn and quercetin. Further the affinity of quercetin towards γ-Syn was estimated using the modified Stern-Volmer plot. γ-Syn was found to bind with quercetin at an equimolar ratio of 1:1. The association constant (K_a) between quercetin and γ-Syn was estimated to be $2.2\times10^{5}M^{-1}$indicating moderate to moderate binding affinity. The binding parameters of quercetin binding to γ-Syn at different temperatures are summarized in Table II. Quercetin was found to bind to γ-Syn with highest affinity at 37°C (310.15 K).

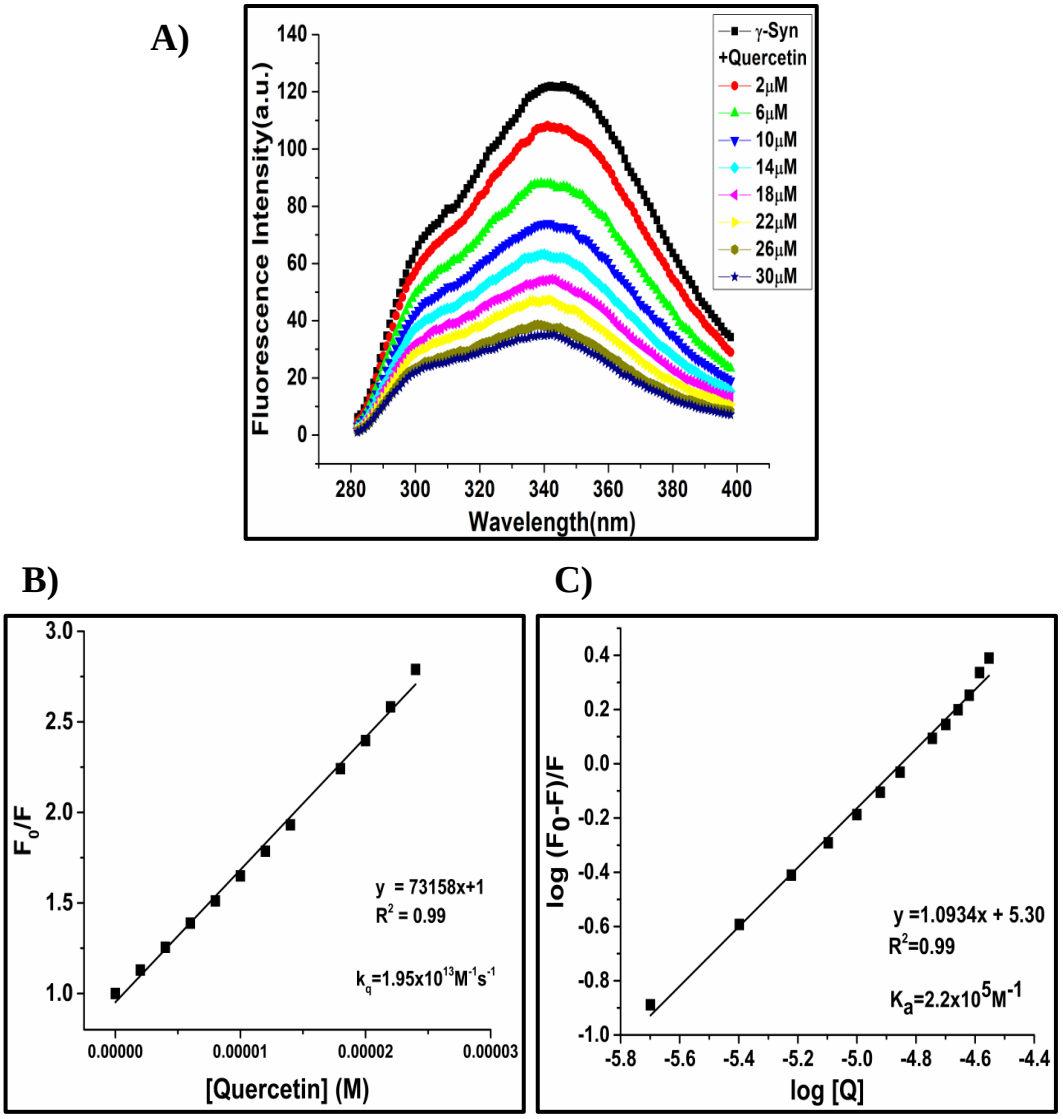

Figure 15. Intrinsic tyrosine fluorescence of γ-Syn in the presence of increasing concentration of quercetin. A) Steady-state fluorescence showing quenching of intrinsic tyrosine fluorescence of γ-Syn (0.3mg/ml) continuously titrated with an increasing concentration of quercetin (2-30μM) at 25°C. B) Plot of F_0/F against quercetin conc. and

(C) Plot of log (F_0-F)/F against log[Q] giving the value for biomolecular quenching constant 'k_q' and binding constant 'K_a' respectively.

Table II. Binding Parameters calculated from Stern- Volmer Plot

Temperature (K)	k_q (Bimolecular quenching constant)	K_a (Binding constant)	N (No. of binding sites)
288.15	$2.19 \times 10^{13} M^{-1} s^{-1}$	$9.08 \times 10^{4} M^{-1}$	~ 1
298.15	$1.95 \times 10^{13} M^{-1} s^{-1}$	$2.2 \times 10^{5} M^{-1}$	~ 1
310.15	$2.69 \times 10^{13} M^{-1} s^{-1}$	$1.43 \times 10^{6} M^{-1}$	~ 1
318.15	$2.58 \times 10^{13} M^{-1} s^{-1}$	$3.48 \times 10^{4} M^{-1}$	0.9 ~ 1

2.6.2 Isothermal Titration Calorimetry of quercetin binding to γ-Syn

To further characterize the thermodynamic parameters of binding interactions between γ-Syn and quercetin, the calorimetric studies on the interaction of quercetin and γ-Syn was carried out at 37°C at 10-fold molar excess ratio of quercetin over γ-Syn. γ-Syn (10.4 μM) was titrated with equal injections of 4 μl quercetin at an equal interval of 420 s, with continuous stirring at 329 rpm. As shown in Figure 16, the binding isotherm shows a moderate binding interaction between quercetin and γ-Syn fitted to a single binding site model. Quercetin binds with γ-Syn spontaneously with a net exothermic reaction. The negligible negative entropy (ΔS) and high negative enthalpy (ΔH) demonstrates that the interaction is an enthalpically driven reaction. The moderate binding affinity with an association constant of ~$1.96 \times 10^{6} M^{-1}$ suggests the role of non-covalent, hydrogen bonding interactions between quercetin and γ-Syn. The data further supports the observations made by the steady-state fluorescence and are in agreement with each other.

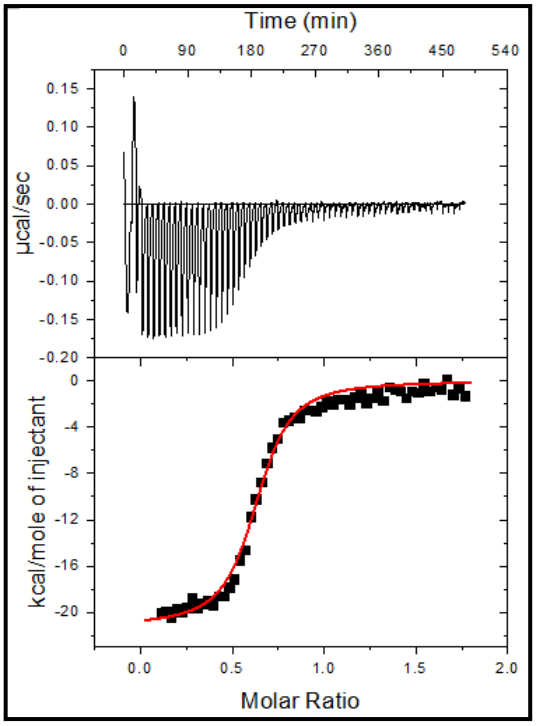

Figure 16. Isothermal titration calorimetry of quercetin binding to γ-Syn. The reaction was carried out at 37 °C with γ-Syn and quercetin ratio of 1:10. *Upper panel*: A raw data plot of heat flow against time for titration of quercetin into γ-Syn and lower panel: Plot of normalized heat released as a function of ligand concentration for the titration. The red solid line shows the single-site fit for the obtained data.

Table III. Thermodynamic parameters of γ-Synuclein binding to quercetin by isothermal titration calorimetry at 37°C

$K_a \times 10^6 (M^{-1})$	ΔH° (kcal / mol)	ΔS° (cal / mol / deg)	ΔG° (kcal / mol)
1.93 ± 0.2	-21.2 ± 0.03	-39.6	-8.7

2.7 Cytotoxic effects of Quercetin generated γ-Synuclein species studied by MTT assay:

To investigate the cytotoxic effects of quercetin generated species, MTT assay was carried out on both breast cancer (MCF-7) and neuroblastoma (SH-SY5Y) cells.

2.7.1 MTT assay on MCF-7 cells

γ-Syn was incubated with an increasing concentration of quercetin (10, 30 and 50μM) under fibrillation conditions and samples were withdrawn at different time intervals (0, 24 and 48h) to investigate the cytotoxic effects of the various γ-Syn species formed at different stages of fibrillation in the presence and absence of quercetin. As shown in Figure 17, the treatment of cells with various concentration of quercetin in the absence of γ-Syn, taken as control, significantly reduced the viability of MCF-7 cells, suggesting that quercetin alone is toxic to the MCF-7 cells. At 0h, the viability of cells in the presence of untreated γ-Syn was reduced by approximately 30%, which was marginally rescued to 20% in the presence of increasing concentration of quercetin. At 24h, the viability of MCF-7 cells was marginally reduced in the presence of quercetin treated γ-Syn species. Interestingly, at 48h of fibrillation where untreated γ-Syn fibrils were found to reduce viability by approximately 25%, the fibrils formed by quercetin at all concentrations were significantly toxic to MCF-7, reducing their viability by nearly 40%, indicating that quercetin generated fibrils are toxic to MCF-7 cells.

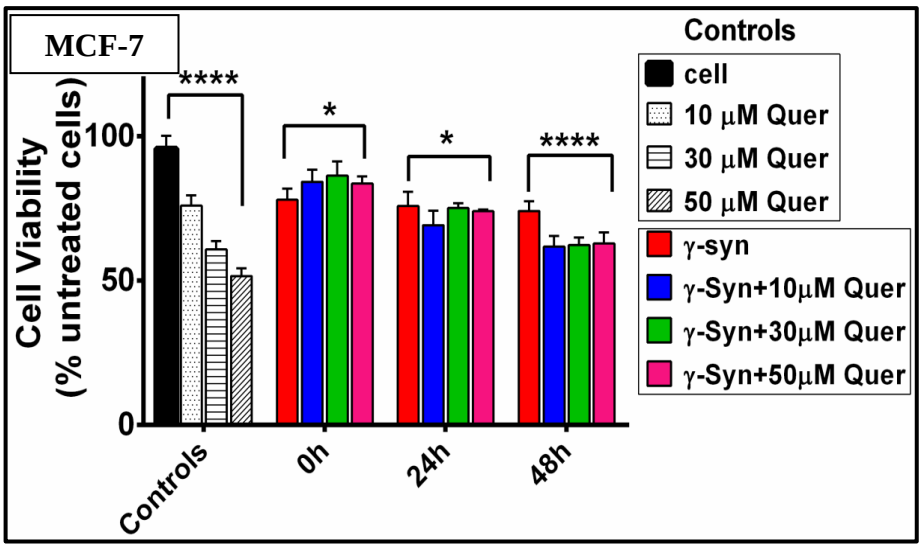

Figure 17. Cytotoxic effects of quercetin treated γ-Syn species on MCF-7 cells by MTT assay. MTT assay reveals that quercetin alone is significantly toxic to MCF-7 cells (****$p < 0.0001$, with respect to untreated cells). At 0h, the viability of cells in the presence of quercetin treated γ-Syn is marginally increased (*$p < 0.05$), as compared to cells treated with γ-Syn alone. The 24h data shows a marginally reduced viability in the presence of quercetin treated γ-Syn (*$p < 0.05$), as compared to cells treated with γ-Syn alone. At 48h, the γ-Syn fibrils formed in the presence of increasing concentration of quercetin were found to

significantly reduce the viability of MCF-7 cells (****$p < 0.0001$, with respect to cells treated with only γ-Syn in the absence of quercetin). The statistical analysis was done using one-way ANOVA. The error bar represents ±SD (n=5).

2.7.2 MTT assay on SH-SY5Y cells

γ-Syn was incubated with an increasing concentration of quercetin (10, 30 and 50μM) under fibrillation conditions and the assay was carried out as mentioned above. As observed in MCF-7 cells (Figure 17), a similar decrease in the SH-SY5Y cell viability was observed in the presence of quercetin alone, used as control (Figure 18A). This suggests that quercetin is inherently toxic to both the cell lines used in the present study. At different time intervals of fibrillation, as shown in Figure 18, the viability of cells were unaffected in the presence of untreated γ-Syn, whereas a significant decrease in the cell viability was observed in the presence of quercetin- treated γ-Syn species. Interestingly, at 24h of fibrillation, the untreated γ-Syn species were found to reduce the cell viability by approximately 50%, which was significantly rescued by the quercetin treated γ-Syn species by increasing the cell viability by almost 20%. At 48h of fibrillation, the γ-Syn fibrils formed in the presence of higher concentration of quercetin (30 and 50 μM), the viability was further found to reduce by ~40%.

Additionally, the cytotoxic effects of the disaggregated species of γ-Syn formed in the presence of quercetin were investigated on the SH-SY5Y cells (Figure 18B). The untreated γ-Syn fibrils formed at the end of fibrillation was found to reduce viability by approximately 35%, which was maintained even in the presence of disaggregated γ-Syn fibrils formed in the presence of quercetin (50 μM). The disaggregated fibrils were thus observed to be equally toxic to the untreated γ-Syn fibrils.

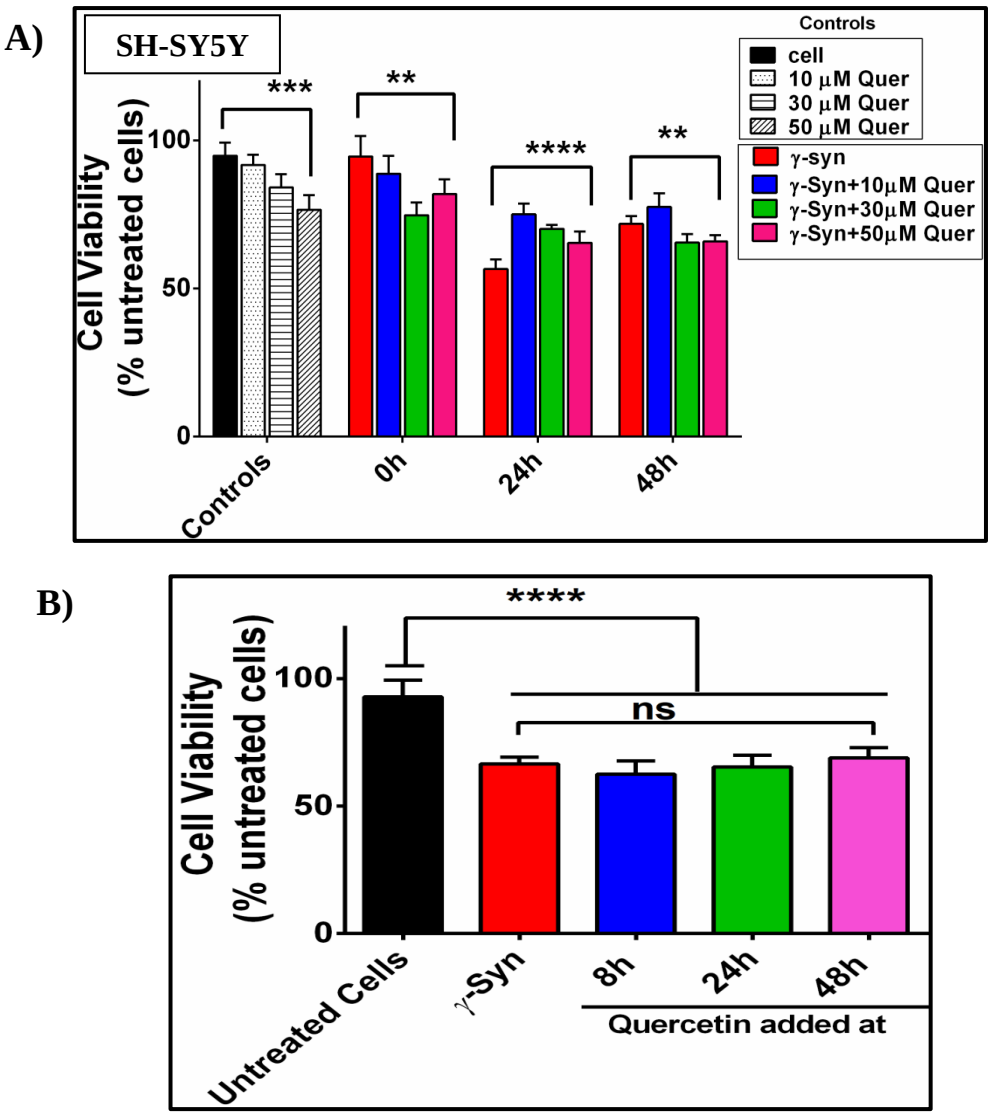

Figure 18. Cytotoxic effects of quercetin treated γ-Syn species on SH-SY5Y cells by MTT assay. A) MTT assay reveals that quercetin alone is significantly toxic to SH-SY5Y cells (***$p < 0.0005$, with respect to untreated cells). At 0h, the viability of cells in the presence of quercetin treated γ-Syn is marginally reduced (**$p < 0.005$), as compared to cells treated with γ-Syn alone. The 24h data shows an increased viability in the presence of quercetin treated γ-Syn (****$p < 0.0001$), as compared to cells treated with γ-Syn alone. At 48h, the γ-Syn fibrils formed in the presence of higher concentration of quercetin (30 and 50 μM) were found to reduce the viability of SH-SY5Y cells (**$p < 0.005$, with respect to cells treated with only γ-Syn in the absence of quercetin). B) MTT assay showing the cytotoxic effects of the disaggregated species of γ-Syn. The untreated γ-Syn fibrils were found to be significantly toxic to SH-SY5Y cells (****$p < 0.0001$, with respect to untreated cells). The disaggregated γ-Syn fibrils formed in the presence of quercetin were found to be equally toxic as untreated γ-Syn fibrils, showing no significant difference in the toxicity. The statistical analysis was done using one-way ANOVA. The error bar represents ±SD (n=5).

3. Discussion

The study emphasises on elucidating the inhibitory effect and the mechanism of quercetin mediated modulation of γ-Syn fibrillation pathway. Quercetin has been previously reported to inhibit amyloidogenesis of many fibril forming proteins such as α-Synuclein (X. Meng et al., 2010; Caruana et al., 2011), Aβ- peptide (Jiménez-Aliaga et al., 2011), insulin (Wang et al., 2011), amylin (López et al., 2016), etc. The results showed here establish a concentration dependent inhibition of γ-Syn fibrillation by quercetin. However, as observed in the presence of EGCG, a complete suppression at a higher concentration of even 50 μM was not observed (Section 3.1). The differences in their inhibitory effects could be explained by the difference in the number of the hydroxyl groups (OH) present in their chemical structures where a direct relationship between an increase in the number of hydroxyl groups in the polyphenols and anti-amyloidogenic activity has been established (Ono et al., 2006). Quercetin in comparison to EGCG has also been previously classified as a good inhibitor that increased the lag time of α-Syn fibrillation by 4 to 5- fold, while EGCG was classified as a strong inhibitor leading to complete suppression of α-Syn fibrillation (X. Meng et al., 2009). A detectable but reduced light scattering intensity in the presence of increasing concentration of quercetin (Figure 2) indicate the formation of smaller species that reduce the overall fibrillar yield of γ-Syn. It is further observed as a concentration dependent disappearance of mature γ-Syn fibrils along with the appearance of short spherical and protofibrillar species visualized by TEM (Figure 3) and AFM (Figure 4) analysis respectively. The effect of quercetin on different stages of γ-Syn fibrillation reveals that quercetin, inhibits fibril elongation and attenuates the protofibrillar assembly when added at earlier and mid stage of fibrillation (8 and 24h respectively). Upon addition of quercetin on the preformed γ-Syn fibrils at saturation (48h) leads to the disassembly of the mature fibrils to form short, disaggregated fragments of reduced fibril diameter as shown in Figure 7 and 8. The disaggregation of mature fibrils of other amyloidogenic proteins such as bovine insulin (Wang et al., 2011), Aβ-peptide (Jiménez-Aliaga et al., 2011) and α-Synuclein (X. Meng et al., 2010; Zhu et al., 2013) by quercetin has also been reported previously. The chemical structure of quercetin facilitates hydrophobic interactions, aromatic stacking and hydrogen bonding with the amyloid forming

regions in proteins that are reported to be the driving forces that lead to fibril inhibition and destabilization (Wang et al., 2011).

The SEC profiles of γ-Syn species formed in the presence and absence of quercetin during fibrillation (Figure 9) reveal a time-dependent increase in γ-Syn oligomerization in the presence of quercetin, predominant at 24h, which is the exponential phase of fibrillation. At 24h, the γ-Syn population appears to be in near equilibrium between the oligomeric and monomeric species of γ-Syn with the appearance of additional population of species that elute later at ~22 min which possibly are the compact conformations of γ-Syn species that get retarded for a longer duration in the column. The SEC profiles monitored at 378 nm (Figure 9B) demonstrate an increased affinity of quercetin towards γ-Syn oligomers and establish that quercetin inhibits γ-Syn fibrillation by binding with the oligomers of γ-Syn formed specifically at the exponential phase of the pathway and modulate them to form compact structures that lead to suppression of fibrillation and thus are the resultant inhibitory species of the γ-Syn fibrillation pathway. These quercetin modulated oligomers of γ-Syn, however were found to be unstable which are SDS-labile and disappear by the end of fibrillation, demonstrated by negligible trace of soluble protein present at 48h of fibrillation. This could also arise due to the reduction in the soluble protein concentration during fibrillation, since complete suppression of fibrillation was not observed even at 50 μM of quercetin. The presence of monomeric peak at 48h of fibrillation in the SEC profile of untreated γ-Syn demonstrates the transient and unstable nature of the γ-Syn species which oscillate between constant association and dissociation during fibril formation. The denaturation of quercetin generated γ-Syn oligomers in the presence of denaturant like SDS, further suggests that quercetin generated oligomers are unstable and are similar in nature to the untreated oligomers of γ-Syn. Unlike the observation made in this study, quercetin has previously been reported to inhibit α-Syn fibrillation by stabilizing both the oligomeric and monomeric forms of α-Syn (X. Meng et al., 2010). The inhibitory effect of quercetin and the other polyphenols investigated in the previous study has been attributed to the vicinal hydroxyphenyl moiety present in flavonoids that are shown to bind non-covalently to α-Syn and also lead to covalent modifications using the flavonoid quinone moiety that restricts the conformational changes in the natively unfolded α-Syn, thus imparting stability (X. Meng et al., 2010).

One of the important aspects of understanding the underlying mechanisms of inhibition is to decipher the nature of the modulated species formed under the effect of small molecule inhibitors. The seeding studies reveal that the quercetin generated species do not act as templates for fibril polymerization and thus are *off-pathway* in nature (Figure 11). The kinetic parameters i.e. lag time (t_{lag}) and apparent rate of fibrillation (k_{app}) estimated for the non-seeded, γ-Syn seeded and quercetin treated seeded pathway reveal that the quercetin treated γ-Syn seeds exhibit a t_{lag} and k_{app} intermediate between non-seeded and γ-Syn seeded kinetics, assuming them to be on-pathway. However, the incomplete suppression of γ-Syn fibrillation in the presence of quercetin and only a marginal difference in the t_{lag} and k_{app} between the non-seeded and quercetin-treated seeded fibrillation rather suggest the role of residual species of γ-Syn that remain unaffected and thus act as seeds giving the differences in the kinetic parameters of fibrillation. The formation of long mature fibrils with reduced fibrillar yield in the presence of quercetin- generated seeds as seen by TEM images (Figure 12) further substantiate the *off-pathway* nature of the quercetin-generated species.

Structural characterization of γ-Syn in the presence of quercetin by far-UV CD analysis both under native and fibrillating conditions reveal that the overall secondary structure of γ-Syn in the presence of quercetin remains unaffected during fibrillation. The structural transition of natively unfolded γ-Syn to the characteristic β-sheet conformation remains unaffected even in the presence of quercetin (Figure 13B) but interestingly as revealed by ANS binding assay the γ-Syn species were observed to maintain an overall reduced hydrophobicity in the presence of quercetin during fibrillation (Figure 14). The reduced ANS intensity in the presence of quercetin during fibrillation could be explained by the formation of oxidized quercetin that is formed upon prolonged incubation during fibrillation, as also reported previously for α-Syn (Zhu et al., 2013). Quercetin possibly interacts with amine side chains of γ-Syn and increases the hydrogen- bonding probability by increasing polarity and thus lowers the exposed surface hydrophobicity. The overlapping ANS spectra both in the presence and absence of quercetin at 8h of fibrillation (Figure 14B) and the subsequent reduction in the ANS intensity with increasing time of fibrillation (Figure 14C to E) indicate the time-dependent oxidation of quercetin after prolonged incubation (after ~20h), which in turn results in reduced surface hydrophobicity. The hydrophilic nature of quercetin as well as

quinone, which is the oxidized form of quercetin, as reported to form multiple hydrogen bonds with α-Syn and thus impart surface hydrophilicity (Zhu et al., 2013), could also be a possible mechanism that play role in inhibition of γ-Syn fibrillation by quercetin.

The presence of strong covalent binding interactions between quercetin and γ-Syn is also supported by the steady-state fluorescence and isothermal titration calorimetry (Figure 15 and 16 respectively). Quercetin binds with a 1:1 binding ratio with γ-Syn with an association constant (k_a) of $10^6 M^{-1}$ at 37°C. An increase in the binding affinity with an increasing temperature, except at 45°C, as shown in Table III, reveals a complex formation between quercetin and γ-Syn with a highest affinity at 37°C. A previous report on quercetin effect of α-Syn fibrillation demonstrates the binding interaction between the ortho-dihyroxyl group in quercetin and α-Syn, suggesting the ortho-dihydroxyl group as the key structure that plays role in fibril inhibition (Zhu et al., 2013).

Several reports have suggested that the ordered prefibrillar oligomers, or protofibrils formed during the fibrillation are mainly responsible for cell death and that the mature fibrils which are end products of fibrillation are neuroprotective (Bucciantini et al., 2002; Caughey and Lansbury Jr, 2003; Ferreira et al., 2007). Investigations on the cytotoxic effect of quercetin generated γ-Syn species on breast cancer (MCF-7) and neuroblastoma (SH-SY5Y) cells reveal a differential effect on these cells as also observed in the presence of EGCG. The difference in the toxicity could arise due to the pharmacological activities of quercetin that affect the signalling pathways differentially in neurons compared with malignant cells, governing cell death or survival in a cell type and metabolism specific manner (Dajas, 2012). The study shows that quercetin alone in the absence of γ-Syn is significantly toxic to both MCF-7 and SH-SY5Y cells but in MCF-7 cells, a 50 % reduction in the viability in the presence of 50 μM quercetin is observed. The doses of quercetin in the range of 3- 50 μM have also been reported to exhibit anti-proliferative properties (Dajas, 2012), however in the case of neuronal cells, only 1-10μM was sufficient to induce cytotoxicity in pure neuronal cells (Ossola et al., 2009). Application of quercetin to the neuronal cell is reported to readily permeate the cells and upon reaching the nucleus increasingly interact with the cytoplasmic and nuclear molecules that give rise to multiple cellular targets responsible for its therapeutic as well as toxic properties (Dajas, 2012). As shown in Figure 17, the

viability of MCF-7 cells was only marginally increased in the presence of quercetin at 0h of fibrillation, while the viability in the presence of quercetin generated fibrils at 48h was significantly reduced, clearly demonstrating the toxic effects of the quercetin treated fibrils of γ-Syn. The reduction in cell viability in the presence of γ-Syn generated species formed in the presence of quercetin however could be majorly attributed to the toxic effect of quercetin alone rather than that incurred by γ-Syn species. The data shows that the reduction in cell viability is much pronounced when quercetin is present alone than when quercetin is present along with γ-Syn fibrils. This leads to a speculation that γ-Syn fibrils bound with quercetin may prevent quercetin from permeating the cell membrane and thus prevent acute toxicity. The complex behaviour of quercetin thus needs to be carefully investigated.

Contrary to the observations made in the presence of MCF-7 cells, the viability of SH-SY5Y cells at 24h of fibrillation was increased in the presence of quercetin generated species (Figure 18A), suggesting that the γ-Syn oligomers formed at 24h of fibrillation as observed in SEC profiles (Figure 9) were neuroprotective. The fibrils of γ-Syn formed in the presence of quercetin at 48h of fibrillation were however found to be neurotoxic. The disaggregated γ-Syn species formed under the effect of quercetin (Figure 18B) on the other hand were found to be neutral species that did not affect the toxicity caused by the untreated γ-Syn fibrils. The study thus provides alternate evidence where the mature fibrils formed at the end of fibrillation in the presence of small molecule inhibitor are more toxic than its oligomeric counterparts and the disaggregated end products are neutral species found to be equally toxic to the untreated fibrils of protein.

Chapter 3.3

Effect of Silibinin on the Structure and Aggregation of γ-Synuclein

1. Background

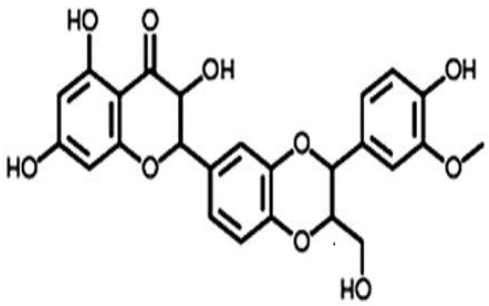

Chemical Structure of Silibinin

Silibinin (Sb), also anonymously called as silybin is the main component of the silymarin complex comprising mostly of polymeric and unoxidized polyphenolic compounds. Silymarin is the active component of the plant of *Silybum marianum* (milk thistle). For over 2000 years, due to the strong anti-oxidant properties, the seeds of this plant have been used to treat plethora of diseases related to liver disorders including hepatitis, cirrhosis, and jaundice and also protect liver from various toxins like drugs and alcohol thus being a strong hepatoprotectant (Křen and Walterova, 2005). Apart from the hepatoprotective activities of silibinin, the neuroprotective and anticancer properties of Sb have also emerged extensively. The promising effects of Sb as an anticancer agent is attributed to its antioxidant property where it is reported to protect the tissues from the oxidative damage caused by several chemotherapeutic agents used simultaneously (Křen and Walterova, 2005). Sb is established to suppress proliferation of wide range of tumours such as colon, prostrate, breast, ovary etc. and also act as a strong chemoprotective agent against various tumour promoters by multiple pathways and mechanisms reported previously (Agarwal et al., 2006). The neuroprotective effects of Sb are demonstrated by its anti-amyloidogenic activities on many amyloid forming proteins such as hIAPP (Cheng et al., 2012; Young et al., 2013), Aβ-peptide (Yin et al., 2011) etc. Sb also imparts neuroprotection in several ways such as, protecting primary hippocampal neurons against oxidative stress (Kittur et al., 2002), protecting against drug induced neuropathy (Mannelli et al., 2012), preventing Alzheimer's disease by inhibiting acetylcholinesterase and modulating the synaptic deficits to prevent the impairment in learning and memory (Duan et al., 2015), neuroprotection against Parkinson's disease by attenuating motor deficit and loss in the dopaminergic neurons (Y. Lee et al., 2015), protecting central nervous system (CNS) against oxidative stress in a state of diabetes (Marrazzo et al., 2011), acting as a strong β-breaker by inhibiting fibrillation of polygalacturonase which is an all β-protein (Chinisaz et al., 2014), etc.

While the antiamyloidogenic effect of Sb on fibrillation pathway of Aβ-peptide is established, the direct effect of silibinin on any of the synucleins (α-, β-, γ- Syn) is not reported till date, ruling out the direct evidence of protective effects of silibinin against Parkinson's disease.

The study presented here demonstrates the effect of Sb on the fibrillation pathway of γ- Syn and elucidates the underlying mechanism of interaction as well as the cytotoxic effects of the Sb modulated γ- Syn species on neuronal (SH-SY5Y) and breast cancer (MCF-7) cells respectively. The data reveal the absence of any antiamyloidogenic activity of Sb on γ- Syn fibrillation at the concentrations of Sb used in the study. A weak binding interaction in the range of ~10mM, along with differential cytotoxicity for MCF-7 and SH-SY5Y cells is further established. The results demonstrate that although γ- Syn fibrillation is not inhibited in the presence of Sb, the fibrillation pathway is nevertheless modulated by Sb to form species that imparts altered cytotoxicity. The observations thus suggest that the mode of action of polyphenols or such small molecule modulators are not completely universal and possibly are governed by the specific protein-ligand interactions that regulate the propensity of the fibrillation pathway to become inhibited or more accelerated under the effect of such modulators. This in turn demands a need for detailed in-depth investigations on the effects of polyphenols on various classes of amyloid forming pathogenic proteins before being used as therapeutics.

2. Results

2.1 Effect of Silibinin on the fibrillation kinetics of γ-Syn:

2.1.1 Thioflavin T assay

The fibrillation kinetics of γ-Syn studied in the presence of increasing concentration of Sb (5 – 50 μM) by ThT assay showed negligible decrease in the ThT fluorescence in the presence of Sb as unlike observed for the other two polyphenols, EGCG and quercetin (chapter 3.1 and 3.2, respectively). In the presence of 25 and 35 μM of Sb, although the final ThT fluorescence was found to be reduced, the decrease in the ThT fluorescence was not concentration-dependent and the overall kinetics remained nearly unaffected in the presence of all the concentration of Sb. This suggests an absence of γ-Syn inhibition by Sb in the concentration range between 5-50 μM.

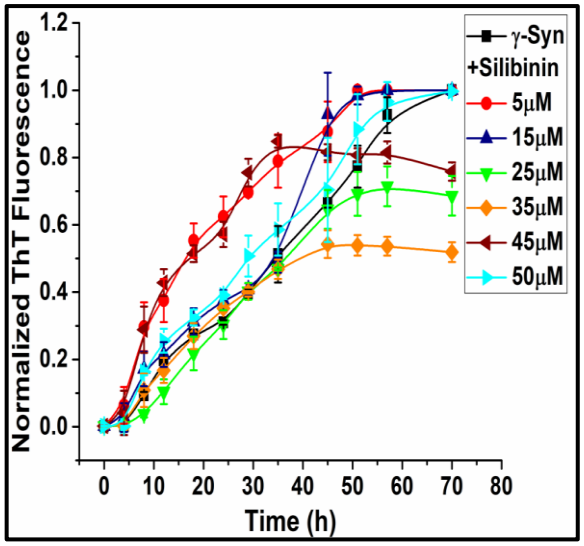

Figure 1. Fibrillation kinetics of γ-Syn in the presence of increasing concentration of Silibinin by Thioflavin T assay. Monomeric γ-Syn was incubated in the presence of increasing concentration of silibinin (5- 50μM) under fibrillating conditions and the ThT fluorescence was recorded at regular interval of time. The overlapping ThT spectra in the presence of Sb show absence of fibrillation inhibition by Sb. The error bars represent the ±SD (n=3).

2.1.2 Transmission Electron Microscopy of γ-Syn fibrils formed in the presence of Silibinin

The morphology of γ-Syn fibrils formed in the absence and presence of Sb was further investigated by TEM. The untreated γ-Syn formed dense network of mature fibrils as also observed earlier. In the presence of increasing concentration of Sb (20 and 30μM), similar networks of mature fibrils were observed, indicating absence of fibrillation inhibition by Sb as also observed in ThT assay. Although mature fibrils were observed at 50 μM Sb, the morphology of the fibrils appeared different than the mature thick fibrils and they were found to be thin and disintegrated, lacking intricate fibrillar network. This suggest that while the fibrillar yield is not significantly reduced in the presence of even 50 μM of Sb, the change in the fibrillar morphology suggests a possible inhibition at concentrations higher than 50 μM, making it a weak modulator of γ-Syn fibrillation.

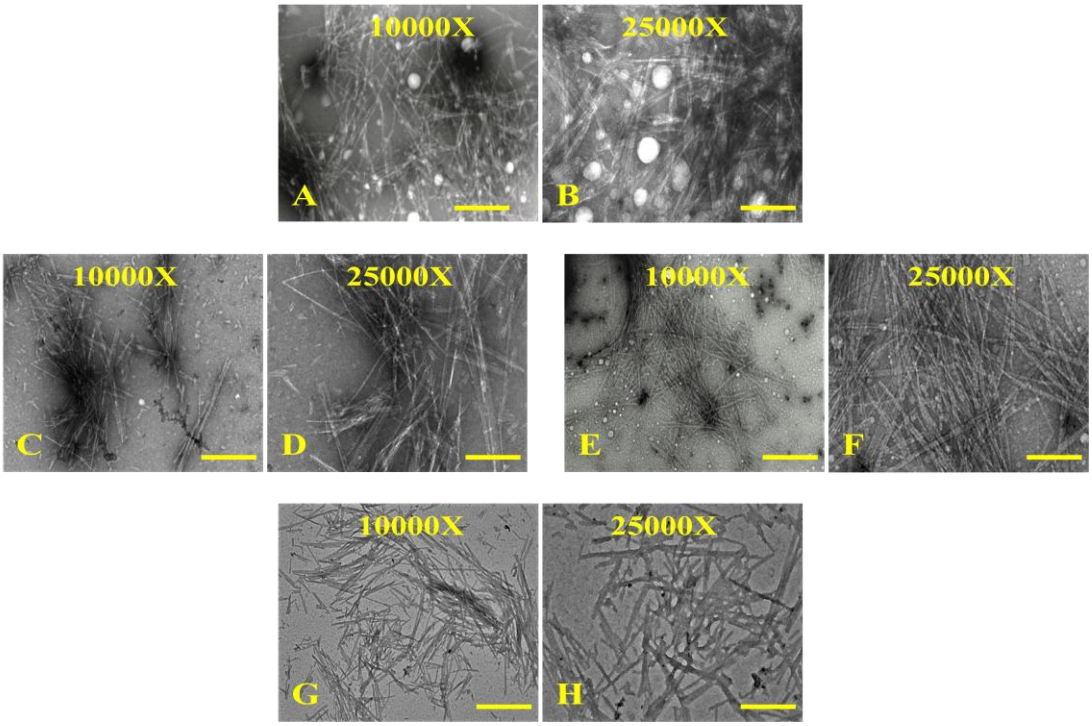

Figure 2. Morphology of γ-Syn fibrils formed in the presence of Silibinin visualized by transmission electron microscope. TEM images of γ-Syn fibrils formed upon saturation (end of fibrillation) in the absence of Sb (A, B) and in the presence of 20μM (C, D), 30 μM (E, F) and 50 μM (G, H) Sb respectively. Scale bar: 100nm.

2.2 Size-exclusion chromatography of γ-Syn species formed in the presence of Silibinin:

In order to investigate how Sb modulates the γ-Syn population in the absence of fibrillation inhibition, size-exclusion chromatography of γ-Syn species formed during fibrillation in the presence of Sb was carried out. The SEC profile of the soluble fraction of γ-Syn species formed in the presence of Sb during fibrillation showed a time-dependent depletion of both the oligomeric and monomeric species of γ-Syn with increased heterogeneity. This suggest that majority of monomeric γ-Syn is converted into insoluble fibrils which are removed during centrifugation leaving only traces of soluble γ-Syn species present in the population.

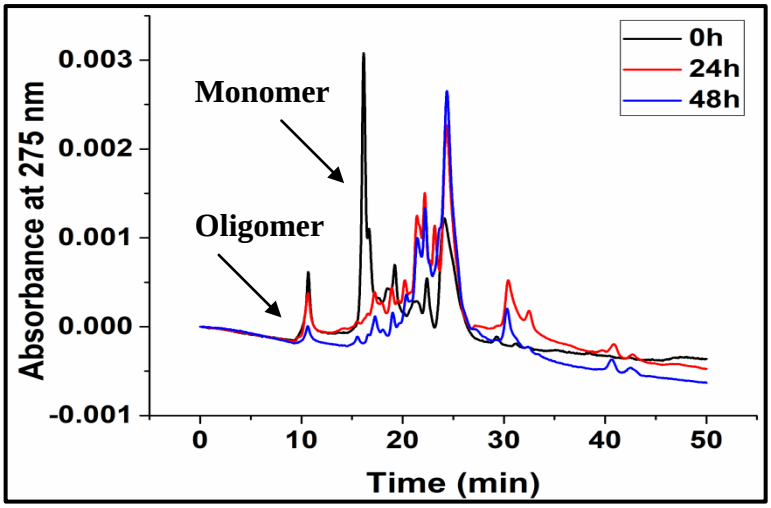

Figure 3. Size-exclusion chromatography of γ-Syn species formed in the presence and absence of Silibinin. The SEC profiles of γ-Syn species formed in the presence of Sb at regular time-intervals during fibrillation.

2.3 Effect of Silibinin on the structure of γ-Syn under both native and fibrillation conditions:

The effect of Sb on the structure of γ-Syn both under native and fibrillating conditions was monitored by far-UV CD and ANS binding assay.

2.3.1 Far-UV CD of γ-Syn in the presence of Sb

The far-UV CD spectra of γ-Syn in the absence and presence of Sb both under native and fibrillating conditions are shown in Figure 4A and B, respectively. Under native conditions, in the presence of Sb, an increase in the negative ellipticity at 200 nm is observed indicating the unfolding of the residual structure of γ-Syn by Sb. During fibrillation at 24 and 48h, an increase in the negative ellipticity at ~218 nm was observed both in the presence and absence of γ-Syn, indicating the formation of characteristic β-sheet structure. The negative ellipticity at ~218 nm increased in the presence of Sb as compared to the untreated γ-Syn, further indicating an increased β-sheet forming propensity in the presence of Sb.

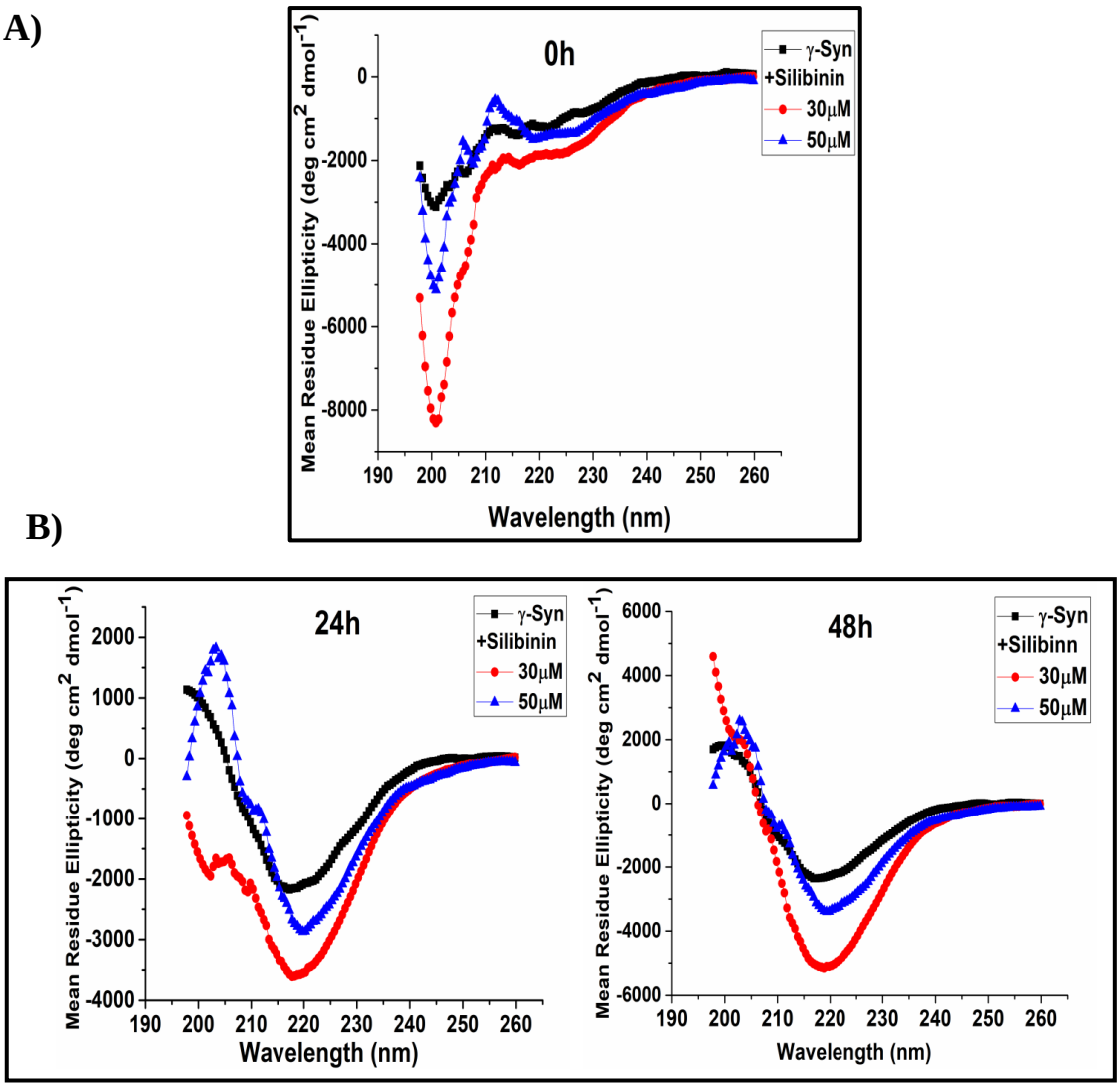

Figure 4. Far-UV CD spectra of γ-Syn in the presence of Silibinin both under native and fibrillating conditions. (A-B) The far-UV CD of γ-Syn in the presence and absence of Sb under native and fibrillating conditions, respectively were monitored at 25 °C using a cuvette of 1mm path length. A) Far-UV CD spectra of γ-Syn (0.3 mg/ml) dissolved 20 mM phosphate buffer, pH7.4 in the presence of increasing concentration of Sb (30 and 50μM), monitored under native conditions. B) Far-UV CD spectra of γ-Syn (0.3 mg/ml) in the presence of increasing concentrations of Sb (30 and 50μM) monitored at time- intervals of 24h *(left panel)* and 48h *(right panel)* during fibrillation showing a shift in the negative ellipticity from 200 nm to ~ 218 nm both in the absence and presence of Sb, depicting the formation of characteristic β-sheet conformation.

2.3.2 ANS binding assay

The effect of Sb on the exposed surface hydrophobicity of γ-Syn was assessed by ANS binding assay both under native and fibrillating conditions. Binding of ANS to

γ-Syn under native conditions both in the absence and presence of Sb showed overlapping spectra with an emission at ~520 nm (Figure 5A). At 24h of fibrillation (Figure 5B, *left panel*), an increase in the ANS intensity with a characteristic blue-shift at ~ 480 nm was observed in the untreated γ-Syn. In the presence of Sb, compared to the untreated γ-Syn an increase in the ANS intensity with the similar blue - shift emission was seen. The increase in the ANS intensity was found to decrease with an increasing concentration of Sb with the ANS spectrum in the presence of 50 μM Sb overlapping with the spectrum of untreated γ-Syn. At the maturation stage of fibrillation (48h), the ANS intensity of untreated γ-Syn was further increased which was found to decrease in the presence of Sb in a concentration-dependent manner (Figure 5B, *right panel*). Interestingly, in the presence of 50 μM Sb, although the emission intensity was reduced, the spectrum was further blue-shifted to ~456 nm. The results indicate an overall increase in the surface hydrophobicity of γ-Syn in the presence of Sb with altered fibrillar surface properties.

A)

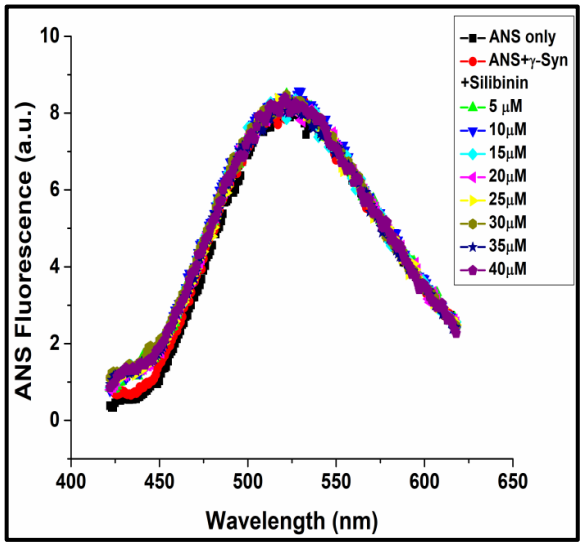

B)

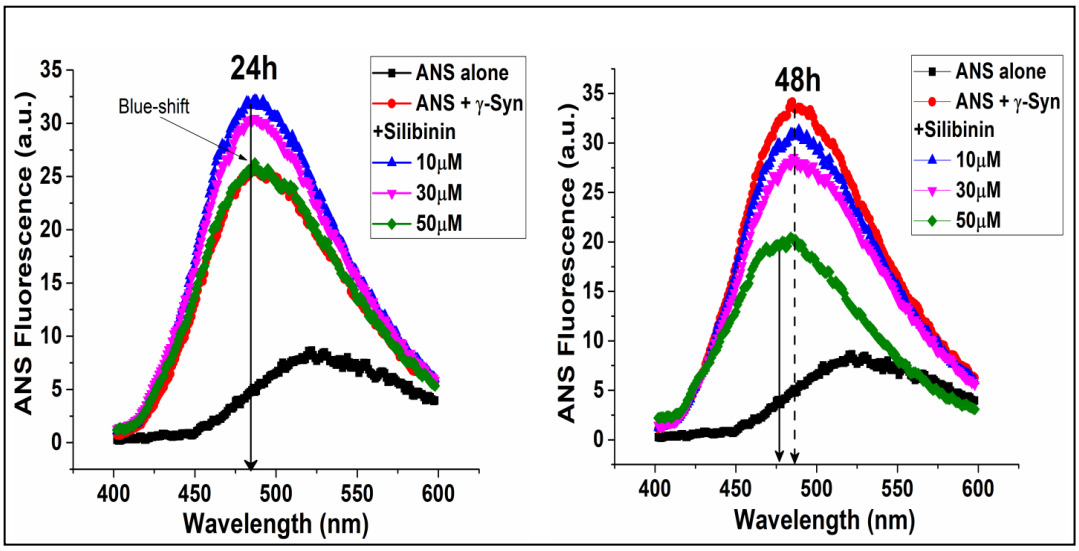

Figure 5. ANS binding analysis of γ-Syn in the absence and presence of Silibinin. A) ANS spectra of γ-Syn in the presence of increasing concentration of Sb (5-40μM) under native conditions showing overlapping ANS spectra. B) ANS binding to γ-Syn in the presence of Sb (10, 30 and 50μM) under fibrillating conditions (24h and 48h) showing characteristic blue-shifted emission (*black arrows*) at 480 nm.

2.4 Binding interaction between γ-Syn and Silibinin:

The binding interaction between Sb and γ-Syn was further studied by fluorescence quenching, van't- Hoff plot and isothermal titration calorimetry.

2.4.1 Effect of Sb on intrinsic tyrosine fluorescence of γ-Synuclein

The effect of Sb on the intrinsic tyrosine fluorescence in γ-Syn was studied by monitoring the changes in the tyrosine fluorescence upon continuous titration of γ-Syn with an increasing concentration of Sb carried out at different temperatures. As shown in Figure 6A, titration of γ-Syn with an increasing concentration of Sb showed a concentration-dependent decrease in the ThT fluorescence, indicating quenching of tyrosine fluorescence and interaction between Sb and γ-Syn. Titration of γ-Syn with an increasing concentration of Sb was accompanied by a red-shift in the emission spectra of tyrosine (Figure 6A (i) and (ii)) around 358 nm, indicating the shift of tyrosine to a more polar environment in the presence of Sb. Using the Stern-Volmer quenching plot, the bimolecular quenching constant (k_q) was calculated to be more than the diffusion-controlled value ($>10^{10} M^{-1}s^{-1}$) indicating a static quenching mechanism and thus complex formation between γ-Syn and Sb

(Figure 6A (iii)). The binding affinity (K_a) between γ-Syn and Sb was estimated by using the modified Stern-Volmer equation (Figure 6A (iv)). Sb was found to bind to γ-Syn with a weak binding interaction with a dissociation constant in the range of ~10 mM, suggesting the role weak non-covalent interactions between Sb and γ-Syn.

The binding interaction between Sb and γ-Syn were also studied at different temperatures (15, 25 and 45°C) and the plots giving their bimolecular quenching constant (k_q) as well as association constant (K_a) are shown in Figure 6 B to D respectively. The binding parameters estimated at different temperatures from the Stern-Volmer plot is summarized in Table I. The binding affinity was found to decrease with an increasing temperature indicating the role of non-covalent interactions between Sb binding to γ-Syn**.**

A)

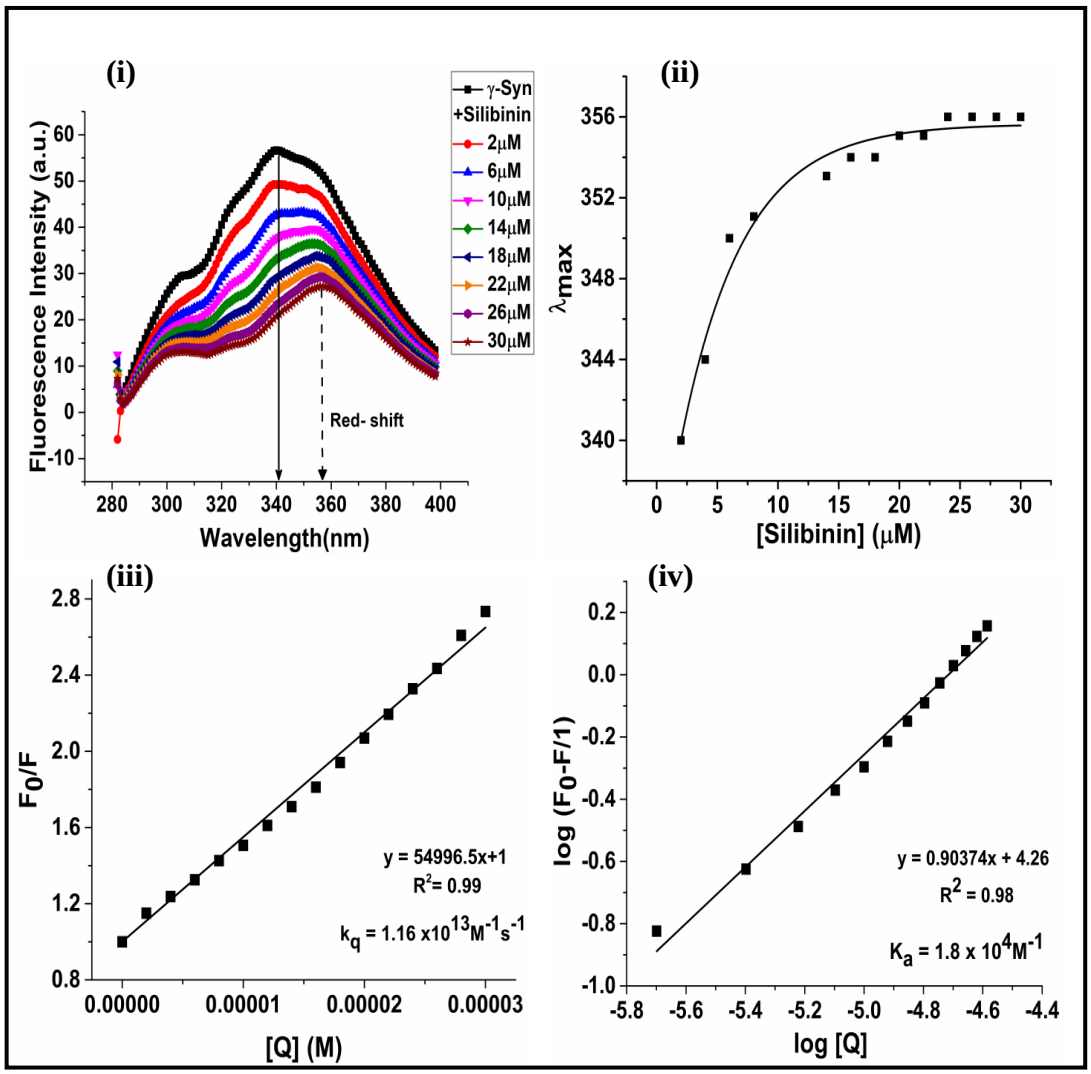

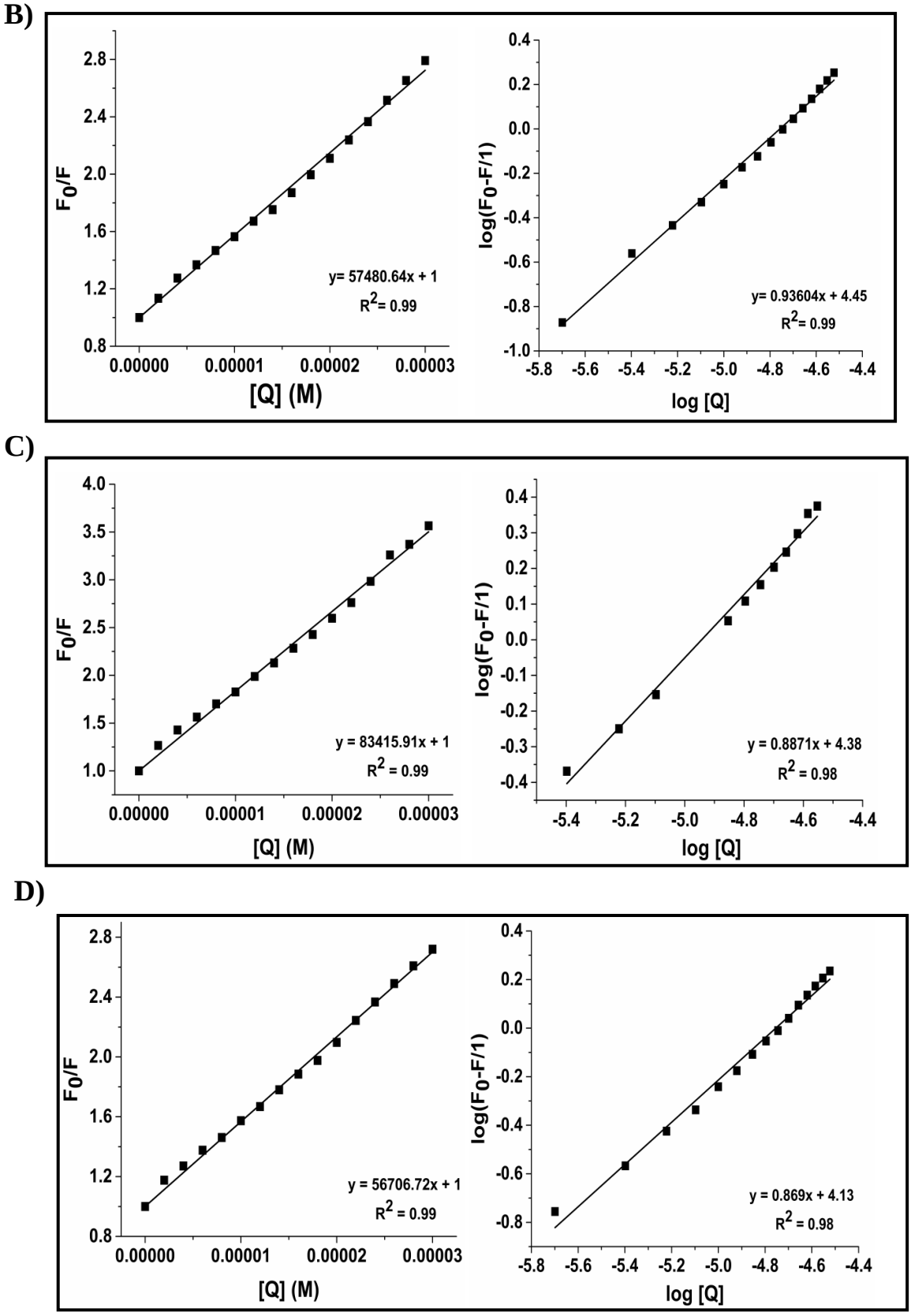

Figure 6. Intrinsic tyrosine fluorescence of γ-Syn in the presence of increasing concentration of Silibinin. A) (i) Steady-state fluorescence showing quenching of intrinsic tyrosine fluorescence of γ-Syn (0.3mg/ml) continuously titrated with an increasing

concentration of Sb (2-30μM) at 37°C with a red-shift in the emission (*black arrows*), (ii) Plot of emission maxima of tyrosine (λ_{max}) with respect to increasing concentration of Sb shows a concentration –dependent shift in the emission wavelength with a red-shifted emission. (iii) Stern-Volmer plot of F_0/F vs [Q] (Sb concentration) giving the value of 'bimolecular quenching constant' (k_q) and (iv) Modified Stern-Volmer plot of log (F_0-F)/F against log[Q] giving the binding affinity or association constant (K_a). B to D) (*left panel*) Plot of F_0/F vs [Q] and (*right panel*) plot of log (F_0-F)/F against log [Q] at 15, 25 and 45°C respectively.

Table I. Binding Parameters calculated from Stern- Volmer Plot

Temp. (K)	$k_q \times 10^{13}$ $M^{-1}s^{-1}$	$K_a \times 10^4$ M^{-1}	n	ΔG° (kcalmol^{-1})	ΔH° (kcalmol^{-1})	ΔS° (cal mol^{-1}deg^{-1})
288.15	1.20	2.81	0.9~ 1	-5.87	-4.56	0.004
298.15	1.75	2.39	0.8~ 1	-5.92		
310.15	1.16	1.8	0.9~ 1	-5.97		
318.15	1.19	1.3	0.8 ~ 1	-6.02		

2.4.2 Mode of binding interaction by using van't-Hoff plot

An insight into the binding mode between γ-Syn and Sb was gained by estimating the free energy of binding (ΔG°), enthalpy (ΔH°) and entropy (ΔS°) by analyzing the temperature dependence of the binding constant using van't-Hoff equation and the binding constants obtained for γ-Syn and Sb from the modified Stern-Volmer plot were used for analysis. The binding parameters of the γ-Syn-Sb complex at four different temperatures obtained by van't –Hoff plot is shown in Figure 7. The negative enthalpy (ΔH° = -19.1kJ mol^{-1}) and a small positive entropy (ΔS° = 19.3 $JK^{-1}mol^{-1}$) indicate that binding of Sb to γ-Syn is a spontaneous reaction driven by electrostatic interactions. The negative free energy is contributed by a large negative enthalpy further suggesting the role of van der Waals and hydrogen bonding interaction between Sb and γ-Syn.

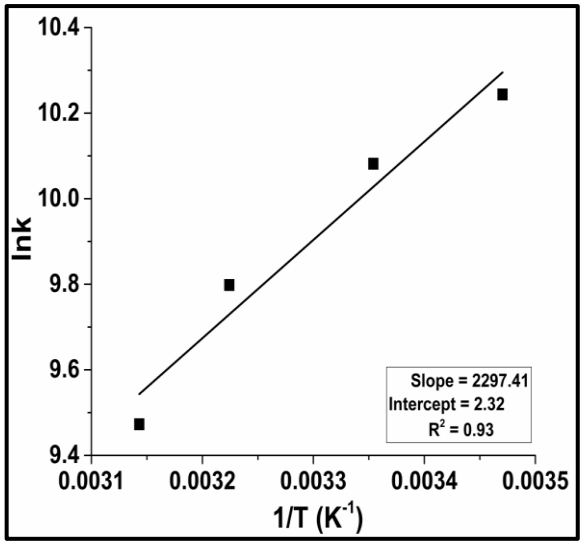

Figure 7. van't-Hoff plot showing the temperature dependence of the binding constants of Sb- γ-Syn interaction. The data is fitted to a least-square regression line (*black line*).

2.4.3 Isothermal titration calorimetry of γ-Syn binding to Silibinin

The thermodynamic parameters of Sb binding to γ-Syn were further characterized by ITC analysis. The ITC binding isotherm, as shown in Figure 8, suggests a sequential binding of γ-Syn to Sb with a negative cooperativity ($K_2 < K_1$) and a moderate to weak binding interaction between Sb and γ-Syn. The negative enthalpy with negligible entropy indicates an enthalpically driven reaction and the role of non-covalent interactions between Sb and γ-Syn.

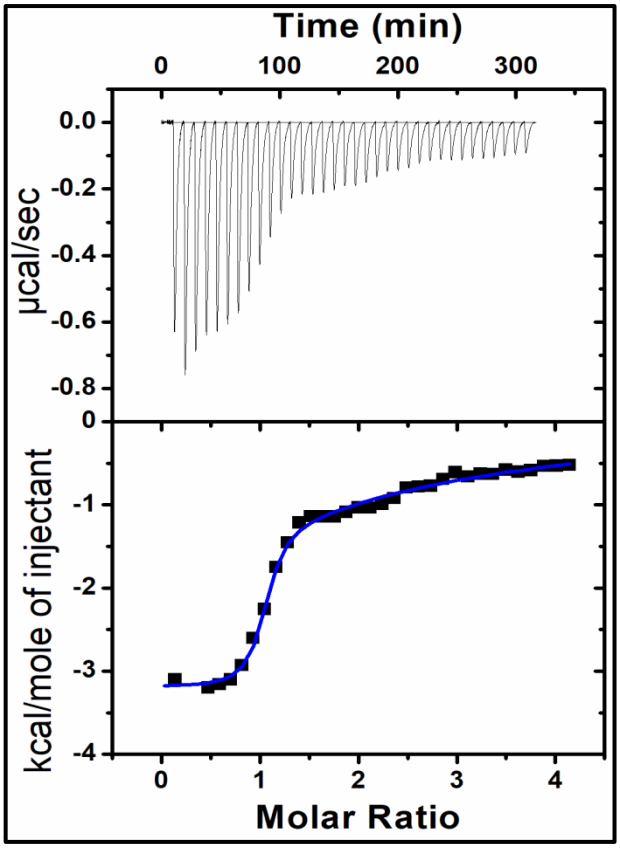

Figure 8. Isothermal titration calorimetry of silibinin binding to γ-Syn. The reaction was carried out at 37 °C with γ-Syn and Silibinin ratio of 1:20. *Upper panel*: A raw data plot of heat flow against time for titration of Sb into γ-Syn and lower panel: Plot of normalized heat released as a function of ligand concentration for the titration. The blue solid line shows the two-site sequential-fit for the obtained data.

Table II. Thermodynamic parameters of Silibinin binding to γ-Synuclein

Thermodynamic parameters	Values
K_1 (M^{-1})	$5.72 \times 10^5 \pm 9.8 \times 10^4$
K_2 (M^{-1})	$1.03 \times 10^3 \pm 0.001$
ΔH_1 (kcal/mol)	-3.20 ± 0.03
ΔH_2 (kcal/mol)	-7.85 ± 0.004
ΔS_1 (cal/mol/deg)	15.6
ΔS_2 (cal/mol/deg)	-12.6

2.5 Cytotoxic effects of Quercetin generated γ-Synuclein species studied by MTT assay

In the absence of fibrillation inhibition by Sb, it was important to investigate if the nature of the γ-Syn fibrils formed in the presence of Sb were different from the untreated fibrils of γ-Syn and whether the γ-Syn fibrillation pathway was modulated by Sb in the absence of inhibition. The MTT assay was carried out on both MCF-7 and SH-SY5Y cells to investigate the cytotoxic effects of γ-Syn species formed in the absence and presence of Sb.

2.5.1 MTT assay on MCF-7 cells

The cytotoxic effects of γ-Syn species formed at different intervals (0, 24 and 48h) during fibrillation in the presence of Sb are shown in Figure 9. At 0h and 48h of fibrillation, the viability of MCF-7 cells in the presence of Sb was found to decrease with an increasing concentration of Sb. The γ-Syn species formed in the presence of 50 μM Sb were found to reduce the viability by almost 50 % and ~20% with respect to untreated cells and only γ-Syn treated cells respectively. Contrastingly, at 24h of fibrillation, the viability was significantly increased in the presence of γ-Syn species formed in the presence of 50 μM Sb. This suggests that the γ-Syn species (monomers and fibrils) formed in the presence of Sb are overall toxic to MCF-7 cells and the increased viability in the presence of 50 μM Sb at 24h indicate the modulation of oligomeric species of γ-Syn.

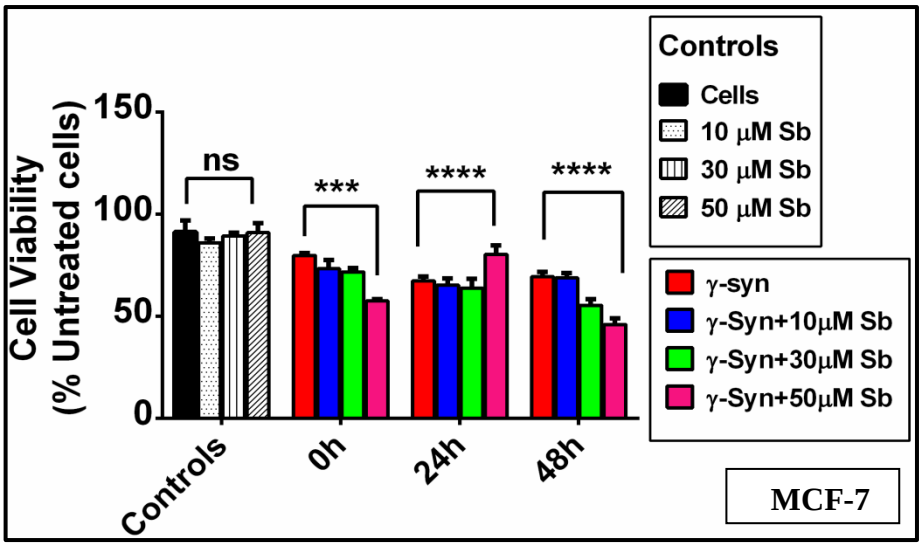

Figure 9. MTT assay showing cytotoxic effects of γ-Syn species formed in the absence and presence of Silibinin on MCF-7 cells. At 0h of fibrillation, MTT assay

shows a concentration- dependent increase in cytotoxicity in the presence of Sb (***p < 0.0004, with respect to untreated cells). At 24h, a significant increase in the viability in the presence of 50μM Sb is seen (****p < 0.0001, with respect to untreated cells). At 48h of fibrillation, a significant reduction in cell viability with an increasing concentration of Sb is seen (****p < 0.0001, compared to untreated cells). The statistical analysis was done using one-way ANOVA. The error bar represents ±SD (n=5).

2.5.2 MTT assay on SH-SY5Y cells

The effect of γ-Syn species on the viability of SH-SY5Y cells are shown in Figure 10. The viability of SH-SY5Y cells at 0h remained unaffected in the presence of Sb treated γ-Syn species. While the viability was marginally reduced in the presence of Sb treated γ-Syn fibrils at 48 h of fibrillation, the viability at all the concentrations of Sb for 24h species was significantly increased that rescued the cells from complete toxicity, indicating variable effects of Sb on different species of γ-Syn.

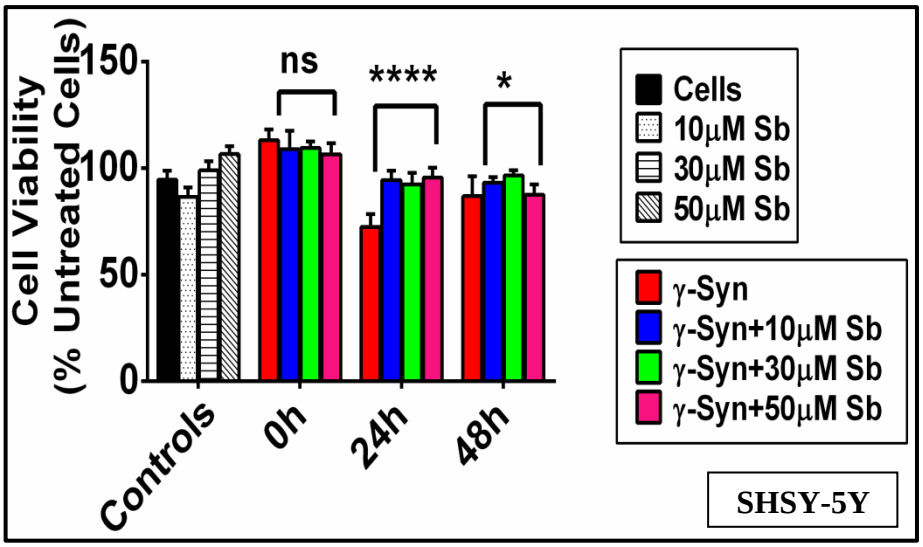

Figure 10. MTT assay showing cytotoxic effects of γ-Syn species formed in the absence and presence of Silibinin on SH-SY5Y cells. At 0h of fibrillation, the viability of cells in the presence of Sb treated cells remains unaffected. MTT assay show an increased viability in the presence of Sb treated γ-Syn species at 24h of fibrillation (****p < 0.0001, with respect to untreated cells). At 48h of fibrillation, the viability was marginally affected in the presence of Sb irrespective of Sb concentration (*p < 0.05, compared to untreated cells). The statistical analysis was done using one-way ANOVA. The error bar represents ±SD (n=5).

3. Discussion

The medicinal and therapeutic properties of silibinin have been widely established for various liver diseases as well as for neurodegenerative diseases and cancer. Although Sb has been reported to inhibit fibrillation of some amyloid forming proteins such as Aβ-peptide (Yin et al., 2011), polygalacturonase (Chinisaz et al., 2014) and hIAPP (Cheng et al., 2012; Young et al., 2013), the direct effect of Sb on fibrillation pathways of many other amyloid-forming proteins, such as Synucleins is unavailable.

This study investigates the anti-amyloidogenic effects of Sb on the γ-Syn fibrillation pathway and observes an absence of any fibrillation inhibition by Sb. In a previous report, Sb was found to inhibit fibrillation of polygalacturonase at a higher concentration range between 50 – 250 μM, with best inhibitory concentration of ~200 μM (Chinisaz et al., 2014), a much higher concentration than that used in this study. This suggests that Sb affects the fibrillation pathways only when present at a several fold molar excess than the fibril forming protein thus indicating Sb to be a weak small-molecule modulator as compared to other polyphenols like EGCG which bring complete suppression even at sub-stoichiometric concentrations (Bieschke et al., 2010) and as observed in chapter 3.1. The change in the fibrillar morphology of γ-Syn in the presence of 50 μM Sb and reduction in the overall fibrillar yield, as observed by TEM (Figure 2) gives rise to the possibility of inhibition of γ-Syn fibrillation pathway by Sb at a concentration higher than that used in the study (> 50 μM)

A sub-stoichiometric concentration of Sb was used (5 – 50 μM) in order to compare the anti-amyloidogenic activities of the three polyphenols (EGCG, quercetin and Sb) used in the present study.

Investigation on the effects of Sb on the γ-Syn structure reveals a characteristic gain in the β-sheet structure indicating fibril formation and thus absence of inhibition (Figure 4). The ANS binding assay suggest that the fibrils formed in the presence of Sb have increased surface polarity (Figure 5) which possibly in turn gives rise to altered fibril morphology (Figure 2). The decrease in the ANS intensity with an increasing concentration of Sb at 48h of fibrillation could possibly occur due to the inaccessibility of ANS to its binding sites on the ordered fibrillar structures also observed previously (Bolognesi et al., 2010), and

demonstrated in this study by a pronounced blue-shifted emission of ANS at ~456 nm in the presence of 50μM Sb.

The mode of binding interaction between Sb and γ-Syn as studied by fluorescence quenching, van't Hoff plot and ITC (Figure 6, 7 and 8 respectively) establish a weak binding affinity with an association constant (k_a) of ~$10^4 M^{-1}$. Binding of Sb to γ-Syn increases the polarity around tyrosine which is clearly demonstrated by the red-shift emission at an increasing concentration of Sb, an effect also observed for Sb binding to human serum albumin reported previously (Maiti et al., 2008). Sb forms a weak binding complex with γ-Syn and the decrease in the binding affinity with an increasing temperature further establishes the role of van de Waals and hydrogen bonding interactions between Sb and γ-Syn.

Even though the oligomeric and protofibrillar species of amyloid- forming proteins are although increasingly being observed to be more toxic than the mature fibrils (Caughey and Lansbury Jr, 2003), the ability of mature fibrils to impart toxicity under the effects of small molecule modulators cannot be ruled out. As revealed by MTT assay, the viability of MCF-7 cells was significantly reduced in the presence of Sb treated monomers as well as the mature fibrils (Figure 9), while the viability of SH-SY5Y cells remained unaffected with a marginal increase in the viability in the presence Sb generated fibrillar species, demonstrating differential toxicity as also observed for EGCG and quercetin. Interestingly, the protective effect of Sb generated γ-Syn oligomers formed at the 24h of fibrillation on both the MCF-7 and SH-SY5Y cells suggest that Sb modulates the oligomeric species of γ-Syn that render them less toxic. The variable effects of Sb generated species on both the MCF-7 and SH-SY5Y cells indicate species specific interaction of Sb with γ-Syn that govern the toxic characteristics of these species and possibly involve a complex mechanism that needs to be further investigated for better understanding of the differential effect.

CONCLUSION

The study gives an insight into the modulating effects of three different classes of polyphenols on the fibrillation pathway of γ-Syn and demonstrates different mechanisms of polyphenol mediated inhibition/modulation of γ-Syn fibrillation pathway. Among the three polyphenols namely, EGCG, quercetin and silibinin used in this study, EGCG containing maximum number of hydroxyl (-OH) groups in its structure, suppresses γ-Syn fibrillation most effectively, which is followed by quercetin, while no suppression is observed in the presence of silibinin. Quercetin and silibinin although contain an equal number of –OH groups (five), the different aromatic ring compositions of these polyphenols possibly give rise to their different antiamyloidogenic activities. Both EGCG and quercetin show a concentration dependent suppression and disaggregation of the protofibrillar and fibrillar species formed in the fibrillation pathway of γ-Syn. While EGCG diverts the fibrillation pathway to form two kinds of SDS-resistant higher order but kinetically retarded *on-pathway* oligomers, quercetin modulates the oligomerization stage (exponential phase) of the γ-Syn fibrillation pathway to form smaller aggregates that are SDS-labile and *off-pathway* in nature. Although silibinin shows no significant effect on the overall fibrillation pathway of γ-Syn, it increases the surface polarity around the fibrillar species that in turn give rise to altered fibrillar morphology in the presence of high concentration (50μM) of silibinin.

The binding interaction of these polyphenols with γ-Syn, interestingly reveal that EGCG despite being the most effective inhibitor of γ-Syn fibrillation pathway among the polyphenols used, interacts most weakly with γ-Syn with a dissociation constant in the range of mM. Quercetin on the other hand interacts with a moderate binding affinity (k_d ~ μM), while silibinin also binds with a weaker affinity with dissociation constant in the range of 10mM. The weakest binding interaction of EGCG with γ-Syn despite its strong suppression of fibrillation indicates the role of weak binding interactions in polyphenol mediated modulation of amyloidogenesis. The weak binding of polyphenols to the amyloid forming species possibly facilitate their transient stacking in the amyloid forming cavities which constantly associate and dissociate from the binding sites to provide barrier for side-to-side β-stacking, a prerequisite for amyloidogenesis. The study also demonstrates differential

cytotoxicity of the polyphenol modulated species of γ-Syn. While EGCG generated γ-Syn oligomers are observed to be toxic for the SH-SY5Y cells but protective for MCF-7 cells, the quercetin modulated γ-Syn species formed in the oligomerization stage are protective to SH-SY5Y cells and only marginally toxic to MCF-7 cells. Interestingly, the quercetin modulated fibrillar species of γ-Syn, despite being *off-pathway* are found to be toxic for both the MCF-7 and SH-SY5Y cells. This observation provides an evidence for the quercetin mediated fibrillar toxicity and demonstrate the complexities involved in the mechanisms that govern the amyloid toxicity in the presence of such small molecule modulators like polyphenols. Also, silibinin which is observed to negligibly affect the fibrillation pathway of γ-Syn, is found to modulate the fibrillar toxicity by increasing the cell viability in the presence of silibinin treated protofibrillar species of γ-Syn.

Together, the study demonstrates the various consequences of polyphenol treatment on fibrillation pathway of a moderately fibrillogenic but highly oligomeric protein like γ-Syn and suggests that the inherent complexities involved in the process of amyloidogenesis, owing to a highly transient and intermittent nature of the amyloid forming species (oligomers and protofibrils), result in further modulation in the presence of polyphenols that affect the fibrillation equilibrium by forming species with altered cytotoxicity. The study suggests a further in-depth investigation on the combined use of such polyphenols on moderately fibrillogenic proteins, including mapping of the binding sites to be able to develop effective therapeutic strategies in future.

Chapter 4

Effect of Polyols on the Structure and Aggregation of γ-Synuclein

The work described in this chapter has been published as:

Roy, S. and Bhat, R. (2018). Effect of polyols on the structure and aggregation of recombinant human γ-Synuclein, an intrinsically disordered protein. *Biochim. Biophys. Acta, Proteins Proteomics* **(doi.org/10.1016/j.bbapap.2018.07.003)**

1. Background

Among the protective osmolytes, the effects of polyol osmolytes (polyhydric alcohols) on the structure, stability and aggregation of globular proteins have been widely established (Gerlsma, 1968; Xie and Timasheff, 1997; Kaushik and Bhat, 1998; Mishra et al., 2005; Tiwari and Bhat, 2006; Vagenende et al., 2009; Khan et al., 2017). Polyols have been reported to impart protective effects by increasing thermal stability (Back et al., 1979; J. C. Lee and Timasheff, 1981) as well as by increasing the surface tension of the aqueous solutions thus facilitating protein folding (Kaushik and Bhat, 1998; Tiwari and Bhat, 2006). A linear relationship between the increasing number of hydroxyl (-OH) groups in the polyols, with the increasing thermal stability (Gerlsma, 1968; Fujita et al., 1982), increasing surface tension and thus increased protein stability (Kaushik and Bhat, 1998; Tiwari and Bhat, 2006) due to the excluded volume effect of polyols has been established previously. Additionally, polyols have also been demonstrated to induce a native-like structure from the denatured state by process of cooperative folding (Devaraneni et al., 2012) and also inhibit aggregation as well as promote refolding of a highly aggregation prone protein, citrate synthase (Mishra et al., 2005).

While the effect of osmolytes on the folding and aggregation of globular proteins is well established, the understanding of the osmolyte-mediated regulation of intrinsically disordered proteins with respect to their aggregation and fibrillation is not very clear. In this study the effect of the series of polyols comprising ethylene glycol, glycerol, erythritol, xylitol and sorbitol with an increment of single hydroxyl groups from 2 to 6 respectively, on the structure and aggregation of γ-Syn is investigated. The physicochemical properties of these polyols in aqueous solution and the experimental transfer free energies of the amino acid chains and the peptide backbone have also been estimated based on the values reported previously. The study observes varying effects of polyols on γ-Syn aggregation ranging from no effect to aggregation as well as suppression depending on the polyol concentration. The experimental findings suggest that the polyols affect γ-Syn nucleation and reduces overall fibrillation. However unlike for the effect on globular proteins, a linear relationship between the increasing number of –OH group in polyols and their effects on structure and aggregation has not been evident. Together, the study

suggests that the effect of polyol osmolytes on the stability and aggregation of IDPs, like γ-Syn is much more complex than their effect on globular proteins. It is further proposed that the modulatory effects of polyols on IDPs are largely governed by a fine balance between the favourable solvent – side chain and unfavourable peptide backbone-solvent interactions.

The chemical structures of the polyols used in the study are shown below:

Ethylene glycol

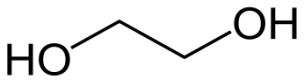

Glycerol

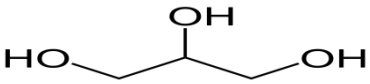

Erythritol

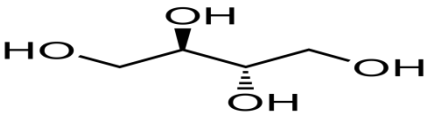

Xylitol

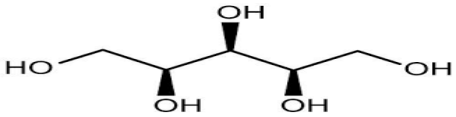

Sorbitol

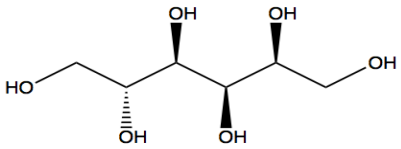

2. Results

2.1 Effect of polyols on the fibrillation kinetics of γ-Syn:

2.1.1 Thioflavin T assay

The effect of the polyol series with an increment of hydroxyl groups from 2 to 6 in ethylene glycol (EG), glycerol, erythritol, xylitol and sorbitol respectively on the fibrillation kinetics of γ-Syn was monitored using ThT assay. γ-Syn was incubated in the presence of an increasing concentration of polyols and the ThT fluorescence was recorded at regular intervals as a function of time. As shown in Figure 1A, in the presence of increasing concentration of EG (0.5 – 7.5M), ThT fluorescence increases initially at intermediate concentrations and diminishes at a concentration > 4.5M. The change in the ThT fluorescence with respect to increasing concentration of EG is shown in the Figure 1A (*right panel*), where suppression of fibrillation is

observed at a higher concentration of EG. In the presence of an increasing concentration of glycerol (0.5 – 4.5M), a concentration dependent decrease in the ThT fluorescence was observed indicating suppression of fibrillation (Figure 1B). While no noticeable difference in the ThT fluorescence in the presence of erythritol (0.5 – 2.5M) and xylitol (0.5 – 3M) was observed (Figure 1C and D respectively), the ThT fluorescence was significantly reduced in the presence of increasing concentrations of sorbitol (0.5 – 2M) thus indicating suppression of fibrillation by sorbitol (Figure 1E). As shown in Figure 1F, the ThT fluorescence measured at an equimolar concentration of polyols (2M) showed a reduced ThT fluorescence in the presence of only glycerol and sorbitol, while the effect of other polyols were observed to only marginally or negligibly affect the fibrillation of γ-Syn. This suggests that among the polyols, glycerol and sorbitol inhibit γ-Syn fibrillation effectively.

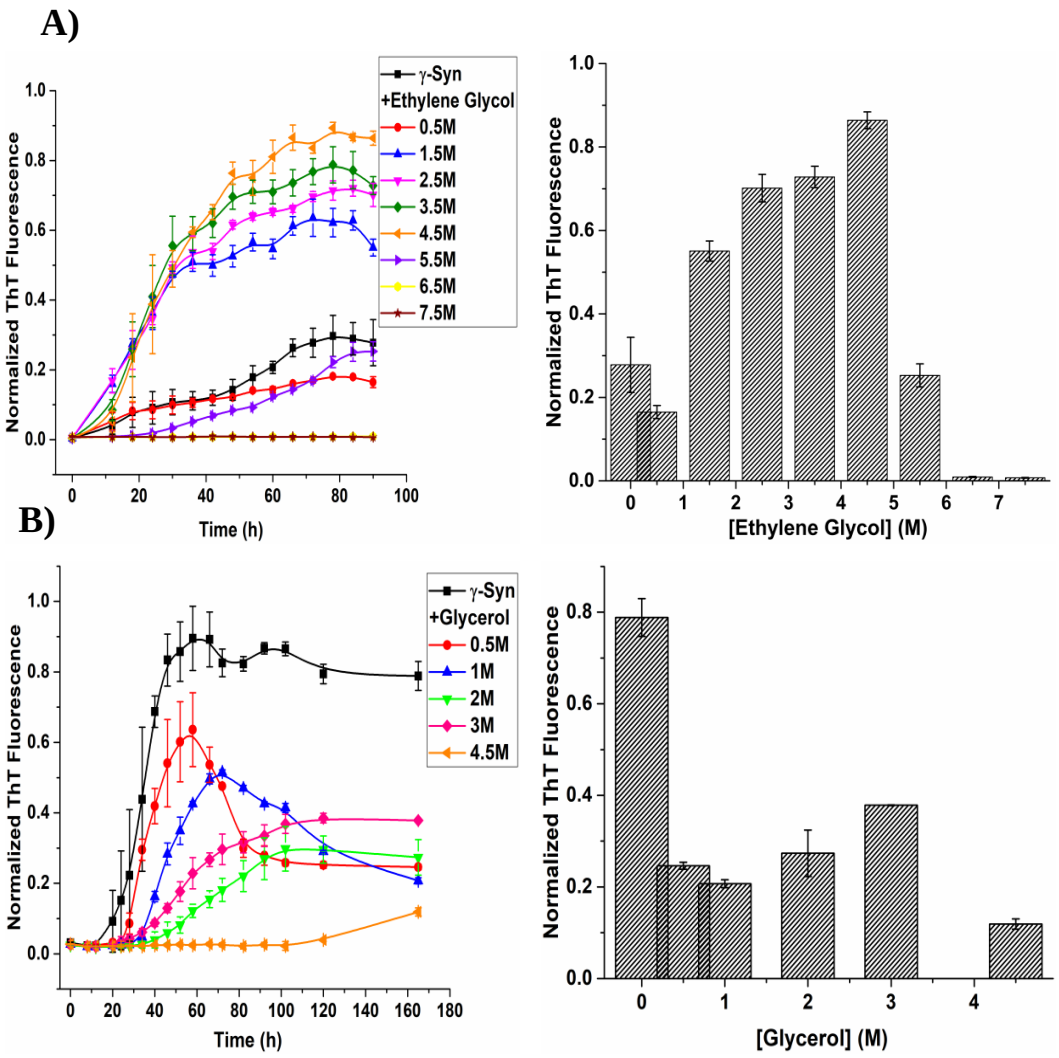

C)

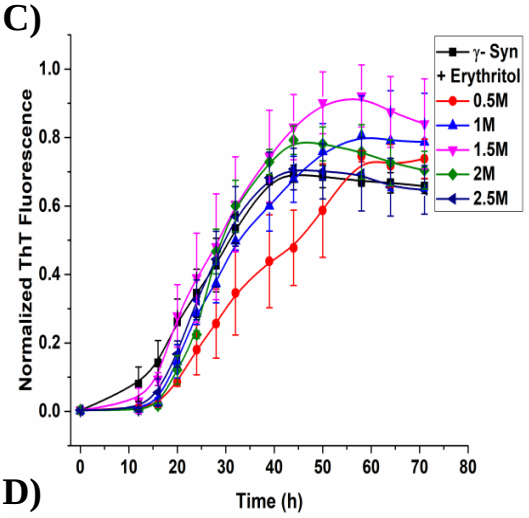
γ- Syn
+ Erythritol
0.5M
1M
1.5M
2M
2.5M
Normalized ThT Fluorescence
Time (h)

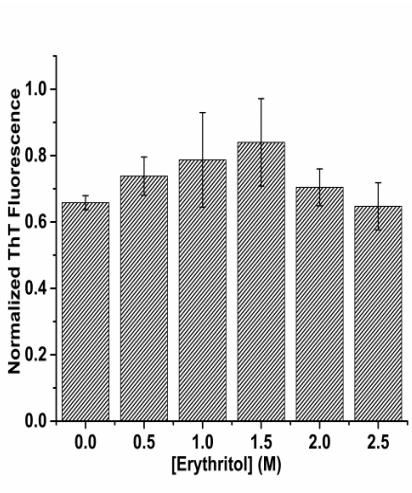
Normalized ThT Fluorescence
[Erythritol] (M)

D)

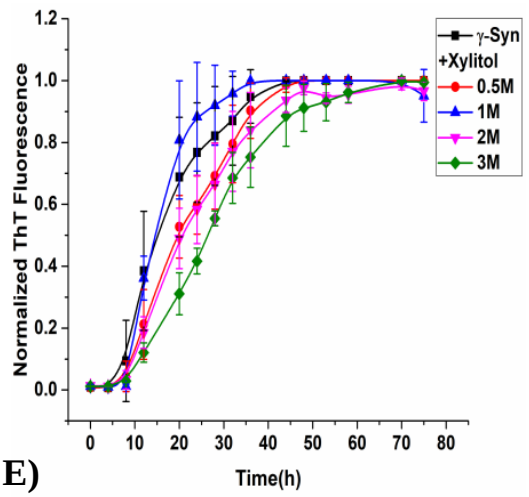
γ-Syn
+Xylitol
0.5M
1M
2M
3M
Normalized ThT Fluorescence
Time(h)

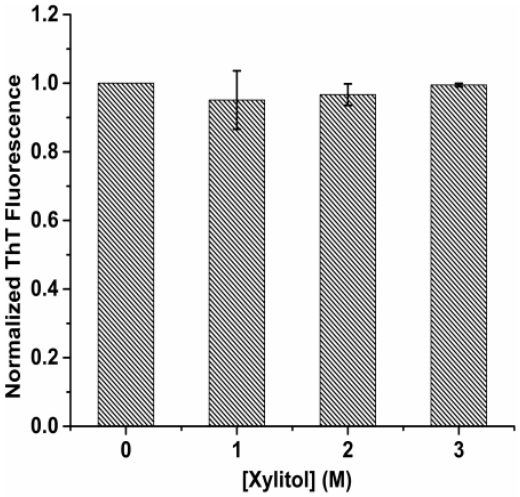
Normalized ThT Fluorescence
[Xylitol] (M)

E)

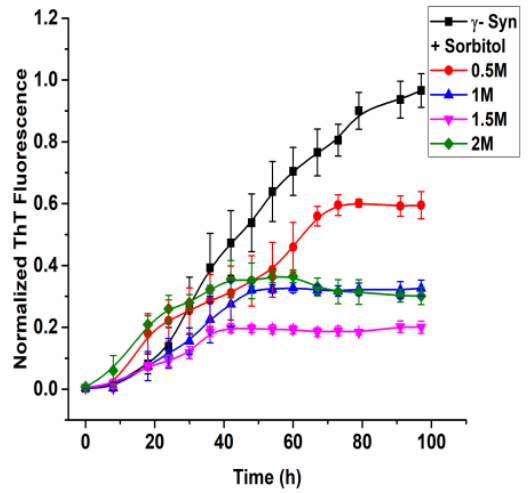
γ- Syn
+ Sorbitol
0.5M
1M
1.5M
2M
Normalized ThT Fluorescence
Time (h)

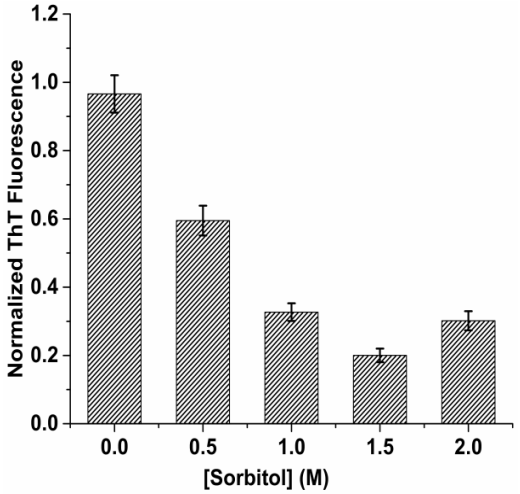
Normalized ThT Fluorescence
[Sorbitol] (M)

F)

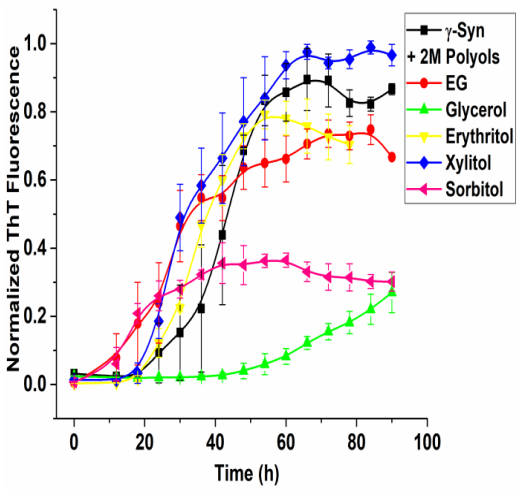

Figure 1. Fibrillation kinetics of γ-Syn in the presence of increasing concentrations of polyols monitored by Thioflavin T assay. The changes in the ThT fluorescence with *:(left and right)* an increasing time of fibrillation and increasing concentration of polyols, *A to E:* EG, glycerol, erythritol, xylitol and sorbitol respectively are shown. F) The relative ThT fluorescence at equimolar concentration (2M) of polyols. ThT was excited at 445 nm and the emission maximum was monitored at 480 nm with an excitation and emission slit widths of 5 nm. The error bars show ±SD (n=3).

2.1.2 Kinetic parameters of γ-Syn fibrillation in the presence of polyols

In order to further understand the effect of polyols on the fibrillation pathway of γ-Syn, the kinetic parameters of fibrillation, i.e. the lag time (t_{lag}) and apparent rate of fibrillation (k_{app}) were estimated using the equations described previously (Ban et al., 2003). Due to the absence of sigmoidal aggregation curve and poor fit quality, the effect of EG on the kinetic parameters of γ-Syn fibrillation could not be estimated. As shown in Figure 2A, a concentration dependent increase in the t_{lag} and a simultaneous decrease in the k_{app} were observed in the presence of an increasing concentration of glycerol. This suggests that glycerol suppresses γ-Syn fibrillation by inhibiting γ-Syn nucleation and retarding fibril polymerization. In the presence of erythritol (Figure 2B), an increase in the lag time with an increasing erythritol concentration was observed. Although the apparent rate of fibrillation (k_{app}) showed an overall increase in the trend, a direct dependence with increasing erythritol concentration was not established. The increase in the lag time in the presence of erythritol also suggests retardation of nucleation but the faster rate of fibrillation on the contrary suggests faster fibril polymerization, indicating a dual effect of erythritol on γ-Syn fibrillation. As shown in Figure 2C, an inverse relationship

between the lag time and rate of fibrillation was observed in the presence of xylitol, just as observed in the case of glycerol. The increased lag time and reduced rate of fibrillation in the presence of xylitol suggests stabilization of the natively unfolded monomer of γ-Syn that retards nucleation as well as stabilization of the protofibrillar species of the pathway that reduces the rate of fibrillation. Interestingly, as opposed to the observation made in the ThT fluorescence data that demonstrates suppression of γ-Syn fibrillation by sorbitol (Figure 1E), the kinetic parameters showed an initial increase in the lag time at lower concentrations which further decreased with an increasing sorbitol concentration (>0.5M), demonstrating sorbitol mediated oligomerization of γ-Syn monomers at higher concentrations. Also, a concentration dependent increase in the rate of fibrillation (k_{app}) in the presence of sorbitol suggests accelerated polymerization (Figure 2D).

Figure 2E, shows the comparison between the relative lag times of γ-Syn fibrillation at equimolar concentration (2M) of the polyols. The data demonstrate an inverse relationship between the increasing –OH groups in the polyols and the lag time of fibrillation, with the lag time of fibrillation decreasing with an increasing number of –OH groups. This suggests that polyols with higher number of –OH groups exclude strongly from the protein vicinity and facilitate γ-Syn nucleation, required for fibrillation.

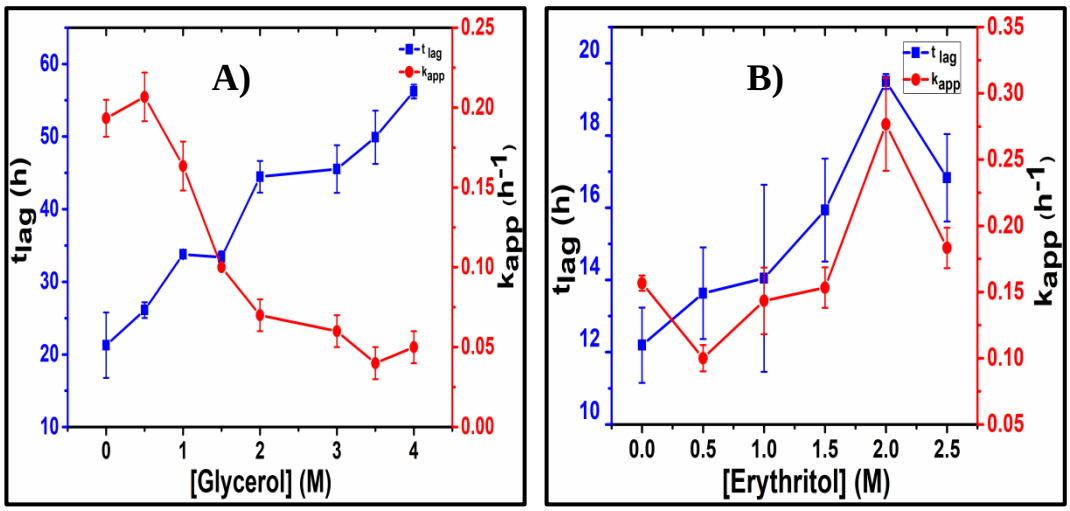

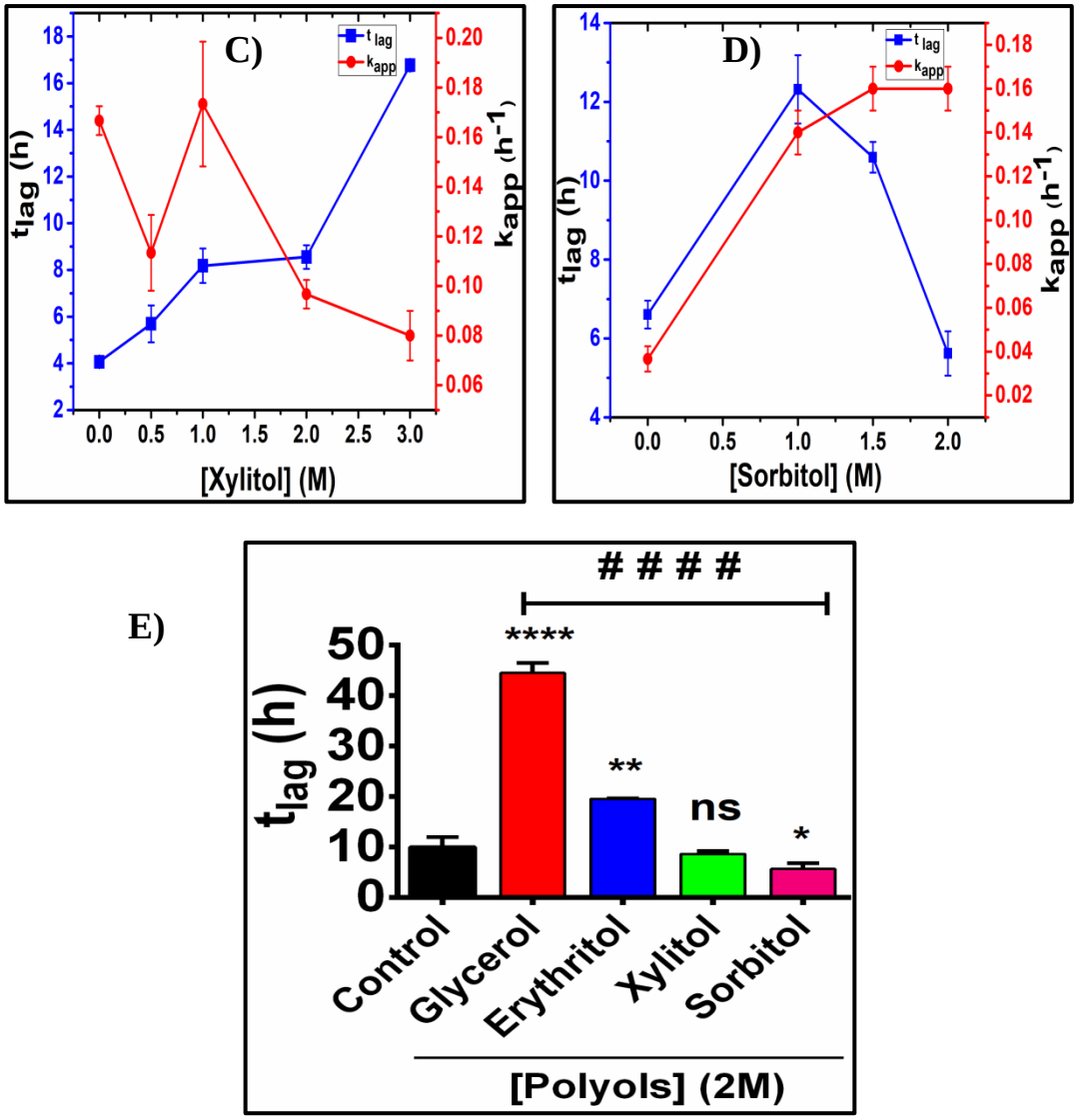

Figure 2. Kinetic parameters of γ-Syn fibrillation. Relationship between lag time (t_{lag}) and an apparent rate of fibrillation (k_{app}) of γ-Syn fibrillation in the presence of increasing concentration of polyols (*A to D:* glycerol, erythritol, xylitol and sorbitol respectively) is shown. E) Bar graph showing the comparison between the lag times of fibrillation in the presence of equimolar concentration (2M) of polyols. An increased lag time in the presence of glycerol and erythritol (****$p < 0.0001$ and **$p<0.005$ with respect to control in presence of glycerol and erythritol, respectively) is seen. In the presence of xylitol, no significant difference in the lag time was observed with respect to control and in the presence of sorbitol, the lag time was marginally reduced (*$p< 0.05$) with respect to control. The statistical analysis for the control and the polyol treated samples were analyzed using unpaired t-test. The data further show significant reduction in the lag time of fibrillation with increasing –OH group in the presence of 2M polyols ($^{####}p< 0.0001$, analyzed by one-way ANOVA). The error bars show ±SD (n=3).

2.1.3 Light scattering by γ-Synuclein species formed during fibrillation in the presence of polyols:

The effect of polyols on the aggregation propensity of γ-Syn was also validated by Rayleigh light scattering. γ-Syn was incubated in the presence of increasing concentration of polyols and the light scattering was monitored at regular intervals during fibrillation. As shown in Figure 3, an overall reduction in the scattering intensity in the presence of all the polyols was observed, indicating an overall reduced fibrillation as well as aggregation in the presence of polyols. In the presence of EG and glycerol (Figure 3A and B respectively), an early increase in the scattering intensity indicates the formation of amorphous aggregates in the earlier stages of the fibrillation pathway. The late rise in the scattering intensity in the presence of xylitol, indicates delayed aggregation, which was also validated by the increased lag time and reduced rate of fibrillation (Figure 2C). The significant decrease in the scattering intensity in the presence of sorbitol (Figure 3E) further validates the reduced fibrillation as observed by reduced overall fluorescence of ThT (Figure 1E).

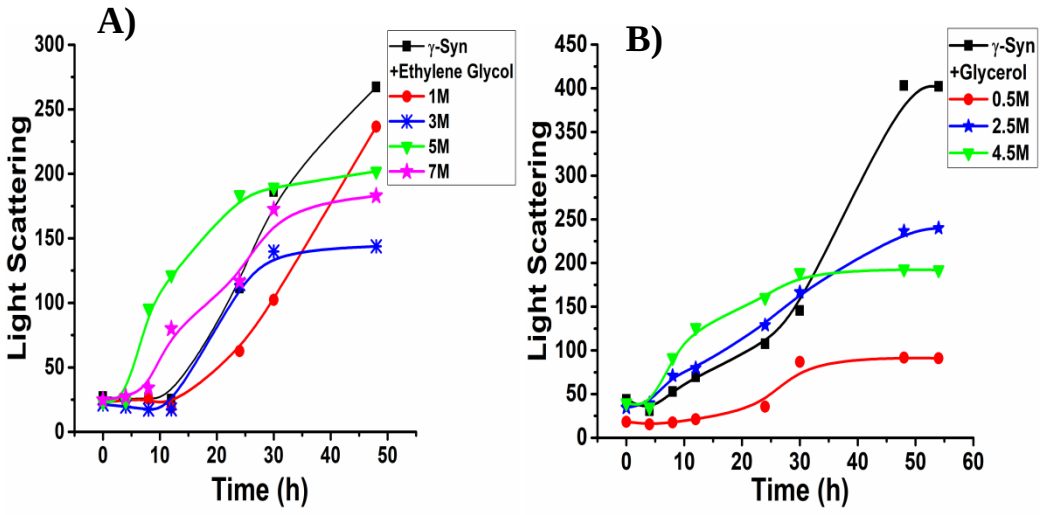

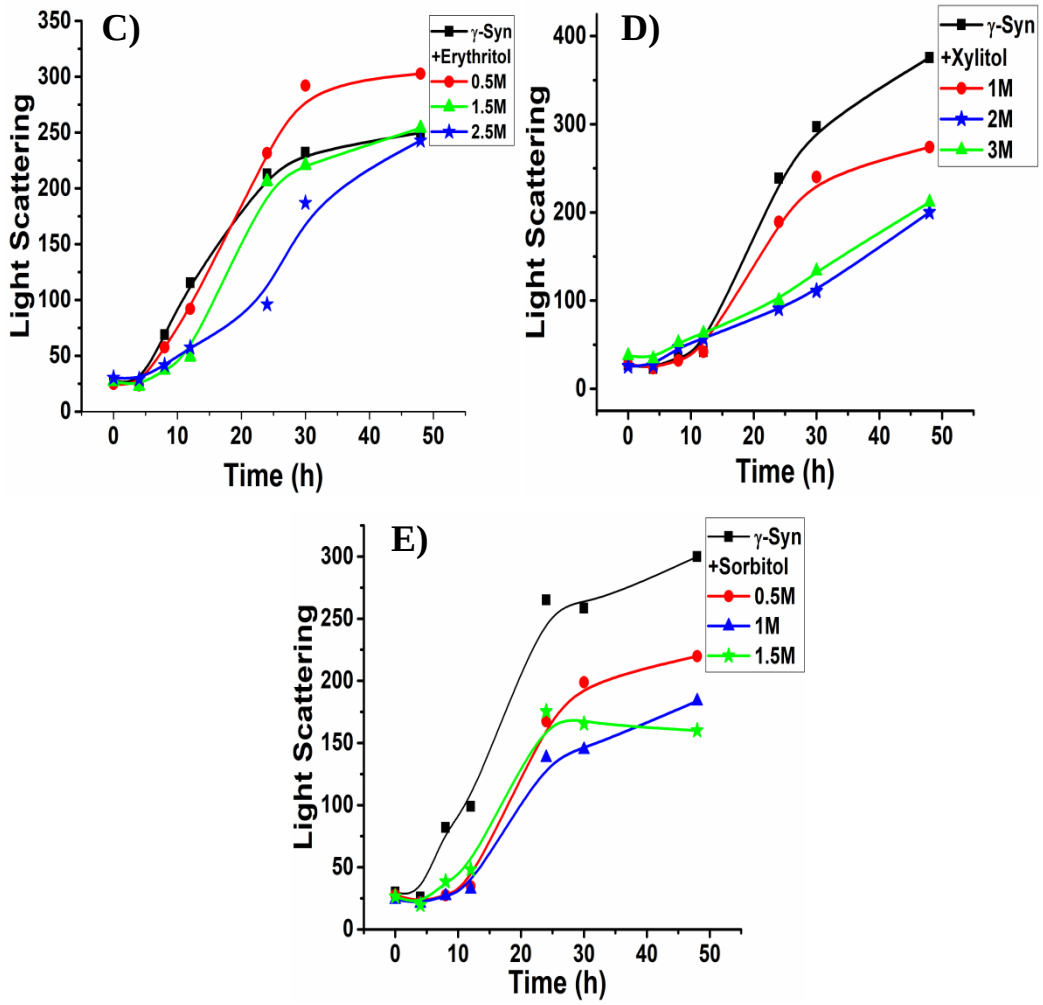

Figure 3. Light scattering by γ-Syn species formed in the absence and presence of polyols during fibrillation. The change in the scattering intensity with respect to the increasing concentration of polyols (*A to E:* EG, glycerol, erythritol, xylitol and sorbitol, respectively was monitored at regular time interval (0h, 4h, 8h, 12h, 24h, 30h and 48h) during fibrillation.

2.1.4 Morphology of the γ-Syn fibrils formed in the presence of polyols visualized by transmission electron microscopy (TEM):

The morphology of the γ-Syn fibrils formed in the presence of lower and higher concentrations of polyols were analyzed by TEM studies. As shown in Figure 4, the overall fibrillar yield in the presence of all the polyols was found to be reduced as compared to the fibrils formed by the untreated γ-Syn. In the presence of high concentration of ethylene glycol (7M), a significant disappearance of the mature fibrils along with the presence of disintegrated small structures was observed corresponding to the reduced ThT fluorescence observed in Figure 1A. In the

presence of glycerol and erythritol, along with reduced fibrillar yields, amorphous aggregates were also seen adhering to the fibrillar surface. In the presence of xylitol and sorbitol short and broken fibrils were also observed. Thus the TEM images obtained were in accordance with the overall reduced scattering observed in the presence of polyols (Figure 3).

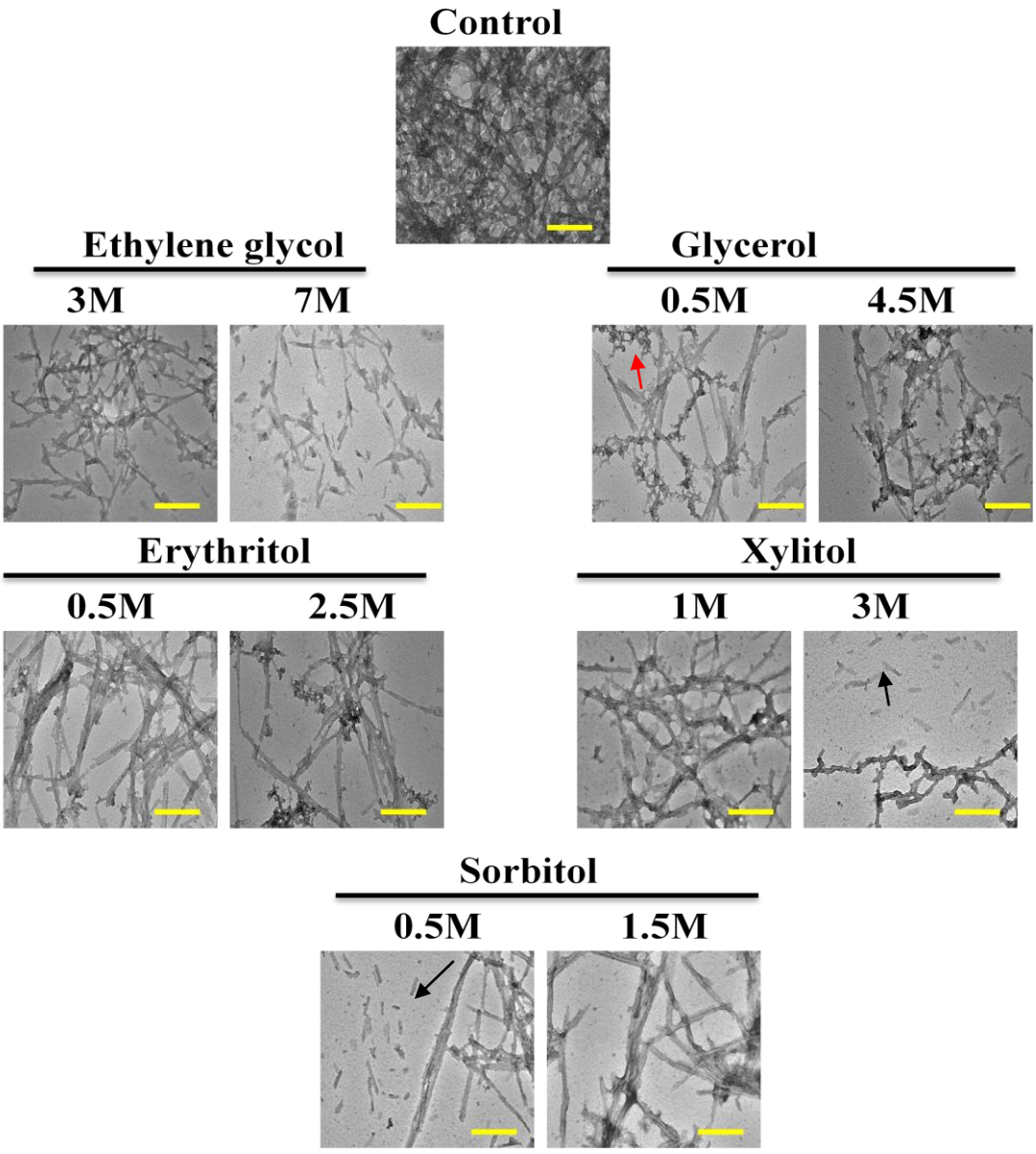

Figure 4. Morphology of γ-Syn fibrils formed in the presence of polyols visualized by transmission electron microscopy.TEM images of γ-Syn fibrils formed upon saturation in the (*top to bottom*) absence of polyols and in the presence of increasing concentration of EG, glycerol, erythritol, xylitol and sorbitol. *Red arrow* shows the formation of amorphous aggregates sticking on fibrillar surface and *black arrows* depict the formation of shorter fibrils in presence of xylitol and sorbitol. A scale bar of 100 nm is shown.

2.2 Effect of polyols on the structure of γ-Syn both under native and fibrillation conditions

The effect of polyols on the secondary structure of γ-Syn both under native and fibrillation conditions was also investigated by using far-UV circular dichroism (CD) spectroscopy and ANS binding assay.

2.2.1 Far-UV CD spectroscopy

2.2.1.1 Native conditions: In order to investigate the effects of polyols on the natively unfolded (intrinsically disordered) conformation of γ-Syn under non-fibrillating conditions, the far-UV CD spectra of γ-Syn in the absence and presence of increasing concentration of polyols were recorded (Figure 5A). The untreated γ-Syn showed a large negative ellipticity at ~200 nm and a small value at ~222 nm, characteristic of natively unfolded proteins. In the presence of EG, a concentration dependent increase in the negative ellipticity at 200 nm as well as 222 nm was observed indicating a partial unfolding of the residual structure of γ-Syn. While no such concentration dependence is observed in the presence of glycerol, the polyols next in the series, i.e. erythritol, xylitol and sorbitol were found to stabilize the natively unfolded conformation of γ-Syn with increasing number of –OH groups from 4 to 6 respectively. In the presence of erythritol, the negative ellipticity of γ-Syn at 200nm was maintained at a higher concentration of erythritol. Hence, a linear relationship between the increasing numbers of –OH groups in polyols with increased stabilization of the natively unfolded conformation of γ-Syn was observed.

2.2.1.2 Fibrillation conditions:

The effect of polyols on the structural transitions of γ-Syn occurring during aggregation both in the absence and presence of polyols was further investigated by incubating γ-Syn in the presence of equimolar concentration of polyols (2M) and recording the far-UV CD spectra at regular time intervals during fibrillation (0, 8, 24 and 48h). As shown in Figure 5B, except in the presence of EG, an increased α-helical propensity with the two characteristic minima at ~208 nm and ~222 nm during the exponential phase (24h) of γ-Syn fibrillation were observed. In the presence of EG, a structural transition from a natively unfolded conformation to a characteristic β-sheet structure with a negative ellipticity at ~218 nm was observed. Erythritol and xylitol were observed to retain α-helicity of γ-Syn even at the

saturation stage of fibrillation (48h). It is also noteworthy, that the α-helical propensity induced in the presence of polyols is retained by the intermediate polyols in the series, i.e. glycerol, erythritol and xylitol even at a saturation stage whereas polyols with 2 and 6 –OH groups, (EG and sorbitol, respectively) result in the formation of a predominant β-sheet structure upon saturation. The combined far-UV CD spectra of γ-Syn in the presence of equimolar concentration of polyols at 24h of fibrillation (Figure 5C) clearly demonstrate an increased α-helical tendency with the increasing number of –OH group in the polyols.

A)

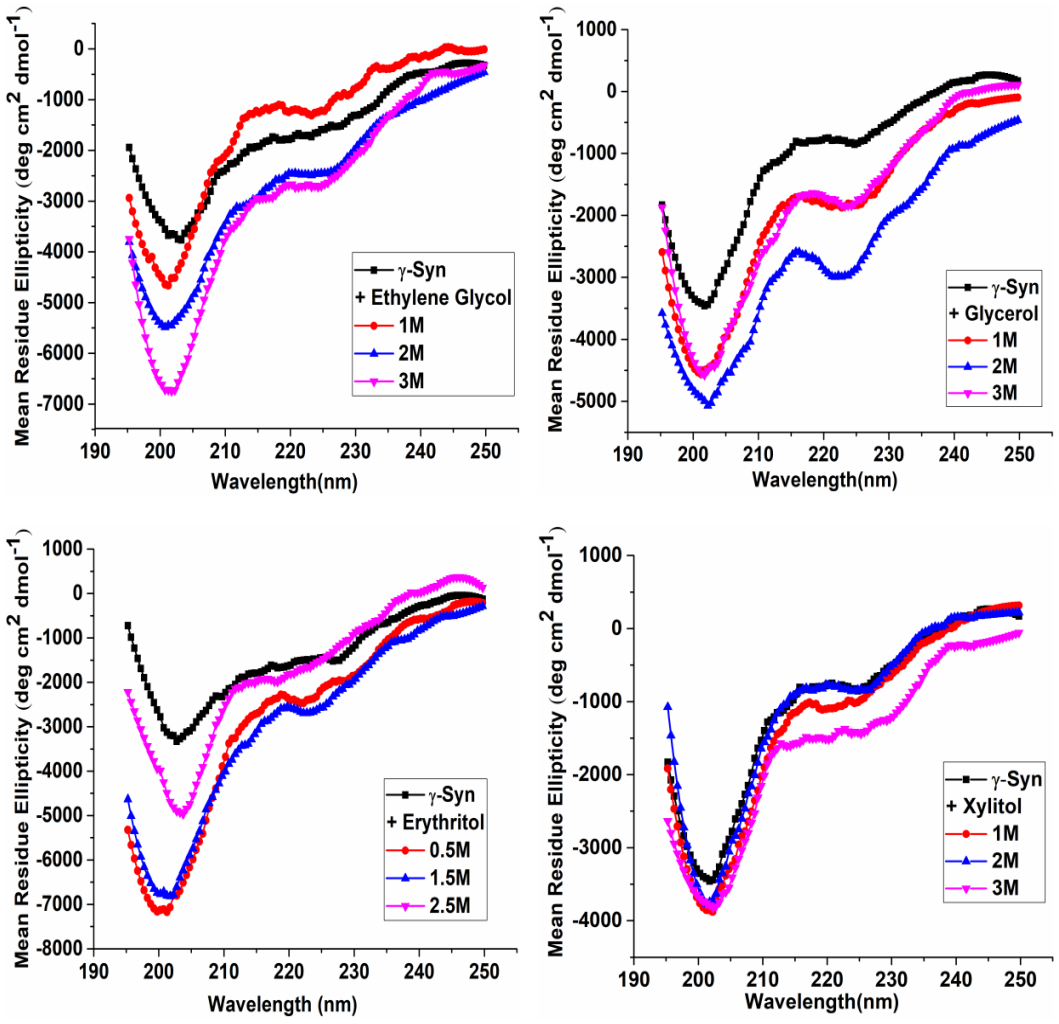

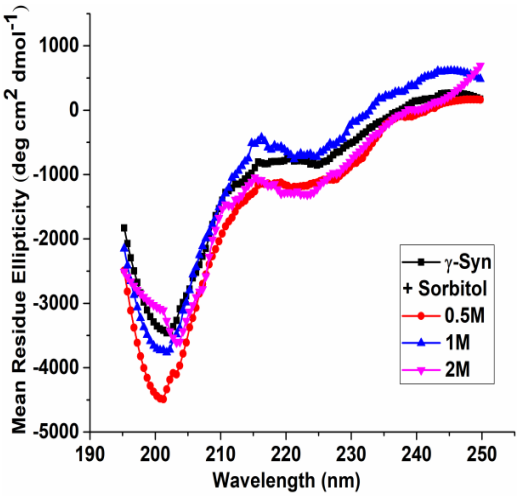
Mean Residue Ellipticity (deg cm^2 dmol^{-1})
Wavelength (nm)
γ-Syn
+ Sorbitol
0.5M
1M
2M

B)

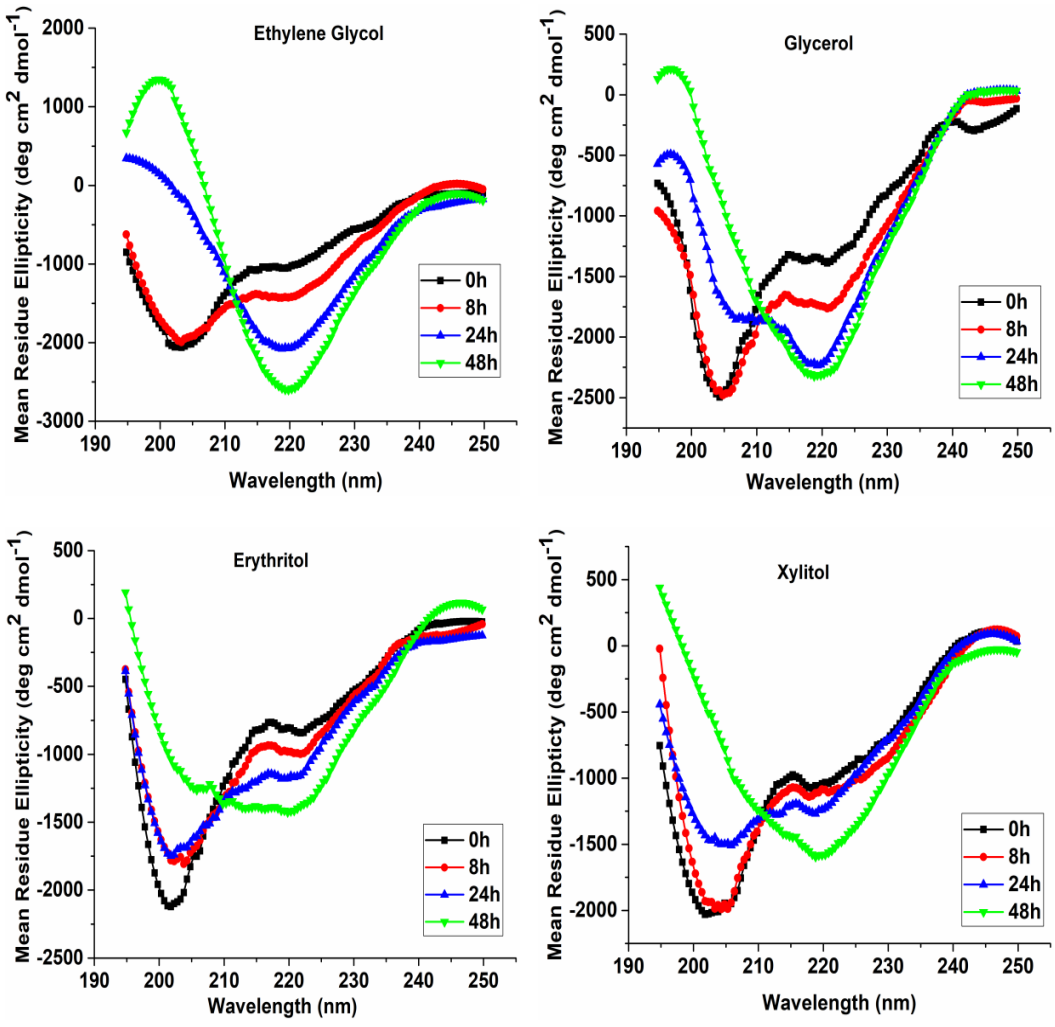
Ethylene Glycol
Glycerol
Erythritol
Xylitol
Mean Residue Ellipticity (deg cm^2 dmol^{-1})
Wavelength (nm)
0h
8h
24h
48h

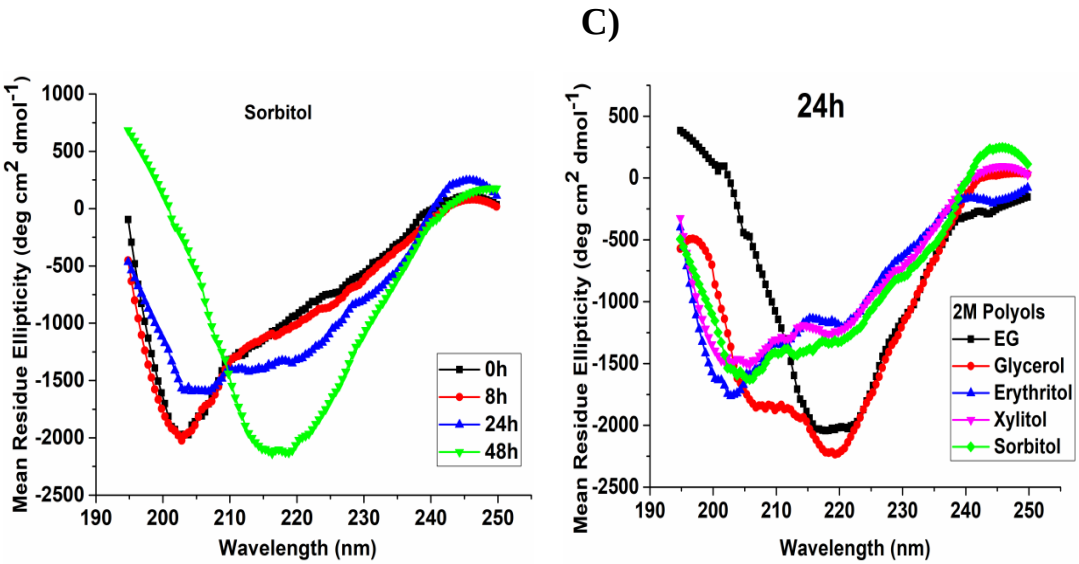

Figure 5. Structural characterization of γ-Syn in the presence of polyols by far-UV circular dichroism spectroscopy. The far-UV CD of γ-Syn in the presence and absence of polyols both under native and fibrillating conditions respectively were monitored at 25 °C using a cuvette of 1mm path length. A) Far-UV CD spectra of γ-Syn (0.5 mg/ml) dissolved in 20 mM phosphate buffer, pH 7.4 in the presence of increasing concentrations of polyols monitored under native conditions. B) Far-UV CD spectra of γ-Syn (0.3 mg/ml) in the presence of increasing concentrations of polyols monitored at time- intervals of 0h, 8h, 24h and 48h during fibrillation. C) Combined far-UV CD spectra at 24h of fibrillation taken from panel B (EG to Sorbitol) comparing the differences between the secondary structure propensities of γ-Syn in the presence of 2M polyols.

2.2.2 ANS binding assay

The effect of polyols on the extent of exposed hydrophobic surface area in γ-Syn was assessed by ANS binding assay. The ANS fluorescence spectra of monomeric γ-Syn in the absence and presence of 2M polyols nearly overlapped with each other, with an emission around 505 ± 0.5 nm (Figure 6A). Under fibrillating condition (24h), an increase in the ANS intensity with an increasing number of hydroxyl groups (-OH) in the polyols was observed with the blue-shifted emission maxima at ~480 nm (Figure 6B and C) with the exception of sorbitol. Although, the ANS emission in the presence of sorbitol was further blue-shifted, the ANS intensity was much reduced in its presence. The diminished ANS fluorescence in the presence of sorbitol could possibly be due to the sorbitol mediated compaction of γ-Syn leading to the burial of the sites required for ANS binding. Except sorbitol, overall these results demonstrate that the

extent of exposed surface hydrophobicity of γ-Syn species increases with the increasing number of –OH groups in the polyols, thus pointing to stronger preferential exclusion of polyols with higher number of –OH groups from the protein surface.

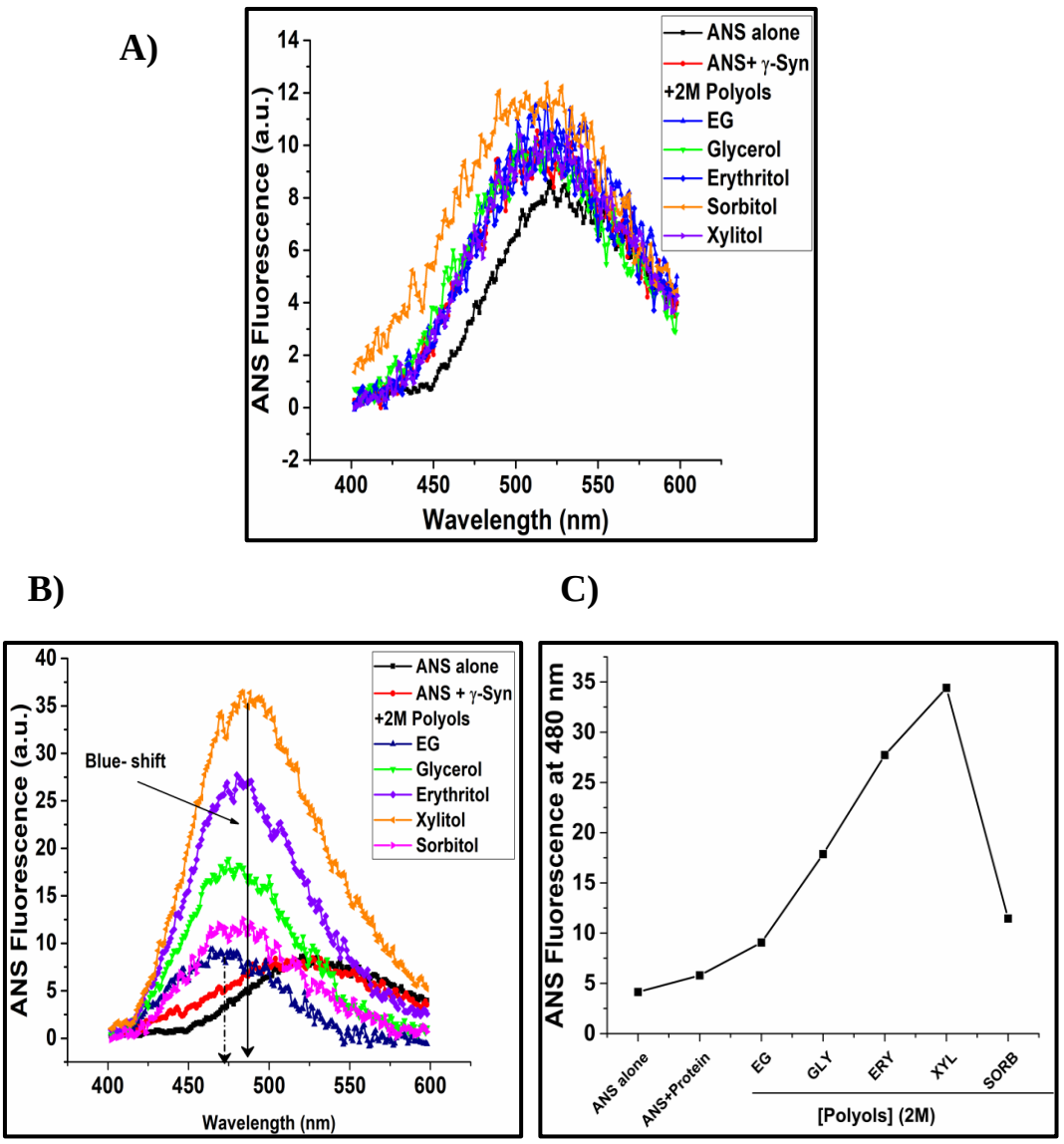

Figure 6. ANS binding to γ-Syn in the presence of polyols. A) Emission spectra of ANS binding to γ-Syn under native conditions in the presence of 2M polyols. B) ANS binding to aggregating species of γ-Syn formed after 24h of fibrillation in the presence of polyols showing an increase in the ANS intensity with increasing –OH groups in polyols with a characteristic blue-shifted emission (s*olid arrow*) at ~480 nm. A larger blue-shift is observed in the presence of EG (*dashed arrow*). C) Plot of ANS binding fluorescence intensity of γ-Syn at 480 nm in 2M polyols.

2.3 The transfer free energy values of γ-Syn from water to polyols

In order to gain an insight into the mechanism of varied effects of polyols on the fibrillation pathway of γ-Syn as observed in this study, the contribution by the amino acid side chains in γ-Syn to its stability and aggregation in the presence of polyols was investigated by estimating the free energy of transfer of γ-Syn from water into the 1M glycerol and 1M sorbitol, based on the amino acid composition of γ-Syn. The transfer free energies of free amino acids from water to 1M glycerol and 1M sorbitol were taken from the previously estimated values by Bolen and co-workers (Auton and Bolen, 2004, 2005; Auton et al., 2008). Such values for other polyols were not available in the literature. The amino acid side chain values were calculated by subtracting the glycine values from those of the given free energy transfer values of amino acids. As shown in the Table I, the free energy of transfer of γ-Syn to 1M sorbitol (3.9 kcal/mol) is more unfavourable than in 1M glycerol (3.2 kcal/mol), which demonstrates the role of a stronger preferential exclusion of sorbitol than glycerol. The calculations based on the amino acid compositions further suggest that the amino acid composition of γ-Syn as well as that of other IDPs and the interaction of polyols with the side chain if IDPs would govern the modulatory effects of polyols other than only the preferential exclusion effect.

Table I. Transfer free energies (cal/mol) of γ-Synuclein from water to 1M Glycerol and 1M Sorbitol calculated from its amino acid composition data.

Amino acid side chain	No. of Residues	1M Glycerol[a] ($\Delta G°_{tran}$)	Total residues value ($\Delta G°_{tran}$)	1M Sorbitol[a] ($\Delta G°_{tran}$)	Total residues value ($\Delta G°_{tran}$)
Nonpolar					
Ala	16	7.76	124.16	18.02	288.32
Phe	2	59.8	119.6	36.6	73.2
Leu	1	-34.4	-34.4	53.4	53.4
Ile	2	38.2	76.4	55	110
Val	22	-1.4	-30.8	40	880
Pro	2	-60.6	-121.2	-24	-48
Met	2	13.9	27.8	21.7	43.4
Tyr[c]	-	-	-	-	-
Polar					
Gly	10	0	0	0	0
Ser	10	6.3	63	-3.9	-39
Thr	10	17.5	175	20.7	207
Gln	6	-2.8	-16.8	-18.6	-111.6
Asn	4	51.6	206.4	-20.5	-82
Acidic					
Asp	3	52.1	156.3	-76	-228
Glu	19	63.4	1204.6	-63.1	-1198.9
Basic					
Lys	15	-34	-510	-21.6	-324
Arg	2	-30.7	-61.4	-18.9	-37.8
Backbone	126	15[b]	1890	35[b]	4410
Total ($\Delta G°_{transfer}$)			**3268.6**		**3996**

a. The side chain free energy transfer values from water to 1M glycerol and 1M sorbitol calculated by using values described by Auton et. al (Auton et al., 2008).

b. Peptide backbone contribution to free energy of transfer from water to 1M glycerol and 1M sorbitol described from previous reports (Auton and Bolen, 2004) and (Auton and Bolen, 2004, 2005), respectively.

c. Single Tyr of γ-Syn was not included in the calculations as $\Delta G^{\circ}_{transfer}$ was available only in 1M sorbitol.

3. Discussion

Studies on the effect of polyols on the structure and aggregation of intrinsically disordered proteins, which are otherwise known to stabilize the folded or native state of globular proteins (Mishra et al., 2005; Tiwari and Bhat, 2006; Vagenende et al., 2009; Devaraneni et al., 2012), is critical to answer a question as to how does a cell simultaneously regulate the balance between the globular and intrinsically disordered proteins under conditions of stress and preserve the physiological function of the proteins involved?

In this study the effect of a series of polyols on the structure and aggregation of γ-Syn is investigated and the relationship between the increasing number of –OH groups in polyols with enhanced protein stability and aggregation/fibrillation is examined. The ThT fluorescence data, monitored in the presence of polyols (Figure 1), reveal a varied effect on the fibrillation pathway of γ-Syn ranging from promoting aggregation to suppression or having a negligible effect, unlike reported for globular proteins previously (Mishra et al., 2005).The kinetic parameters (Figure 2), i.e. the lag time (t_{lag}) and apparent rate of γ-Syn fibrillation (k_{app}), estimated from the ThT assay (Figure 1), reveal that polyols act on the initial stages of γ-Syn fibrillation and a decrease in the lag time with increasing number of -OH groups in polyols is seen, except for ethylene glycol (EG) (Figure 1A) where no lag time was observable (Figure 2E).

Ethylene glycol shows a dual effect on γ-Syn fibrillation which is dependent on its concentration where the fibrillation is promoted at lower concentrations but is almost completely suppressed at higher concentration (>4.5M) (Figure 1A). Such a concentration mediated suppression of fibrillation by EG can be attributed to the increasing viscosity of the polyol (Munishkina et al., 2004; Kumar, 2009; Theillet et al., 2014) that possibly restricts the diffusion of protein molecules and inhibits protein-protein association giving rise to partially polymerized or reduced number of fibrils as seen in the electron micrographs (Figure 4). EG has earlier been observed to

affect the folding kinetics of the protein CI2 depending on its concentration, wherein an inverse relationship between the concentration of EG and rate of folding of the protein was observed. This effect has been related to the concentration-dependent changes in the viscosity of EG (Silow and Oliveberg, 2003). Light scattering studies show an overall reduced scattering by γ-Syn species in the presence of high concentration of EG (Figure 3A). Unlike complete suppression observed in the ThT assay, an increase in the scattering intensity was observed in the presence of higher concentration of EG, which indicates the formation of amorphous aggregates that do not bind to ThT and result in reduced fluorescence intensity in the ThT assay. However, the masking of ThT binding sites on γ-Syn fibrils at higher concentrations of polyols leading to reduced fluorescence intensity in ThT assay (Figure 1A) also can also not be ruled out.

Glycerol, known to be the smallest protein stabilizer among osmolytes (Vagenende et al., 2009) suppresses γ-Syn fibrillation in a concentration dependent manner that prolongs nucleation as well as retards the apparent rate of fibrillation (k_{app}) thereby preventing oligomerization and γ-Syn polymerization (Figure 1B, 2A and 3B).TEM images further reveal an overall reduction in the fibrillar yield along with the formation of amorphous aggregates, adhering to the fibrillar surface, in the presence of glycerol. The effect of glycerol observed on γ-Syn fibrillation could be explained by the 'solvophobic effect' of glycerol (Tiwari and Bhat, 2006) where it may favour the interaction between water molecules and protein surfaces, inhibiting the unfolding of the residual structure present in γ-Syn (Uversky et al., 2002; Marsh et al., 2006). The inhibition of γ-Syn fibrillation in the presence of glycerol could be explained by its preferential interaction with the exposed hydrophobic patches on the protein, possibly the NAC domain in γ-Syn (George, 2001), that stabilizes the aggregation-prone intermediates, thus imparting a dual effect based on the nature of the protein and the physicochemical properties of glycerol (Tiwari and Bhat, 2006; Vagenende et al., 2009). Contrary to the inhibition of γ-Syn fibrillation in the presence of glycerol observed in this study, glycerol has been previously reported to promote fibrillation of α-Synuclein (Munishkina et al., 2004) protein while both α - and γ-Syn belong to the same family of synuclein proteins (George, 2001). The contrasting effect of glycerol on the two members of the same family of proteins highlights the complexity of the effect of osmolytes toward the stability of IDPs. The early rise in the scattering intensity followed by an early saturation (Figure 3B) in the

presence of higher concentrations of glycerol could also be explained by the dual effect of glycerol where it possibly favours the collapse of the unfolded structure of γ-Syn at initial stages of fibrillation and leads to the formation of amorphous aggregates that do not participate in γ-Syn fibrillation.

The next polyols in the series, erythritol and xylitol lead to no significant change in the overall ThT fluorescence. The kinetic parameters of γ-Syn fibrillation reduced light scattering intensity and appearance of short fibrils in the TEM studies (Figure 2C, 3D and 4 respectively) in the presence of xylitol clearly indicate retarded fibril elongation and delayed nucleation. Thus, xylitol affects the fibrillation pathway of γ-Syn by acting on both the initial and the intermediate stages of fibrillation, as also seen in the presence of glycerol.

Sorbitol, a polyol with six –OH groups, reported to impart stability to globular proteins predominantly by preferential exclusion (Tiwari and Bhat, 2006) suppresses overall γ-Syn fibrillation and aggregation with increasing concentration (Figure 1E and 3E). Interestingly, the kinetic parameters of γ-Syn fibrillation show a concentration dependent decrease in the lag time (t_{lag}) and a simultaneous increase in the rate of fibrillation (k_{app}) (Figure 2D) which suggests that at lower concentrations, sorbitol being a predominantly hydrophilic solvent relative to the other polyols used (Hydrophobicity index being sorbitol<Xylitol<Erythritol<Glycerol<EG and proportional to the number of OH groups) (Abbas et al., 2011), possibly interacts with the polar side chains of γ-Syn but with a weaker affinity as compared to its interactions with the surrounding water molecules. At higher concentrations of sorbitol, the sorbitol-water interaction is likely to get further strengthened resulting in stronger preferential exclusion of sorbitol from γ-Syn surface, leading to the repulsive interaction between the hydrophobic NAC domain in γ-Syn (George, 2001) and surrounding water molecules, resulting in contraction of the unfolded γ-Syn. The compaction possibly brings the hydrophobic side chains in the close vicinity of each other facilitating intramolecular interactions which then promote intermolecular interactions, resulting in γ-Syn self-association and oligomerization. A similar effect of the osmolyte TMAO was also reported for the denatured ensemble of carboxyamidated RNase (Qu et al., 1998). Reduced ThT fluorescence along with low scattering intensity (Figure 1E and 3E), and a faster kinetics suggests the formation of early aggregating species that attain faster saturation and reduce the overall fibrillar

yield, leading to the formation of short fibrils of γ-Syn as also observed in TEM studies (Figure 4).

With increasing number of –OH groups in polyols, we observe a decrease in the lag time of fibrillation (Figure 2E) except in EG wherein no lag time was observable (Figure 1A). While glycerol, erythritol, xylitol and sorbitol show a decreasing trend for lag time of γ-Syn fibrillation with increasing –OH group, the effect is inversely proportional to their general stabilizing effect for globular proteins (Mishra et al., 2005). The increasing ANS intensity with increasing number of –OH groups in the polyols, except sorbitol further demonstrates the role of preferential-exclusion that leads to the formation of a molten-globule like state in γ-Syn leading to compaction that in turn promotes early nucleation and polymerization.

Free energy of transfer of amino acid side chains and the peptide backbone from water to various osmolytes including glycerol and sorbitol, evaluated by Bolen and co-workers, results in the net free energy of transfer of γ-Syn (based on its amino acid composition) from water to 1M glycerol and 1M sorbitol of 3.27 kcal/mol and 3.99 kcal/mol, respectively (Table I). This suggests that free energy of transfer of γ-Syn in sorbitol is much more unfavourable than in glycerol, which is in accordance with the reduced lag time observed in the presence of sorbitol relative to glycerol. The data in the table suggest varying free energies of transfer contributions by the polar, nonpolar and charged side chains in the presence of polyols used. It is noteworthy that except EG and sorbitol, all other polyols with respect to control, lead to an increase in the lag time of γ-Syn fibrillation, despite their preferential-exclusion property, whereas polymeric crowders like Ficoll and dextran are reported to reduce the lag time of α-Syn aggregation and promote fibrillation (Munishkina et al., 2004). These findings demonstrate that a fine balance between the preferential interaction of the polyol osmolytes with the polar and charged side chains and preferential exclusion due to unfavourable interaction with the peptide-backbone as well as with the non-polar side chains is significant in governing the stability of IDPs in the presence of polyol osmolytes. Thus, it can be concluded that in the case of IDPs, the stabilizing /destabilizing effect of osmolytes, and hence, their effect on fibrillation and aggregation would be governed by the strength of protein-solvent interactions and solute-solvent interactions which could vary from one IDP to another.

The TEM studies in the presence of polyols show clumping of fibrils and an overall reduction in the fibrillar yield without altering the fibrillar morphology, an

observation commonly reported in the presence of other osmolytes previously (Munishkina et al., 2004; Seeliger et al., 2013; Choudhary et al., 2015). Also, with increasing –OH group in the series that is, from erythritol to sorbitol, much shorter fibrillar species are formed which possibly arises due to macromolecular crowding (Latshaw et al., 2014). The far-UV CD and ANS binding studies reveal a relationship between increasing number of –OH group in polyols with increasing stability (Figure 5A and 6A) where the natively unfolded conformation of γ-Syn is maintained almost linearly with the increasing number of –OH groups in the polyols. The far-UV CD under fibrillation conditions shows that polyols with the increasing number of –OH groups delay the early structural transitions to β-sheet structures during fibrillation and induces the formation of an α-helical intermediate during the exponential stage of fibrillation which is marked by an increase in negative ellipticity with two minima at ~208 nm and ~222 nm (Figure 5B). Osmolytes have also been previously reported to predominantly induce an α-helical conformation in IDPs (Uversky, 2009; Levine et al., 2015) and regulate the IDPs by shuffling the different protein conformations of IDPs rather than giving rise to fundamentally new structures (Levine et al., 2015).

CONCLUSION

In conclusion, the study suggests that a fine balancing of general preferential exclusion effect of polyols based dominantly on the peptide backbone repulsion, weak and non-specific interaction with side chains of IDPs and the physico-chemical nature of the solution especially at higher concentration of polyols is expected to regulate and govern the formation of different conformational states of IDPs. The various conformational states of an IDP that arises in the presence of polyols could either be prone to aggregation/ fibril formation or could lead to the stability of the monomeric form, leading to suppression of fibrillation. Overall, the effect of polyol osmolytes on the conformation, stability, aggregation and fibril formation of an IDP like γ-Syn seems to be much more complex than observed for their effect on globular protein stability and aggregation. The findings suggest that under stress in cellular systems, the effect of polyol osmolyte on IDPs would vary depending on the physicochemical properties of polyols, amino acid side chain composition of IDP as well as active concentration of polyol in the protein vicinity. This would govern fine tuning of the osmolyte production at optimal concentrations in cellular systems under stress, in

order to generate a balance between the stability of globular proteins as well as various conformational states of IDPs to enable the cellular systems to combat stress in an effective way.

Summary

Summary

γ-Syn is the third member of the synuclein family, belonging to the class of intrinsically disordered proteins (IDPs), which fibrillates with a lesser propensity than its highly fibrillogenic counterpart α-Syn, and whose increased self-associating and oligomerization tendency has been implicated in a wide range of diseases including neurodegeneration and various forms of cancer. Despite its involvement in a plethora of diseases as well as its coexistence with the fibrillar plaques of α-Syn, called Lewy bodies, the knowledge of the effect of various modulators on the fibrillation pathway of γ-Syn remain unknown, which otherwise are widely being used as intervention strategies for other amyloidogenic proteins.

Another important aspect in biology, which till date remains elusive, is the understanding of the parallel regulation of the structure and function of the globular as well as intrinsically disordered proteins in cellular systems under stress. The accumulation of small organic solutes called osmolytes by a wide range of prokaryotic and eukaryotic organisms under extreme environmental conditions such as water stress, extreme temperatures, salt stress etc. have been reported to stabilize the tertiary structure of globular proteins by a mechanism of preferential exclusion but a unified view about their effect on the structure, aggregation and fibrillation properties of an IDP is still puzzling.

In view of the above background, this study is divided into two major sections. In the first section, the modulatory effect of naturally occurring small molecule compounds called polyphenols, epigallocatechin-3-gallate (EGCG), quercetin and silibinin have been investigated for their effect on the structure and fibrillation properties of γ-Syn. Second section investigates the effect of the polyol series f compounds comprising ethylene glycol (EG), glycerol, erythritol, xylitol and sorbitol containing an increasing number of hydroxyl groups (-OH groups) from 2 to 6 respectively on the fibrillation and structural properties of γ-Syn. The selection of the series enabled us to probe a correlation between increasing number of –OH groups in polyols with their effect on the stability and aggregation of γ-Syn, if any. A number of biophysical techniques such as steady-state and time-resolved fluorescence spectroscopy, circular dichroism spectroscopy, size-exclusion chromatography, electrophoresis, isothermal titration calorimetry and cytotoxicity

assays have been used to probe the mechanisms of polyphenol mediated modulation of γ-Syn fibrillation.

Studies on the effect of green tea polyphenol EGCG demonstrate strong modulation of γ-Syn fibrillation in the presence of EGCG. EGCG is observed to inhibit more than 50% of γ-Syn fibrillation at a sub-stoichiometry of even 5μM, indicating the role of EGCG in inhibiting the early stages of γ-Syn nucleation. It is further observed that EGCG also attenuates γ-Syn polymerization and leads to fibrillar disaggregation when added at different stages of γ-Syn fibrillation. The effect of EGCG on the secondary structure propensities of γ-Syn reveals that EGCG delays the structural transition of the natively unfolded conformation of γ-Syn to characteristic β-sheet structure during fibrillation. The study establishes that EGCG modulates γ-Syn fibrillation pathway to form α-helical containing higher ordered oligomers (~158 kDa and ~670 kDa) that are SDS-resistant and conformationally restricted in nature. It is also observed that the SDS-resistant higher ordered oligomers are also the resultant species formed upon EGCG mediated fibrillar disaggregation. The seeding studies reveal that these oligomers act as partial templates for γ-Syn polymerization and are thus kinetically retarded but on-pathway in nature that increases the kinetic barrier for γ-Syn elongation. Absence of fibrillation upon addition of EGCG to preformed γ-Syn seeds further establishes the inhibitory effect of EGCG on γ-Syn polymerization. Steady-state and time-resolved fluorescence spectroscopy and isothermal titration calorimetry (ITC) reveals a weak non-covalent interaction between EGCG and γ-Syn with the dissociation constant in the mM range (k_d ~ 2-10 mM). Interestingly, the cytotoxicity assays reveal that while EGCG-generated oligomers completely rescue the breast cancer (MCF-7) cells from γ-Syn toxicity, it reduces the viability of neuroblastoma (SH-SY5Y) cells. However, the disaggregated oligomers of γ-Syn are more toxic than the disaggregated fibrils for MCF-7cells.

Quercetin, the second polyphenol used in the study which is richly present in red wine also showed a concentration-dependent inhibition of γ-Syn fibrillation but unlike in the presence of EGCG, complete suppression of fibrillation was not observed. Thioflavin T (ThT) assay, transmission electron microscopy and atomic force microscopy (TEM and AFM respectively) demonstrates that quercetin, like EGCG also attenuates different stages of γ-Syn fibrillation and disaggregates the mature γ-Syn fibrils. Although the secondary structure propensity of γ-Syn both

under native and fibrillating conditions is not affected by the presence of quercetin, the ANS binding assay reveals that the species formed in the presence of quercetin maintains an overall low hydrophobicity. The interaction studies by steady-state fluorescence and isothermal titration calorimetry (ITC) along with the size-exclusion chromatography (SEC) further suggest that quercetin binds to γ-Syn with a moderate binding interaction with a dissociation constant in the ~μM range and preferentially interacts with the oligomers formed during the exponential stage of fibrillation to modulate them into SDS-labile off-pathway species. Interestingly, it is observed that quercetin modulated species (aggregates and some compact species) despite being off-pathway are significantly toxic to both the breast cancer (MCF-7) and neuroblastoma (SH-SY5Y) cell lines, thus providing an evidence of quercetin mediated fibrillar toxicity. Quercetin alone used as a control for both the cell lines was observed to be significantly toxic to both the cell lines, cautioning the use of quercetin as a therapeutic.

Lastly, among the three polyphenols used in the study, investigations on the effect of silibinin on γ-Syn structure and aggregation reveal an absence of fibrillation inhibition by silibinin within the concentrations used. While the ThT fluorescence remained unaffected in the presence of increasing concentration of silibinin, the morphology of the γ-Syn fibrils as visualized by TEM showed a reduced yield as well as slightly altered fibrillar morphology in the presence of higher concentration of silibinin (50μM), indicating the possibility of inhibitory activity at molar excess concentrations of silibinin. Silibinin like quercetin does not affect the overall secondary structure of γ-Syn but a concentration- dependent decrease in the overall hydrophobicity of γ-Syn during fibrillation is observed by ANS binding studies in the presence of silibinin. The overall reduction in exposed surface hydrophobicity in γ-Syn is further supported by the steady-state fluorescence analysis where an increasing red-shifted emission of single tyrosine present in γ-Syn is observed with respect to increasing concentration of silibinin, suggesting an increased solvent polarity around tyrosine in the presence of silibinin. The mode of binding interactions between γ-Syn and silibinin as studied by steady-state fluorescence, van't- Hoff analysis and ITC studies establish that silibinin forms a weak binding complex with γ-Syn with a dissociation constant in the range of ~10mM, indicating the role of non-covalent interactions between γ-Syn and silibinin. The decrease in the binding affinity between γ-Syn and silibinin with increasing temperature further

substantiates the formation of weak binding complex between γ-Syn and silibinin. The MTT assay used for studying the cytotoxic effects of silibinin generated γ-Syn species on MCF-7 and SH-SY5Y cells interestingly reveals an altered cytotoxicity for both the cells where the cell viabilities are increased in the presence of silibinin treated γ-Syn species formed at the 24h of fibrillation, which corresponds to the exponential stage involving oligomerization. This suggests that silibinin affects the toxic characteristics of γ-Syn species even in the absence of inhibition.

The other aspect of the study investigates the various effects of polyols on the γ-Syn structure and aggregation. Polyols used were ethylene glycol, glycerol, erythritol, xylitol and sorbitol having 2 – 6 –OH groups in them respectively. The effect of polyols on the fibrillation kinetics of γ-Syn as studied by ThT assay shows an absence of any linear correlation between the increasing number of –OH groups in the polyols and their effect on fibrillation which varies from suppression to no effect as well as promotion of fibrillation. While the ThT assay shows a mixed effect of polyols on γ-Syn fibrillation, the TEM and light scattering studies demonstrate an overall reduced fibrillar yield, and, thus aggregation. The kinetic parameters collectively suggest that the polyols act on the nucleation phase of the pathway and a decrease in the lag time of γ-Syn fibrillation with an increasing –OH groups in the polyols are observed that demonstrates the role of stronger preferential exclusion resulting in enhanced self-association and γ-Syn oligomerization. The polyols show a variable effect on the rate of γ-Syn fibrillation that indicates the role of the favourable amino acid side chains and polyol interactions. The polyols with increasing number of–OH groups were found to stabilize the natively unfolded conformation of γ-Syn and delay the structural transition to β-sheet structures by forming an α-helical intermediates during fibrillation. The study also estimates the free energy transfer of γ-Syn from water to 1M glycerol and 1M sorbitol based on its amino acid composition and demonstrates that the free energy of transfer to sorbitol is more unfavourable than glycerol, due to preferential exclusion. Based on the observations made in this study, it is proposed that the conformational states of an IDP like γ-Syn in the presence of polyol osmolytes would be governed by the interplay between the favourable solvent side chain interactions and unfavourable peptide backbone-solvent interactions, which in turn would depend on the physicochemical properties of polyols like viscosity as well amino acid composition of an IDP.

Taken together, the study provides detailed investigation on polyphenol mediated modulation of γ-Syn fibrillation pathway and demonstrates the various mechanisms by which the fibrillation pathway of a moderately fibrillogenic, yet pathogenic protein like γ-Syn is affected. The differential toxicity involving different modes of inhibition shown by γ-Syn species in the presence of therapeutic modulators like polyphenols throw light on its involvement in propagation of diseases and suggest that an understanding of the effects of such modulators on a highly oligomeric protein like γ-Syn could pave the way for development of potential intervention strategies. Additionally, these findings emphasise that the outcome of the osmolyte effects on IDP is much complex than their effect on globular proteins and the effects of a wide range of osmolytes on different IDPs need to be investigated in order to understand the mechanism of regulation of cellular homoeostasis including the balance between the stability of globular and intrinsically disordered proteins in cellular systems under stress.

References

Abbas, S. A., Sharma, V. K., Patapoff, T. W., & Kalonia, D. S. (2011). Solubilities and transfer free energies of hydrophobic amino acids in polyol solutions: Importance of the hydrophobicity of polyols. *Journal of Pharmaceutical Sciences, 100*(8), 3096-3104.

Abbas, S. A., Sharma, V. K., Patapoff, T. W., & Kalonia, D. S. (2012). Opposite effects of polyols on antibody aggregation: thermal versus mechanical stresses. *Pharmaceutical Research, 29*(3), 683-694.

Agarwal, R., Agarwal, C., Ichikawa, H., et al. (2006). Anticancer potential of silymarin: from bench to bed side. *Anticancer Research, 26*(6B), 4457-4498.

Ahmad, B., & Lapidus, L. J. (2012). Curcumin prevents aggregation in α-synuclein by increasing reconfiguration rate. *Journal of Biological Chemistry, 287*(12), 9193-9199.

Ahmad, M., Attoub, S., Singh, M., et al. (2007). Gamma-synuclein and the progression of cancer. *FASEB Journal, 21*(13), 3419-3430.

Alam, P., Chaturvedi, S. K., Siddiqi, M. K., et al. (2016). Vitamin k3 inhibits protein aggregation: implication in the treatment of amyloid diseases. *Scientific Reports, 6*, 26759.

Alam, P., Siddiqi, M. K., Chaturvedi, S. K., et al. (2017). Vitamin B12 offers neuronal cell protection by inhibiting Aβ-42 amyloid fibrillation. *International Journal of Biological Macromolecules, 99*, 477-482.

Amijee, H., Bate, C., Williams, A., et al. (2012). The N-Methylated Peptide SEN304 Powerfully Inhibits Aβ(1–42) Toxicity by Perturbing Oligomer Formation. *Biochemistry, 51*(42), 8338-8352.

Anfinsen, C. B. (1973). Principles that govern the folding of protein chains. *Science, 181*(4096), 223-230.

Apetri, M. M., Maiti, N. C., Zagorski, M. G., et al. (2006). Secondary structure of α-synuclein oligomers: characterization by raman and atomic force microscopy. *Journal of Molecular Biology, 355*(1), 63-71.

Arakawa, T., & Timasheff, S. N. (1983). Preferential interactions of proteins with solvent components in aqueous amino acid solutions. *Archives of Biochemistry and Biophysics, 224*(1), 169-177.

Arimon, M., Grimminger, V., Sanz, F., & Lashuel, H. A. (2008). Hsp104 targets multiple intermediates on the amyloid pathway and suppresses the seeding capacity of Aβ fibrils and protofibrils. *Journal of Molecular Biology, 384*(5), 1157-1173.

Auluck, P. K., Caraveo, G., & Lindquist, S. (2010). α-Synuclein: membrane interactions and toxicity in Parkinson's disease. *Annual Review of Cell and Developmental Biology, 26*, 211-233.

Auton, M., & Bolen, D. W. (2004). Additive transfer free energies of the peptide backbone unit that are independent of the model compound and the choice of concentration scale. *Biochemistry, 43*(5), 1329-1342.

Auton, M., & Bolen, D. W. (2005). Predicting the energetics of osmolyte-induced protein folding/unfolding. *Proceedings of the National Academy of Sciences, 102*(42), 15065-15068.

Auton, M., Bolen, D. W., & Rösgen, J. (2008). Structural thermodynamics of protein preferential solvation: osmolyte solvation of proteins, aminoacids, and peptides. *Proteins: Structure, Function, and Bioinformatics, 73*(4), 802-813.

Azam, S., Hadi, N., Khan, N. U., & Hadi, S. M. (2004). Prooxidant property of green tea polyphenols epicatechin and epigallocatechin-3-gallate: implications for anticancer properties. *Toxicology in vitro, 18*(5), 555-561.

Azriel, R., & Gazit, E. (2001). Analysis of the Minimal Amyloid-forming Fragment of the Islet Amyloid Polypeptide an experimental support for the key role of phenylalanine residue in amyloid formation. *Journal of Biological Chemistry, 276*(36), 34156-34161.

Babu, M. M. (2016). The contribution of intrinsically disordered regions to protein function, cellular complexity, and human disease. *Biochemical Society Transactions, 44*(5), 1185-1200.

Babu, M. M., van der Lee, R., de Groot, N. S., & Gsponer, J. (2011). Intrinsically disordered proteins: regulation and disease. *Current Opinion in Structural Biology, 21*(3), 432-440.

Back, J. F., Oakenfull, D., & Smith, M. B. (1979). Increased thermal stability of proteins in the presence of sugars and polyols. *Biochemistry, 18*(23), 5191-5196.

Bah, A., & Forman-Kay, J. D. (2016). Modulation of intrinsically disordered protein function by post-translational modifications. *Journal of Biological Chemistry, 291*(13), 6696-6705.

Bai, J., Liu, M., Pielak, G. J., & Li, C. (2017). Macromolecular and Small Molecular Crowding Have Similar Effects on α-Synuclein Structure. *ChemPhysChem, 18*(1), 55-58.

Ban, T., Hamada, D., Hasegawa, K., et al. (2003). Direct observation of amyloid fibril growth monitored by thioflavin T fluorescence. *Journal of Biological Chemistry, 278*(19), 16462-16465.

Barral, J. M., Broadley, S. A., Schaffar, G., & Hartl, F. U. (2004). Roles of molecular chaperones in protein misfolding diseases. *Seminars in Cell & Developmental Biology, 15* (1), 17-29.

Baughman, H. E. R., Clouser, A. F., Klevit, R. E., & Nath, A. (2018). HspB1 and Hsc70 chaperones engage distinct tau species and have different inhibitory effects on amyloid formation. *Journal of Biological Chemistry*.

Bennett, M. C. (2005). The role of α-synuclein in neurodegenerative diseases. *Pharmacology & Therapeutics, 105*(3), 311-331.

Biere, A. L., Wood, S. J., Wypych, J., et al. (2000). Parkinson's disease-associated α-synuclein is more fibrillogenic than β-and γ-synuclein and cannot cross-seed its homologs. *Journal of Biological Chemistry, 275*(44), 34574-34579.

Bieschke, J., Russ, J., Friedrich, R. P., et al. (2010). EGCG remodels mature α-synuclein and amyloid-β fibrils and reduces cellular toxicity. *Proceedings of the National Academy of Sciences, 107*(17), 7710-7715.

Bolen, D., & Baskakov, I. V. (2001). The osmophobic effect: natural selection of a thermodynamic force in protein folding1. *Journal of Molecular Biology, 310*(5), 955-963.

Bolognesi, B., Kumita, J. R., Barros, T. P., et al. (2010). ANS binding reveals common features of cytotoxic amyloid species. *ACS Chemical Biology, 5*(8), 735-740.

Bom, A. P. A., Rangel, L. P., Costa, D. C., et al. (2012). Mutant p53 aggregates into prion-like amyloid oligomers and fibrils implications for cancer. *Journal of Biological Chemistry, 287*(33), 28152-28162.

Boothby, T. C., Tapia, H., Brozena, A. H., et al. (2017). Tardigrades use intrinsically disordered proteins to survive desiccation. *Molecular Cell, 65*(6), 975-984.

Brighina, L., Okubadejo, N. U., Schneider, N. K., et al. (2007). Beta-synuclein gene variants and Parkinson's disease: a preliminary case-control study. *Neuroscience Letters, 420*(3), 229-234.

Brockhaus, K., Böhm, M. R., Melkonyan, H., & Thanos, S. (2018). Age-related Beta-synuclein Alters the p53/Mdm2 Pathway and Induces the Apoptosis of Brain Microvascular Endothelial Cells In Vitro. *Cell Transplantation, 27*(5), 796-813.

Brockwell, D. J., & Radford, S. E. (2007). Intermediates: ubiquitous species on folding energy landscapes? *Current Opinion in Structural Biology, 17*(1), 30-37.

Bucciantini, M., Giannoni, E., Chiti, F., et al. (2002). Inherent toxicity of aggregates implies a common mechanism for protein misfolding diseases. *Nature, 416*(6880), 507-511.

Calamai, M., Canale, C., Relini, A., et al. (2005). Reversal of protein aggregation provides evidence for multiple aggregated states. *Journal of Molecular Biology, 346*(2), 603-616.

Campioni, S., Mannini, B., Zampagni, M., et al. (2010). A causative link between the structure of aberrant protein oligomers and their toxicity. *Nature Chemical Biology, 6*(2), 140.

Caruana, M., Högen, T., Levin, J., et al. (2011). Inhibition and disaggregation of α-synuclein oligomers by natural polyphenolic compounds. *FEBS Letters, 585*(8), 1113-1120.

Caughey, B., & Lansbury Jr, P. T. (2003). Protofibrils, pores, fibrils, and neurodegeneration: separating the responsible protein aggregates from the innocent bystanders. *Annual Review of Neuroscience, 26*(1), 267-298.

Chang, Y. C., & Oas, T. G. (2010). Osmolyte-induced folding of an intrinsically disordered protein: folding mechanism in the absence of ligand. *Biochemistry, 49*(25), 5086-5096.

Cheng, B., Gong, H., Li, X., et al. (2012). Silibinin inhibits the toxic aggregation of human islet amyloid polypeptide. *Biochemical and Biophysical Research Communications, 419*(3), 495-499.

Cheng, B., Gong, H., Xiao, H., et al. (2013). Inhibiting toxic aggregation of amyloidogenic proteins: a therapeutic strategy for protein misfolding diseases. *Biochimica et Biophysica Acta (BBA)-General Subjects, 1830*(10), 4860-4871.

Cherny, R. A., Atwood, C. S., Xilinas, M. E., et al. (2001). Treatment with a copper-zinc chelator markedly and rapidly inhibits β-amyloid accumulation in Alzheimer's disease transgenic mice. *Neuron, 30*(3), 665-676.

Chinisaz, M., Ghasemi, A., Larijani, B., & Ebrahim-Habibi, A. (2014). Amyloid formation and inhibition of an all-beta protein: a study on fungal polygalacturonase. *Journal of Molecular Structure, 1059*, 94-100.

Chiti, F., Calamai, M., Taddei, N., et al. (2002). Studies of the aggregation of mutant proteins in vitro provide insights into the genetics of amyloid diseases. *Proceedings of the National Academy of Sciences, 99*(4), 16419-16426.

Chiti, F., Stefani, M., Taddei, N., et al. (2003a). Rationalization of the effects of mutations on peptide and protein aggregation rates. *Nature, 424*, 805.

Chiti, F., Stefani, M., Taddei, N., et al. (2003b). Rationalization of the effects of mutations on peptide andprotein aggregation rates. *Nature, 424*(6950), 805.

Chiti, F., Taddei, N., Baroni, F., et al. (2002). Kinetic partitioning of protein folding and aggregation. *Nature Structural & Molecular Biology, 9*(2), 137-143.

Choudhary, S., Kishore, N., & Hosur, R. V. (2015). Inhibition of insulin fibrillation by osmolytes: Mechanistic Insights. *Scientific Reports, 5*(1).

Clayton, D. F., & George, J. M. (1998). The synucleins: a family of proteins involved in synaptic function, plasticity, neurodegeneration and disease. *Trends in Neurosciences, 21*(6), 249-254.

Close, W., Neumann, M., Schmidt, A., et al. (2018). Physical basis of amyloid fibril polymorphism. *Nature Communications, 9*(1), 699.

Cookson, M. R. (2005). The biochemistry of Parkinson's disease. *Annual Review of Biochemistry, 74*, 29-52.

Cremades, N., Cohen, S. I., Deas, E., et al. (2012). Direct observation of the interconversion of normal and toxic forms of α-synuclein. *Cell, 149*(5), 1048-1059.

Dajas, F. (2012). Life or death: neuroprotective and anticancer effects of quercetin. *Journal of Ethnopharmacology, 143*(2), 383-396.

Danzer, K. M., Haasen, D., Karow, A. R., et al. (2007). Different species of α-synuclein oligomers induce calcium influx and seeding. *Journal of Neuroscience, 27*(34), 9220-9232.

de la Paz, M. L., Goldie, K., Zurdo, J., et al. (2002). De novo designed peptide-based amyloid fibrils. *Proceedings of the National Academy of Sciences, 99*(25), 16052-16057.

de la Paz, M. L., & Serrano, L. (2004). Sequence determinants of amyloid fibril formation. *Proceedings of the National Academy of Sciences, 101*(1), 87-92.

del Amo, J. M. L., Fink, U., Dasari, M., et al. (2012). Structural properties of EGCG-induced, nontoxic Alzheimer's disease Aβ oligomers. *Journal of Molecular Biology, 421*(4-5), 517-524.

Demuro, A., Mina, E., Kayed, R., et al. (2005). Calcium dysregulation and membrane disruption as a ubiquitous neurotoxic mechanism of soluble amyloid oligomers. *Journal of Biological Chemistry, 280*(17), 17294-17300.

Devaraneni, P. K., Mishra, N., & Bhat, R. (2012). Polyol osmolytes stabilize native-like cooperative intermediate state of yeast hexokinase A at low pH. *Biochimie, 94*(4), 947-952.

Dill, K. A., & Chan, H. S. (1997). From Levinthal to pathways to funnels. *Nature Structural Biology, 4*, 10-19.

Dill, K. A., & Chan, H. S. (1997). From Levinthal to pathways to funnels. *Nature Structural and Molecular Biology, 4*(1), 10.

Dill, K. A., & MacCallum, J. L. (2012). The protein-folding problem, 50 years on. *Science, 338*(6110), 1042-1046.

Dobson, C. M. (2003a). Protein folding and disease: a view from the first Horizon Symposium. *Nature Reviews Drug Discovery, 2*(2), 154.

Dobson, C. M. (2003b). Protein folding and misfolding. *nature, 426*(6968), 884.

Dobson, C. M. (2004). Principles of protein folding, misfolding and aggregation, *Seminars in Cell & Developmental Biology, 15*, 3-16.

Dobson, C. M., Šali, A., & Karplus, M. (1998). Protein folding: a perspective from theory and experiment. *Angewandte Chemie International Edition, 37*(7), 868-893.

Duan, S., Guan, X., Lin, R., et al. (2015). Silibinin inhibits acetylcholinesterase activity and amyloid β peptide aggregation: a dual-target drug for the treatment of Alzheimer's disease. *Neurobiology of Aging, 36*(5), 1792-1807.

Ducas, V. C., & Rhoades, E. (2014). Investigation of intramolecular dynamics and conformations of α-, β-and γ-synuclein. *PloS One, 9*(1), e86983.

Dunker, A. K., Lawson, J. D., Brown, C. J., et al. (2001). Intrinsically disordered protein. *Journal of Molecular Graphics and Modelling, 19*(1), 26-59.

Dyson, H. J. (2016). Making sense of intrinsically disordered proteins. *Biophysical Journal, 110*(5), 1013.

Dyson, H. J., & Wright, P. E. (2005). Intrinsically unstructured proteins and their functions. *Nature Reviews Molecular Cell Biology, 6*(3), 197.

Ecroyd, H., & Carver, J. A. (2008). Unraveling the mysteries of protein folding and misfolding. *IUBMB life, 60*(12), 769-774.

Ecroyd, H., Koudelka, T., Thorn, D. C., et al. (2008). Dissociation from the oligomeric state is the rate-limiting step in fibril formation by κ-casein. *Journal of Biological Chemistry, 283*(14), 9012-9022.

Ehrnhoefer, D. E., Bieschke, J., Boeddrich, A., et al. (2008). EGCG redirects amyloidogenic polypeptides into unstructured, off-pathway oligomers. *Nature Structural & Molecular Biology, 15*(6), 558-566.

Ehrnhoefer, D. E., Duennwald, M., Markovic, P., et al. (2006). Green tea (−)-epigallocatechin-gallate modulates early events in huntingtin misfolding and reduces toxicity in Huntington's disease models. *Human Molecular Genetics, 15*(18), 2743-2751.

Ellis, R. J. (2001a). Macromolecular crowding: an important but neglected aspect of the intracellular environment. *Current Opinion in Structural Biology, 11*(1), 114-119.

Ellis, R. J. (2001b). Macromolecular crowding: obvious but underappreciated. *Trends in Biochemical Sciences, 26*(10), 597-604.

Farmer, K., Gerson, J. E., & Kayed, R. (2017). Oligomer Formation and Cross-Seeding: The New Frontier. *Israel Journal of Chemistry, 57*(7-8), 665-673.

Ferreira, S. T., Vieira, M. N., & De Felice, F. G. (2007). Soluble protein oligomers as emerging toxins in Alzheimer's and other amyloid diseases. *IUBMB life, 59*(4-5), 332-345.

Fink, A. L. (1999). Chaperone-mediated protein folding. *Physiological Reviews, 79*(2), 425-449.

Forman, M. S., Trojanowski, J. Q., & Lee, V. M. (2004). Neurodegenerative diseases: a decade of discoveries paves the way for therapeutic breakthroughs. *Nature Medicine, 10*(10), 1055.

Fowler, D. M., Koulov, A. V., Balch, W. E., & Kelly, J. W. (2007). Functional amyloid–from bacteria to humans. *Trends in Biochemical Sciences, 32*(5), 217-224.

Fujita, Y., Iwasa, Y., & Noda, Y. (1982). The effect of polyhydric alcohols on the thermal denaturation of lysozyme as measured by differential scanning calorimetry. *Bulletin of the Chemical Society of Japan, 55*(6), 1896-1900.

Galvin, J. E., Uryu, K., Lee, V. M.-Y., & Trojanowski, J. Q. (1999). Axon pathology in Parkinson's disease and Lewy body dementia hippocampus contains α-, β-, and γ-synuclein. *Proceedings of the National Academy of Sciences, 96*(23), 13450-13455.

Gekko, K. (1981). Mecbanism of polyol-induced protein stabilization: solubility of amino acids and diglycine in aqueous polyol solutions. *The Journal of Biochemistry, 90*(6), 1633-1641.

Gekko, K., & Ito, H. (1990). Competing solvent effects of polyols and guanidine hydrochloride on protein stability. *The Journal of Biochemistry, 107*(4), 572-577.

Gekko, K., & Timasheff, S. N. (1981). Mechanism of protein stabilization by glycerol: preferential hydration in glycerol-water mixtures. *Biochemistry, 20*(16), 4667-4676.

George, J. M. (2001). The synucleins. *Genome Biology, 3*(1).

Gerlsma, S. (1968). Reversible denaturation of ribonuclease in aqueous solutions as influenced by polyhydric alcohols and some other additives. *Journal of Biological Chemistry, 243*(5), 957-961.

Glabe, C. G. (2006). Common mechanisms of amyloid oligomer pathogenesis in degenerative disease. *Neurobiology of Aging, 27*(4), 570-575.

Goldberg, A. L. (2003). Protein degradation and protection against misfolded or damaged proteins. *Nature, 426*(6968), 895.

Golebiewska, U., Zurawsky, C., & Scarlata, S. (2014). Defining the oligomerization state of γ-synuclein in solution and in cells. *Biochemistry, 53*(2), 293-299.

Gosal, W. S., Morten, I. J., Hewitt, E. W., et al. (2005). Competing pathways determine fibril morphology in the self-assembly of β 2-microglobulin into amyloid. *Journal of Molecular Biology, 351*(4), 850-864.

Greenwald, J., & Riek, R. (2010). Biology of amyloid: structure, function, and regulation. *Structure, 18*(10), 1244-1260.

Haataja, L., Gurlo, T., Huang, C. J., & Butler, P. C. (2008). Islet amyloid in type 2 diabetes, and the toxic oligomer hypothesis. *Endocrine Reviews, 29*(3), 303-316.

Harper, J. D., & Lansbury Jr, P. T. (1997). Models of amyloid seeding in Alzheimer's disease and scrapie: mechanistic truths and physiological consequences of the time-dependent solubility of amyloid proteins. *Annual Review of Biochemistry, 66*(1), 385-407.

Hartl, F. U., & Hayer-Hartl, M. (2009). Converging concepts of protein folding in vitro and in vivo. *Nature Structural and Molecular Biology, 16*(6), 574.

Hibi, T., Mori, T., Fukuma, M., et al. (2009). Synuclein-γ is closely involved in perineural invasion and distant metastasis in mouse models and is a novel prognostic factor in pancreatic cancer. *Clinical Cancer Research, 15*(8), 2864-2871.

Higashimoto, Y., Asanomi, Y., Takakusagi, S., et al. (2006). Unfolding, Aggregation, and Amyloid Formation by the Tetramerization Domain from Mutant p53 Associated with Lung Cancer. *Biochemistry, 45*(6), 1608-1619.

Hipp, M. S., Park, S.-H., & Hartl, F. U. (2014). Proteostasis impairment in protein-misfolding and-aggregation diseases. *Trends in Cell Biology, 24*(9), 506-514.

Horwich, A. (2002). Protein aggregation in disease: a role for folding intermediates forming specific multimeric interactions. *The Journal of Clinical Investigation, 110*(9), 1221-1232.

Hudson, S. A., Ecroyd, H., Kee, T. W., & Carver, J. A. (2009). The thioflavin T fluorescence assay for amyloid fibril detection can be biased by the presence of exogenous compounds. *The FEBS Journal, 276*(20), 5960-5972.

Illes-Toth, E., Ramos, M. R., Cappai, R., et al. (2015). Distinct higher-order α-synuclein oligomers induce intracellular aggregation. *Biochemical Journal, 468*(3), 485-493.

Ishii, T., Mori, T., Tanaka, T., et al. (2008). Covalent modification of proteins by green tea polyphenol (–)-epigallocatechin-3-gallate through autoxidation. *Free Radical Biology and Medicine, 45*(10), 1384-1394.

Jahn, T. R., & Radford, S. E. (2005). The Yin and Yang of protein folding. *The FEBS Journal, 272*(23), 5962-5970.

Jahn, T. R., & Radford, S. E. (2008). Folding versus aggregation: polypeptide conformations on competing pathways. *Archives of Biochemistry and Biophysics, 469*(1), 100-117.

Jain, M. K., & Bhat, R. (2014). Modulation of human α-synuclein aggregation by a combined effect of calcium and dopamine. *Neurobiology of Disease, 63*, 115-128.

Jain, M. K., Singh, P., Roy, S., & Bhat, R. (2018). Comparative analysis of the conformation, aggregation, interaction and fibril morphologies of human α, β and γ synuclein proteins. *Biochemistry, 57*(26), 3830-3848.

Jakes, R., Spillantini, M. G., & Goedert, M. (1994). Identification of two distinct synucleins from human brain. *FEBS Letters, 345*(1), 27-32.

Jang, J.-Y., Rhim, H., & Kang, S. (2018). NABi, a novel β-sheet breaker, inhibits Aβ aggregation and neuronal toxicity: Therapeutic implications for Alzheimer's disease. *Biochimica et Biophysica Acta (BBA)-General Subjects, 1862*(1), 71-80.

Jia, T., Liu, Y. E., Liu, J., & Shi, Y. E. (1999). Stimulation of breast cancer invasion and metastasis by synuclein γ. *Cancer Research, 59*(3), 742-747.

Jiang, Y., Liu, Y. E., Goldberg, I. D., & Shi, Y. E. (2004). γ synuclein, a novel heat-shock protein-associated chaperone, stimulates ligand-dependent estrogen receptor α signaling and mammary tumorigenesis. *Cancer Research, 64*(13), 4539-4546.

Jiménez-Aliaga, K., Bermejo-Bescós, P., Benedí, J., & Martín-Aragón, S. (2011). Quercetin and rutin exhibit antiamyloidogenic and fibril-disaggregating effects in vitro and potent antioxidant activity in APPswe cells. *Life Sciences, 89*(25-26), 939-945.

Jinghui, L., & Pieter, A. J. (2014). Cyclic Peptides as Inhibitors of Amyloid Fibrillation. *Chemistry – A European Journal, 20*(9), 2410-2419.

Karplus, M., & Weaver, D. L. (1976). Protein-folding dynamics. *Nature, 260*, 404-406.

Kaushik, J. K., & Bhat, R. (1998). Thermal stability of proteins in aqueous polyol solutions: role of the surface tension of water in the stabilizing effect of polyols. *The Journal of Physical Chemistry B, 102*(36), 7058-7066.

Kaushik, J. K., & Bhat, R. (2003). Why is trehalose an exceptional protein stabilizer? An analysis of the thermal stability of proteins in the presence of the compatible osmolyte trehalose. *Journal of Biological Chemistry, 278*(29), 26458-26465.

Kayed, R., Head, E., Thompson, J. L., et al. (2003). Common structure of soluble amyloid oligomers implies common mechanism of pathogenesis. *Science, 300*(5618), 486-489.

Khan, M. V., Ishtikhar, M., Rabbani, G., et al. (2017). Polyols (Glycerol and Ethylene glycol) mediated amorphous aggregate inhibition and secondary structure restoration of metalloproteinase-conalbumin (ovotransferrin). *International Journal of Biological Macromolecules, 94*, 290-300.

Kim, H., Park, B.-S., Lee, K.-G., et al. (2005). Effects of naturally occurring compounds on fibril formation and oxidative stress of β-amyloid. *Journal of Agricultural and Food Chemistry, 53*(22), 8537-8541.

Kim, Y. E., Hipp, M. S., Bracher, A., et al. (2013). Molecular chaperone functions in protein folding and proteostasis. *Annual Review of Biochemistry, 82*, 323-355.

Kittur, S., Wilasrusmee, S., Pedersen, W. A., et al. (2002). Neurotrophic and neuroprotective effects of milk thistle (Silybum marianum) on neurons in culture. *Journal of Molecular Neuroscience, 18*(3), 265-269.

Klunk, W. E., Pettegrew, J., & Abraham, D. J. (1989). Quantitative evaluation of congo red binding to amyloid-like proteins with a beta-pleated sheet conformation. *Journal of Histochemistry & Cytochemistry, 37*(8), 1273-1281.

Koo, E. H., Lansbury, P. T., & Kelly, J. W. (1999). Amyloid diseases: abnormal protein aggregation in neurodegeneration. *Proceedings of the National Academy of Sciences, 96*(18), 9989-9990.

Kopito, R. R., & Ron, D. (2000). Conformational disease. *Nature Cell Biology, 2*, E207-E209.

Křen, V., & Walterova, D. (2005). Silybin and silymarin–new effects and applications. *Biomed papers, 149*(1), 29-41.

Kumar, R. (2009). Role of naturally occurring osmolytes in protein folding and stability. *Archives of biochemistry and biophysics, 491*(1-2), 1-6.

Lackowicz, J. R. (1983). Principles of fluorescence spectroscopy. *Plenum Press,(New York, 1983) Chapter, 5*, 111-150.

Lasagna-Reeves, C. A., Castillo-Carranza, D. L., Guerrero-Muñoz, M. J., et al. (2010). Preparation and characterization of neurotoxic tau oligomers. *Biochemistry, 49*(47), 10039-10041.

Lasagna-Reeves, C. A., Castillo-Carranza, D. L., Sengupta, U., et al. (2012). Alzheimer brain-derived tau oligomers propagate pathology from endogenous tau. *Scientific Reports, 2*, 700.

Lashuel, H. A., Hartley, D. M., Balakhaneh, D., et al. (2002). New Class of Inhibitors of Amyloid-β Fibril Formation Implications for the Mechanism of pathogenesis in Alzheimer's Disease. *Journal of Biological Chemistry, 277*(45), 42881-42890.

Latshaw, D. C., Cheon, M., & Hall, C. K. (2014). Effects of macromolecular crowding on amyloid beta (16-22) aggregation using coarse-grained simulations. Journal of Physical Chemistry B, *118*(47), 13513-13526.

Lee, D., Paik, S. R., & Choi, K. Y. (2004). β-Synuclein exhibits chaperone activity more efficiently than α-synuclein. *FEBS Letters, 576*(1-2), 256-260.

Lee, J. C., & Timasheff, S. N. (1981). The stabilization of proteins by sucrose. *Journal of Biological Chemistry, 256*(14), 7193-7201.

Lee, S. J. C., Nam, E., Lee, H. J., et al. (2017). Towards an understanding of amyloid-β oligomers: characterization, toxicity mechanisms, and inhibitors. *Chemical Society Reviews, 46*(2), 310-323.

Lee, Y., Park, H. R., Chun, H. J., & Lee, J. (2015). Silibinin prevents dopaminergic neuronal loss in a mouse model of Parkinson's disease via mitochondrial stabilization. *Journal of Neuroscience Research, 93*(5), 755-765.

Leitao, A., Bhumkar, A., Hunter, D. J., et al. (2018). Unveiling a Selective Mechanism for the Inhibition of α-Synuclein Aggregation by β-Synuclein. *International Journal of Molecular Sciences, 19*(2), 334.

Levine, Z. A., Larini, L., LaPointe, N. E., et al. (2015). Regulation and aggregation of intrinsically disordered peptides. *Proceedings of the National Academy of Sciences, 112*(9), 2758-2763.

Libertini, L. J., & Small, E. W. (1985). The intrinsic tyrosine fluorescence of histone H1. Steady state and fluorescence decay studies reveal heterogeneous emission. *Biophysical Journal, 47*(6), 765-772.

Lim, W. K., Rösgen, J., & Englander, S. W. (2009). Urea, but not guanidinium, destabilizes proteins by forming hydrogen bonds to the peptide group. *Proceedings of the National Academy of Sciences, 106*(8), 2595-2600.

López, L. C., Varea, O., Navarro, S., et al. (2016). Benzbromarone, quercetin, and folic acid inhibit amylin aggregation. *International Journal of Molecular Sciences*, *17*(6), 964.

Lorenzen, N., Nielsen, S. B., Yoshimura, Y., et al. (2014). How epigallocatechin gallate can inhibit α-synuclein oligomer toxicity in vitro. *Journal of Biological Chemistry, 289*(31), 21299-21310.

Lu, J. H., Ardah, M. T., Durairajan, S. S. K., et al. (2011). Baicalein Inhibits Formation of α-Synuclein Oligomers within Living Cells and Prevents Aβ Peptide Fibrillation and Oligomerisation. *ChemBioChem, 12*(4), 615-624.

Ludtmann, M. H., Angelova, P. R., Horrocks, M. H., et al. (2018). α-synuclein oligomers interact with ATP synthase and open the permeability transition pore in Parkinson's disease. *Nature Communications, 9*(1), 2293.

Macchi, F., Eisenkolb, M., Kiefer, H., & Otzen, D. E. (2012). The effect of osmolytes on protein fibrillation. *International Journal of Molecular Sciences, 13*(3), 3801-3819.

Maiti, T. K., Ghosh, K. S., Samanta, A., & Dasgupta, S. (2008). The interaction of silibinin with human serum albumin: A spectroscopic investigation. *Journal of Photochemistry and Photobiology A: Chemistry, 194*(2-3), 297-307.

Manivel, P., Muthukumaran, J., Kannan, M., & Krishna, R. (2011). Insight into residues involved in the structure and function of the breast cancer associated protein human gamma synuclein. *Journal of Molecular Modeling, 17*(2), 251-263.

Mannelli, L. D. C., Zanardelli, M., Failli, P., & Ghelardini, C. (2012). Oxaliplatin-induced neuropathy: oxidative stress as pathological mechanism. Protective effect of silibinin. *The Journal of Pain, 13*(3), 276-284.

Marrazzo, G., Bosco, P., La Delia, F., et al. (2011). Neuroprotective effect of silibinin in diabetic mice. *Neuroscience Letters, 504*(3), 252-256.

Marsh, J. A., Singh, V. K., Jia, Z., & Forman-Kay, J. D. (2006). Sensitivity of secondary structure propensities to sequence differences between α-and γ-synuclein: Implications for fibrillation. *Protein Science, 15*(12), 2795-2804.

Mattson, M. P., Cheng, B., Davis, D., et al. (1992). beta-Amyloid peptides destabilize calcium homeostasis and render human cortical neurons vulnerable to excitotoxicity. *Journal of Neuroscience, 12*(2), 376-389.

Meier, J. J., Kayed, R., Lin, C.-Y., et al. (2006). Inhibition of human IAPP fibril formation does not prevent β-cell death: evidence for distinct actions of oligomers and fibrils of human IAPP. *American Journal of Physiology-Endocrinology and Metabolism, 291*(6), 1317-1324.

Meng, F.-G., Park, Y.-D., & Zhou, H.-M. (2001). Role of proline, glycerol, and heparin as protein folding aids during refolding of rabbit muscle creatine kinase. *The International Journal of Biochemistry & Cell Biology, 33*(7), 701-709.

Meng, X., Munishkina, L. A., Fink, A. L., & Uversky, V. N. (2009). Molecular mechanisms underlying the flavonoid-induced inhibition of α-synuclein fibrillation. *Biochemistry, 48*(34), 8206-8224.

Meng, X., Munishkina, L. A., Fink, A. L., & Uversky, V. N. (2010). Effects of various flavonoids on the-synuclein fibrillation process. *Parkinson's Disease, 28*(2010). 65-794.

Mezzenga, R., & Adamcik, J. (2018). The Amyloid Polymorphism in the Protein Folding and Aggregation Energy Landscape. *Angewandte Chemie International Edition*.

Mishra, R., Seckler, R., & Bhat, R. (2005). Efficient refolding of aggregation-prone citrate synthase by polyol osmolytes: how well are protein folding and stability aspects coupled? Journal of Biological Chemistry, *280*(16), 15553-15560.

Mittag, T., Kay, L. E., & Forman-Kay, J. D. (2010). Protein dynamics and conformational disorder in molecular recognition. *Journal of Molecular Recognition, 23*(2), 105-116.

Mollica, L., Bessa, L. M., Hanoulle, X., et al. (2016). Binding mechanisms of intrinsically disordered proteins: theory, simulation, and experiment. *Frontiers in Molecular Biosciences, 3*, 52.

Morar, A. S., Olteanu, A., Young, G. B., & Pielak, G. J. (2001). Solvent-induced collapse of α-synuclein and acid-denatured cytochrome c. *Protein Science, 10*(11), 2195-2199.

Mouillon, J. M., Eriksson, S. K., & Harryson, P. (2008). Mimicking the plant cell interior under water stress by macromolecular crowding: disordered dehydrin proteins are highly resistant to structural collapse. *Plant Physiology, 148*(4), 1925-1937.

Munishkina, L. A., Cooper, E. M., Uversky, V. N., & Fink, A. L. (2004). The effect of macromolecular crowding on protein aggregation and amyloid fibril formation. *Journal of Molecular Recognition, 17*(5), 456-464.

Murray, I. V., Lee, V. M.-Y., & Trojanowski, J. Q. (2001). Synucleinopathies: a pathological and molecular review. *Clinical Neuroscience Research, 1*(6), 445-455.

Naiki, H., & Gejyo, F. (1999). [20] Kinetic analysis of amyloid fibril formation *Methods in Enzymology. 309*, 305-318.

Nath, S., Meuvis, J., Hendrix, J., et al. (2010). Early aggregation steps in α-synuclein as measured by FCS and FRET: Evidence for a contagious conformational change. *Biophysical Journal, 98*(7), 1302-1311.

Necula, M., Kayed, R., Milton, S., & Glabe, C. G. (2007). Small molecule inhibitors of aggregation indicate that amyloid β oligomerization and fibrillization pathways are independent and distinct. *Journal of Biological Chemistry, 282*(14), 10311-10324.

Nelson, R., Sawaya, M. R., Balbirnie, M., et al. (2005). Structure of the cross-β spine of amyloid-like fibrils. *Nature, 435*(7043), 773.

Nerelius, C., Sandegren, A., Sargsyan, H., et al. (2009). α-Helix targeting reduces amyloid-β peptide toxicity. *Proceedings of the National Academy of Sciences, 106*(23), 9191-9196.

Neyroz, P., Zambelli, B., & Ciurli, S. (2006). Intrinsically disordered structure of Bacillus pasteurii UreG as revealed by steady-state and time-resolved fluorescence spectroscopy. *Biochemistry, 45*(29), 8918-8930.

Ngoungoure, V. L. N., Schluesener, J., Moundipa, P. F., & Schluesener, H. (2015). Natural polyphenols binding to amyloid: A broad class of compounds to treat different human amyloid diseases. *Molecular Nutrition & Food Research, 59*(1), 8-20.

Ninkina, N., Peters, O., Millership, S., et al. (2009). γ-Synucleinopathy: neurodegeneration associated with overexpression of the mouse protein. *Human Molecular Genetics, 18*(10), 1779-1794.

Novitskaya, V., Bocharova, O. V., Bronstein, I., & Baskakov, I. V. (2006). Amyloid fibrils of mammalian prion protein are highly toxic to cultured cells and primary neurons. *Journal of Biological Chemistry, 281*(19), 13828-13836.

Ono, K., Hamaguchi, T., Naiki, H., & Yamada, M. (2006). Anti-amyloidogenic effects of antioxidants: implications for the prevention and therapeutics of Alzheimer's disease. *Biochimica et Biophysica Acta (BBA)-Molecular Basis of Disease, 1762*(6), 575-586.

Onuchic, J. N., & Wolynes, P. G. (2004). Theory of protein folding. *Current Opinion in Structural Biology, 14*(1), 70-75.

Ossola, B., Kääriäinen, T. M., & Männistö, P. T. (2009). The multiple faces of quercetin in neuroprotection. *Expert Opinion on Drug Safety, 8*(4), 397-409.

Palhano, F. L., Lee, J., Grimster, N. P., & Kelly, J. W. (2013). Toward the molecular mechanism (s) by which EGCG treatment remodels mature amyloid fibrils. *Journal of the American Chemical Society, 135*(20), 7503-7510.

Pan, Z.-Z., Bruening, W., Giasson, B. I., et al. (2002). γ-Synuclein promotes cancer cell survival and inhibits stress-and chemotherapy drug-induced apoptosis by modulating MAPK pathways. *Journal of Biological Chemistry, 277*(38), 35050-35060.

Park, J.-Y., & Lansbury, P. T. (2003). β-Synuclein inhibits formation of α-synuclein protofibrils: a possible therapeutic strategy against Parkinson's disease. *Biochemistry, 42*(13), 3696-3700.

Pawar, A. P., DuBay, K. F., Zurdo, J., et al. (2005). Prediction of "aggregation-prone" and "aggregation-susceptible" regions in proteins associated with neurodegenerative diseases. *Journal of Molecular Biology, 350*(2), 379-392.

Pérez, C., & Griebenow, K. (2001). Improved activity and stability of lysozyme at the water/CH2CI2 interface: enzyme unfolding and aggregation and its prevention by polyols. *Journal of Pharmacy and Pharmacology, 53*(9), 1217-1226.

Pervin, M., Unno, K., Ohishi, T., et al. (2018). Beneficial Effects of Green Tea Catechins on Neurodegenerative Diseases. *Molecules, 23*(6), 1297.

Picotti, P., De Franceschi, G., Frare, E., et al. (2007). Amyloid fibril formation and disaggregation of fragment 1-29 of apomyoglobin: insights into the effect of pH on protein fibrillogenesis. *Journal of Molecular Biology, 367*(5), 1237-1245.

Plakoutsi, G., Bemporad, F., Calamai, M., et al. (2005). Evidence for a mechanism of amyloid formation involving molecular reorganisation within native-like precursor aggregates. *Journal of Molecular Biology, 351*(4), 910-922.

Porat, Y., Abramowitz, A., & Gazit, E. (2006). Inhibition of amyloid fibril formation by polyphenols: structural similarity and aromatic interactions as a common inhibition mechanism. *Chemical Biology & Drug Design, 67*(1), 27-37.

Qu, Y., Bolen, C., & Bolen, D. (1998). Osmolyte-driven contraction of a random coil protein. *Proceedings of the National Academy of Sciences, 95*(16), 9268-9273.

Richardson, J. S., & Richardson, D. C. (2002). Natural β-sheet proteins use negative design to avoid edge-to-edge aggregation. *Proceedings of the National Academy of Sciences, 99*(5), 2754-2759.

Rivera, I., Capone, R., Cauvi, D. M., et al. (2018). Modulation of Alzheimer's amyloid β peptide oligomerization and toxicity by extracellular Hsp70. *Cell Stress and Chaperones, 23*(2), 269-279.

Rose, G. D., Fleming, P. J., Banavar, J. R., & Maritan, A. (2006). A backbone-based theory of protein folding. *Proceedings of the National Academy of Sciences, 103*(45), 16623-16633.

Ross, C. A., & Poirier, M. A. (2004). Protein aggregation and neurodegenerative disease. *Nature Medicine, 10*(7), S10-17.

Sabogal-Guáqueta, A. M., Munoz-Manco, J. I., Ramírez-Pineda, J. R., et al. (2015). The flavonoid quercetin ameliorates Alzheimer's disease pathology and protects

cognitive and emotional function in aged triple transgenic Alzheimer's disease model mice. *Neuropharmacology, 93*, 134-145.

Sahay, S., Anoop, A., Krishnamoorthy, G., & Maji, S. K. (2014). Site-Specific Fluorescence Dynamics of α-Synuclein Fibrils Using Time-Resolved Fluorescence Studies: Effect of Familial Parkinson's Disease-Associated Mutations. *Biochemistry, 53*(5), 807-809.

Santoro, M. M., Liu, Y., Khan, S. M. A., et al. (1992). Increased thermal stability of proteins in the presence of naturally occurring osmolytes. *Biochemistry, 31*(23), 5278-5283.

Scaramozzino, F., Peterson, D. W., Farmer, P., et al. (2006). TMAO promotes fibrillization and microtubule assembly activity in the C-terminal repeat region of tau. *Biochemistry, 45*(11), 3684-3691.

Seeliger, J., Estel, K., Erwin, N., & Winter, R. (2013). Cosolvent effects on the fibrillation reaction of human IAPP. *Physical Chemistry Chemical Physics, 15*(23), 8902-8907.

Selkoe, D. J. (2003). Folding proteins in fatal ways. *Nature, 426*(6968), 900.

Serpell, L. C., Sunde, M., Benson, M. D., et al. (2000). The protofilament substructure of amyloid fibrils1. *Journal of Molecular Biology, 300*(5), 1033-1039.

Silow, M., & Oliveberg, M. (2003). High concentrations of viscogens decrease the protein folding rate constant by prematurely collapsing the coil. *Journal of Molecular Biology, 326*(1), 263-271.

Simmons, L. K., May, P. C., Tomaselli, K. J., et al. (1994). Secondary structure of amyloid beta peptide correlates with neurotoxic activity in vitro. *Molecular Pharmacology, 45*(3), 373-379.

Singer, M. A., & Lindquist, S. (1998). Multiple effects of trehalose on protein folding in vitro and in vivo. *Molecular Cell, 1*(5), 639-648.

Singh, S., & Singh, J. (2003). Effect of polyols on the conformational stability and biological activity of a model protein lysozyme. *Aaps Pharmscitech, 4*(3), 101-109.

Soto, C., Sigurdsson, E. M., Morelli, L., et al. (1998). β-sheet breaker peptides inhibit fibrillogenesis in a rat brain model of amyloidosis: implications for Alzheimer's therapy. *Nature Medicine, 4*(7), 822-826.

Stefani, M. (2004). Protein misfolding and aggregation: new examples in medicine and biology of the dark side of the protein world. *Biochimica et Biophysica Acta (BBA)-Molecular Basis of Disease, 1739*(1), 5-25.

Stefani, M. (2008). Protein folding and misfolding on surfaces. *International Journal of Molecular Sciences, 9*(12), 2515-2542.

Stefani, M., & Dobson, C. M. (2003). Protein aggregation and aggregate toxicity: new insights into protein folding, misfolding diseases and biological evolution. *Journal of Molecular Medicine, 81*(11), 678-699.

Stenvang, M., Dueholm, M. S., Vad, B. S., et al. (2016). Epigallocatechin Gallate Remodels Overexpressed Functional Amyloids in Pseudomonas aeruginosa and Increases Biofilm Susceptibility to Antibiotic Treatment. *Journal of Biological Chemistry, 291*(51), 26540-26553.

Stine, W. B., Dahlgren, K. N., Krafft, G. A., & LaDu, M. J. (2003). In vitro characterization of conditions for amyloid-β peptide oligomerization and fibrillogenesis. *Journal of Biological Chemistry, 278*(13), 11612-11622.

Street, T. O., Bolen, D. W., & Rose, G. D. (2006). A molecular mechanism for osmolyte-induced protein stability. *Proceedings of the National Academy of Sciences, 103*(38), 13997-14002.

Suematsu, N., Hosoda, M., & Fujimori, K. (2011). Protective effects of quercetin against hydrogen peroxide-induced apoptosis in human neuronal SH-SY5Y cells. *Neuroscience Letters, 504*(3), 223-227.

Suganthy, N., Devi, K. P., Nabavi, S. F., et al. (2016). Bioactive effects of quercetin in the central nervous system: Focusing on the mechanisms of actions. *Biomedicine & Pharmacotherapy, 84*, 892-908.

Sunde, M., Serpell, L. C., Bartlam, M., et al. (1997). Common core structure of amyloid fibrils by synchrotron X-ray diffraction1. *Journal of Molecular Biology, 273*(3), 729-739.

Sung, Y.-h., & Eliezer, D. (2007). Residual structure, backbone dynamics, and interactions within the synuclein family. *Journal of Molecular Biology, 372*(3), 689-707.

Surgucheva, I., Park, B.-C., Yue, B. Y., et al. (2005). Interaction of myocilin with γ-synuclein affects its secretion and aggregation. *Cellular and Molecular Neurobiology, 25*(6), 1009-1033.

Surgucheva, I., Sharov, V. S., & Surguchov, A. (2012). γ-Synuclein: seeding of α-synuclein aggregation and transmission between cells. *Biochemistry, 51*(23), 4743-4754.

Surguchov, A., Palazzo, R. E., & Surgucheva, I. (2001). Gamma synuclein: Subcellular localization in neuronal and non-neuronal cells and effect on signal transduction. *Cytoskeleton, 49*(4), 218-228.

Szabo, A., Lynn, K., Krajcarski, D., & Rayner, D. (1978). Tyrosinate fluorescence maxima at 345 nm in proteins lacking tryptophan at pH 7. *FEBS letters, 94*(2), 249-252.

Tamgüney, G., & Korczyn, A. D. (2017). A critical review of the prion hypothesis of human synucleinopathies. *Cell and Tissue Research*, 1-8.

Theillet, F.-X., Binolfi, A., Frembgen-Kesner, T., et al. (2014). Physicochemical properties of cells and their effects on intrinsically disordered proteins (IDPs). *Chemical Reviews, 114*(13), 6661-6714.

Thomas, P. J., Qu, B.-H., & Pedersen, P. L. (1995). Defective protein folding as a basis of human disease. *Trends in Biochemical Sciences, 20*(11), 456-459.

Tian, L., Zhao, Y., Truong, M.-J., et al. (2018). Synuclein gamma expression enhances radiation resistance of breast cancer cells. *Oncotarget, 9*(44), 27435-27447.

Timasheff, S. N. (1995). Solvent stabilization of protein structure *Protein Stability and Folding, 40*, 253-269.

Tiwari, A., & Bhat, R. (2006). Stabilization of yeast hexokinase A by polyol osmolytes: correlation with the physicochemical properties of aqueous solutions. *Biophysical Chemistry, 124*(2), 90-99.

Townsend, D., Hughes, E., Akien, G., et al. (2018). Epigallocatechin-3-gallate remodels apolipoprotein AI amyloid fibrils into soluble oligomers in the presence of heparin. *Journal of Biological Chemistry*, doi: 10.1074/jbc.RA118.002038.

Tran, H. T., Mao, A., & Pappu, R. V. (2008). Role of backbone− solvent interactions in determining conformational equilibria of intrinsically disordered proteins. *Journal of the American Chemical Society, 130*(23), 7380-7392.

Tsao, R. (2010). Chemistry and biochemistry of dietary polyphenols. *Nutrients, 2*(12), 1231-1246.

Tsigelny, I. F., Bar-On, P., Sharikov, Y., et al. (2007). Dynamics of α-synuclein aggregation and inhibition of pore-like oligomer development by β-synuclein. *The FEBS Journal, 274*(7), 1862-1877.

Uversky, V. N. (2002a). Natively unfolded proteins: a point where biology waits for physics. *Protein Science, 11*(4), 739-756.

Uversky, V. N. (2002b). What does it mean to be natively unfolded? *The FEBS Journal, 269*(1), 2-12.

Uversky, V. N. (2008). Amyloidogenesis of natively unfolded proteins. *Current Alzheimer Research, 5*(3), 260-287.

Uversky, V. N. (2009). Intrinsically disordered proteins and their environment: effects of strong denaturants, temperature, pH, counter ions, membranes, binding partners, osmolytes, and macromolecular crowding. *The protein Journal, 28*(7-8), 305-325.

Uversky, V. N. (2011). Intrinsically disordered proteins from A to Z. *The international journal of Biochemistry & Cell Biology, 43*(8), 1090-1103.

Uversky, V. N. (2016). Paradoxes and wonders of intrinsic disorder: Complexity of simplicity. *Intrinsically Disordered Proteins, 4*(1), e1135015.

Uversky, V. N., Li, J., & Fink, A. L. (2001). Evidence for a partially folded intermediate in α-synuclein fibril formation. *Journal of Biological Chemistry, 276*(14), 10737-10744.

Uversky, V. N., Li, J., Souillac, P., et al. (2002). Biophysical Properties of the Synucleins and Their Propensities to Fibrillate Inhibition of α-Synuclein assemble by β-and γ-Synucleins. *Journal of Biological Chemistry, 277*(14), 11970-11978.

Uversky, V. N., Oldfield, C. J., & Dunker, A. K. (2008). Intrinsically disordered proteins in human diseases: introducing the D2 concept. *Annual Review of Biophysics, 37*, 215-246.

Vagenende, V., Yap, M. G., & Trout, B. L. (2009). Mechanisms of protein stabilization and prevention of protein aggregation by glycerol. *Biochemistry, 48*(46), 11084-11096.

Viña, J. (2002). Biochemical adaptation: mechanism and process in physiological evolution. *Biochemistry and Molecular Biology Education, 30*(3), 215-216.

Volles, M. J., & Lansbury, P. T. (2007). Relationships between the sequence of α-synuclein and its membrane affinity, fibrillization propensity, and yeast toxicity. *Journal of molecular biology, 366*(5), 1510-1522.

Wang, J.-B., Wang, Y.-M., & Zeng, C.-M. (2011). Quercetin inhibits amyloid fibrillation of bovine insulin and destabilizes preformed fibrils. *Biochemical and biophysical research communications, 415*(4), 675-679.

Ward, S. M., Himmelstein, D. S., Lancia, J. K., & Binder, L. I. (2012). Tau oligomers and tau toxicity in neurodegenerative disease. *Biochemical Society Transactions, 40*(4), 667-671.

Welch, W. J., & Brown, C. R. (1996). Influence of molecular and chemical chaperones on protein folding. *Cell Stress & Chaperones, 1*(2), 109.

Winner, B., Jappelli, R., Maji, S. K., et al. (2011). In vivo demonstration that α-synuclein oligomers are toxic. *Proceedings of the National Academy of Sciences, 108*(10), 4194-4199.

Wiseman, R. L., Powers, E. T., & Kelly, J. W. (2005). Partitioning conformational intermediates between competing refolding and aggregation pathways: insights into transthyretin amyloid disease. *Biochemistry, 44*(50), 16612-16623.

Wolynes, P. G., Onuchic, J. N., & Thirumalai, D. (1995). Navigating the folding routes. *Science, 267*(5204), 1619-1619.

Wu, C., Lei, H., Wang, Z., et al. (2006). Phenol red interacts with the protofibril-like oligomers of an amyloidogenic hexapeptide NFGAIL through both hydrophobic and aromatic contacts. *Biophysical Journal, 91*(10), 3664-3672.

Xie, G., & Timasheff, S. N. (1997). Mechanism of the stabilization of ribonuclease A by sorbitol: preferential hydration is greater for the denatured than for the native protein. *Protein Science, 6*(1), 211-221.

Xue, W.-F., Hellewell, A. L., Gosal, W. S., et al. (2009). Fibril fragmentation enhances amyloid cytotoxicity. *Journal of Biological Chemistry, 284*(49), 34272-34282.

Yancey, P. H. (2005). Organic osmolytes as compatible, metabolic and counteracting cytoprotectants in high osmolarity and other stresses. *Journal of Experimental Biology, 208*(15), 2819-2830.

Yancey, P. H., Clark, M. E., Hand, S. C., et al. (1982). Living with water stress: evolution of osmolyte systems. *Science, 217*(4566), 1214-1222.

Yang-Hartwich, Y., Soteras, M., Lin, Z., et al. (2015). p53 protein aggregation promotes platinum resistance in ovarian cancer. *Oncogene, 34*(27), 3605.

Yin, F., Liu, J., Ji, X., et al. (2011). Silibinin: a novel inhibitor of Aβ aggregation. *Neurochemistry International, 58*(3), 399-403.

Young, L. M., Cao, P., Raleigh, D. P., et al. (2013). Ion mobility spectrometry–mass spectrometry defines the oligomeric intermediates in amylin amyloid formation and the mode of action of inhibitors. *Journal of the American Chemical Society, 136*(2), 660-670.

Z˘erovnik, E. (2002). Amyloid-fibril formation. Proposed mechanisms and relevance to conformational disease. *European Journal of Biochemistry, 269*(14), 3362-3371.

Zaidi, & Bhat. (2018). Resveratrol Interferes with an Early Step in the Fibrillization Pathway of Human Lysozyme and Modulates it towards Less-Toxic, Off-Pathway Aggregates. *ChemBioChem, 19*(2), 159-170.

Zhang, H., Kouadio, A., Cartledge, D., & Godwin, A. K. (2011). Role of gamma-synuclein in microtubule regulation. *Experimental Cell Research, 317*(10), 1330-1339.

Zhou, H.-X. (2012). Intrinsic disorder: signaling via highly specific but short-lived association. *Trends in Biochemical Sciences, 37*(2), 43-48.

Zhou, W., Zhu, M., Wilson, M. A., et al. (2006). The oxidation state of DJ-1 regulates its chaperone activity toward α-synuclein. *Journal of Molecular Biology, 356*(4), 1036-1048.

Zhu, M., Han, S., & Fink, A. L. (2013). Oxidized quercetin inhibits α-synuclein fibrillization. *Biochimica et Biophysica Acta (BBA)-General Subjects, 1830*(4), 2872-2881.

Zhu, M., Rajamani, S., Kaylor, J., et al. (2004). The flavonoid baicalein inhibits fibrillation of α-synuclein and disaggregates existing fibrils. *Journal of Biological Chemistry, 279*(26), 26846-26857.

Zraika, S., Hull, R., Verchere, C., et al. (2010). Toxic oligomers and islet beta cell death: guilty by association or convicted by circumstantial evidence? *Diabetologia, 53*(6), 1046-1056.

List of Publications:

1. Jain,M.K., Singh,P*., Roy,S*. and Bhat, R. (2018) Comparative Analysis of the Conformation, Aggregation, Interaction, and Fibril Morphologies of Human α-, β-, and γ-Synuclein Proteins. Biochemistry, **57** (26), 3830–3848.

2. Roy,S. and Bhat,R. (2018) Effect of polyols on the structure and aggregation of recombinant human γ-Synuclein, an intrinsically disordered protein *Biochim. Biophys. Acta, Proteins Proteomics* (doi.org/10.1016/j.bbapap.2018.07.003).

Conference Paper:

1. Roy, S. and Bhat, R. Inhibitory Effect of Polyphenol Epigallocatechin-3-gallate on the Fibrillation of Recombinant Human γ-Synuclein. Indian Biophysical Society, IISC, Bangalore, India, February 8-10, 2016.

2. Roy, S. and Bhat, R. EGCG Disaggregates Human γ-Synuclein Fibrils and Modulates the Pathway to Form Stable and Distinct Oligomeric Species. The Protein Society's 31st Annual Symposium, Montreal, Canada, July 24-27, 2017.(doi.org/10.1002/pro.3349).

3. Roy, S. and Bhat, R. Effect of Polyphenols on the Structure and Aggregation of Recombinant Human γ-Synuclein, an Intrinsically Disordered Proteins. Gordon Research Seminars and Conference-Intrinsically Disordered Proteins, Les Diablerets, Switzerland, June 30-July6, 2018.

*****Equal contribution

Turnitin Originality Report

Processed on: 13-Jul-2018 17:44 IST
ID: 982266215
Word Count: 38013
Submitted: 1

Ph. D. thesis By Sneha Roy

Similarity Index	Similarity by Source
12%	Internet Sources: 3% Publications: 11% Student Papers: 1%

1% match (publications)
Narendra Nath Jha, Srivastav Ranganathan, Rakesh Kumar, Surabhi Mehra et al. "Complexation of NAC derived peptide ligands with C-terminus of α-synuclein accelerates its aggregation", Biochemistry, 2017

< 1% match (publications)
Surabhi Mehra, Dhiman Ghosh, Rakesh Kumar, Mrityunjoy Mondal et al. "Glycosaminoglycans have variable effects on α-synuclein aggregation and differentially affect the activities of the resulting amyloid fibrils", Journal of Biological Chemistry, 2018

< 1% match (publications)
Singh, Pradeep K., Vasudha Kotia, Dhiman Ghosh, Ganesh M. Mohite, Ashutosh Kumar, and Samir K. Maji. "Curcumin Modulates α-Synuclein Aggregation and Toxicity", ACS Chemical Neuroscience, 2013.

< 1% match (publications)
Keiko Maeda, Masafumi Kuzuya, Xian Wu Cheng, Toshinobu Asai et al. "Green tea catechins inhibit the cultured smooth muscle cell invasion through the basement barrier", Atherosclerosis, 2003

< 1% match (publications)
Abdullah Sultan, Bakthisaran Raman, Ch. Mohan Rao, Ramakrishna Tangirala. " The Extracellular Chaperone Haptoglobin Prevents Serum Fatty Acid-promoted Amyloid Fibril Formation of β -Microglobulin, Resistance to Lysosomal Degradation, and Cytotoxicity ", Journal of Biological Chemistry, 2013

< 1% match (publications)
Nayere Taebnia, Dina Morshedi, Soheila Yaghmaei, Farhang Aliakbari, Fatemeh Rahimi, Ayyoob Arpanaei. "Curcumin-Loaded Amine-Functionalized Mesoporous Silica Nanoparticles Inhibit α-Synuclein Fibrillation and Reduce Its Cytotoxicity-Associated Effects", Langmuir, 2016

< 1% match (publications)
Thomas R. Jahn, Sheena E. Radford. "Folding versus aggregation: Polypeptide conformations on competing pathways", Archives of Biochemistry and Biophysics, 2008

< 1% match (publications)
M. Maeshima. "A Plasma Membrane-associated Protein of Arabidopsis thaliana AtPCaP1 Binds Copper Ions and Changes Its Higher Order Structure", Journal of Biochemistry, 06/16/2008

< 1% match (student papers from 29-Jul-2015)
Submitted to Savitribai Phule Pune University on 2015-07-29

< 1% match (student papers from 15-Mar-2017)
Submitted to Canterbury Christ Church University on 2017-03-15

< 1% match (publications)
Shuai Jiang, Lingling Wang, Mengmeng Huang, Zhihao Jia et al. "DM9 Domain Containing Protein Functions As a Pattern Recognition Receptor with Broad Microbial Recognition Spectrum", Frontiers in Immunology, 2017

< 1% match (publications)

"Encyclopedia of Cancer", Springer Nature, 2011

< 1% match (student papers from 28-Jul-2016)
Submitted to Jawaharlal Nehru University (JNU) on 2016-07-28

< 1% match (publications)
Xuli Wu, Weiyi He, Li Yao, Haiping Zhang, Zhigang Liu, Wenpu Wang, Ye Ye, Jijuan Cao. "Characterization of Binding Interactions of (−)-Epigallocatechin-3-gallate from Green Tea and Lipase", Journal of Agricultural and Food Chemistry, 2013

< 1% match (publications)
Yanping Li, Yangyang Zhou, Bowen Qi, Tao Gong, Xun Sun, Yao Fu, Zhirong Zhang. " Brain-Specific Delivery of Dopamine Mediated by , -Dimethyl Amino Group for the Treatment of Parkinson's Disease ", Molecular Pharmaceutics, 2014

< 1% match (publications)
Taebnia, Nayere, Dina Morshedi, Mohsen Doostkam, Soheila Yaghmaei, Farhang Aliakbari, Gurvinder Singh, and Ayyoob Arpanaei. "The effect of mesoporous silica nanoparticle surface chemistry and concentration on the α-synuclein fibrillation", RSC Advances, 2015.

< 1% match (publications)
Advances in Experimental Medicine and Biology, 2015.

< 1% match (publications)
"From Protein Structure to Function with Bioinformatics", Springer Nature, 2017

< 1% match (publications)
"Poster Session Abstracts.(Abstracts)(Report)(Author abstract)", Indian Journal of Pharmacology, Dec 2015 Issue

< 1% match (publications)
Matthew Auton. "Structural thermodynamics of protein preferential solvation: Osmolyte solvation of proteins, aminoacids, and peptides", Proteins Structure Function and Bioinformatics, 12/2008

< 1% match (Internet from 18-Jan-2016)
http://www.mdpi.com/1422-0067/10/12/5498/htm

< 1% match (publications)
Xiaoyun Meng, Larissa A. Munishkina, Anthony L. Fink, Vladimir N. Uversky. "Molecular Mechanisms Underlying the Flavonoid-Induced Inhibition of α-Synuclein Fibrillation", Biochemistry, 2009

< 1% match (publications)
Xu, Xiaoqing, Yingdan Qian, Ping Wu, Hui Zhang, and Chenxin Cai. "Probing the anticancer-drug-binding-induced microenvironment alterations in subdomain IIA of human serum albumin", Journal of Colloid and Interface Science, 2015.

< 1% match (publications)
Chi L.L. Pham, Su Ling Leong, Feda E. Ali, Vijaya B. Kenche, Andrew F. Hill, Sally L. Gras, Kevin J. Barnham, Roberto Cappai. "Dopamine and the Dopamine Oxidation Product 5,6-Dihydroxylindole Promote Distinct On-Pathway and Off-Pathway Aggregation of α-Synuclein in a pH-Dependent Manner", Journal of Molecular Biology, 2009

< 1% match (publications)
Xiaolin Sun, William T., Vladimir N.. "Chapter 9 Applications of Bioinformatics and Experimental Methods to Intrinsic Disorder-Based Protein-Protein Interactions", InTech, 2012

< 1% match (publications)
"Main Symposia And Workshops", FEBS Journal, 2013.

< 1% match (publications)
Masoumeh Valipour, Parvaneh Maghami, Mehran Habibi-Rezaei, Mostafa Sadeghpour et al. "Interaction of insulin with methyl tert -butyl ether promotes molten globule-like state and production of reactive oxygen species", International Journal of Biological Macromolecules, 2015

< 1% match (publications)

Parvez Alam, Sumit Kumar Chaturvedi, Mohammad Khursheed Siddiqi, Ravi Kant Rajpoot, Mohd Rehan Ajmal, Masihuz Zaman, Rizwan Hasan Khan. "Vitamin k3 inhibits protein aggregation: Implication in the treatment of amyloid diseases", Scientific Reports, 2016

< 1% match (publications)
Vladimir N. Uversky, Jie Li, Pierre Souillac, Ian S. Millett, Sebastian Doniach, Ross Jakes, Michel Goedert, Anthony L. Fink. "Biophysical Properties of the Synucleins and Their Propensities to Fibrillate", Journal of Biological Chemistry, 2002

< 1% match (publications)
Habchi, Johnny, Peter Tompa, Sonia Longhi, and Vladimir N. Uversky. "Introducing Protein Intrinsic Disorder", Chemical Reviews

< 1% match (publications)
Christopher M. Dobson. "Kinetic partitioning of protein folding and aggregation", Nature Structural Biology, 02/01/2002

< 1% match (publications)
Stefani, Massimo. "Protein Folding and Misfolding, Relevance to Disease, and Biological Function", Enzyme Inhibitors Series, 2007.

< 1% match (publications)
Uversky, Vladimir N.. "Paradoxes and wonders of intrinsic disorder: Complexity of simplicity", Intrinsically Disordered Proteins, 2016.

< 1% match (publications)
Feroz, S.R. Mohamad, S.B. Lee, G.S. Male. "Supramolecular interaction of 6-shogaol, a therapeutic agent of Zingiber officinale with human serum", Phytomedicine: International Journal of , June 15 2015 Issue

< 1% match (Internet from 06-Jul-2016)
http://onlinelibrary.wiley.com/doi/10.1111/j.1742-4658.2008.06257.x/full?identityKey=6cafeb6a-4e94-4b12-9c7c-dfd49f3416d7®ionCode=US-CA&wol1URL=%2Fdoi%2F10.1111%2Fj.1742-4658.2008.06257.x%2Ffull

< 1% match (publications)
Wei Zhu, Yangyang Jia, Jinming Peng, Chun-mei Li. "Inhibitory Effect of Persimmon Tannin on Pancreatic Lipase and the Underlying Mechanism in Vitro", Journal of Agricultural and Food Chemistry, 2018

< 1% match (publications)
Uversky, Vladimir N.. "Flexible Nets of Malleable Guardians: Intrinsically Disordered Chaperones in Neurodegenerative Diseases", Chemical Reviews, 2011.

< 1% match (Internet from 08-Mar-2016)
http://ir.canterbury.ac.nz/bitstream/handle/10092/4415/thesis_fulltext.pdf?isAllowed=y&sequence=1

< 1% match (publications)
Shaltiel-Karyo, Ronit, Dan Davidi, Moran Frenkel-Pinter, Michael Ovadia, Daniel Segal, and Ehud Gazit. "Differential inhibition of Î±-synuclein oligomeric and fibrillar assembly in parkinson's disease model by cinnamon extract", Biochimica et Biophysica Acta (BBA) - General Subjects, 2012.

< 1% match (Internet from 19-Mar-2010)
http://www-bio3d-igbmc.u-strasbg.fr/~mgsb/bms/biblio/Dyson_2005.pdf

< 1% match (publications)
Su Ling Leong. "Modulation of α-Synuclein Aggregation by Dopamine: A Review", Neurochemical Research, 05/15/2009

< 1% match (publications)
Uversky, V.N.. "Conformational constraints for amyloid fibrillation: the importance of being unfolded", BBA - Proteins and Proteomics, 20040506

< 1% match (publications)
Levy-Sakin, Michal, Roni Scherzer-Attali, and Ehud Gazit. "Modifiers of Protein Aggregation-From Nonspecific to Specific Interactions", Protein and Peptide Folding Misfolding and Non-Folding Schweitzer-Stenner/Peptide Folding Misfolding and Nonfold, 2012.

< 1% match (publications)
Marri, Lucia <1977>(Trost, Prof. Paolo Bernardo). "CP12: Intrinsically Unstructured Proteins regulating photosynthetic enzymes through protein-protein interactions", Alma Mater Studiorum - Università di Bologna, 2011.

< 1% match (publications)
Sheena McGowan, Isabelle S Lucet, Jackie K Cheung, Milena M Awad, James C Whisstock, Julian I Rood. "The FxRxHrS Motif: A Conserved Region Essential for DNA Binding of the VirR Response Regulator from Clostridium perfringens", Journal of Molecular Biology, 2002

< 1% match (publications)
Espinoza-Fonseca, L.M.. "Reconciling binding mechanisms of intrinsically disordered proteins", Biochemical and Biophysical Research Communications, 20090508

< 1% match (publications)
Edwin, F.. "Anion-Induced Folding of Rabbit Muscle Pyruvate Kinase: Existence of Multiple Intermediate Conformations at Low pH", Archives of Biochemistry and Biophysics, 20000901

< 1% match (Internet from 22-Aug-2010)
http://www.tau.ac.il/lifesci/departments/biotech/members/gazit/documents/52.pdf

< 1% match (publications)
"Bioremediation in Latin America", Springer Nature, 2014

< 1% match (publications)
Natarajan Suganthy, Kasi Pandima Devi, Seyed Fazel Nabavi, Nady Braidy, Seyed Mohammad Nabavi. "Bioactive effects of quercetin in the central nervous system: Focusing on the mechanisms of actions", Biomedicine & Pharmacotherapy, 2016

< 1% match (Internet from 29-Jun-2016)
http://www.jbc.org/content/283/14/9012.full

< 1% match (Internet from 06-Sep-2017)
http://digitalcommons.fiu.edu/cgi/viewcontent.cgi?article=1471&context=etd

< 1% match (Internet from 04-Sep-2016)
http://www.nature.com/ncomms/2015/150108/ncomms6908/full/ncomms6908.html

< 1% match (publications)
Selva Sharma, Arumugam, and Malaichamy Ilanchelian. "A Comprehensive Multispectroscopic Analysis on the Interaction and Corona Formation of Human Serum Albumin with Gold/Silver Alloy Nanoparticles", The Journal of Physical Chemistry B

< 1% match (publications)
Madeira, Pedro P., Ana Bessa, Luís Álvares-Ribeiro, M. Raquel Aires-Barros, Alírio E. Rodrigues, Vladimir N. Uversky, and Boris Y. Zaslavsky. "Amino acid/water interactions study: a new amino acid scale", Journal of Biomolecular Structure and Dynamics, 2014.

< 1% match (publications)
F Ulrich Hartl, Manajit Hayer-Hartl. "Converging concepts of protein folding in vitro and in vivo", Nature Structural & Molecular Biology, 2009

< 1% match (Internet from 19-Jul-2017)
https://ediss.uni-goettingen.de/bitstream/handle/11858/00-1735-0000-0023-995D-E/Dissertation-YuWang-2013.pdf?sequence=1

< 1% match (publications)
Wolynes, Peter G. Onuchic, Jose N. Thiru. "Navigating the folding routes.(protein folding)", Science, March 17 1995 Issue

< 1% match (publications)
H. Rösner. "Antiproliferative/Cytotoxic Activity of Molecular Iodine and Iodolactones in Various Human Carcinoma Cell Lines. No Interfering with EGF-signaling, but Evidence for Apoptosis", Experimental and Clinical Endocrinology & Diabetes, 07/2010

< 1% match (publications)
Dajas, Federico. "Life or death: Neuroprotective and anticancer effects of quercetin", Journal of Ethnopharmacology, 2012.

< 1% match (publications)
Molecular Science of Fluctuations Toward Biological Functions, 2016.

< 1% match (publications)
Yan Wei. "Rapid glycation with D-ribose induces globular amyloid-like aggregations of BSA with high cytotoxicity to SH-SY5Y cells", BMC Cell Biology, 2009

< 1% match (publications)
Cristina Cecchi, Massimo Stefani. "The amyloid-cell membrane system. The interplay between the biophysical features of oligomers/fibrils and cell membrane defines amyloid toxicity", Biophysical Chemistry, 2013

< 1% match (publications)
Tzviya Zeev-Ben-Mordehai. "The intracellular domain of theDrosophila cholinesterase-like neural adhesion protein, gliotactin, is natively unfolded", Proteins Structure Function and Genetics, 11/15/2003

< 1% match (Internet from 31-Mar-2017)
http://www.ejh.it/index.php/ejh/article/view/2749/2659

< 1% match (publications)
Ellis, R.. "Macromolecular crowding: an important but neglected aspect of the intracellular environment", Current Opinion in Structural Biology, 20010201

< 1% match (publications)
Farabegoli, F.. "(-)-Epigallocatechin-3-gallate downregulates estrogen receptor alpha function in MCF-7 breast carcinoma cells", Cancer Detection and Prevention, 2007

< 1% match (Internet from 06-May-2016)
http://aac.asm.org/content/59/11/6939.full

< 1% match (Internet from 01-Jan-2014)
http://www.science.gov/topicpages/a/accelerates+neurodegenerative+disease.html

< 1% match (publications)
Maeda, K.. "Green tea catechins inhibit the cultured smooth muscle cell invasion through the basement barrier", Atherosclerosis, 200301

< 1% match (publications)
Katharina Schueller, Marc Pignitter, Veronika Somoza. " Sulfated and Glucuronated - Resveratrol Metabolites Regulate Chemokines and Sirtuin-1 Expression in U-937 Macrophages ", Journal of Agricultural and Food Chemistry, 2015

< 1% match (publications)
Nunilo Cremades, Samuel I.A. Cohen, Emma Deas, Andrey Y. Abramov et al. "Direct Observation of the Interconversion of Normal and Toxic Forms of α-Synuclein", Cell, 2012

< 1% match (Internet from 07-Nov-2017)
http://digitalassets.lib.berkeley.edu/etd/ucb/text/Mauldin_berkeley_0028E_10545.pdf

< 1% match (publications)
Danzer, Karin. "Die Beteiligung verschiedener alpha-Synuklein Oligomere in der Entstehung der Parkinson Krankheit", Universität Ulm. Fakultät für Naturwissenschaften, 2007.

< 1% match (publications)
S. A. Pawar. "Characterization of acid-induced unfolding intermediates of glucose/xylose isomerase", European Journal of Biochemistry, 11/2000

< 1% match (publications)
"Study Results from S.J. Jang and Colleagues Broaden Understanding of Breast Cancer (In-vitro antican", Obesity, Fitness & Wellness Week, Oct 15 2016 Issue

< 1% match (publications)
Wu, Xuli, Weiyi He, Haiping Zhang, Yao Li, Zhigang Liu, and Zhendan He. "Acteoside: A lipase inhibitor from the Chinese tea Ligustrum purpurascens kudingcha", Food Chemistry, 2014.

< 1% match (publications)

Quan Van Vuong, Katarina Siposova, Trang Truc Nguyen, Andrea Antosova et al. "Binding of Glyco-Acridine Derivatives to Lysozyme Leads to Inhibition of Amyloid Fibrillization", Biomacromolecules, 2013

< 1% match (publications)
V. N. Uversky. "Protein folding revisited. A polypeptide chain at the folding – misfolding – nonfolding cross-roads: which way to go?", Cellular and Molecular Life Sciences CMLS, 09/01/2003

< 1% match (publications)
M. Teresa Pastor. "Hacking the Code of Amyloid Formation: The Amyloid Stretch Hypothesis", Prion, 01/01/2007

< 1% match (publications)
Otávio Augusto Chaves, Bijo Mathew, Dari Cesarin-Sobrinho, Balasubramanian Lakshminarayanan et al. "Spectroscopic, zeta potential and molecular docking analysis on the interaction between human serum albumin and halogenated thienyl chalcones", Journal of Molecular Liquids, 2017

< 1% match (student papers from 19-Mar-2009)
Submitted to University of Newcastle upon Tyne on 2009-03-19

< 1% match (Internet from 17-Sep-2017)
http://discovery.ucl.ac.uk/1490493/1/Natalello_Co-fibrillogenesis%20of%20Wild-type%20and%20D76N.pdf

< 1% match (Internet from 26-Jan-2017)
https://www.omicsonline.org/2155-6210/images/2155-6210-S12-005-g004.html

< 1% match (publications)
da Silva, Fernanda Luna, Eduardo Coelho Cerqueira, Mônica Santos de Freitas, Daniela Leão Gonçalves, Lilian Terezinha Costa, and Cristian Follmer. "Vitamins K interact with N-terminus α-synuclein and modulate the protein fibrillization in vitro. Exploring the interaction between quinones and α-synuclein", Neurochemistry International, 2013.

< 1% match (publications)
From Protein Structure to Function with Bioinformatics, 2009.

< 1% match (publications)
F. Ulrich Hartl. "Molecular chaperones in protein folding and proteostasis", Nature, 07/20/2011

< 1% match (publications)
Xuhui Zhu, Honghong Yao, Fuwang Peng, Shannon Callen, Shilpa Buch. "PDGF-mediated protection of SH-SY5Y cells against Tat toxin involves regulation of extracellular glutamate and intracellular calcium", Toxicology and Applied Pharmacology, 2009

< 1% match (publications)
Aabgeena Naeem. "Defective Protein Folding and Aggregation as the Basis of Neurodegenerative Diseases: The Darker Aspect of Proteins", Cell Biochemistry and Biophysics, 05/15/2011

< 1% match (publications)
Krigbaum, W.R.. "Local interactions as a structure determinant for protein molecules: II", BBA - Protein Structure, 19790125

< 1% match (publications)
Ja-Young Jang, Hyangshuk Rhim, Seongman Kang. "NABi, a novel β-sheet breaker, inhibits Aβ aggregation and neuronal toxicity: Therapeutic implications for Alzheimer's disease", Biochimica et Biophysica Acta (BBA) - General Subjects, 2018

< 1% match (student papers from 13-Mar-2018)
Submitted to Universiti Putra Malaysia on 2018-03-13

< 1% match (publications)
Elizabeth A. Yates, Justin Legleiter. "Preparation Protocols of Aβ(1–40) Promote the Formation of Polymorphic Aggregates and Altered Interactions with Lipid Bilayers", Biochemistry, 2014

< 1% match (publications)
Indu R. Chandrashekaran, Christopher G. Adda, Christopher A. MacRaild, Robin F. Anders, Raymond S. Norton. " Inhibition by Flavonoids of Amyloid-like Fibril Formation by Merozoite Surface Protein 2 ", Biochemistry, 2010

< 1% match (publications)
Shaikh, S.M.T.. "Binding of the bioactive component isothipendyl hydrochloride with bovine serum albumin", Journal of Molecular Structure, 20060320

< 1% match (student papers from 29-Nov-2017)
Submitted to University of Leicester on 2017-11-29

< 1% match (Internet from 30-Aug-2017)
https://repositorio-aberto.up.pt/bitstream/10216/10638/7/5718_TD_01_P.pdf

< 1% match (Internet from 25-Aug-2015)
http://www.mdpi.com/1420-3049/19/11/17202

< 1% match (Internet from 09-Aug-2017)
https://www.j3.jstage.jst.go.jp/browse/bbb1961/53/1/_contents?from=0

< 1% match (publications)
Zohreh Moradi, Mozhgan Khorasani-Motlagh, Ali Reza Rezvani, Meissam Noroozifar. "Evaluation of DNA, BSA binding, and antimicrobial activity of new synthesized neodymium complex containing 29-dimethyl 110-phenanthroline", Journal of Biomolecular Structure and Dynamics, 2017

< 1% match (publications)
Shashi Prajapati. "Alkaline unfolding and salt-induced folding of bovine liver catalase at high pH", European Journal of Biochemistry, 7/1998

< 1% match (publications)
Fang FANG. "Novel squamosamide derivative (compound FLZ) attenuates $A\beta_{25-35}$-induced toxicity in SH-SY5Y cells", Acta Pharmacologica Sinica, 2/2008

< 1% match (publications)
Mihoko Kinoshita. "Incorporation of ZP1 into perivitelline membrane after *in vivo* treatment with exogenous ZP1 in Japanese quail (*Coturnix japonica*)", FEBS Journal, 07/2008

< 1% match (publications)
Shen, Pei-Hong. "Synuclein-γ suppression mediated by RNA interference inhibits the clonogenicity and invasiveness of MCF-7 cells", Oncology Letters, 2013.

< 1% match (publications)
Choi, Jin Ho, and Gyu Man Kim. "Fabrication of PDMS Stencil using Gas Blowing for Micropatterned 3T3 Cell Culture", Journal of the Korean Society of Precision Engineering, 2013.

< 1% match (publications)
Christopher D. Syme. "A Raman optical activity study of rheomorphism in caseins, synucleins and tau. New insight into the structure and behaviour of natively unfolded proteins", European Journal of Biochemistry, 1/2002

< 1% match (student papers from 10-May-2018)
Submitted to University of Hull on 2018-05-10

< 1% match (student papers from 24-Jan-2014)
Submitted to Tarleton State University on 2014-01-24

< 1% match (Internet from 28-Aug-2017)
http://www.jbc.org/content/287/9/6753.full.pdf

< 1% match (publications)
Arpan Bhattacharya, Soumitra Bhowmik, Amit K. Singh, Prashant Kodgire, Apurba K. Das, Tushar Kanti Mukherjee. "Direct Evidence of Intrinsic Blue Fluorescence from Oligomeric Interfaces of Human Serum Albumin", Langmuir, 2017

< 1% match (publications)
Sunil K. Ravi, Ramesh B. Narasingappa, Bruno Vincent. "Neuro-nutrients as anti-alzheimer's disease agents: A critical review", Critical Reviews in Food Science and Nutrition, 2018

< 1% match (publications)
Kaur, Khushwinder, Raj Kumar, and S.K. Mehta. "Nanoemulsion: A new medium to study the interactions and stability of curcumin with bovine serum albumin", Journal of Molecular Liquids, 2015.

< 1% match (publications)
Seley, K.L.. "Unexpected inhibition of S-adenosyl-l-homocysteine hydrolase by a guanosine nucleoside", Bioorganic & Medicinal Chemistry Letters, 20030616

< 1% match (student papers from 24-Aug-2015)
Submitted to Savitribai Phule Pune University on 2015-08-24

< 1% match (student papers from 19-Dec-2013)
Submitted to Higher Education Commission Pakistan on 2013-12-19

< 1% match (publications)
Meng, Xiaoyun, Larissa A. Munishkina, Anthony L. Fink, and Vladimir N. Uversky. "Molecular Mechanisms Underlying the Flavonoid-Induced Inhibition of α-Synuclein Fibrillation", Biochemistry, 2009.

< 1% match (publications)
Uversky, Vladimir N., and A. Keith Dunker. "Why are we Interested in the Unfolded Peptides and Proteins?", Protein and Peptide Folding Misfolding and Non-Folding Schweitzer-Stenner/Peptide Folding Misfolding and Nonfold, 2012.

< 1% match (publications)
A. Yeo. "Coincident signalling between the Gi/Go-coupled delta-opioid receptor and the Gq-coupled m3 muscarinic receptor at the level of intracellular free calcium in SH-SY5Y cells", Journal of Neurochemistry, 3/15/2001

< 1% match (student papers from 27-Feb-2018)
Submitted to University of Wollongong on 2018-02-27

< 1% match (Internet from 21-Jan-2010)
http://www.ucm.es/info/respira/resources/PDF/008.pdf

< 1% match (Internet from 26-May-2016)
http://spectrum.library.concordia.ca/7531/1/Khalil_Phd_S2011.pdf

< 1% match (Internet from 25-Nov-2016)
http://springerplus.springeropen.com/articles/10.1186/2193-1801-3-360

< 1% match (Internet from 16-Jun-2012)
http://media.wiley.com/product_data/excerpt/43/04705258/0470525843-147.pdf

< 1% match (publications)
Diane Latawiec. "Modulation of Alpha-Synuclein Aggregation by Dopamine Analogs", PLoS ONE, 02/16/2010

< 1% match (publications)
P. Krishnamoorthy, P. Sathyadevi, Alan H. Cowley, Rachel R. Butorac, N. Dharmaraj. "Evaluation of DNA binding, DNA cleavage, protein binding and in vitro cytotoxic activities of bivalent transition metal hydrazone complexes", European Journal of Medicinal Chemistry, 2011

< 1% match (publications)
H. Jane Dyson, Peter E. Wright. "Intrinsically unstructured proteins and their functions", Nature Reviews Molecular Cell Biology, 2005

< 1% match (publications)
Chattoraj, Shyamtanu, and Kankan Bhattacharyya. "Fluorescent Gold Nano-Cluster inside a Live Breast Cell: Etching and Higher Uptake in Cancer Cell", The Journal of Physical Chemistry C

< 1% match (publications)
Johana Plch, Kristyna Venclikova, Olga Janouskova, Jan Hrabeta et al. "Paclitaxel-Loaded Polylactide/Polyethylene Glycol Fibers with Long-Term Antitumor Activity as a Potential Drug Carrier for Local Chemotherapy", Macromolecular Bioscience, 2018

< 1% match (publications)
Rafati, A.A.. "Thermodynamic and binding study of hemoglobin, oxy-hemoglobin and carbamino-hemoglobin upon interaction with cationic surfactants, using surfactant membrane selective electrodes", Journal of Molecular Liquids, 20090210

< 1% match (student papers from 07-Apr-2017)
Submitted to Indian Institute of Technology, Bombay on 2017-04-07

< 1% match (Internet from 26-Jun-2018)
https://pubs.acs.org/doi/full/10.1021/acsomega.7b01472

< 1% match (Internet from 09-Sep-2017)
http://www.jbc.org/content/288/19/13602.full.pdf

< 1% match (Internet from 22-Jun-2017)
https://bmcdevbiol.biomedcentral.com/track/pdf/10.1186/1471-213X-7-29?site=bmcdevbiol.biomedcentral.com

< 1% match (Internet from 14-Sep-2017)
http://jpet.aspetjournals.org/content/jpet/251/2/718.full.pdf

< 1% match (Internet from 24-Nov-2017)
http://journals.plos.org/plosone/article?id=10.1371%2Fjournal.pone.0133154

< 1% match (publications)
Ronit Shaltiel-Karyo, Dan Davidi, Moran Frenkel-Pinter, Michael Ovadia, Daniel Segal, Ehud Gazit. "Differential inhibition of α-synuclein oligomeric and fibrillar assembly in parkinson's disease model by cinnamon extract", Biochimica et Biophysica Acta (BBA) - General Subjects, 2012

< 1% match (publications)
Kentaro Shiraki. "Comparative analyses of the conformational stability of a hyperthermophilic protein and its mesophilic counterpart", European Journal of Biochemistry, 8/2001

< 1% match (publications)
Arshdeep Sidhu, Ine Segers-Nolten, Vinod Subramaniam. "Solution conditions define morphological homogeneity of α-synuclein fibrils", Biochimica et Biophysica Acta (BBA) - Proteins and Proteomics, 2014

< 1% match (publications)
Uversky, V.N.. "Understanding protein non-folding", BBA - Proteins and Proteomics, 201006

< 1% match (publications)
Kronman, Martin J., and Gerald D. Fasman. "Metal-Ion Binding and the Molecular Conformational Properties of α Lactalbumi", Critical Reviews in Biochemistry and Molecular Biology, 1989.

< 1% match (publications)
A. A. Moosavi-Movahedi. "Formation of the Molten Globule-Like State of Cytochrome c Induced by n-Alkyl Sulfates at Low Concentrations", Journal of Biochemistry, 01/01/2003

< 1% match (publications)
Hai-ning Yu, Lan-cui Zhang, Jun-guo Yang, Undurti N. Das, Sheng-rong Shen. "Effect of laminin tyrosine–isoleucine–glycine–serine–arginine peptide on the growth of human prostate cancer (PC-3) cells in vitro", European Journal of Pharmacology, 2009

< 1% match (publications)
Seo, M.. "Membrane depolarization stimulates the proliferation of SH-SY5Y human neuroblastoma cells by increasing retinoblastoma protein (RB) phosphorylation through the activation of cyclin-dependent kinase 2 (Cdk2)", Neuroscience Letters, 20060814

< 1% match (publications)

Liwen Sun. "Protective effects of EUK4010 on β-amyloid(1–42) induced degeneration of neuronal cells", European Journal of Neuroscience, 8/2006

< 1% match (publications)
Bellucci Arianna. "Alpha-synuclein aggregation and cell death triggered by energy deprivation and dopamine overload are counteracted by D2/D3 receptor activation", Journal of Neurochemistry, 4/10/2008

< 1% match (Internet from 23-Jun-2017)
http://publications.aston.ac.uk/30817/1/Dennison_T_2017.pdf

< 1% match (Internet from 26-May-2016)
https://researchspace.auckland.ac.nz/bitstream/handle/2292/6983/whole.pdf?sequence=2

< 1% match (Internet from 13-Apr-2003)
http://www.kcsnet.or.kr/publi/bul/bu96n2/bu96n2t5.html

< 1% match (Internet from 23-Feb-2017)
http://journal.frontiersin.org/article/10.3389/fnins.2016.00408/full

< 1% match (Internet from 30-May-2018)
https://tel.archives-ouvertes.fr/tel-01777947/file/Skilitsi_Anastasia_Ioanna_2017_ED182.pdf

< 1% match (Internet from 15-Jun-2018)
https://www.frontiersin.org/articles/10.3389/fnins.2016.00084/full

< 1% match (Internet from 12-Sep-2017)
https://scholarworks.iupui.edu/bitstream/handle/1805/2917/Cissell%20ETD%20Submission%20%28122-10%29.pdf?isAllowed=y&sequence=1

< 1% match (Internet from 04-Nov-2017)
http://etd.auburn.edu/xmlui/bitstream/handle/10415/3824/MazumderSuman_Dissertation.pdf?isAllowed=y&sequence=2

< 1% match (Internet from 05-May-2012)
http://www.bratislleklisty.sk/2002/10304-04.pdf

< 1% match (Internet from 06-Jan-2018)
https://www.frontiersin.org/articles/10.3389/fmicb.2016.00973/full

< 1% match (Internet from 07-Jun-2018)
https://www.frontiersin.org/articles/10.3389/fmicb.2015.01565/full

< 1% match (Internet from 19-Nov-2006)
http://www.knosof.co.uk/cbook/sent1.pdf

< 1% match (Internet from 18-May-2016)
http://www.mdpi.com/1420-3049/20/10/17976/htm

< 1% match (Internet from 07-Sep-2017)
https://pilot.mass.gov/files/documents/2017/08/31/newengland-power2016.pdf

< 1% match (publications)
Keiko Maeda, Masafumi Kuzuya, Xian Wu Cheng, Toshinobu Asai et al. "Green tea catechins inhibit the cultured smooth muscle cell invasion through the basement barrier", Atherosclerosis, 2003

< 1% match (publications)
Vladimir N. Uversky. "Amyloidogenesis of Natively Unfolded Proteins", Current Alzheimer Research, 06/01/2008

< 1% match (publications)
Vladimir N Uversky. "Targeting intrinsically disordered proteins in neurodegenerative and protein dysfunction diseases: another illustration of the D^2 concept", Expert Review of Proteomics, 08/2010

< 1% match (publications)

Vladimir N. Uversky. "Structural and Conformational Prerequisites of Amyloidogenesis", Protein Reviews, 2006

< 1% match (publications)
Pritam Choudhury, Krishnendu Das, Prasanta Kumar Das. " -Phenylalanine-Tethered, Naphthalene Diimide-Based, Aggregation-Induced, Green-Emitting Organic Nanoparticles ", Langmuir, 2017

< 1% match (publications)
Uversky, V.N.. "Intrinsically disordered proteins from A to Z", International Journal of Biochemistry and Cell Biology, 201108

< 1% match (publications)
Taboada, Pablo, Silvia Barbosa, Josué Juárez, Manuel-Alatorre Meda, and Víctor Mosquera. "Amyloid-Like Fibrils: Origin, Structure, Properties, and Potential Technological Applications", Proteins in Solution and at Interfaces Methods and Applications in Biotechnology and Materials Science, 2013.

< 1% match (publications)
University of Tennessee, Knoxville

< 1% match (publications)
Noval, María G., Mariana Gallo, Sebastián Perrone, Andres G. Salvay, Lucía B. Chemes, and Gonzalo de Prat-Gay. "Conformational Dissection of a Viral Intrinsically Disordered Domain Involved in Cellular Transformation", PLoS ONE, 2013.

< 1% match (publications)
Junwei Fu, Chuanbiao Bie, Bei Cheng, Chuanjia Jiang, Jiaguo Yu. "Hollow CoSx polyhedrons act as high-efficiency cocatalyst for enhancing the photocatalytic hydrogen generation of g-C3N4", ACS Sustainable Chemistry & Engineering, 2018

< 1% match (publications)
N.W. Rizzo. "Characterization of the structure and composition of gecko adhesive setae", Journal of The Royal Society Interface, 06/22/2006

< 1% match (publications)
N. Muryoi. "Cloning and Expression of afpA, a Gene Encoding an Antifreeze Protein from the Arctic Plant Growth-Promoting Rhizobacterium Pseudomonas putida GR12-2", Journal of Bacteriology, 09/01/2004

< 1% match (publications)
Banthit Chetsawang. "Melatonin protects against hydrogen peroxide-induced cell death signaling in SH-SY5Y cultured cells: involvement of nuclear factor kappa B, Bax and Bcl-2", Journal of Pineal Research, 9/2006

< 1% match (publications)
Moza, B.. "Equilibrium studies of the effect of difference in sequence homology on the mechanism of denaturation of bovine and horse cytochromes-c", BBA - Proteins and Proteomics, 20030321

< 1% match (publications)
Kim, Jeong-Mi Noh, Eun-Mi Kwon, Kang-Bea. "Curcumin suppresses the TPA-induced invasion through inhibition of PKC[alpha]-dependent MMP-expressi", Phytomedicine: International Journal of , Sept 15 2012 Issue

< 1% match (publications)
Freyer, M.W.. "Binding of netropsin to several DNA constructs: Evidence for at least two different 1:1 complexes formed from an -AATT-containing ds-DNA construct and a single minor groove binding ligand", Biophysical Chemistry, 200703

< 1% match (publications)
Guevara-Hernandez, Eduardo, Aldo A. Arvizu-Flores, Maria E. Lugo-Sanchez, Enrique F. Velazquez-Contreras, Francisco J. Castillo-Yañez, Luis G. Brieba, and Rogerio R. Sotelo-Mundo. "A novel viral thymidylate kinase with dual kinase activity", Journal of Bioenergetics and Biomembranes, 2015.

< 1% match (student papers from 04-Jun-2015)
Submitted to Vrije Universiteit Brussel on 2015-06-04

< 1% match (publications)
V.N. Uversky, A.K. Dunker. "3.9 Intrinsically Disordered Proteins", Elsevier BV, 2012

< 1% match (publications)
Zhang, L.W.. "Study of the interactions between fluoroquinolones and human serum albumin by affinity capillary electrophoresis and fluorescence method", Analytica Chimica Acta, 20071105

< 1% match (publications)
Jose Roberto S.A. Leite. "Topographical Analysis of Schizolobium Parahyba Chymotrypsin Inhibitor (Spci) by Atomic Force Microscopy", Protein and Peptide Letters, 04/01/2002

< 1% match (publications)
Ghosh, Sudeshna, Nitin K. Pandey, Priyanka Banerjee, Koel Chaudhury, Nóra Veronika Nagy, and Swagata Dasgupta. "Copper(II) directs formation of toxic amorphous aggregates resulting in inhibition of hen egg white lysozyme fibrillation under alkaline salt mediated conditions", Journal of Biomolecular Structure and Dynamics, 2014.

< 1% match (publications)
Ranjeet K. Sinha, Ronak Y. Patel, Naveen Bojjireddy, Anindya Datta, Gosukonda Subrahmanyam. "Epigallocatechin gallate (EGCG) inhibits type II phosphatidylinositol 4-kinases: A key component in pathways of phosphoinositide turnover", Archives of Biochemistry and Biophysics, 2011

< 1% match (publications)
Methods in Molecular Biology, 2012.

< 1% match (publications)
Sinha, R.K.. "Epigallocatechin gallate (EGCG) inhibits type II phosphatidylinositol 4-kinases: A key component in pathways of phosphoinositide turnover", Archives of Biochemistry and Biophysics, 20111201

< 1% match (publications)
Xuli Wu, Weiyi He, Haiping Zhang, Yao Li, Zhigang Liu, Zhendan He. "Acteoside: A lipase inhibitor from the Chinese tea Ligustrum purpurascens kudingcha", Food Chemistry, 2014

< 1% match (publications)
Springer Protocols Handbooks, 2009.

< 1% match (publications)
April Darling, Vladimir Uversky. "Intrinsic Disorder in Proteins with Pathogenic Repeat Expansions", Molecules, 2017

< 1% match (publications)
Johnson, William M., Amy L. Wilson-Delfosse, and John. J. Mieyal. "Dysregulation of Glutathione Homeostasis in Neurodegenerative Diseases", Nutrients, 2012.

< 1% match (publications)
Oscar Conchillo-Solé. "AGGRESCAN: a server for the prediction and evaluation of "hot spots" of aggregation in polypeptides", BMC Bioinformatics, 2007

< 1% match (publications)
Tiantian Yin, Wenjie Xie, Jing Sun, Licong Yang, Jie Liu. "Penetratin Peptide-Functionalized Gold Nanostars: Enhanced BBB Permeability and NIR Photothermal Treatment of Alzheimer's Disease Using Ultralow Irradiance", ACS Applied Materials & Interfaces, 2016

INTRODUCTION Proteins are linear and unbranched chains of amino acids and after water are the most abundant biological molecules that are involved in plethora of biological processes. One of the remarkable characteristics of living entities is the self assembly of the most of the intricate components with precision and accuracy. Protein folding is the most fundamental example of self –assembly where the linear polypeptide chain of amino acids folds into a functional three dimensional state. Important insights into the mechanism of protein folding emphasising on the structural, kinetic and thermodynamic analyses of various intermediate as well as transition states, from information gained by experiments, theory and simulation studies have now emerged (Ref). While the puzzle of protein folding still remains unsolved, the misfolding of proteins into aggregates increases the load on the cellular

machineries that are evolved to avoid aggregation and prevent the underlying aggregate borne diseases, making it inevitable to find the missing links of protein folding and to fully understand factors that are responsible for the deviation from protein folding pathways. An Overview of Protein Folding Historically, Anfinsen's Nobel Prize winning experiment on "scrambled RNase" demonstrated that the proteins fold spontaneously and that all the information needed for a polypeptide chain to fold into a three-dimensional conformation is encoded in its amino acid sequence (Anfinsen, 1973). The denaturation of RNase A enzyme in the presence of a denaturant, i.e. Urea rendered the enzyme inactive with the mixture of several isomeric forms of the reduced disulfide bonds which when subjected to renaturation in the presence of mercaptoethanol underwent disulfide interchange giving rise to a homogenous product indistinguishable from the native state. This led to the emergence of the "Thermodynamic Hypothesis". According to this hypothesis, a protein under denaturing conditions or in an unfolded state posses astronomical conformations which under folding conditions are spontaneously driven to optimize their intramolecular as well as solvent-protein interactions (intermolecular) to attain a lowest minimum free energy, that correspond to its native state. Anfinsen suggested that the retention of the memory of the native structure is one of the factors that lead to the correct folding of the protein to its three-dimensional state. He further suggested that cooperative interactions are essential for the stability of the proteins and proposed that the ability of the denatured protein to fold back to its native state is governed 1 solely by the internal residues that comprise the hydrophobic core of the protein than the residues exposed to the solvent and thus only those residues are required to be conserved that allow natural selection and high degree of mutation of other residues occurring during evolution (Anfinsen, 1973). Cyrus Levinthal made the argument that is famously known as "Levinthal's paradox" that under denaturing conditions the number of possible conformations would take a sizeable amount of time to find the native conformation and attain the functional three- dimensional structure in microsecond to millisecond time-scale within which most proteins fold (Rose et al., 2006) and thus suggested that achieving the global minimum and that too quickly are two mutually exclusive events, which are defined as thermodynamic and kinetic control, respectively. While thermodynamic control is a slow process that is determined by the final native condition irrespective of the denatured state and independent of any pathway, the kinetic control is quick as it is pathway dependent and the final structure could vary depending on the denatured state from which the folding was initiated (Ken A Dill & Hue Sun Chan, 1997). Thus according to Levinthal the native state of a protein is attained by a directed search, but how it is attained remained unexplained, leaving it a paradox. The argument led to the quest for protein folding pathways and gave rise to the 'new- view' that sees folding as "diffusion-like process" (Karplus & Weaver, 1976) where the unfolded polypeptide instead of going through a single route to the native state resembles a multi-dimensional landscape where each conformation with varying degrees of freedom undergo conformational fluctuations that follows myriad of pathways to finally attain the native state (Wolynes et al., 1995; Ken A. Dill & Hue Sun Chan, 1997). A typical protein energy landscape is shown in Figure 1, which is characterized by a tapered end indicating limited population of low energy, native-like conformations and wide open surface at the top that describes the multiple unfolded ensembles that tread their way downhill to the native state (Dill & MacCallum, 2012). Wolynes and colleagues suggested that for a protein to be kinetically foldable there must exist sufficient slope in the energy landscape to go downhill in the funnel to attain global energy minimum and attain the native state with minimum frustrations because the native-like interactions favoured by natural selection are more stable than the non-native states, thus resulting in a smoother funnel (Wolynes et al., 1995). Computer simulation studies have revealed that the folding funnels that appear smoother on a global scale may be rugged on local scales (Dill & MacCallum, 2012) indicating the inherent fluctuations between the unfolded and folded conformations that bring the highly separated amino acids closer and attains the lower energy native state by trial and error (Dobson, 2 2003b). Since the energy landscape is encoded by the amino acid sequence, the shape of the folding funnel also depends on the sequence of each protein where the folding chain proceeds towards lower intra-chain energy by undergoing hydrophobic collapse, salt-bridge formation, intra-chain hydrogen bonding etc. until the conformational possibilities of the chain narrows (Ken A. Dill & Hue Sun Chan, 1997; Dobson et al., 1998; Rose et al., 2006). Proteins are believed to fold by nucleation events comprising of 'key residues' in the structure that form folding nucleus with native-like topology in parts of the polypeptide chain and are characterized by self-dependent units of secondary structures such as helices and turns which act as stepping stones for the successive folding of the polypeptide (Wolynes et al., 1995; Dobson, 2003b; Jahn & Radford, 2005; Dill & MacCallum, 2012). The small single domain proteins

(<100 residues) involve a two –state folding populated with only two kinds of species, unfolded and native resulting in a smoother energy landscape, while large proteins (> 100 residues) have a rough energy surface and form folding intermediates en-route to the native state (Jahn & Radford, 2005). The funnel illustrates that the folding is slowed by a thermodynamic bottleneck which comprises of the transition state reflecting multiple pathways of protein folding giving rise to formation of high energy intermediate structures through which the molecules must pass to attain the native state (Wolynes et al., 1995; Dobson, 2003b; Onuchic & Wolynes, 2004; Brockwell & Radford, 2007). These intermediate states are kinetic traps of misfolded conformers which can act two-way by accelerating protein folding (on-pathway) or become kinetic dead ends that in turn may give rise to off- pathway events, such as protein aggregation, thus becoming rate limiting for protein folding reactions (Brockwell & Radford, 2007; Jahn & Radford, 2008). Figure 1. Funnel -energy landscape of protein folding. The funnel shows multiple high energy conformations wending downhill to attain limited number of low energy conformations. Folding occurs via alternative multiple trajectories. Recreated and reused with permission (Dill & MacCallum, 2012). Protein Misfolding and Aggregation The transiently trapped intermediate species formed during process of protein folding can accumulate under various conditions and favour intermolecular interactions giving rise to aggregates, thus leading to misfolding of protein. These intermediate non-native states have solvent exposed hydrophobic residues and unstructured segments of peptide backbone which tend to self-associate into disordered aggregates in a concentration-dependent manner where their associations are driven by hydrophobic and interchain hydrogen bonding interactions (Horwich, 2002; Dobson, 2003a; Barral et al., 2004; Jahn & Radford, 2005; Ecroyd & Carver, 2008; Y. E. Kim et al., 2013). The advancements in the experimental methods capable of measuring protein folding at a very short time-scale (μs time-scale) such as ultra- rapid mixing, or detection of transient species by using techniques like FRET, NMR spectroscopy or fluorescence correlation spectroscopy (FCS) have revealed the presence of partially folded intermediates in the folding process of even the simplest proteins. The state- of-the-art techniques like NMR relaxation dispersion measurements are capable of detecting the scarcely populated (as low as 1%) non-native protein conformations and also provide 4 residue specific knowledge of the kinetic and thermodynamic properties of the species (Jahn & Radford, 2008). Protein folding in vivo is a much complex process due to the challenges posed by the crowded cellular milieu which the nascent polypeptide chain encounters (Ellis, 2001a, 2001b; Dobson, 2003b; Barral et al., 2004; Stefani, 2008). The extremely high concentration of macromolecules inside the cells, approximately in the range of 300-400 g l- 1 is referred to as macromolecular crowding, where the macromolecules occupy around 20- 30% of the total cellular volume. Crowding effect is also termed as 'excluded-volume' effect, emphasising that it is a physical non-specific effect which originates from steric repulsion. A highly crowded environment means that the effective concentration and thermodynamic activity of each molecule is greater than its actual concentration and the volume freely available to a macromolecule is reduced due to the excluded-volume effect. Such an effect is expected to promote self-association and enhance protein folding by either collapsing the unfolded polypeptide chain into compact state or lead to the association of partially folded intermediates into off-pathway (non-functional) aggregates (Ellis, 2001a, 2001b). The exposed hydrophobic residues on the nascent polypeptide chain during translation and translocation as well as assembled oligomeric complexes of the polypeptide further present obstacles in proper folding of the polypeptide into functional three-dimensional native state (Thomas et al., 1995). In order to ensure correct folding, the cellular machinery has evolved molecular chaperones and folding catalysts which counteract the non-native interactions and facilitate proper folding under cellular conditions (Thomas et al., 1995; Fink, 1999; Dobson, 2003b). Molecular chaperones are defined as proteins that increase the overall efficiency of protein folding by interacting, stabilizing and assisting the nascent polypeptide to acquire correct folding by reducing the probability of non-native, competing interactions, particularly aggregation (Dobson, 2003b; Hartl & Hayer-Hartl, 2009). The chaperones play multiple roles such as de novo protein folding, refolding of stress-denatured protein, intracellular protein transport as well as degradation of misfolded proteins. The class of chaperones that are predominantly involved in protein biogenesis are heat-shock proteins (Hsp) - 70 family and chaperonins (Hsp 60s) that recognize the exposed hydrophobic amino acid side chains in the non-native conformations and promote their correct folding through ATP- dependent cycles of association and dissociation (Hartl & Hayer-Hartl, 2009). Apart from the chaperone-assisted folding of proteins, the folding catalysts comprise of important enzymes such as protein disulphide isomerase and peptidylprolyl isomerase that enhance the rate of formation and 5 reorganization of disulphide bonds and

accelerate the potentially slow steps of protein folding by increasing the rate of cis-trans isomerisation of peptide bonds including proline residues respectively (Fink, 1999). The cells are also equipped with sophisticated quality control system that examines if the proteins are correctly folded and target the misfolded proteins for degradation by generating 'unfolded protein response' (UPR) which involves ubiquitin-proteasome pathway where ubiquitin binds to the target proteins marking them for destruction (Dobson, 2003a; Goldberg, 2003; Stefani & Dobson, 2003). Additionally under evolutionary pressure to avoid aggregation, the functional proteins have developed sequences that are less prone to aggregation, such as presence of proline residues in the membrane α-helices (Jahn & Radford, 2008) and negative designs present in β-sheet containing proteins that prevent the edge-to-edge aggregation (Richardson & Richardson, 2002). The protective role of evolution against aggregation is also explained by the finding that significant part of eukaryotic genome codes for natively unfolded proteins which are characterised by low surface hydrophobicity and high net charge (due to uncompensated charge) that remain unfolded under physiological conditions. Such proteins are collectively defined as natively unfolded proteins or intrinsically disordered proteins (Uversky, 2002a). Even though the cells are evolved to tightly regulate and assist the correct folding of the nascent polypeptide, due to the marginal stability of the native state relative to the denatured state (Jahn & Radford, 2005), the aggregation can be triggered by factors such as mutations (Chiti, Taddei, et al., 2002; Chiti et al., 2003b), changes in the folding environment, chemical modifications (oxidation, proteolysis) reducing conformational stability, aberrant interactions with metal ions, faulty chaperones and defects in the protein control machineries (Stefani & Dobson, 2003; Stefani, 2004; Hipp et al., 2014). Since protein folding plays the central role in biological processes, it is inevitable that malfunctioned protein will give rise to plethora of diseases which are collectively called as conformational diseases or misfolding diseases (Kopito & Ron, 2000; Z˘erovnik, 2002). Protein misfolding predominantly gives rise to highly organized cross β- sheet containing extracellular fibrillar aggregates called 'Amyloids' which contribute majorly to the protein misfolding diseases causing wide range of neurodegenerative diseases such as Creutzfeldt-Jacob's disease, Parkinson's disease, Alzheimer's disease, etc. and some form of cancer (Yang-Hartwich et al., 2015) broadly defined as 'Amyloidoses'(Koo et al., 1999; Selkoe, 2003; Stefani & Dobson, 2003). ? Amyloidogenesis 'Amyloid' term was first coined by Virchow in 1853 to define waxy, eosinophilic tissue deposits that were assumed to be composed of carbohydrates and within ten years of their nomenclature they were identified to be deposits of proteins by Fredrich and Kekule. In 1959 the EM studies revealed the deposits to be fibrillar in nature which were observed to be rigid and unbranched species with characteristic tinctorial properties such as binding to Congo red dye (Horwich, 2002). The wide variety of proteins and peptides associated with the amyloidogenic diseases share no sequence or structural similarity and yet the fibrils formed by such proteins share a strikingly similar morphological as well as structural characteristics (Stefani & Dobson, 2003; Dobson, 2004). The X-ray diffraction studies in 1968 revealed that amyloids exhibit cross β-signature and the β-sheet comprises the strongest repeating unit of the fibril that runs parallel to the fibrillar axis with their strands aligned perpendicular to this axis (Nelson et al., 2005). The amyloids share common characteristics which include formation of fibrils with elongated and unbranched morphology with a diameter of 70-120Å (Sunde et al., 1997; Jahn & Radford, 2008), binding to dye such as Congo red and thioflavin T, resulting in characteristic green-yellow birefringence of Congo red and increased fluorescence with ThT, lag-time dependent rate limiting kinetics with cooperative binding and self-seeding properties which exhibit unusual stability (Nelson et al., 2005). These fibrils are extremely stable species and are resistant to degradation by proteases and denaturants, making them stubborn for elimination by the cell regulatory machinery (Ecroyd & Carver, 2008). The fibrils also usually consist of 2 to 6 protofibrils, which are approximately 2 nm in diameter that are twisted around each other and appear like supercoiled rope-like structures (Serpell et al., 2000). A detailed investigation on the mechanism of cross β-sheet formation in amyloid fibrils studied by X-ray diffraction studies revealed three levels of organization within the fibrils. First, involves the alignment of the protein molecules in a β-sheet form which is followed by the self-complementation of the two sheets forming the sheet pairs containing a dry interface. Dry interface with an absence of any water molecule other than those hydrating the carboxylate ion at the ends of polypeptide chain facilitate tight interdigitation of the same amino acids of the mating sheets giving a 'steric-zipper'-like appearance that involves van der Waals interactions and are stronger than the other protein interface. The third level draws in the interaction between the sheet structures to form fibrils by the non-covalent forces which are relatively weaker than the forces involved in the first two steps. The second level explains the lag phase of

fibrillation since the amide side chains take longer to acquire proper 7 orientation required for interdigitation of the mating sheets and stacking of amide hydrogen bonds in the dry interface. The decrease in entropy gives rise to the kinetic barrier of fibril formation and thus is energetically an unfavourable reaction (Nelson et al., 2005). Although till date a fully objective atomic model for common spine structure has not been available, an array of sophisticated biophysical techniques like solid-state NMR (ss NMR), cryo-electron microscopy, X-ray fiber diffraction and powder diffraction are continuing to provide in-depth insights about the core structure of amyloids (Nelson et al., 2005), such as understanding amyloid polymorphism (Close et al., 2018). The amyloid formation predominantly occurs by 'nucleation –dependent polymerization' mechanism where the protein monomer at nucleation stage, undergoes structural rearrangements and associations giving rise to a thermodynamically unfavourable and rate-limiting step where it is converted into ordered oligomeric nucleus followed by an exponential or growth phase where the nucleus grows rapidly by further addition of competent monomeric/oligomeric species forming the intermediate species such as protofibrils and finally the saturation or steady-state which marks the formation of mature amyloid fibrils where the fibrils and monomer population are in equilibrium with each other (Harper & Lansbury Jr, 1997). An amyloid fibril formation has been characterized by a sigmoidal growth curve that represents the nucleation –dependent polymerization model (Naiki & Gejyo, 1999) as depicted in Figure 2. The characteristic features that identifies such a model are, (a) aggregation only above critical concentration of the protein present, (b) even slightly above critical concentration, lag phase is observed before polymerization and (c) amelioration of lag phase upon addition of seeds, which are the pre-formed fibrillar species containing amyloid forming characteristics (Harper & Lansbury Jr, 1997). Whilst most of the proteins form amyloids by nucleation –dependent phenomena, fibrils have also been reported to form by nucleation-independent kinetics (Gosal et al., 2005; Ecroyd et al., 2008). The formation of amyloids is now believed to be a generic property of the polypeptides. Contrary to earlier hypothesis that amyloids are only formed by disease related proteins, in 1998 it was accidentally observed that proteins unrelated to any disease also forms amyloid fibrils similar to those formed by the pathogenic proteins. Later on it was established that by changing the solution conditions (such as low pH, high temperature, lack of interacting partners, presence of salts and co-solvents etc.) proteins can be deliberately pushed towards amyloid formations such that their native structures are partially or completely disrupted with retention of hydrogen-bonding capacity (Stefani & Dobson, 2003). It has also been observed that short peptides of 4 to 6 residues can form well –defined fibrils 8 with all the characteristics of the fibrils formed by longer (>100 residues) proteins (Manuela López de la Paz et al., 2002). Therefore it is established that the amyloid formation is governed by the inherent physico-chemical property of the polypeptide main chain rather than amino-acid side chains and in the light of this, the generic property of polypeptides to form amyloids with common structural features is well explained as the peptide backbone irrespective of proteins remains unchanged (Stefani & Dobson, 2003). The amino acid side chains however have been observed to govern the fibrillation propensities of polypeptides (Azriel & Gazit, 2001; Chiti, Calamai, et al., 2002; Chiti et al., 2003a; Manuela Lopez de la Paz & Serrano, 2004) and the solvent conditions that affect the ionization states of amino acids, such as changes in pH are reported to form fibrillar species with altered morphology (Gosal et al., 2005). A collective view establishes the fact that native proteins are evolved to contain amino acid sequences and structural adaptations that alleviate aggregation and favour folding of protein into compact states which are dictated primarily by the amino acid side chain interactions that differ for each polypeptide chain. However, factors such as enhanced β-sheet propensity, increased hydrophobicity and decreased overall charge could divert the pathway towards aggregation and amyloid formation from protein folding pathways (Stefani & Dobson, 2003). The observations lead to the consensus that protein folding and aggregation are two distinct yet competing pathways where a polypeptide can undergo aggregation or folding depending on the environmental conditions (Stefani, 2008). The different mechanisms of protein aggregation are illustrated in Figure 3. Destabilization of the native state is a prerequisite for amyloid formation. While destabilizing conditions such as addition of denaturant, high temperature, low pH, mutation or truncation lead to accumulation of partially unfolded intermediates with exposed hydrophobic residues (Jahn & Radford, 2008), a partial folding of the intrinsically disordered proteins to form the molten globule state is key step towards fibrillogenesis (Uversky, 2008). Formation of aggregates by mechanism such as domain swapping (ds), edge- to edge association (ee), strand association (sa) and β-strand stacking (bs) has been proposed to be responsible for amyloid formation (Jahn & Radford, 2008). An early formation of disordered or amorphous aggregate has been

observed in the initial stages of fibrillation which reorganize in the exponential phase and later adopt the characteristic cross β-structure of the amyloids (Plakoutsi et al., 2005). Apart from the pathogenic implications of amyloid formation, recent studies have shown evidence that many of these amyloids have functional properties in many eukaryotic and prokaryotic organisms (Greenwald & Riek, 2010). Several examples of 9 functional amyloids have been observed such as formation of amyloids by curlin protein in E. coli that enables bacteria to colonize by forming biofilms, aggregation of Ure 2p protein in the yeast S. cerevisae that helps in adapting to nitrogen deprived conditions etc.(Theillet et al., 2014). The role of functional amyloids in mammalian cells has also been reported. Disordered Pmel17 protein is reported to form fibrillar species in melanosomes that protects the cells from UV and oxidative damage (Fowler et al., 2007). Figure 2. Representative sigmoidal curve depicting nucleation – dependent polymerization model of amyloid formation. The figure shows sequential steps of fibril polymerization and different aggregation states of a protein formed at different stages of fibrillation. Figure 3. Proposed mechanisms of protein aggregation. The schematic depicts the possible structural rearrangements of a polypeptide which in its different states undergo and form amyloid fibrils. The four main mechanisms shown are domain-swapping (ds), strand association (sa), edge- edge-association (ee) or β-strand stacking (bs) respectively. Reused with permission (Jahn & Radford, 2008). ? Folding and Aggregation: two competing pathways Several studies have demonstrated that the partially unfolded intermediates that predominantly resemble a molten globule state exhibit significant fraction of native-contacts along with non-native contacts and that the intrinsic properties of amino acid side chains that govern the structural preferences such as high hydrophobicity, secondary structure propensity and high net charge are equally important in determining the aggregation propensity (Jahn & Radford, 2008; Mezzenga & Adamcik, 2018). Under crowded cellular milieu, competition between the intramolecular and intermolecular interactions exists, that results in a dramatic increase in the ruggedness of the energy landscape (Jahn & Radford, 2008) . A combined energy landscape of folding and aggregation is illustrated in Figure 4. The evidence for kinetic partitioning between folding and aggregation was also provided by Chiti and co- workers and it was established that the regions on the α/β acylphosphatase (AcP) protein which determine the rate of aggregation are distinct from those that determine the rate of protein folding. It is seen that while the mutations in the highly structured regions in the transition states largely affect the rate of folding, little consequence is observed on rate of aggregation. The study thus established that the AcP residues involved in major interaction in the folding nucleus do not play role in the rate- limiting steps of aggregation (Chiti, Taddei, et al., 2002). Although the entire polypeptide chain is involved in fibril formation, the detailed investigation on the intrinsic properties of the natively unfolded proteins, i.e. Aβ-42, α-Synuclein and tau which readily forms amyloid have revealed that the polypeptide sequences contain two sensitive regions which are categorised as 'aggregation-prone' and 'aggregation-sensitive region' defined as P- and S- region respectively (Pawar et al., 2005). While the P-regions comprise the local regions with high aggregation propensity and promote the aggregation of the entire polypeptide sequence, the S-region is the susceptible region likely to be the part of the amyloid core only upon mutation (Pawar et al., 2005). A similar observation of kinetic partitioning was also made in the case of highly aggregation prone protein Transthyretin (TTR). It was demonstrated that the reassembly of TTR to functional homotetrameric form depends on the concentration of the folded TTR monomer which partitions itself between the reassembly and the aggregation pathway. The reassembly pathway is observed to compete with the aggregation pathway for the TTR monomer but upon accumulation of large amount of aggregates the partitioning tilts towards the aggregation pathway (Wiseman et al., 2005). Further using techniques such as positional scanning mutagenesis, it has been revealed that there is a presence of tolerant and restrictive mutation sequences on amyloid sequence of a protein and fibril formation is a fine balance between the specific side chain interactions and electrostatic interactions within the sequence of the protein (Manuela Lopez de la Paz & Serrano, 2004). The kinetics observed for fibril formation unlike first order kinetics of protein folding involves competition between unimolecular concentration-dependent intrachain interaction and multimolecular interchain interaction that dominates with an increasing protein concentration (Horwich, 2002). The energy landscape of aggregation as shown in Figure 4 depicts the complexity of the protein folding and aggregation and includes the formation of wide range of conformational variants and multitude of pathways that is presented to the polypeptide as it skirts around the landscape. The energy minima on the aggregation side of the landscape is poorly defined due to the heterogeneity and high dynamicity of the intermediate oligomeric species formed in the pathway but the energy minima for the protofibrils and fibrils, which are stable

rigid structures are expected to be well-defined in the landscape. Thus, in the view of the energy landscape theory, the fact that virtually any protein can form amyloids subjected to appropriate conditions suggest that amyloid fibril is the universal global free-energy minima of all polypeptides that may assemble by common mechanisms governed by the physico- chemical properties of the polypeptide chain (Jahn & Radford, 2008). Figure 4. A schematic representation showing partitioning between the energy landscape of protein folding and aggregation. The landscape illustrates a simple folding funnel (light blue) for a conformational search of single polypeptide chain to its native state. A highly rugged energy landscape due to intermolecular protein interactions is shown for the aggregation pathway (dark blue). Reused with permission (Jahn & Radford, 2005). ? Amyloid toxicity and Diseases Amyloids and Neurodegeneration The accumulation of protein aggregates in the form of amyloid plaques in the brain are the key characteristics of wide range of neurodegenerative diseases such as Alzheimer's disease (AD), Parkinson's disease (PD), Huntington's disease (HD), amyotrophic lateral sclerosis (ALS) etc. (Koo et al., 1999; Caughey & Lansbury Jr, 2003; Forman et al., 2004; Ross & Poirier, 2004) and the wide range of amyloidogenic diseases are summarized in Table I. There is a growing evidence that the early aggregates formed as intermediates in the amyloidogenic pathway comprising the soluble oligomeric species, protofibrillar species and amorphous aggregates are more toxic than the mature fibrils and play an important role in cellular dysfunction and death (Caughey & Lansbury Jr, 2003). The lack of correlation between the clinical symptoms and the extent of accumulated fibrils suggests the role of early oligomeric species in the pathogenesis. In the case of neurodegenerative diseases such as AD, an absence of any direct relationship between the amyloid plaque and AD related dementia suggested that the toxic effects of non-fibrillar Aβ42 deposits occur before the plaques are formed and dementia is observed. Also, administration of Aβ oligomers to the live animals resulted in deficits in long-term potentiation and memory loss. On the other hand PD is characterized by the amyloid aggregates of α-Synuclein, called Lewy bodies and out of many mutational variants of α-Syn that gain toxic function, A30P forms spherical protofibrils by slowing aggregation and binds to the membrane with a greater affinity than the mature fibrils or the monomers, establishing that the early oligomers are more pathogenic than the mature fibrils (Caughey & Lansbury Jr, 2003). The increasing experimental evidences have demonstrated the toxic effects of oligomeric species of several amyloidogenic proteins such as Aβ-peptide (Stine et al., 2003; S. J. C. Lee et al., 2017), α-Synuclein (Danzer et al., 2007; Winner et al., 2011), IAPP (Meier et al., 2006; Haataja et al., 2008; Zraika et al., 2010), tau oligomers (Ward et al., 2012) etc. Although the majority of reports demonstrate the cytotoxic effects of amyloid oligomers, the toxic effects of mature fibrils could not be ruled out (Novitskaya et al., 2006). The finding that species formed early in the aggregation of two small globular proteins PI3- SH3 (SH3 domain of phosphatidyl-inositol-3'-kinase) and HypF- N which are not related to any amyloid diseases further suggest that amyloid forming is a general phenomena which is not restricted only to the disease causing proteins. Also, it was proposed that the amyloid oligomers of proteins irrespective of their relatedness to a disease share common structural features as well as common mechanisms of toxicity (Bucciantini et al., 2002). In another study, the binding of the micellar Aβ-specific antibody to amyloid oligomers of various amyloidogenic peptides further supported that the amyloid oligomers share common structural characteristics (Kayed et al., 2003). It was observed that HypF-N protein under fibrillating conditions formed two types of oligomers with similar morphology but the packing of hydrophobic interactions among the protein molecules differed from each other which in turn governed their toxic characteristics. The oligomers with the higher exposed hydrophobic residues with lower packing were observed to have higher cell penetrating ability and thus high toxicity (Campioni et al., 2010), establishing the role of hydrophobic exposure in oligomer toxicity. Although, the structural characterization of amyloid oligomers although is challenging due to their transient and dynamic nature, most of the toxic amyloid oligomers are reported to contain β-sheet structures (Apetri et al., 2006; Lasagna-Reeves et al., 2010; Illes-Toth et al., 2015), and possess seeding capabilities (Farmer et al., 2017) as well as prion like self propagating properties (Lasagna-Reeves et al., 2012). The presence of aggregates both inside and outside the cell has been observed to induce apoptosis and thus is toxic and causes cell death. The increasing 14 experimental evidences majorly suggest that membrane permeabilization by amyloid oligomers leading to the dysregulation of Ca2+ homeostasis is the underlying cause of amyloid-mediated toxicity (Mattson et al., 1992; Demuro et al., 2005; Glabe, 2006). It is suggested that upon exposure to toxic amyloid aggregates the intracellular reactive oxygen species (ROS) elevates due to the influx of Ca2+ ions which is followed by the up-regulation of the oxidative metabolism aimed at generating ATP which in turn is required by the membrane

pumps for the clearance of excess Ca2+ ions from the vicinity. Elevated ROS leads to the oxidation of the proteins which are involved in the ion transfer as well as other downstream signalling required for the clearance of excess Ca2+ ions, thus leading to depletion of ATP and accumulation of Ca2+ ions inside the cells. The depletion of ATP and accumulation of toxic aggregates is much evident in the old age due to which most of the amyloid-borne diseases are a group of chronic diseases that become prevalent with aging (Stefani & Dobson, 2003). The amyloidogenic proteins have been reported to interact with lipid membranes and form pores or single channels on the membrane surface that led to the concept of 'Channel Hypothesis'(Glabe, 2006). The interaction of misfolded species with membrane is reported to occur by two-step mechanism which involves the electrostatic interaction between the positively charged side chain residues and negatively charged or polar head groups of membrane followed by the burial of hydrophobic residues into the hydrophobic interior of the membrane (Stefani & Dobson, 2003). A recent study on the underlying effect of α-Synuclein oligomer toxicity shows an increased swelling and permeability of mitochondrial membrane by selective oxidation of the ATP synthase β subunit that leads to mitochondrial peroxidation and thus cell death (Ludtmann et al., 2018). Together, it is established that the oxidative stress due to accumulated ROS could further amplify the damaging effects by causing the impairment of ion pumps as well as permeabilization of mitochondrial membrane which in turn could lead to the activation of various apoptotic events, thus causing cell death. Amyloids and Cancer Apart from their pronounced effects seen in neurodegenerative diseases, the abnormal accumulation of proteins is also associated with various forms of cancer. The aggregates of the wild-type and mutant p53 protein which is the most important tumour suppressor protein and is also regarded as the gate-keeper of cell growth and division, has been reported to form aggregates of its conformational variants that impair the proapoptotic functions of p53, leading to rise of malignancy. Several cancers such as neuroblastoma, breast cancer, 15 retinoblastoma, colon cancer (Stefani, 2004), ovarian cancer (Yang-Hartwich et al., 2015) etc. are reported to occur due to such aggregates of p53. Additionally, the mutant variant of p53 showed a prion-like behaviour where a dominant negative effect was observed as the protofibrils and oligomeric species of mutant p53 sequester the wild-type p53 into inactive conformations that promote massive aggregation (Stefani, 2004; Bom et al., 2012). The wild- type and mutant p53 have also been reported to associate into tetramers that irreversibly aggregate to form amyloids (Higashimoto et al., 2006). Additionally, the aggregated p53 is also considered to be a marker for chemoresistance, indicating the deleterious effects of aggregated p53 in cancer (Yang-Hartwich et al., 2015). ? Therapeutic Strategies Against Amyloidogenesis The diverse etiology underlying the amyloidogenic diseases suggest broad range of therapeutic strategies which are grouped into four main categories, such as stabilization of the native states by use of structural analogues, reducing the aggregation-prone species, inhibition of the nucleus formation or growth of aggregates and enhancement of housekeeping mechanisms by using chaperones (Dobson, 2003a). A large part of amyloid research now attempts to design and use wide range of inhibitors that bring inhibition by one or all of the above mentioned strategies. The use of synthetically designed peptides such as β- sheet breakers, a five residue peptide has been reported to prevent Aβ fibrillogenesis and also disassemble preformed fibrils and reduce cytotoxicity (Soto et al., 1998). A recent study has reported the use of a novel β-breaker peptide NABi, which inhibits Aβ fibril formation both in vitro and in vivo and prevents neuronal cell death, a hallmark in AD (Jang et al., 2018). The uses of vitamins have also been reported to affect fibrillation of amyloidogenic proteins, such as a concentration dependent inhibition of hen egg white lysozyme (HEWL) and Aβ- peptide fibrillation as well as reduced cytotoxicity is observed in the presence of vitamin K3(Alam et al., 2016). Similarly vitamin B12 is observed to impart neuronal cell protection by inhibiting Aβ fibrillogenesis (Alam et al., 2017). Chaperones which are the controllers of protein folding machinery have also been observed to inhibit amyloid formation in various proteins. Hsp 70 prevents Aβ oligomer formation and reduces cytotoxicity (Rivera et al., 2018), Hsp 104 targets multiple intermediates of the Aβ fibrillation pathway and strongly suppresses Aβ fibrillation in an ATP independent manner by abolishing Aβ fibrils seeding capacity (Arimon et al., 2008), DJ- 1 having structural analogy to the chaperone Hsp 31 is an oxidative stress-induced chaperone that prevents α-Synuclein fibrillogenesis (W. Zhou et al., 2006). Recently, HspB1 and Hsc 70 16 chaperones have been demonstrated to bind to the microtubule binding repeat region of tau protein with different affinities. While HspB1 chaperone delays fibrillation by interacting weakly with the early species of tau protein, the Hsc 70 strongly interacts with amyloidogenic regions to prevent elongation by capping the ends of tau fibrils (Baughman et al., 2018). A new class of inhibitors which are structural analogues of

apomorphine have also previously been reported to inhibit Aβ fibrillation by affecting its polymerization and deposition (Lashuel et al., 2002). Apart from these many small molecule inhibitors such as use of polyphenols (Ngoungoure et al., 2015; Zaidi & Bhat, 2018), cyclic peptides (Jinghui & Pieter, 2014), metal-ion chelators (Cherny et al., 2001) and neurotransmitters (Jain & Bhat, 2014) have been reported to modulate the fibrillation pathways of wide range of amyloidogenic proteins. Cellular Stress and Osmolytes Nature has evolved strategies to protect the structural and the functional integrity of biological systems ranging from prokaryotes to eukarytotes. The natural selcet Intrinsically Disordered Proteins (IDPs) Intrinsically disordered proteins are a group of natively unfolded proteins that are flexible, essentially non-compact and lack a well- folded secondary structure under physiological conditions (Uversky, 2002b). It is now established that approximately 30% of mammalian proteome comprises as a full-length disordered protein and 75% as extended disordered regions in signalling proteins (Theillet et al., 2014). Disordered sequences are also found in the structured and ordered domains of well-folded proteins which are termed as intrinsically disordered regions (IDRs) (Dyson, 2016). These proteins have sequence peculiarities where they are characterized by uncompensated charge groups, i.e. they have high net charge in neutral pH and have reduced hydrophobic amino acid residues. In other words, IDPs are enriched in disorder promoting amino acids (Pro, Arg, Gly, Gln, Ser, Glu, Lys and Ala) and are scarce in order-promoting amino acids (Cys, Trp, Tyr, Phe, Ile, Leu, val and Asn). It has been established that the low mean hydrophobicity and high net charge are the prerequisites for a protein to remain unfolded under physiological conditions, thus generating intrinsically disordered proteins (Uversky, 2002a, 2002b; Dyson & Wright, 2005; Uversky, 2016). The IDPs possess a structural continuum ranging from tightly folded single domains to multidomain proteins containing flexible or disordered regions, to compact yet disordered molten globules and finally highly extended or random heterogeneous states (Dyson & Wright, 2005). The structure-function paradigm was replaced by the 'Protein Trinity' model according to which a native cellular protein can occur in the form of ordered, random coil and molten globule states where the biological function can arise from any of these conformations or the transition between them and any of these states could represent the native state of protein (Dunker et al., 2001). The trinity model was later extended to the 'Protein Quartet' model where pre-molten globule state was also proposed to be one of the conformational and functional states of the protein (Uversky, 2002a). It is suggested that natively unfolded polypeptide in aqueous solutions, splits into two structurally different groups where one group remains in a random coil state with no ordered secondary structure and the other is more compact and is in pre-molten globule state that is, it is less compact than the folded and molten globule state but more compact than a random coil protein (Uversky, 2002a). The IDPs are characterized by larger hydrodynamic dimensions as compared to a globular protein corresponding to same molecular mass, lack of ordered secondary structure and high intramolecular flexibility (Uversky, 2002a). Several experiments suggest that the conformational states of IDPs are largely governed by the solvent conditions which can promote either collapse of the unfolded state such as at low pH and high temperature conditions or maintain the unfolded conformation in the presence of denaturants such as GdmCl and Urea (Uversky, 2002b, 2009; Jain et al., 2018). Due to the lack of a 3D structure in IDPs and the susceptibility of the IDPs to various environmental conditions, a given segment of protein molecule can have varying conformationsat different time points. Thus, the IDPs are also called '4D proteins' since their structure is defined by both time and space and a particular structure in an IDP can be observed at a given time only, making it a complex ensemble of structures to be characterized (Uversky, 2016). The techniques such as gel filtration chromatography, SAXS, FTIR, far-UV CD and NMR spectroscopy, light scattering, sedimentation studies have been used for studying the hydrodynamic properties of the intrinsically disordered proteins (Dyson & Wright, 2005). The functional importance of the disordered proteins have been extensively investigated and it is suggested that the conformational plasticity of the IDPs is an important prerequisite for process of molecular recognition (Uversky, 2002a). The various functions of IDPs include the cellular 2 concept", Expert Review of Proteomics, 08/2010">signal transduction, storage of small molecules, chaperoning, 2 concept", Expert Review of Proteomics, 08/2010">regulation of transcription and translation, protein phosphorylation, cell-cycle regulation, scaffolding and the regulation of the self-assembly of multiprotein complexes such as the bacterial flagellum and the ribosome. Several chaperones and RNA binding proteins are reported to possess unfolded regions that bind to the misfolded proteins and RNA molecules, acting as recognition elements and/or assist the unfolding of the kinetically trapped intermediate (Dyson & Wright, 2005; Mollica et al., 2016). One of the remarkable characteristics of IDPs is to undergo 'disorder-to – order' transition and form more

ordered states or fold into secondary or tertiary structure upon binding with their targets or interacting partners (Dyson & Wright, 2005; Mittag et al., 2010). IDPs are also observed to form 'fuzzy complexes' where the IDPs retain high degree of disorder even in bound states (Mollica et al., 2016; Uversky, 2016). Broadly two mechanisms are observed to be the limiting cases of IDP binding which are, (a) conformational selection, where folding in the IDP occurs before binding and (b) induced fit, where IDP gains structure after binding. However, complex binding mechanisms involving different combinations of these two have also been envisaged (Mollica et al., 2016). The folding and binding of IDPs/IDRs accomplish interaction with their targets by high specificity and low binding affinity, which may facilitate specific ligand binding interactions for the signalling cascades while dissociating when signalling is completed. It is suggested that binding of an IDP due to the loss of conformational entropy 19 gives rise to an unfavourable entropic contribution to binding and uncouples binding strength from specificity, thus facilitating high specificity with a low binding affinity (Dyson & Wright, 2005; H.-X. Zhou, 2012; Babu, 2016; Mollica et al., 2016). Among the other advantages of the specific qualities of IDPs and IDRs that facilitate efficient interaction and regulation are, assembly of complexes due to open access of binding site to an IDP and lack of steric hindrance, susceptibility to modifying enzymes such as kinases, e.g. post- translational modifications of linker region as well as other IDRs (Bah & Forman-Kay, 2016), formation of extended binding interfaces which facilitate even high affinity binding, multiple binding partners or promiscuity due to conformational plasticity and high turnover rate of IDPs that facilitate signalling (Mollica et al., 2016). Due to large heterogeneity of the IDPs and massive mechanistic repertoire that involves diverse functionalities, defining the binding interactions of IDPs by a uniform or a generic mechanism is a challenge. The use of advanced techniques such as NMR spectroscopy, molecular simulations and transient kinetic studies are paving way for better understanding of mechanisms of IDP interactions. While the functional versatilities of IDPs in cellular complexities are now increasingly being appreciated, the importance of IDPs in many diseases is also prevalent. The recent studies on IDPs have raised enormous interest due to their increased fibril forming or amyloidogenic proteins that play role in majority of neurodegenerative diseases as well as cancer (Uversky et al., 2008; Babu et al., 2011). As the IDPs lack a well folded tertiary structure, unlike globular proteins where partial unfolding is required for fibril formation, the IDPs undergo partial folding and attain a molten-globule state, which is a prerequisite for fibrillation (Uversky, 2008). Stabilization of a partially folded conformation both in a globular as well an IDP is must for fibrillation that facilitates the important intermolecular interactions including electrostatic interaction, hydrogen bonding and hydrophobic interactions required for self-association and oligomerization (Uversky, 2008). Synuclein Family Synucleins are a class of intrinsically disordered proteins, comprising of three genes α, β, and γ-synuclein which are small, soluble, highly conserved vertebrate proteins expressed predominantly in neurons (George, 2001; Uversky et al., 2002; Sung & Eliezer, 2007; Ducas & Rhoades, 2014) and are mapped to human chromosome 4q21, 5q35 and 10q23 respectively (Clayton & George, 1998). The α, β, and γ-syn are composed of 140, 134 and 127 amino acid residues, respectively corresponding to a molecular weight of ~14 kDa (Jain et al., 2018). The members of this family share a great level of sequence homology. The synucleins are characterised by a highly conserved N-terminal domain, hydrophobic NAC domain and a least conserved acidic stretch in the –COOH terminal domain. The N-terminal domain is implicated as α- helical lipid binding motif sharing similarity to the class - A2 lipid- binding domain. Within the N-terminal region, lies the NAC domain marked by a repetitive, degenerative amino acid motif KTKEGV with conserved periodicity of 11 amino acid repeats imparting hydrophobicity variations among the proteins (Uversky et al., 2002; Sung & Eliezer, 2007). The α and β-Syn are predominantly localized in the presynaptic nerve terminals, while γ-Syn is abundant in peripheral nervous systems, i.e. spinal cord and sensory ganglia, both primary sensory and sympathetic neurons. γ- Syn among the other members is most widely distributed within neuronal cytoplasm being present throughout the cell bodies and axons, as well as expressed in wide range of tissues such as olfactory epithelium, breast and ovarian tumours (George, 2001; Uversky et al., 2002; Sung & Eliezer, 2007). Among all the synucleins, α-Syn remains most widely studied due to its increased amyloid forming propensity which is predominantly linked to the etiology of Parkinson's disease (PD). The pathognomonic fibrillar deposits of α- Syn are most abundant components of Lewy bodies (LB) or Lewy neuritis (LN) which is a hallmark of PD, characterised by lesions which are the aggregates of proteins and lipids (Cookson, 2005; Auluck et al., 2010). The fibrillar deposits of α-Syn in the form of LB have also been reported to be causative agents for other neurodegenerative diseases such Alzheimer's disease (AD), dementia with

Lewy bodies (DLB) and multiple system atrophy (MSA), thus establishing their prevalent role in neurodegenerative diseases, which are collectively termed as 'Synucleopathies' (Murray et al., 2001; Bennett, 2005). A recent study has also established the similarities between prion protein and α-Syn, suggesting a prion like propagation of synucleopathies (Tamgüney & Korczyn, 2017). Although the three synucleins share high sequence similarities, the subtle differences in their sequences, such as lack of the NAC domain (11-residues stretch) in β-Syn and a shorter or slightly less negative C-terminal in γ-Syn have been observed to impart differences in their fibrillation and secondary structure propensities, and conformational dynamics (Uversky et al., 2002; Marsh et al., 2006; Sung & Eliezer, 2007; Ducas & Rhoades, 2014). The fibrillation propensities of the synucleins are in the following order α-Syn > γ-Syn > β-Syn (Biere et al., 2000; Jain et al., 2018). The absence of the NAC domain in β-Syn is responsible for its negligible fibrillation propensity (Uversky et al., 2002), however, under conditions such as low pH, β-Syn is observed to form fibrils (Jain et al., 2018). β-Syn at high 21 molar concentration is reported to inhibit both α-, and γ-Syn fibrillation (Jain et al., 2018) and the chaperoning effects of β-Syn has been well established previously (Park & Lansbury, 2003; D. Lee et al., 2004; Tsigelny et al., 2007). A recent study, by the use of techniques like single molecule fluorescence spectroscopy and cell-free protein expression systems has demonstrated that β-Syn preferentially incorporates into the smaller oligomers of α-Syn and strongly inhibits fibrillation of A30P and G51D variants compared to E46K, H50Q and A53T, which are the other pathogenic mutants of α-Syn (Leitao et al., 2018). Although the direct involvement of β-Syn in neurodegenerative diseases, is still not evident, the SNPs (single nucleotide polymorphs) of β-Syn have been related to the onset of PD upon aging (Brighina et al., 2007; Brockhaus et al., 2018). γ-Synuclein γ-Synuclein is the third and the least studied member of the synuclein family which lacks the tyrosine rich C-terminal signature domain of α- and β- Syn, containing a single tyrosine residue at 39 position and shares approximately 60% sequence similarity with α-Syn (Uversky et al., 2002). A recent phylogenetic analysis on the relatedness of three synucleins suggest that both α and β-Syn share their parental lineage from γ-Syn, and that γ-Syn has a long evolutionary history, thus being distantly related to the other two synucleins (Jain et al., 2018). γ-Syn is most intriguing in the sense that unlike the other two synucleins it is widely involved in causing both neurodegeneration (Ninkina et al., 2009) and cancer (M. Ahmad et al., 2007), suggesting a connecting link between the progression of these two diseases by complex interplay of the protein that is yet to be deciphered. γ-Syn or SNCG, also called "Persyn" was originally referred to as Breast Cancer Specific Gene-1 (BSG-1) due to its overexpression in late stages of breast cancer (Jia et al., 1999). Till date, disease causing variants of γ-Syn are not evidenced, however, a common polymorphism of γ-Syn (V110E) was reported previously (Ducas & Rhoades, 2014) and is used in this study. The pathogenic effects of γ-Syn are attributed to its overexpression and elevated levels of γ-Syn in many late stages of cancer are considered a prognostic marker for metastasis (M. Ahmad et al., 2007). Several undesirable and cancer promoting effects of over expressed γ-Syn are as follows: over expressed γ-Syn confers antibiotic resistance against microtubule targeted drugs like paclitaxel, a widely used chemotherapeutic agent in cancer cells and promotes association and polymerization of microtubule proteins (Zhang et al., 2011), enhances malignancy by promoting perineural invasion or distant metastasis (Hibi et al., 2009), chaperoning the estrogen receptor (ER-α) to maintain high ligand binding affinity and stimulating hormone responsive mammary tumorigenecity (Jiang et al., 2004), influence cell cycle by co- localizing in the centrosome and spindle pole of mitotic cells thus affecting signalling transduction (Surguchov et al., 2001), wards off the cancer cells from apoptosis by interacting with various MAPKs (Mitogen Activated Protein Kinases) and imparts resistance to chemotherapeutic drugs thus promoting survival of tumour cells (Pan et al., 2002), interacts with myocilin and thus has a possible role in pathology of glaucoma (Surgucheva et al., 2005), enhances resistance to radiation in breast cancer cells (Tian et al., 2018), etc. The other damaging effects of over expressed γ-Syn is the death of motor neurons due to the formation of aggregates at a higher concentration, the effects collectively termed as 'γ-Synucleopathies'(Ninkina et al., 2009), and are summarized in Figure 5. Structural characterization studies reveal that the functional disparities between γ-Syn and α-Syn arises due to their structural differences in the C-terminal tail (Sung & Eliezer, 2007; Manivel et al., 2011), which is more dynamic in γ-Syn than other two synucleins (Ducas & Rhoades, 2014) and adopts a coil-like structure in γ-Syn, while in α-Syn it remains uncoiled and unfolded. Additionally, the C-terminal tail of γ-Syn is reported to be highly exposed to the solvent environment and that the interactions of γ-Syn are also mediated through the C-terminal domain (Manivel et al., 2011). In a previous study, the investigation on the effects of sequence differences and the

fibrillation propensities between α- and γ-Syn revealed that the amyloid forming region in γ-Syn has an increased α-helical propensity compared to α-Syn, which in turn imparts lower fibrillation propensity to γ-Syn (Marsh et al., 2006). From available evidences present in literature for γ-Syn, it is established that γ-Syn is the moderately fibrillogenic but highly oligomeric member of the synuclein family, where it is monomeric at low concentration but associates to form oligomers when concentration increases (Uversky et al., 2002). Biophysical characterization of γ-Syn in terms of its secondary structure, fibrillation propensity as well as hydrodynamic properties reveals that γ-Syn has a smaller hydrodynamic dimension than both the α- and β-syncleins and attains globularity as well as β-sheet propensity at concentrations above or equal to 70μM (Uversky et al., 2002). The severity of γ-Syn in causing neurodegenerative diseases and cancer lies in its tendency to form annular oligomers either on oxidation or at higher concentration, which not only are capable of getting transmitted from one cell to another but are believed to have seeding effect on other intracellular proteins, such as α-Syn, which is a hallmark in PD (Surgucheva et al., 2012). Nevertheless, γ-Syn deposits have also been traced in Lewy bodies in conjunction with the fibrillar deposits of α-Syn (Galvin et al., 1999). Therefore the factors such as high concentration (Uversky et al., 2002), oxidation (Surgucheva et al., 2012) and dissociation of γ-Syn from its interaction partners (Golebiewska et al., 2014) are reported to facilitate oligomerization. Figure 5. Schematic diagram summarizing the involvement of γ-Synuclein in pathogenesis In the light of the current scenario and the established evidences on potentially toxic oligomeric intermediates in the fibrillation pathway of γ-Syn, it is important to employ a strategy for regulating the toxicity of these resultant oligomeric species and investigate the effects of various therapeutic modulators on fibrillation pathway of γ-Syn. Despite the evidence of the vast range of pathogenic implications of γ-Syn, no intervention strategies for the modulation of the fibrillation pathway or oligomerization tendency of γ-Syn have been attempted. In this study we have employed three different polyphenols, namely epigallocatechin- 3-gallate (EGCG), quercetin and silibinin and a series of polyols to investigate their effects on the structure and aggregation of human γ-Syn. In the next sections, the advantages of polyphenols, their characteristics and their use as antiamyloidogenic agents are described as well as the diverse effects of polyols on the stability and aggregation behaviour of IDPs, and the underlying mechanisms and their importance in living systems are discussed. Polyphenols One of the most promising candidates emerging as effective therapeutics against amyloidogenic diseases are the naturally occurring small molecule phytochemical called polyphenols, which are abundant in plant resources and are characterized by one or more aromatic phenolic rings in their structure. The natural polyphenols are richly supplemented in wine, tea, nuts, berries, whole grains, and chocolates and in many other plants. The naturally occurring polyphenols are classified based on their source of origin, biological function and chemical structure and some of the major categories are: vitamins (e.g., b-carotene and α- tocopherol), flavonoid (e.g., flavanone and isoflavone), phenolic acids (e.g., benzoic acid and phenylacetic acid), and other miscellaneous polyphenols (resveratrol, curcumin, rosmarinic acid etc.) (Porat et al., 2006; Tsao, 2010). The polyphenolic compounds are reported to have many pharmacological properties such as antioxidative, anticarcinogenic, neuroprotective, anti-inflammatory etc. (Ngoungoure et al., 2015). While the antiamyloidogenic effects of many polyphenols have been investigated, a universal mechanism of polyphenol mediated inhibition of fibrillation doesn't exist. It is observed that different polyphenols can interact with different amyloidogenic species formed in the pathway such as monomeric, oligomeric or pre-fibrillar form as well as different modes of inhibition and modulation has also been observed. One of the mechanisms by which naturally occurring polyphenols are speculated to inhibit amyloidogenesis is by the process of aromatic stacking where the aromatic rings present in the structure interact with the aromatic residues present in the amyloidogenic protein, thus inhibiting self-assembly process in amyloid formation (Porat et al., 2006; Wu et al., 2006). Due to the growing evidence of amyloid oligomer toxicity in amyloidogenic diseases, attempts are made to use polyphenols in arresting, modulating or rendering the oligomers less toxic with the use of polyphenols. Epigallocatechin-3-gallate (EGCG) is one of the most widely used polyphenol that is reported to affect oligomerization of both α-Syn and Aβ- peptide, modulating them to form off-pathway, non-toxic species (Ehrnhoefer et al., 2008; del Amo et al., 2012). A similar effect of the polyphenol Baicalein on α-Syn and Aβ-peptide is also reported (Lu et al., 2011). The other examples of antiamyloidogenic effects of polyphenols, involving different modes of inhibition are, stabilization of early aggregates of human lysozyme by red wine polyphenol, resveratrol (Zaidi & Bhat, 2018), fibrillation inhibition and disaggregation of preformed fibrils by polyphenol Baicalein (Zhu et al., 2004; Lu et al., 2011), increased reconfiguration rate of α-Syn

leading to inhibition of fibrillation by curcumin (B. Ahmad & Lapidus, 2012), etc. The effects of various polyphenols on different proteins and their mode of actions are consolidated and well documented in a number of reviews (Cheng et al., 2013; Ngoungoure et al., 2015). While an enormous amount of evidence for the use of polyphenols as antiamyloidogenic agents for some proteins are available, no such effect of polyphenols on γ- Syn fibrillation has been investigated. Polyol Osmolytes Outline of present study The involvement of γ-Syn in plethora of diseases ranging from neurodegeneration and cancer led to the commencement of this study with two broad aims. The first aim was to investigate the effects of small molecule modulators, called Polyphenols which are now increasingly being used as therapeutics against amyloidogenic diseases on the structure and aggregation of γ-Syn. The increased tendency of γ-Syn to self –associate and form toxic oligomers despite being moderately fibrillogenic as compared to its fibrillogenic counterpart α-Syn, makes it an important target for small molecule mediated inhibition or modulation and the knowledge of the effects of such modulators on the oligomeric as well as fibrillogenic tendency of γ-Syn, which is yet unknown is expected to lead to a better understanding of the propagation of the underlying synuclein borne diseases. Due to the lack of understanding and unavailability of evidence on the small molecule mediated modulation of γ-Syn fibrillation pathway, this study investigates the effect of three different class of polyphenols, epigallocatechin-3-gallate (EGCG), quercetin and silibinin on the fibrillation pathway of γ-Syn. The study provides the first report on the detailed mechanism on the polyphenol mediated modulation of the γ-Syn fibrillation pathway by investigating the effect of these polyphenols on the fibrillogenic as well as oligomeric tendency of γ-Syn, by studying in detail the effects on γ-Syn structure, the mode of binding interactions between the polyphenols and γ-Syn and most importantly assessing their cytotoxic effects on two different cell lines, breast cancer (MCF-7) and neuroblastoma (SH-SY5Y) cells. The second aim of the study was to investigate the effects of protective osmolytes called Polyols on the structure, stability and aggregation of γ-Syn. The stabilizing effects of the polyol osmolytes which are naturally found in organisms under stress are well established for the globular proteins but with the prevalence of intrinsically disordered proteins in the eukaryotic as well as prokaryotic genome a very important and fundamental question arises as how is the cellular homeostasis maintained in the presence of polyols under stress with the coexistence of globular and IDPs? The previous reports have demonstrated a linear relationship between an increasing –OH group in the polyols with increased protein stability. Thus understanding the effect of these polyols on the structure and aggregation of γ- Syn, which is an IDP, was intriguing to investigate the effect of any such linearity on the stability and aggregation of an IDP. The study uses a polyol series comprising ethylene glycol, glycerol, erythritol, xylitol and sorbitol with increasing –OH group from 2 to 6 respectively and by using various biophysical techniques demonstrates the variable effects of polyols on the fibrillation propensity and structure of γ-Syn. The study gives an important insight into the possible modulatory effects of an osmolytes on an IDP that may help in understanding the simultaneous regulation of globular as well as intrinsically disordered proteins in cellular systems under stress. Chapter 3 Effect of Polyphenols on the Structure and Aggregation of γ -Synuclein Chapter 3.1 Effect of Epigallocatechin-3-gallate (EGCG) on the Structure and Aggregation of γ -Synuclein 1. Background Epigallocatechin-3-gallate (EGCG), the primary catechin present in green tea belonging to the family of flavonones has a well established neuroprotective (Pervin et al., 2018) as well as anticancer properties (Azam et al., 2004). EGCG has been reported to inhibit the fibrillation of a wide range of amyloidogenic proteins like α-Syn, Aβ peptide, Huntingtin (Ehrnhoefer et al., 2006; Ehrnhoefer et al., Chemical Structure of EGCG 2008), wild type apolipoprotein A-I (apo A-I) (Townsend et al., 2018) etc. The most prevalent characteristic of EGCG inhibited fibrillation pathway is the formation of non-toxic, stable oligomeric species or benign protein aggregates which do not further participate in the polymerization process thus rendering them off-pathway (Bieschke et al., 2010; Palhano et al., 2013). Cross-linking of amyloid fibrils by oxidized EGCG (Palhano et al., 2013), covalent modification with the sulfhydryl groups on the protein (Ishii et al., 2008), interference with the aromatic core of amyloidogenic protein like Aβ resulting in the formation of structured non-toxic aggregates (del Amo et al., 2012), immobilization of the C- terminal region of α-Syn leading to the reduced degree of oligomer binding to the membrane (Lorenzen et al., 2014) and formation of a molecular zipper by EGCG to facilitate the assembly of EGCG-containing oligomers (Ehrnhoefer et al., 2008) are the proposed mechanisms of EGCG mediated inhibition and altered oligomer as well as amyloid toxicity. By using techniques like ion-mobility mass spectrometry, it has also been revealed that EGCG alters the oligomerization and fibrillation assembly of hIAPP protein by binding to the specific conformers among the dynamic ensembles of the protein (Young et al., 2013). The antiamyloidogenic

property of EGCG also imparts it an antimicrobial activity which is demonstrated by the EGCG mediated remodelling of the Fap fibrils, required for the quorum sensing in pathogenic organisms like P. aeruginosa (Stenvang et al., 2016). In the light of the above background, in this study the effect of EGCG on the structure and aggregation of γ -Syn has been investigated. The study demonstrates that EGCG retards nucleus formation leading to deceleration of fibril polymerization and mediates its inhibitory effect by modulating the on-going fibrillation pathway to form two separate populations of SDS- resistant higher- ordered γ-Syn oligomers (~ 4 and 10 mer), that are conformationally restrained and gain an α-helical propensity during fibrillation. It is demonstrated that the EGCG generated oligomers act as partial templates for γ-Syn polymerization and the kinetic characteristics suggest that they are on-pathway but are kinetically retarded species (increased lag time) that fail to build-up into mature fibrils during polymerization. Investigation on the mode of binding interaction between EGCG and γ-Syn, reveal that the pronounced effect of EGCG is mediated by weak, non-covalent interactions (Kd ~ mM), that points to the importance of weak binding interactions in modulating the γ-Syn fibrillation pathway. The study also establishes that EGCG attenuates the protofibrillar stages of the pathway and disaggregates protofibrils as well as the mature fibrils into similar kind of SDS-resistant oligomers. Interestingly, the EGCG-generated oligomers are observed to be differentially toxic to the breast cancer (MCF-7) and neuroblastoma (SH-SY5Y) cells, where they completely rescue the MCF-7 cells from γ-Syn toxicity but are more toxic than the untreated γ-Syn oligomers for the SH-SY5Y cells. This indicates the critical role of γ-Syn and complexities it may impart in the treatment of amyloidogenic diseases. The investigation on the cytotoxic effects of the disaggregated γ-Syn oligomers reveal a high toxicity of MCF-7 cells relative to the disaggregated γ-Syn fibrils that highlights an early gain of toxic characteristics by species of γ-Syn which is governed by the morphology of the species formed. The observations made in this study suggest that the modulators that could inhibit the early stages of γ-Syn fibrillation without leading to disaggregation may prove to be potential candidates for preventing synucleopathies. Additionally, the study observes differences in the mechanism of EGCG-mediated modulation of γ-Syn fibrillation from that previously reported for α-Syn, which indicates a critical role of γ-Syn in underlying pathogenesis and suggest that an in-depth investigation on the effects of such modulators on γ-Syn fibrillation will help to better understand the events leading to the onset of synucleopathies and help in the development of effective intervention strategies. 2. Results 2.1 Effect of EGCG on the fibrillation kinetics of γ-Syn: 2.1.1 Thioflavin T assay The effect of EGCG on the kinetics of γ-Syn fibrillation was analyzed by Thioflavin T binding assay. ThT is a benzothiazole dye that fluoresces strongly upon binding with the cross β-sheet structures which are a signature for amyloid fibrils (Ban et al., 2003). The ThT 32 fluorescence was found to decrease by almost 8-fold in magnitude upon binding with γ -Syn fibrils formed in the presence of EGCG and an apparent fibrillation rate (kapp) of untreated γ- Syn was found to be 0.36 ± 0.02 h-1. Incubation of γ-Syn in the presence of increasing concentration of EGCG (5-50 μM) resulted in a concentration -dependent decrease in ThT fluorescence (Figure 1A and 1B) with negligible rise in ThT fluorescence recorded in the presence of EGCG at higher concentrations (>30 μM). The decrease in the apparent fibrillation rate (kapp) of γ-Syn with respect to EGCG is shown in Figure 1C. A) B) C) Figure 4. Fibrillation kinetics of γ -Syn in the presence of increasing concentration of EGCG by Thioflavin T assay. Monomeric γ-Syn was incubated in the presence of increasing concentration of EGCG (5- 50μM) under fibrillating conditions and the ThT fluorescence was recorded at regular interval of time during fibrillation. The concentration dependent decrease in the ThT fluorescence in 33 the presence of EGCG, (A) with respect to time (h) and (B) with respect to EGCG concentration (μM) shows inhibition of fibrillation. (C) The decrease in the apparent rate of fibrillation (kapp) (h-1) with respect to increasing EGCG concentration shows retardation of fibrillation. The error bars represent the ±SD (n=3). 2. 1.2 Light scattering by γ-Syn species formed during fibrillation in the presence of EGCG. The effect of EGCG on the aggregation propensity of γ-Syn was also validated by Rayleigh scattering since ThT does not bind to the amorphous aggregates and is also reported to be interfered by the presence of exogenous compounds (Hudson et al., 2009). γ-Syn was incubated under fibrillating conditions in the presence of an increasing concentration of EGCG and the scattering intensity was recorded at regular intervals during fibrillation. During the initial stages of γ-Syn fibrillation an early rise in the scattering intensity in the presence of 50μM EGCG was observed indicating the formation of higher ordered oligomers by EGCG. The overall scattering was however reduced in the presence of EGCG, suggesting inhibition of γ-Syn aggregation by EGCG (Figure 2A). To further confirm the formation of higher ordered oligomers by EGCG, the scattering intensity of the soluble γ-Syn species formed in the presence of EGCG, obtained after centrifugation was monitored. A

concentration dependent increase in the scattering intensity by the soluble γ-Syn species formed in the presence of EGCG was observed, further suggesting the formation of higher ordered oligomers by EGCG (Figure 2B). A) B) Figure 5. Light scattering by γ-Syn species formed in the presence of an increasing concentration of Quercetin. (A) The concentration-dependent decrease in the scattering intensity shows inhibition of aggregation by EGCG. Early increase in the scattering intensity in the presence of 50 μM EGCG indicates the formation of higher –ordered oligomers. (B) Light scattering by soluble γ- Syn species formed in the presence of EGCG obtained by centrifugation confirms formation of higher-ordered oligomers by EGCG. γ-Syn was incubated with increasing concentration of quercetin (10, 30 and 50μM) and incubated at 37 °C, 200 rpm. The scattering intensity was recorded using a quartz cuvette of 1 cm path length at λex=λem (Δλ=0). 2.1.3 Transmission Electron Microscopy of γ -Syn fibrils formed in the presence of EGCG The effect of EGCG on the morphology of γ-Syn fibrils was studied by negatively stained transmission electron microscopy. Incubation of monomeric γ-Syn with EGCG (5-50 μM) during fibrillation showed a concentration dependent disappearance of the γ-Syn fibrils (Figure 3A) corresponding well with the decrease in ThT fluorescence (Figure 1A). At higher concentrations of EGCG (50 μM), amorphous protein aggregates and some spherical oligomers were also seen which were also confirmed by Rayleigh scattering (Figure 3B). Also, the TEM images of the successive stages of fibril formation showed a time-dependent build-up of γ-Syn monomers into mature fibrils, whereas in presence of EGCG, shorter fragments of γ-Syn were observed (Figure 3B). Control A) 100nm +EGCG 10 μM 30 μM 50 μM 100nm 100nm 100nm B) No EGCG 0h 8h 12h 100nm 100nm 100nm 24h 48h 100nm 100nm +EGCG 12h +EGCG +EGCG 0h 8h 12h 100nm 100nm 24h 48h 100nm 100nm 100nm Figure 6. Morphology of γ -Syn fibrils formed in the presence of EGCG visualized by transmission electron microscope. (A) Transmission electron microscopy images of fibrils formed at the end of fibrillation in presence of increasing concentration of EGCG (Scale bars, 100nm). (B) 36 Time-dependent polymerization of monomeric γ-Syn in absence (upper panels) and presence (lower panels) of EGCG (50μM) at 0h, 8h, 12h, 24h and 48h of fibrillation shows the formation of mature γ- Syn fibrils in absence of EGCG. In presence of EGCG, short and partially polymerized fibrils were seen (Scale bars, 100nm). The arrows ( ) at 24h of fibrillation in absence and presence of EGCG shows the differences in fibril morphology. 2.1.4 Atomic Force Microscopy of γ-Syn species formed in the presence of EGCG AFM measurements of γ -Syn fibrils formed both in presence and absence of EGCG (50 μM), demonstrated a significant suppression of fibril formation in presence of EGCG. γ -Syn in the absence of EGCG formed mature intertwined fibrils with their average height of ~11 nm. However, in the presence of EGCG no mature fibrils were observed and highly populated large spherical oligomers with an average height of 26.2 nm ± 4.05 nm and sparsely populated smaller oligomers with an average height of 12.28 nm ± 4.23 nm were observed. These oligomers were found to self-associate with each other giving rise to a beaded appearance as shown in Figure 4. + 50 μM EGCG Control Figure 7. AFM analysis of the γ-Syn species formed in the presence of EGCG (50μM). Atomic force microscopy images showing disappearance of mature γ -Syn fibrils in the presence of EGCG (50 μM), along with an appearance of self-associated large spherical oligomers, depicted clearly in the cross section of the oligomers (right panel; below). 2.2 Effect of EGCG on different stages of γ-Syn fibrillation: 2.2.1 Thioflavin T assay The effect of EGCG on different stages of γ-Syn fibrillation was further probed by adding EGCG (50 μM) at different time intervals (8h, 24h and 48h) which respectively correspond to lag, log and saturation stage of γ-Syn fibrillation under conditions used. The ThT fluorescence was found to decrease substantially at all time-points when EGCG was added (Figure 5A), indicating attenuation of fibrillation both at nucleation and exponential stages in the presence of EGCG. The decrease in ThT fluorescence upon addition of EGCG on preformed fibrils further indicated disaggregation of γ-Syn fibrils by EGCG (Figure 5B). A) B) Figure 8. Fibrillation kinetics of γ-Syn upon addition of EGCG at different stages of fibrillation studied by ThT assay. A) Thioflavin T assay showing decrease in ThT fluorescence and inhibition of γ-Syn fibrillation at all three stages upon addition of EGCG at 8h, 24h and 48h. B) EGCG mediated disaggregation of preformed γ-Syn fibrils depicted by a continuous decrease in the ThT fluorescence upon addition of EGCG. The error bars represent ±S.D. (n=3). 2.2 .2 TEM images of γ-Syn fibrils formed upon addition of EGCG at different stages of γ-Syn fibrillation 38 The TEM images of the fibrils, formed upon addition of EGCG at lag, log and saturation phases (8h, 24h and 48h respectively) of γ-Syn fibrillation, reveal the presence of shorter and disintegrated fragments indicating the disaggregation of protofibrils and pre-formed γ-Syn fibrils (Figure 2C and D respectively). Control 100nm EGCG addition at 8h 24h 48h 100nm 100nm 100nm Figure 9. TEM images of γ-Syn species formed upon addition of EGCG (50μM) at different stages of fibrillation. TEM images of γ-Syn

fibrils formed at different stages of EGCG mediated inhibition. (Left to Right): Control, EGCG added at 8h, 24h and 48h respectively, shows formation of short and disintegrated fibrils, indicating fibril disaggregation (Scale bars, 100 nm). 2.2.3 Atomic Force Microscopy (AFM) of γ -Syn fibrils formed in presence of EGCG The morphology of the γ-Syn fibrils formed upon addition of EGCG at different stages of fibrillation was also analyzed by AFM studies. Addition of EGCG at initial late lag and log phase of fibrillation resulted in the formation of protofibrillar and oligomeric species at 8 and 24h respectively. The average heights of both the oligomeric and protofibrillar species were ~9.5nm. At 48h of EGCG addition, short disaggregated fibrils along with formation of spherical oligomers were observed with an average height of ~12 nm. Control 8h addition 24h addition 48h addition Figure 10. AFM images of γ-Syn fibrils formed upon addition of EGCG at different stages of fibrillation. AFM images showing disaggregation of γ-Syn fibrils upon addition of EGCG at different stages of fibrillation (Left to Right) : Control, EGCG added at 8h, 24h and 48h respectively. Addition of EGCG at 48 h shows broken fibrils (red arrow) and disaggregated spherical oligomers (yellow encircled). 2.3 Modulation of γ-Syn fibrillation pathway in the absence and presence of EGCG: The EGCG mediated inhibition and modulation of γ-Syn fibrillation pathway was further investigated by studying the effect of EGCG on the population of various γ-Syn species formed during aggregation by size-exclusion chromatography and investigating the nature of the species formed by SDS- and Native-PAGE analysis. 2.3.1 Size-exclusion chromatography of γ -Syn fibrils formed in the presence and absence of EGCG 2.3.1.1 Absorbance monitored at 275nm: The γ-Syn species formed both in the presence and absence of EGCG (50 μM) during fibrillation were withdrawn at regular time intervals (0, 24 and 48h) and the soluble fractions obtained after centrifugation were subjected to SEC at an absorbance of 275 nm (Figure 8B). Untreated γ-Syn solution in the absence of fibrillation eluted with a major monomeric peak at ~15.6 min and a small oligomeric peak at ~10.5 min, corresponding to an apparent molecular weight of ~44 kDa and ~670 kDa (> 10 mer), respectively as calculated from the standard calibration curve (Figure 8A). The SEC profiles of γ-Syn during aggregation showed an increase in the oligomeric peak area during the exponential phase (24h) of fibrillation, whereas during the end of fibrillation (48h) the soluble protein was significantly reduced eluting as monomers with only a negligible trace of oligomers present (Figure 8B). There were appearances of low absorbance multiple peaks eluting immediately after the major monomeric peak (~10.5 min) which disappeared with an increasing time of fibrillation, suggesting the presence of small fractions of various conformations which are getting retarded for a longer period of time in the column. The possibility that these peaks were a resultant of different γ-Syn conformations was further validated by estimating the hydrodynamic radii of γ-Syn using the empirical equations established for calculating the hydrodynamic properties of a protein from the apparent molecular weights obtained from SEC (Uversky et al., 2002). The Stoke's radius (Rs) of the monomeric γ-Syn as calculated using the apparent molecular mass (~44 kDa) was found to be ~28.7Å, which corresponds nearly with the previously reported value for monomeric γ-Syn (Uversky et al., 2002). Upon addition of EGCG (50 μM), at 0h, an immediate rise in the oligomer peak eluting at ~10.3 min was observed. During the exponential phase of fibrillation (24h), the EGCG treated γ-Syn eluted with the appearance of another significant peak at ~13.4 min corresponding to an apparent molecular weight of ~158 kDa, indicating the formation of second type of oligomer (~ 4mer) in the presence of EGCG which otherwise was absent in the SEC profiles of untreated γ-Syn species. These results indicate EGCG mediated formation of γ-Syn oligomers during fibrillation. 2.3.1.2 Absorbance monitored at 270nm: The binding of EGCG to different species of γ- Syn was further investigated by monitoring absorbance at 270 nm, where EGCG absorbs (Figure 8C). Although, the contribution by the tyrosine present in γ-Syn in this region cannot 41 be ruled out, the area under the curve was calculated to nullify the effect of tyrosine on the absorbance measured. The quantitation of the area under the respective peaks at all time intervals (0, 24 and 48h), showed an increase in the oligomeric peak area as compared to the area covered by the monomeric peak, and thus indicated an increased affinity of EGCG towards oligomers of γ-Syn. 2.3.1.3 SEC of γ-Syn species formed upon addition of EGCG at different stages of fibrillation: In order to investigate the disaggregated products of the protofibrillar and fibrillar species of γ-Syn, the SEC profiles of γ-Syn formed upon addition of EGCG (50 μM) at the lag (8h), log (24h) and exponential phase (48h) of the pathway were subjected to the column and elutions were monitored at 275 nm (Figure 8D). The incubation samples with EGCG added at different time intervals were withdrawn at the end of fibrillation and the samples were similarly centrifuged to analyze the soluble aggregates of the pathway. The SEC profiles clearly demonstrated the formation of γ-Syn oligomers at all the three stages

of EGCG addition. The increased oligomeric peak area (Figure 8E) even at 48h of EGCG addition further validated the EGCG mediated disaggregation of γ-Syn fibrils into higher- ordered oligomers (~158 kDa and 670 kDa). A) B) C) D) Figure 11. Size-exclusion chromatography of γ-Syn species in the presence of EGCG during fibrillation. A) Calibration curve of protein standards of known molecular weights obtained by size- exclusion chromatography. The protein standards mixture contained Thyroglobulin (670 kDa), γ- globulin (158 k Da), ovalbumin (44 kDa), myoglobulin (17 kDa) and vitamin B12 (1.3 kDa). The standard calibration curve was used to determine the apparent molecular weights of γ-Syn species eluting through the column. B) SEC-HPLC of γ-Syn during fibril formation monitored at regular time intervals 0, 24 and 48h (left to right) respectively showing formation of two types of oligomers in presence of EGCG which are absent in the untreated population. The formation of second type of oligomer at 24h of fibrillation is shown with an arrow ( ). C) The SEC profile at wavelength of 270 nm indicating preferential binding of EGCG with γ-Syn oligomers (left panel) with the relative percent area distribution of the different γ-Syn species depicting the formation of oligomers (right panel). D) SEC-profile (left panel) and percent area distribution (right panel) of γ-Syn species formed upon addition of EGCG at 8h, 24h and 48h showing disaggregation of pre-existing fibrils of γ-Syn 44 into oligomeric forms, designated in the plot as olig A and olig B corresponding to apparent molecular weights of ~670 kDa and ~158 kDa respectively. The error bars represent ±S.D. from three independent chromatographic runs (n=3). 2.3.2 Native-PAGE analysis The observations made by SEC were also validated by polyacrylamide gel electrophoresis under native conditions (Figure 9), where bands migrating just below the stacking gel were visualized only in the EGCG treated samples and showed large intensities with increasing time of fibrillation, thus indicating the formation of higher ordered oligomers by EGCG. EGCG (50μM) M _ + _ + _ + 200 kDa 45 kDa 31 kDa 0h 24h 48h Oligomers Monomers Figure 12. Native-PAGE analysis of γ-Syn species formed at different stages of fibrillation in the presence of EGCG (50μM). The protein molecular weight marker is depicted by lane M. The appearance of bands near ~200 kDa in the presence of EGCG shows formation of higher ordered oligomers. 2.3.3 SDS-PAGE analysis The nature of the oligomers formed in the presence of EGCG were further investigated by performing electrophoresis under denaturing conditions as shown in Figure 10A. The formation of two discrete bands in EGCG-treated γ-Syn samples depicts the formation of SDS-stable γ -Syn oligomers in the presence of EGCG with an apparent molecular weight of ~200 kDa and above, not seen in the untreated γ-Syn samples. A similar observation was made with the disaggregated species of γ-Syn (Figure 10B), where SDS- stable oligomers were observed to be formed in the presence of EGCG. A) EGCG (50μM) M _ + _ + _ + EGCG (μM) M _ 30 40 50 200 kDa 200 kDa 31 in vivo treatment with exogenous ZP1 in Japanese quail (*Coturnix japonica*)", FEBS Journal, 07/2008">kDa 31 kDa 21 kDa 14 in vivo treatment with exogenous ZP1 in Japanese quail (*Coturnix japonica*)", FEBS Journal, 07/2008">kDa 0h in vivo treatment with exogenous ZP1 in Japanese quail (*Coturnix japonica*)", FEBS Journal, 07/2008">B) 200 kDa 31 in vivo treatment with exogenous ZP1 in Japanese quail (*Coturnix japonica*)", FEBS Journal, 07/2008">kDa 21 in vivo treatment with exogenous ZP1 in Japanese quail (*Coturnix japonica*)", FEBS Journal, 07/2008">kDa 14 in vivo treatment with exogenous ZP1 in Japanese quail (*Coturnix japonica*)", FEBS Journal, 07/2008">kDa 24h in vivo treatment with exogenous ZP1 in Japanese quail (*Coturnix japonica*)", FEBS Journal, 07/2008">M 21 kDa 14 kDa 48h 48h EGCG addition at Control 8h 24h 48h Figure 13. SDS-PAGE analysis of γ-Syn species formed in the presence of EGCG. A) SDS-PAGE at regular intervals of fibrillation (left panel) in the presence of EGCG (50 μM) and (right panel) in the presence of increasing concentration of EGCG demonstrating the formation of SDS- stable oligomeric species in the presence of EGCG. B) SDS-PAGE of disaggregated oligomers showing EGCG-mediated formation of SDS- resistant oligomers at all stages of EGCG addition. The molecular weight marker lane in all the gels is depicted as M. 2.3.4 Dynamic Light Scattering The hydrodynamic properties of γ-Syn species formed during aggregation in the presence and the absence of EGCG were also studied by dynamic light scattering. The mean particle size distribution measured at different time intervals during fibrillation are shown in Figure 11. The hydrodynamic radii (Rh) of the γ-Syn oligomers formed both in presence and absence of EGCG were found to be within a range of 50-80 nm, suggesting the formation of higher - ordered oligomers as seen in SEC profiles. (i) (ii) (iii) (iv) (v) (vi) Figure 14. Mean particle size distribution of γ -Syn oligomers formed in presence and absence of EGCG during fibrillation measured by dynamic light scattering. The polydispersity of γ-Syn species during aggregation in absence (i to iii: 0h, 24h and 48h respectively) and presence of EGCG (iv to vi: 0h, 24h and 48h respectively) fitted into a Gaussian distribution of hydrodynamic radii (Rh) shows the formation of γ-Syn oligomers of the hydrodynamic radii ranging

between 50-80 nm. The increase in the (Rh) seen upon addition of EGCG at 0h (iv), shows immediate oligomerization of γ- Syn by EGCG. 2.4 Effects of EGCG treated and untreated seeds on γ-Syn fibrillation pathway: 2.4.1 Fibrillation kinetics in the presence of EGCG-treated and untreated γ-Syn seeds by ThT assay In order to investigate the stage at which EGCG specifically acts and whether the EGCG-generated oligomers act as templates for γ-Syn polymerization, the fibrillation was carried out in the presence of EGCG (50 μM) treated and untreated seeds (20% v/v) incubated for 48h. The fibrillation kinetics was monitored at regular intervals under shaking conditions using ThT fluorescence assay. As shown in Figure 12, the lag time of fibrillation in the presence of γ-Syn seed fibrils was reduced by approximately 10h, compared to the non- seeded γ-Syn fibrillation, whereas the EGCG-treated seeds were found to decrease the lag time by ~6h subsequently delaying fibril elongation. Addition of EGCG (50 μM) to the preformed γ-Syn seeds incubated with the monomeric γ-Syn showed negligible ThT fluorescence, suggesting that EGCG inhibits polymerization of γ-Syn fibrils and that the EGCG-generated oligomers are on-pathway that act as partial templates for γ-Syn polymerization and are thus kinetically retarded in nature. Figure 15. Fibrillation kinetics of γ -Syn in the presence of EGCG treated and untreated seeds studied by ThT assay. Fibrillation kinetics of γ -Syn in presence of EGCG-treated (50 μM) and untreated seeds (20% v/v) (left panel) formed after 48h of incubation and bar graph showing the significant difference in the lag time (right panel) in the EGCG-generated seeds as compared to the seeds formed without EGCG (**p < 0.001) and between non-seeded γ-Syn and EGCG-generated γ-Syn seeds (***p < 0.0005). The lag time of fibrillation in the presence of untreated γ-Syn seeds was significantly shorter than the non-seeded kinetics (****p < 0.0001). Negligible ThT fluorescence in the presence of EGCG (50 μM) added to the fibrillation reaction of seeded γ-Syn (green line) shows elongation inhibition. 2.4.2 TEM images of γ -Syn species formed in the absence and presence of EGCG treated γ-seeds The TEM images of the fibrils formed in the presence and absence of EGCG treated seeds (Figure 13A) showed that γ-Syn is capable of self seeding its fibrillation pathway giving rise to thick intertwined mature fibrils whereas only short and partially polymerized fragments were observed in presence of EGCG- treated seeds. This validates the EGCG-mediated formation of unfavourable γ-Syn oligomers that prevent nucleus formation and hence, fibril maturation. Additionally, the formation of short and diffused fibrillar species in the presence of EGCG added to seeded γ-Syn indicated the inhibition of fibril polymerization by EGCG (Figure 13B). A) 100nm 100nm 100nm B) 100nm Figure 16. Transmission electron microscopy images of fibrils formed in presence of EGCG- treated and untreated seeds. A) The TEM images showing the morphology of the fibrils formed (left to right: no seed, 20% (v/v) γ-Syn seed and 20% (v/v) EGCG treated γ-Syn seeds respectively). B) TEM image of the species formed upon addition of EGCG (50μM) to preformed γ-Syn. A magnification of 10,000 was used for all the images. (Scale bars, 100 nm). 2.5 Effect of EGCG on the structure of γ-Syn both under native and fibrillation conditions 2.5.1 Far-UV circular dichroism (CD) spectroscopy of γ-Syn in the presence of EGCG 2. 5.1.1 Far-UV CD analysis of γ-Syn under native and fibrillation conditions: To gain insight into the effect of EGCG on the secondary structure of γ -Syn, far-UV CD spectroscopy of the γ-Syn species incubated with an increasing concentration of EGCG (10, 30 and 50 μM) under native and fibrillating conditions was carried out. Monomeric and untreated γ-Syn showed far-UV CD spectra of a typical natively unfolded conformation with a large negative ellipticity at ~200 nm and a small value at ~222 nm, which was also maintained at all the concentrations of EGCG used (Figure 14A). The far-UV CD spectra of γ-Syn, monitored after 24h and 48h of fibrillation (Figure 14B), showed a shift in negative ellipticity to 218 nm, indicating a structural transition from the natively unfolded conformation to a characteristic β-sheet structure. This structural transition was found to be significantly delayed in presence of EGCG in a concentration-dependent manner, with an increase in negative ellipticity at ~208 nm and ~221nm at higher concentration of EGCG (50 μM), indicating the formation of an α-helical like structure by EGCG. 2.5.1.2 Far-UV CD analysis of soluble γ -Syn oligomers formed in the presence and absence of EGCG during fibrillation: The structure of γ -Syn oligomers formed both in the absence and the presence of EGCG were further characterized by far-UV CD spectra measurements of the soluble oligomers obtained after centrifugation of the fibrillating samples carried out as a function of time (Figure 14C). The far-UV CD spectra of soluble γ- Syn oligomers measured at different time intervals, i.e. 0h, 8h, 24h and 48h, showed spectra characteristic of natively unfolded protein, with a negative peak at ~200 nm. The differences in the intensities of the negative ellipticity indicated slight perturbations in the structure. In contrast, the EGCG generated oligomers during aggregation were found have increased secondary structure propensity showing a decrease in ellipticity at 200 nm and appearance of negative ellipticity with two minima at 208 nm and 220

nm, indicating increased α-helicity in the conformation. These results indicate an EGCG induced gain in the α-helical propensity in the γ-Syn oligomers which otherwise retain the natively unfolded conformation during fibrillation. A) B) . 24h 48h Figure Continued… C) 0h 8h 24h 48h Figure 17. Far-UV CD analysis of γ -Syn in the presence and absence of EGCG under native and fibrillation conditions. A) Far-UV CD spectra of γ-Syn (0.5 mg /ml) dissolved 20 mM phosphate buffer, pH-7.4 conditions in the presence of increasing concentration of EGCG (10, 30 and 50μM), monitored under native conditions. B) Far-UV CD spectra of γ-Syn (0 .3 mg/ml) in presence of increasing concentrations of EGCG (10, 30 and 50μM) monitored at time- intervals of 24h (left panel) and 48h (right panel) during fibrillation showing a shift in the negative ellipticity from 200 nm to ~ 218 nm in the untreated γ-Syn, depicting the formation of characteristic β-sheet conformation. C) Far- UV CD analysis of γ -Syn oligomers in presence of EGCG (50 μM) during fibrillation (left to right : 0h, 8h, 24h and 48h) was carried out at 25 °C using a cuvette of 0.1 mm path length to avoid interference in the measurement by 100 mM NaCl present in the fibrillation buffer (see Methods). Far-UV spectra of EGCG-treated oligomers at 48h showing double minima at ~208 nm and ~220 nm indicate α-helical structure. 2.5.2 ANS binding assay The extent of exposed hydrophobic surface area in γ-Syn was assessed by ANS binding assay. ANS (1-anilino-8-naphthalenesulfonic acid), a widely used solvent-sensitive dye is known to fluoresce with a blue-shifted emission upon binding with hydrophobic surroundings (Bolognesi et al., 2010) The ANS fluorescence spectra of monomeric γ-Syn in the presence of increasing concentration of EGCG overlapped with that of the fluorophore in buffer alone, with an emission around 525 nm ± 0.5 nm (Figure 15A). The ANS fluorescence spectra measured at different time intervals (0h, 24h and 48h) during fibrillation (Figure 15B), showed an increase in the fluorescence intensity with a characteristic blue shifted emission (λem at 480 nm) in the untreated γ-Syn fibrils. The ANS emission spectra obtained in EGCG treated γ-Syn fibrils were also blue shifted but the increments in the intensity were much reduced at all the time-points (Figure 15B). These results demonstrate that the extent of exposed hydrophobic surface area in γ -Syn species increases during aggregation which to a large extent is prevented by EGCG, suggesting that EGCG modulated species maintain an overall low surface hydrophobicity. A) B) Figure 15. ANS binding to γ-Syn in presence of EGCG shows an overall low surface hydrophobicity. A) Emission spectra of ANS binding to γ-Syn with increasing concentration of EGCG under native conditions. B) ANS binding to aggregating species of γ-Syn in presence and absence of EGCG with a characteristic blue-shift shown at ~480 nm. 2.6 Binding interactions between γ-Syn and EGCG The mode of binding interaction between EGCG and γ-Syn was further investigated by using steady-state and time-resolved fluorescence as well as isothermal titration calorimetry (ITC). 2.6.1 Steady-state fluorescence studies: Effect of EGCG on the intrinsic tyrosine fluorescence of γ-Syn To investigate the accessibility of EGCG to the lone tyrosine present in γ-Syn, tyrosine fluorescence of γ-Syn in the presence of increasing concentration of EGCG (2-30 μM) was monitored upon excitation at 275 nm with emission intensity recorded from 280-400 nm. The single tyrosine in γ-Syn has an emission maximum at 342 nm due to tyrosinate formation upon excitation as also reported for other proteins containing single tyrosine in absence of tryptophan (Szabo et al., 1978; Libertini & Small, 1985). A concentration dependent decrease in tyrosine fluorescence indicated an interaction between γ-Syn and EGCG (Figure 16A). Using the Stern-Volmer quenching equation, the bimolecular quenching constant (kq) was found to be more than 1010 M-1s-1 (kq = 9.6x1012 M-1s-1) (Figure 16B) indicating a static quenching mechanism and a binding interaction between EGCG and γ-Syn. The binding parameters were evaluated by employing the modified Stern-Volmer equation which resulted in a linear dependence between fluorescence quenching intensity and EGCG concentration from a plot of log (Fo-F/F) vs. log (Q) (Figure 16C). γ-Syn was found to bind with EGCG at an approximately equimolar ratio of 1:1. An interaction with a binding constant (Ka) of 6.9 103 M-1 was obtained suggesting the role of weak non-covalent interactions in EGCG mediated inhibition of γ-Syn fibrillation. In addition, the binding of EGCG to the different species of γ-Syn formed during fibrillation was carried out and the samples of γ-Syn withdrawn at time intervals of 0h, 24h and 48h were similarly titrated with increasing concentrations of EGCG at 25 °C. The modified Stern-Volmer plot showing the binding affinity (Ka) of EGCG to different species of γ-Syn is shown in Figure 16D and Table 1 respectively. EGCG was found to bind with highest affinity with the species formed during exponential phase of fibrillation (24h) validating the increased affinity of EGCG to γ- Syn oligomers as also revealed by SEC. A) B) C) Figure Continued… D) 0h 24h y = 0.9596 x + 4.14 R2 = 0.99 y = 1.3295 x + 5.72 R2 = 0.98 48h y = 0.8540 x + 3.71 R2 = 0.99 Figure 16. Intrinsic tyrosine fluorescence of γ-Syn in the presence of increasing concentration of EGCG. A) Steady-state fluorescence showing quenching of intrinsic tyrosine fluorescence of γ-Syn (0.3

mg/ml) continuously titrated with an increasing concentration of EGCG (2-30 μM) at 25ºC. B) The bimolecular quenching constant (kq = 7.4 x 1012 M-1s-1) at 25ºC indicates a static quenching mechanism between EGCG and γ-Syn. C) Modified Stern-Volmer plot of log (F0-F)/F vs log [Q] showing weak binding between γ-Syn and EGCG (Ka= 6.9x103M-1). D) Modified Stern-Volmer plots showing binding affinities of EGCG to different aggregating species of γ-Syn. EGCG showed higher affinity (Ka=105 M-1) at 24h of fibrillation, indicating increased affinity for oligomeric species of γ- Syn formed during exponential phase of the pathway (24h). Table 1. Binding of γ-Syn with different aggregating species of γ-Syn. Time (h) Ka (Binding Constant) 0 1.4 x 104 M-1 24 5.2 x105 M-1 48 5.1 x 103M-1 2.6.2 Time-Resolved Fluorescence measurements of γ-Syn in presence of EGCG 2.6.2.1 Fluorescence decay measurements of tyrosine in γ-Syn under native conditions: The binding mechanism between EGCG and γ-Syn was also investigated by time resolved fluorescence measurements of the single tyrosine present in γ-Syn, carried out in the presence of increasing concentration of EGCG (5-25 μM). The fluorescence intensity decay curves and the autocorrelation of the weighted residual mean used for deciding the goodness of the fit are shown in Figure 17A and B respectively. The decay curves both in the presence and absence of EGCG were described by three discrete decay components distributed into shorter lifetime (τ1 < 0.5ns), intermediate lifetime (τ2 ~2ns) and longer lifetime (τ3~ 6ns). The decay lifetimes observed in the presence of EGCG were found to be only marginally less than the average lifetime (τm) of native γ-Syn and the decay curves were indistinguishable from each other yielding the ratio of τ0/τ ~1(Table 2). This indicates that the changes in the fluorescence intensity were brought dominantly due to the changes in the decay amplitudes suggesting the existence of static quenching mechanism and a complex formation between EGCG and γ- Syn, as also observed in the steady-state fluorescence measurements. 2.6.2.2 Conformational dynamics of soluble γ-Syn oligomers formed in the presence of EGCG during aggregation: The conformational dynamics of γ-Syn oligomers formed both in the presence and absence of EGCG during fibrillation was further assessed by monitoring the lifetime decay of the lone tyrosine in γ-Syn at regular intervals of fibrillation. The samples of soluble oligomeric species of γ-Syn characterized by far-UV CD were also characterized by time-resolved fluorescence spectroscopy and the differences in the lifetimes between the EGCG generated and untreated γ-Syn oligomers were investigated. The fluorescence intensity decay curves at time intervals of (0h, 8h, 24h and 48h) and the autocorrelation of the weighted residual mean used for deciding the goodness of the fit are shown in Figure 17C. Time-resolved fluorescence measurements of γ -Syn oligomers both in the presence and absence of EGCG at all the time intervals are appropriately described by three discrete decay components as also observed under native state. The results showing the amplitudes of respective lifetimes along with their mean lifetimes are summarized in Table 3. The data show a faster decay in the EGCG-generated oligomers as compared to the untreated oligomers in the initial stages of fibrillation which become slower during the course of fibrillation, thus indicating a time- dependent confinement in the overall structure in the EGCG-generated oligomers. The untreated γ-Syn oligomers on the other hand show a decreasing fluorescence lifetime with an increase in the time of fibrillation, much evident during the exponential (24h) and saturation phase (48h) which indicates a solvent-exposed or an unfolded conformation. The increase in the amplitude (α1) of the shortest lifetime (τ1) and a concomitant decrease in the amplitude (α3) of the longest lifetime (τ3) in the untreated γ-Syn oligomers and vice-versa in the EGCG- generated oligomers during fibrillation (Figure 17D and E) clearly demonstrate the unfolded state of the untreated γ-Syn oligomers which when formed in presence of EGCG becomes conformationally more restrained and structured upon prolonged incubation. These observations thus further support the results obtained from far-UV CD of the γ-Syn oligomers (Figure 14C). A) B) Figure Continued… C) 48h Figure Continued… D) E) Figure 17. Time-resolved fluorescence measurements of γ-Syn species in the presence and absence of EGCG. A) Time-resolved fluorescence intensity decay of γ-Syn under native conditions in the presence of increasing concentrations of EGCG and B) plots of the autocorrelation function of the weighted residuals used to judge the goodness of the fit (left to right: no EGCG, 5, 10, 15, 20 and to 25 μM EGCG respectively) . The fluorescence decay curves were obtained upon excitation at 284 nm and monitoring emission at 342 nm. γ-Syn concentration of 1mg/ ml in 20 mM phosphate buffer, containing 100 mM NaCl at pH 7.4 was used. C) Lifetime decay curves of γ-Syn oligomers formed at 0, 8, 24 and 48h of fibrillation both in the presence and absence of EGCG along with their respective residuals (0 to 24h -upper: γ-Syn, lower: with EGCG and in 48h, left residual : γ-Syn, right residual : with EGCG). D) The plot of average lifetime (τm) versus the time of fibrillation demonstrates the difference in the decay kinetics in the EGCG generated and untreated oligomers. E) The relationship between the change in the amplitudes of the

fastest (τ1) and slowest (τ3) time constants (α1 and α3 respectively) with respect to the increasing time of fibrillation in the control and EGCG-treated samples. Table 2. Lifetime decay Parameters of γ-Syn in the presence of EGCG at 25 °C. γ-Syn τ1 [ns] (α1) τ2[ns](α2) τ3[ns](α3) τm [ns] χ2 γ-Syn (Control) 0. 41 (4.29) 2.00 (22.32) 5.83 (73.38) 4.74 1.04 +5μM EGCG 0.35 (4.22) 1.92 (23.08) 5.82 (72.70) 4.68 1.07 +10μM EGCG 0.38 (4.59) 1.93 (21.79) 5.82 (73.61) 4.72 1.09 +15μM EGCG 0.36(4.84) 1.91 (22.97) 5.82 (72.19) 4.66 1.03 +20μM EGCG 0.30 (4.91) 1.80 (23.06) 5.77 (72.03) 4.58 1.07 +25μM EGCG 0.31 (5.62) 1.83 (24.01) 5.78 (70.37) 4.52 1.08 Table 3. Lifetime decay Parameters of γ-Syn oligomers formed in the presence and absence of EGCG at 25 °C. Time (h) Sample τ1 [ns] (α1) τ2 [ns] (α2) τ3 [ns] (α3) τm [ns] χ2 0 γ-Syn +EGCG 0.30 (3.81) 0.20 (8.81) 2.04 (23.31) 1.63 (26.47) 5.72 (72.88) 5.58 (64.71) 4.65 4.06 1.05 1.06 8 γ-Syn +EGCG 0.35 (3.82) 0.23 (8.56) 2.08 (23.46) 1.77 (26.69) 5.73 (72.72) 5.71 (64.74) 4.66 4.18 1.04 1.06 24 γ-Syn +EGCG 0.25 (4.81) 0.10 (8.33) 2.07 (24.03) 1.59 (21.09) 5.71 (71.15) 5.58 (70.58) 4.57 4.28 1.10 1.10 48 γ-Syn +EGCG 0.098 (11.54) 0.09 (7.35) 1.58 (23.74) 1.78 (23.44) 5.606 (64.73) 5.64 (69.20) 4.00 4.32 1.07 1.09 2.6.3 Isothermal Titration Calorimetry of EGCG binding to γ-Syn The binding of EGCG to γ-Syn was further investigated by ITC analysis. The calorimetric study of the interaction of EGCG with γ-Syn was carried out at 25 °C with a 30 fold molar excess ratio of EGCG over γ-Syn. The representative ITC is displayed in Figure 18. The dissociation constant (Kd) obtained from the binding isotherm was of weak magnitude and in the mM range (Kd = 2.19 mM), thereby substantiating the role of weak non-covalent interactions in facilitating the binding of EGCG to γ-Syn. Due to the weak nature of binding interactions, enthalpy and entropy values could not be accurately deduced. ITC results were, however, in accordance with the steady-state fluorescence titration data indicating a weak binding interaction between EGCG and γ-Syn. Figure 18. Isothermal titration calorimetry of EGCG interaction with γ-Syn shows a weak binding interaction. The reaction was carried out at 25 ^{o}C with a γ-Syn and EGCG ratio of 1:30.Upper panel: A raw data plot of heat flow against time for titration of EGCG into γ-Syn and Lower panel: Plot of total normalized heat released as a function of ligand concentration for the titration. The solid line shows the one-site fit for the obtained data. 2.7 Cytotoxic effects of EGCG generated γ-Syn species 2.7.1 MTT Assay The cytotoxic effects of EGCG generated species by MTT assay was carried out on both breast cancer (MCF-7) and neuroblastoma (SH-SY5Y) cells due to the involvement of γ-Syn in both neurodegeneration and cancer. 2.7.1.1 MTT assay on MCF-7 cells γ -Syn was incubated both in the presence and absence of EGCG (50μM) for 24h and the effect of the γ-Syn species on the metabolic activity of the MCF-7 cells were assessed by MTT assay. The treatment of the MCF-7 cells with the protofibrillar and oligomeric species of γ-Syn generated after 24h of fibrillation, resulted to the decrease in MTT reduction by approximately 20 % indicating reduced cell viability (Figure 19A). On the other hand, the treatment of the cells with the EGCG generated oligomers was found to significantly increase the metabolic activity and thus cell viability by almost completely rescuing the MCF-7 cells from γ-Syn toxicity. The cytotoxic effect of EGCG-generated disaggregated γ-Syn species were further investigated on MCF-7cells. The toxicity of the disaggregated oligomers and the whole population of disaggregated γ-Syn fibrils containing various forms of γ-Syn disaggregates, were assessed separately by MTT assay. As the EGCG-diverted γ-Syn oligomers were found to be protective on MCF-7 cells (Figure 19A), it was interesting to compare the cytotoxic effects of the disaggregated oligomers on the same. For the assay, the disaggregated γ-Syn species formed after addition of EGCG (50 μM) at 8h, 24h and 48h (corresponding to lag, log and saturation phase respectively) of fibrillation, were withdrawn at the end of fibrillation (~72 h) and were separated into two groups where in one group only the soluble species obtained after centrifugation were used for the treatment of the cells and in the other group the disaggregated species as a whole were used without centrifugation. The disaggregated oligomers at all the time intervals (8, 24 and 48h) were found to be equally toxic to MCF-7 cells as the untreated γ-Syn oligomers (Figure 19B). On the other hand, the disaggregated fibrils were found to be less toxic than the γ-Syn oligomers. This indicates an early gain of toxic characteristics by γ-Syn which cannot be reversed upon fibril disaggregation by EGCG. A) MCF-7 B) Figure 19. Cytotoxic effects of EGCG treated γ-Syn species on MCF-7 cells by MTT assay. A) MTT assay reveal an increased viability of MCF-7 cells in the presence of EGCG generated oligomers (*p < 0. 01 and ***p < 0. 0005, related to the cells treated with γ-Syn oligomers and with respect to the untreated cells respectively). B) MTT assay show the reduction (****p < 0.0001) in the MTT absorbance with respect to the controls taken as untreated cells indicate that the disaggregated oligomers are significantly toxic to cells, whereas the whole population of disaggregated fibrils formed upon fragmentation are marginally toxic (**p < 0.001) to the untreated cells. The error bars represent ±S.D. (n = 3). The

statistical analysis was done using one-way ANOVA 2.7.1.2 MTT assay on SH-SY5Y cells The effect of 24h incubation samples of γ -Syn formed in the presence of EGCG (50μM) were also investigated by MTT assay on SH-SY5Y cells. A contrasting effect of γ-Syn oligomers on the viability of neuronal cells (SH-SY5Y) was observed. As otherwise observed in MCF-7 cells, the γ-Syn oligomers were found to be only moderately toxic to SH-SY5Y cells (Figure 20) whereas the EGCG generated oligomers were found to reduce viability by almost 50% as compared to the untreated and γ-Syn treated cells. Thus a differential toxicity of EGCG generated oligomers of γ-Syn on MCF-7 and SH-SY5Y cells were observed. SH-SY5Y Figure 20. Cytotoxic effects of EGCG treated γ-Syn species on SH-SY5Y cells by MTT assay. MTT assay on SH-SY5Y cells show a significant reduction in cell viability in the presence of EGCG generated oligomers (****p < 0.0001, related to the untreated cells), which only marginally reduced in presence of untreated γ-Syn oligomers (*p < 0.01 with respect to untreated cells). 2.7.2 LDH Assay on MCF-7 and SH-SY5Y cells The cytotoxic effects of the EGCG generated γ-Syn oligomers on both MCF-7 and SH-SY5Y cells were also validated by investigating the non-viability of the cells by LDH release assay (Figure 21A and B). The treatment of MCF-7 cells by the EGCG generated 24h γ-Syn oligomers increased the viability of MCF-7 cells and contrastingly decreased the viability of SH-SY5Y cells, as also observed in the MTT assay (Figure 19 and 20). The release of LDH into the culture medium is directly related to the extent of cellular damage and thus cell death, thus the reduced LDH release in the MCF-7 cells as well as increased LDH release in SH-SY5Y cells upon treatment with the EGCG generated γ-Syn oligomers indicates the contrasting effects of EGCG on these two cell lines, where on one hand it is protective and on the other is toxic respectively. Additionally the cytotoxic effects of the disaggregated γ-Syn oligomers on MCF-7 cells were also validated by the LDH assay. The disaggregated γ-Syn oligomers resulted in an increased release of LDH into the medium as compared to the disaggregated fibrils, thus establishing the membrane permeabilizing and membrane damaging effects of disaggregated γ-Syn oligomers on MCF-7 cells (Figure 21C). A) B) C) Figure 21. Cytotoxic effects of EGCG treated γ-Syn species on MCF-7 and SH-SY5Y cells by LDH release assay. A) LDH assay on MCF-7 cells show an increased cytotoxicity in presence of γ- Syn oligomers (**p < 0.005 related to the untreated cells) which is completely rescued in the presence of EGCG generated oligomers (**p < 0. 005 with respect to the γ-Syn treated cells). B) LDH assay on SH-SY5Y cells shows an increased cell death of SH-SY5Y cells in presence of EGCG-generated oligomers (***p < 0.0005 and **p < 0.005 related to untreated cells and γ-Syn treated cells respectively). The statistical analysis was done using unpaired t-test. C) The cytotoxic effects of the disaggregated γ-Syn oligomers by LDH assay showing an increased cell death in the presence of EGCG-mediated disaggregated oligomers as compared to disaggregated fibrils (# and * denote the significant difference between the disaggregated oligomers and disaggregated fibrils with respect to untreated cells respectively). The statistical analysis was done using unpaired t-test and the error bars represent ±S.D. (n=3). 3. DISCUSSION EGCG has previously been reported to inhibit fibrillation of other amyloidogenic proteins such as α-Synuclein and Aβ peptide but at a ratio of 5 to 10-fold molar excess over protein concentration (Ehrnhoefer et al., 2008; Palhano et al., 2013) which in the case of γ-Syn interestingly suppresses 50% of fibrillation even at a 15-fold less stoichiometry and a ratio of less than 1:1 is needed to bring complete inhibition (Figure 1A). The strong suppression of γ- Syn fibrillation by a significantly lower concentration of EGCG suggests that it acts on the nucleation phase of the pathway where it interacts with the nucleus or seeds present in low concentration as reported for small molecule mediated inhibition of Aβ fibrillation (Necula et al., 2007). Size-exclusion chromatography of γ-Syn species formed in the presence of EGCG monitored under fibrillating conditions demonstrate that EGCG diverts the on-going fibrillation pathway and disaggregates the existing fibrils into two similar kinds of SDS- resistant higher ordered oligomers with apparent molecular weights of ~158 kDa and ~670 kDa (Figure 8 and 10), with the formation of bigger oligomers (~ 670 kDa) favoured over the smaller one. The disaggregation of the pre-existing fibrils and protofibrils of γ-Syn into SDS- resistant oligomers by EGCG without forming amorphous aggregates, has also been reported for polyphenol Baicalein which shows a similar effect on mature fibrils of α-Syn (Zhu et al., 2004). The appearance of short and broken fibrils as observed in the TEM and AFM studies (Figure 6 and 7), further substantiates the attenuation of γ-Syn fibrillation at all the stages in the presence of EGCG as well as indicates EGCG mediated disaggregation. The light scattering results further demonstrate the formation of soluble aggregates as well as higher order oligomers by EGCG (Figure 2 and 11). The apparent molecular weight of monomeric γ-Syn is found to be ~44 kDa, an overestimated value which results from the natively unfolded nature of the intrinsically disordered protein (Golebiewska et al., 2014). The hydrodynamic radius (Rs) of the monomeric γ-Syn

under the experimental conditions was found to be 28.7Å which is smaller than that estimated for completely random coil form indicating compactness in the overall structure which in turn suggests a high self-associating tendency of γ-Syn, also reported in previous studies (Uversky et al., 2002). The values calculated by using the apparent molecular weight obtained from the SEC differs slightly from the Rs value calculated previously, possibly arising due to the differences in the protein concentrations used, emphasizing the role of concentration dependent self association of γ- Syn. The gradual build up of γ-Syn oligomers during the exponential phase of the pathway and their subsequent decline by the end of fibrillation in the absence of EGCG (Figure 8B) demonstrates the transient nature of these highly reactive species which possibly remain in a dynamic equilibrium with the monomer and disassemble into unstructured monomers under denaturing conditions unlike the EGCG generated oligomers (Figure 10). Although the exact mechanism of EGCG induced stability of γ-Syn is still unclear, the effect of EGCG could be understood in light of a previous study where it is reported that the hydroxyl rich aromatic structure of EGCG could form stable hydrogen bonds with the unfolded polypeptide such as α-Synuclein and Aβ-peptide, thus establishing that intermolecular interactions facilitate the self assembly of the EGCG stabilised oligomers (Ehrnhoefer et al., 2008). 70 Seeding studies (Figure 12) reveal that the EGCG-generated γ-Syn oligomers act only as partial templates for monomer addition for fibril polymerization and are intermediates of the γ-Syn fibrillation pathway. The intermediate lag time observed in the presence of EGCG- treated seeds suggest that the EGCG-generated oligomers increase the kinetic barrier for nucleus formation and delay fibril formation by retarding the apparent rate of fibrillation (kapp) (Table 1). It is interesting to note that EGCG has been previously reported to modulate α-Syn fibrillation pathway into SDS- resistant, higher ordered oligomers which are off- pathway in nature (Ehrnhoefer et al., 2008) unlike the oligomers of γ-Syn, which are observed to be on-pathway in this study. Such contrasting effect of a polyphenol on two closely related members of the same family indicates the involvement of complex modulating mechanisms that needs to be further investigated. The inhibition of fibril polymerization by EGCG and the presence of short or partially polymerized fibrils formed in the presence of EGCG-generated γ-Syn seeds (Figure 12 and 13) further suggests the formation of kinetically modulated and unfavourable species by EGCG Also, the shortened lag phase of γ-Syn fibrillation in the presence of preformed seeds (Figure 4A) indicates a nucleation dependent polymerization mechanism as also seen in α-Syn fibrillation (Uversky et al., 2002). Since the presence of EGCG shifts the equilibrium towards formation of oligomeric species, it is also suggested that EGCG favours conformations that have less likelihood of being the precursors for γ-Syn fibrillation. Far-UV CD analysis and ANS binding studies reveal stabilization of natively unfolded conformation in presence of EGCG, depicted by a negative ellipticity at ~198 nm (Figure 14A) and a weak ANS fluorescence intensity (Figure 15A), corresponding to the low mean hydrophobicity of these intrinsically disordered proteins (Uversky, 2011). It is well established that formation of β-sheet is a signature for amyloid fibrils (Klunk et al., 1989; Simmons et al., 1994; Chiti, Taddei, et al., 2002) and an increase in the hydrophobicity is one of the important physicochemical properties that is known to be involved in driving the formation of β-sheet structures leading to the build-up of toxic oligomeric species (Chiti, Taddei, et al., 2002; Pawar et al., 2005; Bolognesi et al., 2010; Campioni et al., 2010). It is observed in this study that the formation of characteristic β-sheet structures in γ-Syn during fibrillation is significantly delayed by an increasing concentration of EGCG which is also accompanied by the gain of an α-helical propensity (negative ellipticity and double minima at~208 nm and ~221nm) (Figure 14B). Supporting these results, an increasing ANS fluorescence intensity upon its binding with the aggregating species of γ-Syn indicating a molten-globule like state, a prerequisite for intrinsically disordered proteins for formation of fibrils, (Uversky, 2008) is substantially diminished in the 71 presence of EGCG (Figure 15B). The α-helical propensity of the γ-Syn oligomers as observed by far-UV CD analysis further highlights the increased structural stability of these oligomers that demonstrates their role in inhibiting the maturation of γ-Syn fibrils (Figure 14C). Formation of an α-helical structure by small molecule ligands in Aβ-peptide has also been reported to reduce Aβ-oligomer toxicity (Nerelius et al., 2009). The increased tendency of γ-Syn to form α-helical structure in its amyloid forming region, is reported to be an intrinsic property that can be induced under various conditions making it less prone to fibrillation compared to α-Syn which possess a high β-sheet forming propensity in that region (Marsh et al., 2006). The results such as immediate oligomerization upon EGCG addition (Figure 8), also depicted by an early increase in the light scattering intensity (Figure 2), clearly suggests that the EGCG mediated γ-Syn oligomerization occurs spontaneously and is relatively faster than γ-Syn amyloidogenesis alone which agrees with the theory of competitive binding (Gosal et al., 2005; Ehrnhoefer et al.,

2008). In the light of this theory, it is proposed that EGCG competes out the self-associating unfolded γ-Syn monomers binding preferentially with the unstructured oligomers, and thereby reducing the formation of β-sheet containing species and remodelling the pathway to form kinetically retarded α-helix containing oligomeric species majorly divided into two higher-ordered forms. The binding interaction between EGCG and γ-Syn using the steady-state and time- resolved fluorescence spectroscopy as also validated by isothermal titration calorimetry reveal the role of weak non-covalent interactions between EGCG and γ-Syn that bring significant modulation of the γ-Syn fibrillation pathway. The lone tyrosine present in γ-Syn that shows a characteristic tyrosinate emission at 342nm, as also observed for unfolded histone H1 protein containing single tyrosine (Libertini & Small, 1985). The quenching of tyrosine fluorescence in presence of increasing concentration of EGCG at 25 °C (Figure 16A and B), with a bimolecular quenching constant higher than the diffusion controlled value (kq > 1010 M-1) and the lifetime decay profiles of γ-Syn showing negligible change in the presence of EGCG under non-aggregating conditions (Figure 16B and Table 3), establish a static quenching mechanism indicating a complex formation between γ-Syn and EGCG. Isothermal titration calorimetry of γ-Syn binding to EGCG further reveals a weak binding affinity with a dissociation constant in the mM range. In agreement to this, the association constant (Ka) deduced from the modified Stern-Volmer plot (Figure 16C) obtained from steady-state fluorescence studies also reveals a weak binding affinity between EGCG and γ-Syn, although estimating a ~10-fold higher value than that observed in ITC. 72 This is likely due to the nature of two techniques, wherein fluorescence relies on the single tyrosine probe and ITC is based on global heat changes. The steady-state fluorescence spectra of different aggregating species of γ-Syn in presence of EGCG further reveal a higher affinity of EGCG towards oligomers of γ-Syn (Table 2 and Figure 16C), substantiating the observation made by SEC (Figure 8C). Additionally, the conformational dynamicity of these oligomers as studied by time-resolved fluorescence spectroscopy under fibrillating conditions (Figure 17C) reveals a time-dependent increase in the overall structural confinement in the EGCG-generated γ-Syn oligomers which upon prolonged fibrillation becomes more structured, thus supporting the gain of an α-helical propensity in EGCG-generated oligomers during fibrillation (Figure 14B). The faster decay kinetics of untreated γ-Syn oligomers during fibrillation (Figure 17C) as also supported by the retention of natively unfolded conformation of γ-Syn oligomers observed by far-UV CD (Figure 14C) describes the increased structural dynamicity of the oligomers of γ-Syn. This suggest that EGCG promotes the formation of conformationally restrained, α-helical structure by perturbing the local conformations in the natively unfolded γ-Syn to become more solvent exposed during the early stages of fibrillation which is depicted by faster fluorescence decay in the EGCG-generated oligomers during the initial stages of fibrillation. One of the important aspects of small molecule mediated modulation of fibrillation pathways is to investigate their cytotoxic effects as the oligomers and the protofibrillar intermediates formed during amyloidogenesis have previously been reported to be more toxic than the mature fibrils (Bucciantini et al., 2002; Caughey &Lansbury Jr, 2003; Ferreira et al., 2007). Given the fact that γ-Syn is involved in both cancer and neurodegeneration, the study compares the cytotoxic effects of EGCG-generated γ-Syn oligomers on breast cancer (MCF- 7) and neuroblastoma (SH-SY5Y) cells, taken as representatives of the diverse diseases, respectively. The increase in cell viability of MCF-7 cells (Figure 19A and 21A) and a reduction in viability of SH-SY5Y cells (Figure 20A and 21B) in the presence of EGCG- generated oligomers point toward the cell-specific behaviour of γ-Syn that could possibly play a critical role in the propagation of such diseases. This highlights the complexities in the use of EGCG and other polyphenols in the prevention of synucleopathies and needs further exploration. Furthermore, the mature fibrils of several amyloidogenic proteins have also been known to disaggregate under several conditions such as prolonged incubation during fibrillation (Cremades et al., 2012), changes in pH (Picotti et al., 2007) and chemical denaturants (Calamai et al., 2005). The toxic characteristics of the disaggregated oligomers 73 playing role in pathogenesis has also been observed previously (Cremades et al., 2012). The reduction in the viability of MCF-7 cells in presence of EGCG-disaggregated species (Figure 19B and 21C) suggest that γ-Syn gains toxic characteristics early during the nucleation which otherwise in the presence of EGCG at earlier stages fails to form toxic oligomeric intermediates (Figure 19A). Interestingly, the significant toxicity of the disaggregated oligomers observed against the partial toxicity of the fragmented fibrils (Figure 19B and 21C) demonstrate the increased membrane permeabilizing and thus damaging potential of γ-Syn oligomers causing cell death as compared to the disaggregated fibrils. The observation in turn highlights the critical role of the length and physical structure of the amyloid species that could possibly affect their cellular permeability and in turn govern their cytotoxicity. A

relationship between the fibril length and the amyloid toxicity has also been reported previously for amyloidogenic proteins like β2m, lysozyme and α-Synuclein where a reduction in the fibril length by fragmentation was associated with increased cytotoxicity (Xue et al., 2009). These results suggest that several factors such as stage of inhibition, morphology of aggregating species as well as the cell type together play a role in governing the toxicity of these species. A schematic representation of the mechanism of EGCG –mediated modulation of γ-Syn fibrillation is summarized in Figure I. Black arrow ( ): γ-Syn fibrillation pathway in the absence of EGCG Black dashed arrow ( ): EGCG-mediated γ-Syn fibrillation pathway Red arrow ( ): Disaggregation pathway of γ-Syn in the presence of EGCG Highly toxic: ++++ Partially toxic: + Chapter 3.2 Effect of Quercetin on the Structure and Aggregation of γ-Synuclein 1. Background Quercetin (3, 3′, 4′, 5, 7-pentahydroxylflavone) is the most widely studied flavonoid that comprises 65- 70% of dietary flavonoid and has beneficial effects in wide range of diseases such as cancer therapy, neurodegenerative diseases, cardiovascular diseases, inflammatory diseases etc. (Dajas, 2012; Suganthy et al., 2016). Quercetin was first isolated in the year 1936 by the physiologist Albert Szent-Györgyi de Nagyràpolt, winning the Nobel Prize in the field of Chemical Structure of Quercetin physiology and medicine (Suganthy et al., 2016). Quercetin is ubiquitously present in most plants, fruits, vegetables, nuts, grains, phenolic acids and alcohols. Red wine and tea infusions are considered to be the richest sources of quercetin that contain highest concentrations ranging from 4 to 16 and 10 to 25 mg/l respectively (Suganthy et al., 2016). The chemical structure of quercetin comprising of five hydroxyl groups which includes the 3′,4′ dihydroxy structure in the B-ring and 2,3 double bond in the C-ring with 4- oxo function confers the compound a high antioxidant property (Meng et al., 2009) that also is responsible for most of its pharmacokinetic properties. Quercetin has been demonstrated to have both anticancer and neuroprotective properties which are extensively documented in reviews published previously (Ossola et al., 2009; Dajas, 2012). The direct oxygen scavenging role of quercetin has been demonstrated to be responsible that protects neuronal cells from ROS mediated damage and prevent neurodegeneration (Dajas, 2012). Oxidative stress has been indentified to be the major cause of neurodegenerative diseases such as Parkinson's disease, Alzheimer's disease etc., where the accumulation of reactive oxygen species lead to neuronal cell loss and dysfunction (Zhu et al., 2013). Among many neuroprotective effects, quercetin has been reported to protect the neuronal SH-SY5Y cells from the H2O2 induced apoptotic damage (Suematsu et al., 2011), reverse the histopathological features of Alzheimer's disease (AD) by ameliorating the cognitive and emotional impairments in disease mice model (Sabogal-Guáqueta et al., 2015), inhibit fibrillation of many amyloid forming proteins and disaggregate the preformed fibrils of proteins such as α-Synuclein (Meng et al., 2010; Zhu et al., 2013), Aβ-peptide (H. Kim et al., 2005; Jiménez-Aliaga et al., 2011), bovine insulin (Wang et al., 2011) etc. The involvement of γ-Syn in both neurodegeneration and cancer makes it an important target for investigation of the inhibitory effects of quercetin on γ-Syn fibrillation. The study demonstrates a concentration- dependent inhibition of γ-Syn fibrillation as well as disaggregation with absence of complete suppression. Quercetin preferentially binds with the oligomeric species of γ-Syn formed in the exponential phase of the pathway by a strong binding interaction (kd ~ μM) and modulates the pathway to form SDS-labile species that are less fibrillogenic and off-pathway in nature. It is shown that quercetin does not affect the overall secondary structure of γ-Syn but maintains an overall low surface hydrophobicity of γ-Syn that possibly decelerates fibrillation. Interestingly, the quercetin generated species (fibrils and compact species) although off-pathway in nature were observed to be toxic to both the breast cancer (MCF-7) and neuroblastoma (SH-SY5Y) cells, providing the evidence for the toxic characteristics of the small molecule generated mature fibrils compared to the oligomeric counterparts. The study observes a high cytotoxic effect of lone quercetin on both the cell lines cautioning the use of quercetin as a universal therapeutics against both neurodegeneration as well as cancer. Lastly, the study suggests that the small molecule mediated intervention of fibrillation leading to inhibition may not always be desirable to combat adverse effects of amyloid-borne diseases and cancer. 2. Results 2.1. Effect of Quercetin on the fibrillation kinetics of γ-Syn 2.1.1 Thioflavin T Assay The fibrillation kinetics of recombinant human γ-Syn in the presence of increasing concentration of quercetin (5-50μM) was monitored using Thioflavin T (ThT) fluorescence. Monomeric γ-Syn was incubated under fibrillating conditions in the presence of quercetin dissolved in 1% DMSO and the ThT fluorescence was measured at regular time intervals during fibrillation. As shown in Figure 1, the ThT fluorescence was found to decrease in the presence of quercetin in a concentration dependent manner. Although a significant decrease in ThT fluorescence was observed in the presence of quercetin, a complete suppression of

fibrillation was not observed at any concentration. Upon saturation, approximately 30% of the amyloid was bound to ThT compared to the amyloid formed by the untreated γ-Syn, indicating ~70% reduction in fibrillation in the presence of 50μM quercetin. These results suggest an inhibitory effect of quercetin on γ-Syn fibrillation. Figure 1. Fibrillation kinetics of γ -Syn in the presence of increasing concentration of Quercetin by Thioflavin T assay. Monomeric γ -Syn was incubated in the presence of increasing concentration of quercetin (5- 50μM) under fibrillating conditions and the ThT fluorescence was recorded at regular interval of time. The concentration dependent decrease in the ThT fluorescence in the presence of quercetin showed fibrillation inhibition. The error bars represent the ±SD (n=3). 2.1.2 Light scattering by γ-Syn species formed during fibrillation in the presence of quercetin. The presence of exogenous compounds such as polyphenols due to their strong absorptive and fluorescent properties are reported to interfere with the ThT fluorescence assay, leading to quenching of ThT fluorescence (Hudson et al., 2009). The effect of quercetin on the fibrillation propensity was thus also validated by Rayleigh scattering. γ-Syn was incubated under fibrillating conditions in the presence of an increasing concentration of quercetin and the scattering intensity was recorded at regular intervals during fibrillation. The concentration dependent decrease in the scattering intensity as shown in Figure 2, clearly demonstrated inhibition of γ-Syn aggregation by quercetin, however as observed in the ThT assay complete suppression even at 50μM was not observed. Figure 2. Light scattering by γ-Syn species formed in the presence of an increasing concentration of Quercetin. The concentration-dependent decrease in the scattering intensity shows inhibition of aggregation by quercetin. γ-Syn was incubated with increasing concentration of quercetin (10, 30 and 50μM) and incubated at 37 °C, 200 rpm. The scattering intensity was recorded using a quartz cuvette of 1 cm path length at λex=λem (Δλ=0). 2.1.3 Transmission Electron Microscopy of γ -Syn fibrils formed in the presence of Quercetin The morphology of the γ-Syn fibrils formed in the absence and presence of quercetin was analyzed by negatively stained images using transmission electron microscopy (TEM). As shown in Figure 3, the untreated γ-Syn formed thick intertwined fibrils upon completion or saturation stage of fibrillation. In the presence of quercetin, a concentration-dependent disappearance of mature γ-Syn fibrils was observed thus indicating inhibition of γ-Syn fibrillation by quercetin. Figure 3. Morphology of γ -Syn fibrils formed in the presence of Quercetin visualized by transmission electron microscope. TEM images of γ-Syn fibrils formed upon saturation (end of fibrillation) in absence of Quercetin (A, B) and in presence of 5μM (C, D), 30 μM (E, F), 40 μM (G, H) and 50 μM (I, J) Quercetin respectively. Scale bar: 100nm. 2.1.4 Atomic Force Microscopy (AFM) of γ -Syn fibrils formed in presence of Quercetin The morphology of the γ -Syn fibrils formed in the presence and absence of quercetin was also studied by AFM analysis (Figure 4). The AFM analysis clearly demonstrated the formation of long intertwined fibrils in the untreated γ-Syn (control) with the average height of fibrils ~11 nm. In the presence of quercetin, a concentration dependent disappearance of mature fibrils was observed. At a higher concentration of quercetin (50 μM), the average height of the fibrillar species were reduced to ~7 nm, indicating inhibition of fibrillation. In the presence of 30 μM of quercetin, there were appearances of small spherical as well as fragmented protofibrillar species, resulting in amorphous aggregate formation with an increased height of ~17 nm. These results thus establish the inhibitory effect of quercetin on γ-Synuclein fibrillation. Control +10 μM Quer +30 μM Quer +50 μM Quer Figure 4. AFM analysis of the γ -Syn species formed in the presence of an increasing concentration of quercetin. The AFM images showing a concentration-dependent disappearance of mature fibrils in the presence of quercetin (left to right: control and in the presence of 10, 30 and 50 μM quercetin respectively). 2.2. Effect of Quercetin on different stages of γ-Syn fibrillation: 2.2.1 Thioflavin T Assay To investigate the effect of quercetin on different stage of γ-Syn fibrillation, quercetin (50μM) was added to the incubation sample at different time intervals (8, 24 and 48h) which correspond to the lag, log and exponential phase of fibrillation as previously mentioned in (Section). The ThT fluorescence was recorded at regular intervals immediately after adding quercetin at above mentioned time-points. Upon addition of quercetin, an immediate drop in the ThT fluorescence was observed which was followed by an overall decrease in ThT 82 fluorescence during fibrillation (Figure 5). The drop in the ThT fluorescence immediately upon addition of quercetin could be due to the known interference between ThT and coloured polyphenols like quercetin (Hudson et al., 2009). However, the successively reduced ThT fluorescence in the later stages suggested attenuation of fibril polymerization and disaggregation of mature γ-Syn fibrils by quercetin. The disassembly of the mature γ-Syn fibrils under the effect of quercetin was also further confirmed by the light scattering assay as mentioned below. Figure 5. Fibrillation kinetics of γ-Syn upon addition of quercetin at different stages of fibrillation studied by ThT assay. The decrease in the ThT

fluorescence upon addition of quercetin (50μM) at lag, log and saturation phase of fibrillation (8, 24 and 48h respectively) suggested attenuation of fibrillation and fibrillar disaggregation by quercetin. The error bars represent ±SD (n=3). 2.2.2 Light scattering by γ-Syn species formed after addition of quercetin at different stages of fibrillation The fibrillation samples used above for the ThT assay were further analyzed by light scattering assay. The scattering intensities of the fibrils formed at the end of fibrillation with quercetin added at 8, 24 and 48h of fibrillation showed a reduced scattering at all the time points with respect to control suggesting inhibition of protofibrillar polymerization and disaggregation of mature γ-Syn fibrils in the presence of quercetin (Figure 6). Also, the scattering intensity was found to decrease in the order of 8h >24h > 48h of quercetin addition demonstrating pronounced effect of quercetin on the saturation stage of fibrillation leading to disaggregation of mature γ-Syn fibrils into smaller structures. Figure 6. Rayleigh light scattering by γ-Syn species formed after addition of quercetin at different stages of fibrillation. The scattering intensity by the γ-Syn species formed at saturation after addition of quercetin at different stages (8, 24 and 48h) of fibrillation, recorded at an λex=λem (Δλ=0) using a 1 cm quartz cuvette showed a significant reduction in the scattering intensity at all the time points with respect to control (****p < 0.0001), indicating disaggregation pre-formed protofibrils and fibrils by quercetin. The statistical analysis was performed using unpaired t-test. The error bars represent ±SD (n=3). 2.2.3 TEM images of γ-Syn fibrils formed upon addition of quercetin at different stages of γ-Syn fibrillation The morphology of the γ-Syn species formed upon addition of quercetin at above mentioned time-points of fibrillation were also studied by TEM analysis (Figure 7). The untreated fibrils of γ-Syn as also observed previously formed dense network of mature fibrils. The γ-Syn fibrils formed upon addition of quercetin at 8 and24h of fibrillation although showed network of long fibrils, the fibrillar yield with respect to untreated fibrils was found to be much reduced. At 48h of quercetin addition, short and disintegrated fibrillar species was observed with an absence of mature fibrils, thus clearly demonstrating disaggregation of mature γ-Syn fibrils by quercetin. Figure 7. Transmission electron microscopy images of fibrils formed upon addition of quercetin at different stages of fibrillation. Morphology of the fibrils observed in absence of quercetin addition, (upper panel): Control and upon addition of quercetin at (left to right): 8h, 24h and 48h respectively. Addition of quercetin at all three time-points (8, 24 and 48h) showed diminished fibrils and disaggregation of mature γ-Syn fibrils at 48h of quercetin addition. A 100-nm scale bar is shown for comparison. A magnification of 10,000 X was used for all the images. 2.2.4 AFM analysis of γ-Syn fibrils formed upon addition of quercetin at different stages of fibrillation The morphology of the fibrils formed upon addition of quercetin at different stages of γ-Syn fibrillation was further studied by AFM analysis (Figure 8). The γ -Syn fibrils formed in the absence of quercetin showed long fibrillar networks with an average height ranging between 12 – 15 nm. Upon addition of quercetin at 8h (lag phase) of fibrillation, there was an appearance of numerous oligomeric and protofibrillar structures with an average height between 9-10 nm. This indicated an attenuation of nucleation and thus fibril polymerization, when quercetin is added in the early stages of γ-Syn fibrillation. Addition of quercetin during the exponential phase of fibrillation (24h) formed isolated fibrils lacking dense networks along with the appearance of short protofibrillar species, indicating inhibition of elongation 85 and fibril disaggregation. At 48h of quercetin addition, short and disintegrated fibrillar species were observed with a reduced average height ranging between 6-8 nm, demonstrating disassembly and dissolution of mature γ-Syn fibrils in the presence of quercetin. The results clearly demonstrate that quercetin effectively acts on all the stages of γ-Syn fibrillation and leads to inhibition of fibril polymerization at early and mid-stage of fibrillation while disaggregating preformed mature γ-Syn fibrils upon saturation. A) B) C) D) Figure 8. AFM analysis of γ-Syn species formed upon addition of quercetin at different stages of fibrillation. AFM images showing the morphology of the γ-Syn fibrils formed in the absence of quercetin addition (A) and disaggregation of γ-Syn fibrils upon addition of quercetin at 8, 24 and 48h of quercetin addition (B to D respectively). 2.3 Modulation of γ-Syn fibrillation pathway in the absence and presence of quercetin In order to elucidate the mechanism of inhibition by quercetin, it was important to investigate the effect of quercetin on the population heterogeneity of γ-Syn species formed during fibrillation and understand how quercetin modulate the fibrillation pathway of γ-Syn to bring inhibition. 2.3.1 Size-exclusion chromatography of γ-Syn fibrils formed in the presence and absence of quercetin The SEC-HPLC analysis of the soluble fraction of the fibrillation reaction was carried out to investigate the population distribution among various γ-Syn species formed in the absence and presence of quercetin during fibrillation. The analysis was done at an absorption wavelength of 275 nm and 378 nm to record the absorbance of γ-Syn, indicating the heterogeneity of γ-Syn species formed during

fibrillation and by recording quercetin absorbance indicating the affinity of quercetin to various species of γ-Syn respectively. 2.3.1.1 Absorbance monitored at 275 nm: The soluble fractions of γ-Syn obtained after centrifugation of the incubated γ-Syn samples during course of aggregation in the presence and absence of quercetin (50μM) were studied at regular time interval (0, 24 and 48h) of γ-Syn fibrillation and the SEC profiles monitored at 275 nm are shown in Figure 9A. The SEC profile of untreated γ-Syn both under native and fibrillating conditions is mentioned previously in (Section.). In the presence of quercetin (50μM), during exponential phase of the pathway (24h), a gradual rise in the oligomer peak at ~10.5 min along with an increasing peak eluting at ~22min was observed. By the end of fibrillation (48h), the SEC-profile of quercetin treated γ-Syn showed a substantial decrease in the oligomer peak as well as only a trace of monomeric species were present. 2.3.1.2 Absorbance monitored at 378 nm: To investigate the affinity of quercetin to different species of γ-Syn formed during fibrillation, the SEC analysis was carried out by monitoring absorbance at 378 nm, the absorbance wavelength for quercetin (Figure 9B). At 24h of fibrillation, a predominant rise in the oligomer peak was observed with a successive decline at saturation (Figure 9B). At 48h (saturation stage), slight rise in the peak eluting between 20-23 min was observed. This demonstrates that quercetin has a higher affinity toward the oligomeric species of γ-Syn. A) Figure Continued… B) Figure 9. Size-exclusion chromatography of γ-Syn species formed in the presence and absence of quercetin. A) Size-exclusion profiles of γ-Syn species formed at different intervals (0, 24 and 48h) during fibrillation in the presence and absence of quercetin (50 μM). At 24h of fibrillation, an increase in the peak at ~23 min is shown with an arrow ( ). (B) SEC profiles of quercetin bound γ-Syn species, the absorbance monitored at 378 nm, indicating increased affinity of quercetin to oligomeric γ-Syn. 2.3.2 SDS - PAGE analysis To investigate the nature of the γ-Syn species formed in the presence of increasing concentration of quercetin (30 and 50μM), SDS-PAGE analysis of the soluble and insoluble fraction of γ-Syn species formed after 48h of incubation was carried out. The supernatant was obtained after centrifugation at 14 ,000×g for 30 minutes. In the absence of quercetin, a thick fibrillar pellet band was observed which decreased in the intensity in the presence of increasing concentration of quercetin, indicating that majority of the soluble fraction (monomer and oligomers) of γ-Syn is converted to fibrils in the absence of quercetin. The soluble fraction was indistinguishable in the absence and presence of 30μM quercetin but in the presence of 50μM quercetin, the soluble fraction was not visible along with the reduced intensity in the pellet fraction. Since the SDS-stable species were not observed in the stacking gel in the fibrillar pellet formed in the presence of 50μM quercetin, the reason behind reduction of both soluble and insoluble fraction in the presence of 50μM quercetin needs to be further investigated. Overall, it is demonstrated that γ-Syn forms SDS-labile species both in the absence and presence of quercetin. Quercetin (μM) - - +30 +30 +50 +50 M S P S P S P 66 kDa 45 kDa 31 kDa 21 kDa 14 kDa Figure 10. SDS- PAGE analysis of γ-Syn species formed in the absence and presence of increasing concentration (30 and 50 μM) of quercetin at 48h of fibrillation. The molecular weight marker is denoted by M and the soluble (supernatant) and the insoluble (pellet) fractions are denoted by S and P respectively. 2.3.3 Dynamic light scattering The soluble aggregates of γ-Syn formed in the presence of quercetin used for SEC-HPLC studies were further used to characterize their hydrodynamic properties by DLS. The summary of the mean particle size distribution of γ-Syn species formed in the presence of increasing concentration of quercetin at different time intervals is given in Table1. The hydrodynamic radii (Rh) of monomeric γ-Syn were measured to be around 28.08nm. On addition of quercitin an overall increase in the Rh of the γ-Syn species were observed. Table I. Hydrodynamic Properties of γ -Syn Formed in the Presence of Quercetin 2.4 Effects of Quercetin treated and untreated seeds on γ-Syn fibrillation pathway 2.4.1 Fibrillation kinetics in the presence of quercetin-treated and untreated γ-Syn seeds by ThT assay: To investigate whether the quercetin generated species act as template for γ-Syn polymerization and understand the underlying mechanism of inhibition, the seeding studies were carried out. Preformed γ-Syn seeds formed in the absence and presence of quercetin (50 μM) were used to seed the monomeric γ-Syn and the fibrillation kinetics of monomeric γ -Syn in the presence and absence of seeds was monitored by ThT assay. As shown in Figure 11 (A and B), the lag time of fibrillation was significantly reduced in the presence of untreated γ- Syn seeds, a characteristics of nucleation-dependent polymerization mechanism as also mentioned previously (Section). The lag time of fibrillation in the presence of quercetin treated seeds showed a lag time shorter than the non-seeded but longer than the γ-Syn seeded kinetics. Although a difference in the lag time between the quercetin treated and non-seeded fibrillation was observed, it was found to be only marginally significant (*p < 0.05), 91 indicating that the quercetin generated species do not act as templates for

γ-Syn fibrillation. Additionally the apparent rate (kapp) of γ-Syn fibrillation in the presence of quercetin- treated seeds and non-seeded fibrillation differed only marginally from each other (Figure 11C), indicating that the overall fibrillation remains unaffected in the presence of quercetin generated species. Thus the results suggest that quercetin-generated species are off-pathway in nature. A) B) Figure Continued… C) Figure 11. Fibrillation kinetics of γ -Syn in the presence of quercetin treated and untreated seeds studied by ThT assay. A) ThT assay in the presence of quercetin treated and untreated seeds showing a shortened lag time in the presence of untreated γ-Syn seeds (red circle) with respect to both non- seeded kinetics (black square) and quercetin treated γ-Syn seeds (blue triangle). Data shows a marginally reduced lag time of fibrillation in the presence of quercetin treated seeds with respect to non-seeded kinetics. B) Bar graph showing the significance of the difference in the lag time (tlag) of fibrillation. The data shows that the tlag (h) is significantly reduced in the presence of untreated γ-Syn seeds (***$p < 0.001$, with respect to non-seeded reaction). The tlag (h) of fibrillation in the presence of quercetin treated seeds is only marginally reduced (*$p < 0.05$) than the non-seeded fibrillation. C) Bar graph showing the significance of the difference in the apparent rate of fibrillation (kapp). The data shows that the rate of fibrillation is increased in the presence of untreated γ-Syn seeds as compared to non-seeded reaction (**$p < 0.005$), whereas the difference in the (kapp) (h-1) between the quercetin – treated and non-seeded reaction was only marginally different (* $p < 0.05$), indicating that quercetin generated species are off-pathway in nature. The statistical analysis was performed using unpaired t- test and the error bars represent ±SD (n=3). 2.4.2 TEM images of γ -Syn species formed in the absence and presence of quercetin treated γ-seeds The morphology of the γ-Syn species formed in the presence and absence of quercetin generated seeds was further was visualized by TEM studies (Figure 12). In the presence of untreated γ-Syn seeds, thick fibrils with well-defined boundaries were observed, whereas in the presence of the non-seeded γ-Syn, long and thinner fibrils were observed with reduced yield as compared to the seeded fibrils. In the presence of quercetin-generated seeds, significant reduction in the fibrillar yield was further observed with respect to both seeded and non-seeded γ-Syn. Thus, the formation of mature fibrils in the presence of quercetin- treated seeds suggest that quercetin inhibited species are off-pathway in nature. No Seed γ-Syn Seed Quercetin treated γ-Syn Seed Figure 12. Transmission electron microscopy images of fibrils formed in presence of Quercetin- treated and untreated seeds. The TEM images showing the morphology of the fibrils formed (left to right: no seed, 20% (v/v) γ-Syn seed and 20% (v/v) Quercetin treated γ-Syn seeds respectively) A magnification of 10,000 was used for all the images. (Scale bars, 100 nm). 2.5 Effect of quercetin on the structure of γ -Syn under both native and fibrillation conditions 2.4.1 Far-UV CD analysis of γ -Syn in the presence of quercetin To gain insight into the effect of quercetin on γ-Syn structure and fibrillation, circular dichroism spectroscopy of the γ-Syn species incubated with an increasing concentration of quercetin (10, 30 and 50 μM) under native and fibrillating conditions was carried out. Untreated and freshly prepared solutions of γ-Syn showed far-UV CD spectra of a typical natively unfolded conformation with a large negative ellipticity at ~200 nm and a small value at ~222 nm, which was also maintained at all the concentrations of quercetin used (Figure 13A). However, in the presence of higher concentration of quercetin (30 and 50 μM), a decrease in the negative ellipticity at ~200 nm was observed indicating a gain of secondary structure along with a decrease in the natively unfolded conformation in γ-Syn. The far-UV CD spectra of γ -Syn both in the absence and presence of quercetin, monitored after 24h and 48h of fibrillation (Figure 13B), showed a shift in negative ellipticity to 218 nm, indicating a 94 structural transition from the natively unfolded conformation to a characteristic β-sheet structure. A) B) Figure 13. Far-UV CD spectra of γ -Syn in the presence of quercetin both native and fibrillating conditions. (A-B) The far-UV CD of γ-Syn in the presence and absence of quercetin both under native and fibrillating conditions respectively were monitored at 25 °C using a cuvette of 1mm path length. A) Far-UV CD spectra of γ-Syn (0. 3 mg /ml) dissolved 20 mM phosphate buffer, pH-7.4 conditions in the presence of increasing concentration of quercetin (10, 30 and 50μM), monitored under native conditions. B) Far-UV CD spectra of γ-Syn (0 .3 mg/ml) in presence of increasing concentrations of quercetin (10, 30 and 50μM) monitored at time- intervals of 24h (left panel) and 48h (right panel) during fibrillation showing a shift in the negative ellipticity from 200 nm to ~ 218 nm both in the absence and presence of quercetin, depicting the formation of characteristic β- sheet conformation. 2.4.2 ANS binding assay The effect of quercetin on the exposed surface hydrophobicity of γ-Syn was further assessed by ANS binding assay. ANS fluoresces strongly with a blue shifted emission upon binding with the hydrophobic patches in a protein. Binding of ANS to γ-Syn in the presence of increasing concentration of quercetin under native conditions results to a concomitant

decrease in the ANS fluorescence intensity (Figure 14A). This indicates a competitive binding between ANS and quercetin on γ-Syn leading to displacement of bound ANS at higher concentrations of quercetin (Figure 14A). ANS fluorescence measured at regular time intervals during γ-Syn fibrillation (Figure 14B to E) in the absence of quercetin showed an increase in the ANS fluorescence intensity with a characteristic blue shifted emission at ~480 nm. On the other hand, the increments in the ANS intensity in the presence of quercetin were significantly reduced during aggregation. It is to be noted that at 8h of fibrillation (Figure 14B), an overlapping spectra of ANS bound with the protein both in the absence and presence of quercetin was observed, indicating the conformational changes in the protein, minimizing the interference between ANS and quercetin. During the later stages of fibrillation (24 and 48h) (Figure 14C and D), the significant decrease in the ANS intensity in the presence of quercetin indicated an overall low hydrophobicity in the γ-Syn species formed by quercetin. Changes in the ANS fluorescence intensity at emission maxima of 480 nm, with an increasing concentration of quercetin at regular time intervals during fibrillation is shown in Figure 14 E. A) B) C) Figure Continued… D) E) Figure 14. ANS binding analysis of γ -Syn in the absence and presence of quercetin. A) Emission spectra of ANS binding to γ-Syn under native conditions in the presence of increasing concentration of quercetin. B to D) ANS binding to aggregating species of γ-Syn formed in the presence of increasing concentration of quercetin showing blue shifted emission at ~480 nm. E) Bar showing the difference in the ANS fluorescence intensities at an emission maximum of 480 nm at regular intervals of fibrillation in the presence of quercetin. 2.5 Binding interactions between γ-Syn and quercetin The mode of binding interaction between quercetin and γ-Syn was further investigated using steady- state fluorescence and isothermal titration calorimetry (ITC) to gain an in-depth understanding of the mechanism underlying the quercetin mediated inhibition of the γ-Syn fibrillation pathway. 2.6.1 Effect of quercetin on intrinsic tyrosine fluorescence of γ-Synuclein To investigate the mode of binding interaction between quercetin and γ-Syn and probe the accessibility of quercetin to the single tyrosine present in γ-Syn, the changes in the tyrosine fluorescence intensity in the presence of increasing concentration of quercetin (2-30μM) was monitored at different temperatures. As shown in Figure 15A, continuous titration of γ-Syn with an increasing concentration of quercetin at 25°C, showed a concentration dependent decrease in the tyrosine fluorescence. The quenching of tyrosine fluorescence in the presence of quercetin thus indicated an interaction between γ-Syn and quercetin. Using the Stern- Volmer equation, the bimolecular quenching constant (kq) was calculated to be more than 1010M-1s-1 (kq = 1.95×1013M-1s-1) (Figure 15B) indicating a static quenching mechanism and complex formation between γ-Syn and quercetin. Further the affinity of quercetin towards γ- Syn was estimated using the modified Stern-Volmer plot. γ-Syn was found to bind with quercetin at an equimolar ratio of 1:1. The association constant (Ka) between quercetin and γ- Syn was estimated to be 2.2×105M-1indicating moderate to strong binding affinity. The binding parameters of quercetin binding to γ-Syn at different temperatures are summarized in Table II. Quercetin was found to bind to γ-Syn with highest affinity at 37°C (310.15 K). A) B) C) Figure 15. Intrinsic tyrosine fluorescence of γ-Syn in the presence of increasing concentration of quercetin. A) Steady-state fluorescence showing quenching of intrinsic tyrosine fluorescence of γ- Syn (0.3mg/ml) continuously titrated with an increasing concentration of quercetin (2-30μM) at 25 °C. B) Plot of F0/F against quercetin conc. and (C) Plot of log (F0-F)/F against log[Q] giving the value for biomolecular quenching constant 'kq' and binding constant 'Ka' respectively. Table II. Binding Parameters calculated from Stern- Volmer Plot Temperature (K) kq (Bimolecular quenching constant) Ka (Binding constant) N (No. of binding sites) 288.15 2.19 × 1013M-1 s-1 9.08 × 104M-1 ~ 1 298.15 1.95 × 1013M-1 s-1 2.2 × 105M-1 ~ 1 310.15 2.69 × 1013M-1 s-1 1.43 × 106M-1 ~ 1 318.15 2.58 × 1013M-1 s-1 3.48 × 104M-1 0.9 ~ 1 2.6.2 Isothermal Titration Calorimetry of quercetin binding to γ-Syn To further characterize the thermodynamic parameters of binding interactions between γ-Syn and quercetin, the calorimetric study of the interaction of quercetin and γ-Syn was carried out at 37°C at 10-fold molar excess ratio of quercetin over γ-Syn. γ-Syn (10.4 μM) was titrated with equal injections of 4 μl quercetin at an equal interval of 420 s, with continuous stirring at 329 rpm. As shown in Figure 16, the binding isotherm shows a strong binding interaction between quercetin and γ-Syn fitted to a single binding site model. Quercetin binds with γ-Syn spontaneously with a net exothermic reaction. The negligible negative entropy (ΔS) and high negative enthalpy (ΔH) demonstrates that the interaction is an enthalpically driven reaction. The strong binding affinity with an association constant of ~1.96 × 106M-1 suggests the role of non-covalent, hydrogen bonding interactions between quercetin and γ-Syn. The data further supports the observations made by the steady-state fluorescence and are in agreement with each

other. Figure 16. Isothermal titration calorimetry of quercetin binding to γ-Syn. The reaction was carried out at 37 °C with γ-Syn and quercetin ratio of 1:10. Upper panel: A raw data plot of heat flow against time for titration of quercetin into γ-Syn and lower panel: Plot of normalized heat released as a function of ligand concentration for the titration. The red solid line shows the single-site fit for the obtained data. Table III. Thermodynamic parameters of γ-Synuclein binding to quercetin by isothermal titration calorimetry Ka × 106 (M-1) ΔH° (kcal / mol) ΔS° (cal / mol / deg) ΔG° (kcal / mol) 1.93 ± 0. 2 -21.2 ± 0.03 -39.6 -8.7 2.7 Cytotoxic effects of Quercetin generated γ-Synuclein species studied by MTT assay To investigate the cytotoxic effects of quercetin generated species, MTT assay was carried out on both breast cancer (MCF-7) and neuroblastoma (SH-SY5Y) cells. 2.7.1 MTT assay on MCF-7 cells γ-Syn was incubated with an increasing concentration of quercetin (10, 30 and 50μM) under fibrillation conditions and samples were withdrawn at different time intervals (0, 24 and 48h) to investigate the cytotoxic effects of the various γ-Syn species formed at different stages of fibrillation in the presence and absence of quercetin. As shown in Figure 17, the treatment of cells with various concentration of quercetin in the absence of γ-Syn, taken as control, significantly reduced the viability of MCF-7 cells, suggesting that quercetin alone is toxic to the MCF-7 cells. At 0h, the viability of cells in the presence of untreated γ-Syn was reduced by approximately 30%, which was marginally rescued to 20% in the presence of increasing concentration of quercetin. At 24h, the viability of MCF-7 cells was marginally reduced in the presence of quercetin treated γ-Syn species. Interestingly, at 48h of fibrillation where untreated γ-Syn fibrils were found to reduce viability by approximately 25%, the fibrils formed by quercetin at all concentrations were significantly toxic to MCF-7, reducing their viability by nearly 40%, indicating that quercetin generated fibrils are toxic to MCF-7 cells. MCF-7 Figure 17. Cytotoxic effects of quercetin treated γ-Syn species on MCF-7 cells by MTT assay. MTT assay reveals that at quercetin alone is significantly toxic to MCF-7 cells (****p < 0.0001, with respect to untreated cells). At 0h, the viability of cells in the presence of quercetin treated γ-Syn is marginally increased (*p < 0.05), as compared to cells treated with γ-Syn alone. The 24h data shows a marginally reduced viability in the presence of quercetin treated γ-Syn (*p < 0.05), as compared to cells treated with γ-Syn alone. At 48h, the γ -Syn fibrils formed in the presence of increasing concentration of quercetin were found to significantly reduce the viability of MCF-7 cells (****p < 0.0001, with respect to cells treated with only γ-Syn in the absence of quercetin). The statistical analysis was done using one-way ANOVA. The error bar represents ±SD (n=5). 2.7.2 MTT assay on SH-SY5Y cells γ-Syn was incubated with an increasing concentration of quercetin (10, 30 and 50μM) under fibrillation conditions and the assay was carried out as mentioned above. As observed in MCF-7 cells (Figure 17), a similar decrease in the SH-SY5Y cell viability was observed in the presence of quercetin alone, used as control (Figure 18A). This suggests that quercetin is inherently toxic to both the cell lines used in the present study. At different time intervals of fibrillation, as shown in Figure 18, the viability of cells were unaffected in the presence of untreated γ-Syn, whereas a significant decrease in the cell viability was observed in the presence of quercetin- treated γ-Syn species. Interestingly, at 24h of fibrillation, the untreated γ-Syn species were found to reduce the cell viability by approximately 50%, which was significantly rescued by the quercetin treated γ-Syn species by increasing the cell viability by almost 20%. At 48h of fibrillation, the γ -Syn fibrils formed in the presence of higher concentration of quercetin (30 and 50 μM), the viability was further found to reduce by ~40%. Additionally, the cytotoxic effects of the disaggregated species of γ-Syn formed in the presence of quercetin were investigated on the SH-SY5Y cells (Figure 18B). The untreated γ- Syn fibrils formed at the end of fibrillation was found to reduce viability by approximately 35%, which was maintained even in the presence of disaggregated γ -Syn fibrils formed in the presence of quercetin (50 μM). The disaggregated fibrils were thus observed to be equally toxic to the untreated γ-Syn fibrils. A) SH-SY5Y B) Figure 18. Cytotoxic effects of quercetin treated γ-Syn species on SH-SY5Y cells by MTT assay. A) MTT assay reveals that at quercetin alone is significantly toxic to SH-SY5Y cells (***p < 0.0005, with respect to untreated cells). At 0h, the viability of cells in the presence of quercetin treated γ-Syn is marginally reduced (**p < 0.005), as compared to cells treated with γ-Syn alone. The 24h data shows an increased viability in the presence of quercetin treated γ-Syn (****p < 0.0001), as compared to cells treated with γ-Syn alone. At 48h, the γ -Syn fibrils formed in the presence of higher concentration of quercetin (30 and 50 μM) were found to reduce the viability of SH-SY5Y cells (**p < 0.005, with respect to cells treated with only γ-Syn in the absence of quercetin).. B) MTT assay showing the cytotoxic effects of the disaggregated species of γ-Syn. The untreated γ-Syn fibrils were found to be significantly toxic to SH-SY5Y cells (****p < 0. 0001, with respect to untreated

cells). The disaggregated γ-Syn fibrils formed in the presence of quercetin were found to be equally toxic as untreated γ-Syn fibrils, showing no significant difference in the toxicity. The statistical analysis was done using one-way ANOVA. The error bar represents ±SD (n=5). 3. Discussion The study emphasises on elucidating the inhibitory effect and the mechanism of quercetin mediated modulation of γ-Syn fibrillation pathway. Quercetin has been previously reported to inhibit amyloidogenesis of many fibril forming proteins such as α-Synuclein (Meng et al., 2010; Caruana et al., 2011), Aβ- peptide (Jiménez-Aliaga et al., 2011), insulin (Wang et al., 2011), amylin (López et al., 2016), etc. The results demonstrated here establish a concentration dependent inhibition of γ-Syn fibrillation by quercetin however, as observed in the presence of EGCG (Section), a complete suppression at a higher concentration of even 50 μM was not observed (Section 3.1). The differences in their inhibitory effects could be explained by the difference in the number of the hydroxyl groups (OH) present in their chemical structures where a direct relationship between an increase in the number of hydroxyl groups in the polyphenols and anti-amyloidogenic activity has been established (Ono et al., 2006). Quercetin in comparison to EGCG has also been previously classified as a good inhibitor that increased the lag time of α-Syn fibrillation by 4 to 5- fold, while EGCG was classified as a strong inhibitor leading to complete suppression of α-Syn fibrillation (Meng et al., 2009). A detectable but reduced light scattering intensity in the presence of increasing concentration of quercetin (Figure 2) indicate the formation of smaller species that reduce the overall fibrillar yield of γ-Syn. It is further observed as a concentration dependent disappearance of mature γ-Syn fibrils along with the appearance of short spherical and protofibrillar species visualized by TEM (Figure 3) and AFM (Figure 4) analysis respectively. The effect of quercetin on different stages of γ-Syn fibrillation reveal that quercetin, like EGCG (Section) inhibits fibril elongation and attenuates the protofibrillar assembly when added at earlier and mid stage of fibrillation (8 and 24h respectively), while addition of quercetin on the preformed γ-Syn fibrils at saturation (48h) leads to the disassembly of the mature fibrils to form short, disaggregated fragments of reduced fibril diameter as shown in Figure 5. The disaggregation of mature fibrils of other amyloidogenic proteins such as bovine insulin (Wang et al., 2011), Aβ-peptide (Jiménez-Aliaga et al., 2011) and α-Synuclein (Meng et al., 2010; Zhu et al., 2013) by quercetin has also been reported previously. The chemical structure of quercetin facilitates hydrophobic interactions, aromatic stacking and hydrogen bonding with the amyloid forming regions in proteins that are reported to be the driving forces that lead to fibril inhibition and destabilization (Wang et al., 2011). The SEC profiles of γ-Syn species formed in the presence and absence of quercetin during fibrillation (Figure 9) reveal a time-dependent increase in γ-Syn oligomerization in the presence of quercetin, predominant at 24h, which is the exponential phase of fibrillation. At 24h, the γ-Syn population appears to be in near equilibrium between the oligomeric and monomeric species of γ-Syn with the appearance of additional population of species that elute later at ~22 min which possibly are the compact conformations of γ-Syn species that get retarded for a longer duration in the column. The SEC profiles monitored at 378 nm (Figure 9B) demonstrate an increased affinity of quercetin towards γ-Syn oligomers and establish that quercetin inhibits γ-Syn fibrillation by binding with the oligomers of γ-Syn formed specifically at the exponential phase of the pathway and modulate them to form compact structures that lead to suppression of fibrillation and thus are the resultant inhibitory species of the γ-Syn fibrillation pathway. These quercetin modulated oligomers of γ-Syn, however were found to be unstable which are SDS-labile and disappear by the end of fibrillation, demonstrated by negligible trace of soluble protein present at 48h of fibrillation. This could also arise due to the reduction in the soluble protein concentration occurred during fibrillation in the presence of quercetin, since complete suppression of fibrillation was not observed even at 50 μM of quercetin concentration. The presence of monomeric peak at 48h of fibrillation in the SEC profile of untreated γ-Syn demonstrates the transient and unstable nature of the γ- Syn species which oscillate between constant association and dissociation during fibril formation. The denaturation of quercetin generated γ-Syn oligomers in the presence of denaturant like SDS, further suggest that quercetin generated oligomers are unstable and are similar in nature to the untreated oligomers of γ-Syn. Unlike the observation made in this study, quercetin has previously been reported to inhibit α-Syn fibrillation by stabilizing both the oligomeric and monomeric forms of α-Syn (Meng et al., 2010). The inhibitory effect of quercetin and the other polyphenols investigated in the previous study has been attributed to the vicinal hydroxyphenyl moiety present in flavonoids that are shown to bind non-covalently to α-Syn and also lead to covalent modifications using the flavonoid quinone moiety that restricts the conformational changes in the natively unfolded α-Syn, thus imparting stability (Meng et al., 2010). One of the important aspects of understanding the underlying

mechanisms of inhibition is to decipher the nature of the modulated species formed under the effect of small molecule inhibitors. The seeding studies reveal that the quercetin generated species do not act 106 as templates for fibril polymerization and thus are off-pathway in nature (Figure 11). The kinetic parameters i.e. lag time (tlag) and apparent rate of fibrillation (kapp) estimated for the non-seeded, γ-Syn seeded and quercetin treated seeded pathway reveal that the quercetin treated γ-Syn seeds exhibit a tlag and kapp intermediate between non-seeded and γ-Syn seeded kinetics, assuming them to be on-pathway. However, the incomplete suppression of γ-Syn fibrillation in the presence of quercetin and only a marginal difference in the tlag and kapp between the non-seeded and quercetin-treated seeded fibrillation rather suggest the role of residual species of γ-Syn that remain unaffected and thus act as seeds giving the differences in the kinetic parameters of fibrillation. The formation of long mature fibrils with reduced fibrillar yield in the presence of quercetin- generated seeds as seen by TEM images (Figure 12) further substantiate the off-pathway nature of the quercetin-generated species. Structural characterization of γ-Syn in the presence of quercetin by far-UV CD analysis both under native and fibrillating conditions reveal that the overall secondary structure of γ -Syn in the presence of quercetin remains unaffected during fibrillation. The structural transition of natively unfolded γ-Syn to the characteristic β-sheet conformation remain unaffected even in the presence of quercetin (Figure 13B) but interestingly as revealed by ANS binding assay the γ-Syn species were observed to maintain an overall reduced hydrophobicity in the presence of quercetin during fibrillation (Figure 14). The reduced ANS intensity in the presence of quercetin during fibrillation could be explained by the formation of oxidized quercetin that is formed upon prolonged incubation during fibrillation, as also reported previously for α-Syn (Zhu et al., 2013), interacts with amine side chains of γ-Syn and increases the hydrogen- bonding probability by increasing polarity and thus lowering the surface hydrophobicity. The overlapping ANS spectra both in the presence and absence of quercetin at 8h of fibrillation (Figure 14B) and then subsequent reduction in the ANS intensity with increasing time of fibrillation (Figure 14C to E) indicate the time- dependent oxidation of quercetin after prolonged incubation (after ~20h), which in turn results in reduced surface hydrophobicity. The hydrophilic nature of quercetin as well as quinone, which is the oxidized form of quercetin, as reported to form multiple hydrogen bonds with α-Syn and thus impart surface hydrophilicity (Zhu et al., 2013), could also be a possible mechanism that play role in inhibition of γ-Syn fibrillation by quercetin. The presence of strong covalent binding interactions between quercetin and γ-Syn is also supported by the steady-state fluorescence and isothermal titration calorimetry (Figure 15 and 16 respectively). Quercetin binds with a 1:1 binding ratio with γ-Syn with an association constant (ka) of 106M-1 at 37°C. An increase in the binding affinity with an 107 increasing temperature, except at 45°C, as shown in Table III, reveal a complex formation between quercetin and γ-Syn with a highest affinity at 37°C. A previous report on quercetin effect of α-Syn fibrillation demonstrate the binding interaction between the ortho-dihroxyl group in quercetin and α-Syn, suggesting the ortho-dihydroxyl group as the key structure that play role in fibril inhibition (Zhu et al., 2013). Several reports have suggested that the ordered prefibrillar oligomer, or protofibrils formed during the fibrillation are mainly responsible for cell death and that the mature fibrils which are end products of fibrillation are neuroprotective (Bucciantini et al., 2002; Caughey &Lansbury Jr, 2003; Ferreira et al., 2007). Investigations on the cytotoxic effect of quercetin generated γ-Syn species on breast cancer (MCF-7) and neuroblastoma (SH-SY5Y) cells reveal a differential effect on these cells as also observed in the presence of EGCG (Section). The difference in the toxicity could arise due to the pharmacological activities of quercetin that affect the signalling pathways differentially in neurons compared with malignant cells, governing cell death or survival in a cell type and metabolism specific manner (Dajas, 2012). The study shows that lone quercetin in the absence of γ-Syn is significantly toxic to both MCF-7 and SH-SY5Y cells but in MCF-7 cells, a 50 % reduction in the viability in the presence of 50 μM quercetin is observed. The doses of quercetin in the range of 3- 50 μM have also been reported to exhibit anti-proliferative properties (Dajas, 2012), however in the case of neuronal cells, only 1-10μM was sufficient to induce cytotoxicity in pure neuronal cells (Ossola et al., 2009). Application of quercetin to the neuronal cell is reported to readily permeate the cells and upon reaching the nucleus increasingly interact with the cytoplasmic and nuclear molecules that give rise to multiple cellular targets responsible for its therapeutic as well as toxic properties (Dajas, 2012). As shown in Figure 17, the viability of MCF-7 cells was only marginally increased in the presence of quercetin at 0h of fibrillation, while the viability in the presence of quercetin generated fibrils at 48h was significantly reduced, clearly demonstrating the toxic effects of the quercetin treated fibrils of γ-Syn. The reduction in cell viability in the presence of γ-Syn generated

species formed in the presence of quercetin however majorly could be attributed to the toxic effect of quercetin alone rather than that incurred by γ-Syn species. The data shows that the reduction in cell viability is much pronounced when quercetin is present alone than when quercetin is present along with γ-Syn fibrils. This leads to a speculation that γ-Syn fibrils bound with quercetin may prevent quercetin from permeating the cell membrane and thus prevent acute toxicity. The complex behaviour of quercetin thus needs to be carefully investigated. Contrary to the observations made in the presence of MCF-7 cells, the 25–35-induced toxicity in SH-SY5Y cells", Acta Pharmacologica Sinica, 2/2008">viability of SH-SY5Y cells at 24h 25–35-induced toxicity in SH-SY5Y cells", Acta Pharmacologica Sinica, 2/2008">of fibrillation was increased in the presence of quercetin generated species (Figure 18A), suggesting that the γ-Syn oligomers formed at 24h of fibrillation as observed in SEC profiles (Figure 9) were neuroprotective. The fibrils of γ -Syn formed in the presence of quercetin at 48h of fibrillation were however found to be neurotoxic. The disaggregated γ-Syn species formed under the effect of quercetin (Figure 18B) on the other hand were found to be neutral species that did not affect the toxicity caused by the untreated γ-Syn fibrils. The study thus provides alternate evidence where the mature fibrils formed at the end of fibrillation in the presence of small molecule inhibitor is more toxic than its oligomeric counterparts and the disaggregated end products are neutral species found to be equally toxic to the untreated fibrils of protein. Chapter 3.3 Effect of Silibinin on the Structure and Aggregation of γ-Synuclein 1. Background Silibinin (Sb), also anonymously called as silybin is the main component of the silymarin complex comprising mostly of polymeric and unoxidized polyphenolic compounds. Silymarin is the active component of the plant of Silybum marianum (milk thistle). For over 2000 years, due to the strong anti- Chemical Structure of Silibinin oxidant properties, the seeds of this plant have been used to treat plethora of diseases related to liver disorders including hepatitis, cirrhosis, and jaundice and also protect liver from various toxins like drugs and alcohol thus being a strong hepatoprotectant (Křen & Walterova, 2005). Apart from the hepatoprotective activities of silibinin, the neuroprotective and anticancer properties of Sb have also emerged extensively. The promising effects of Sb as an anticancer agent is attributed to its antioxidant property where it is reported to protect the tissues from the oxidative damage caused by several chemotherapeutic agents used simultaneously (Křen & Walterova, 2005). Sb is established to suppress proliferation of wide range of tumours such as colon, prostrate, breast, ovary etc. and also act as a strong chemoprotective agent against various tumour promoters by multiple pathways and mechanisms reported previously (Agarwal et al., 2006). The neuroprotective effects of Sb are demonstrated by its anti-amyloidogenic activities on many amyloid forming proteins such hIAPP (Cheng et al., 2012; Young et al., 2013), Aβ-peptide (Yin et al., 2011) etc. Sb also imparts neuroprotection in several ways such as, protecting primary hippocampal neurons against oxidative stress (Kittur et al., 2002), protecting against drug induced neuropathy (Mannelli et al., 2012), preventing Alzheimer's disease by inhibiting acetylcholinesterase and modulating the synaptic deficits to prevent the impairment in learning and memory (Duan et al., 2015), neuroprotection against Parkinson's disease by attenuating motor deficit and loss in the dopaminergic neurons (Y. Lee et al., 2015), protect central nervous system (CNS) against oxidative stress in a state of diabetes (Marrazzo et al., 2011), acting as a strong β- breaker by inhibiting fibrillation of polygalacturonase which is an all β-protein (Chinisaz et al., 2014) etc. While the antiamyloidogenic effect of Sb on fibrillation pathway of Aβ-peptide is established, the direct effect of silibinin on any of the synucleins (α-, β-, γ-Syn) is not reported till date, ruling out the direct evidence of protective effects of silibinin against Parkinson's disease. 111 The study presented here demonstrates the effects of Sb on the fibrillation pathway of γ- Syn and elucidates the underlying mechanism of interaction as well as the cytotoxic effects of the Sb modulated γ- Syn species on neuronal (SH-SY5Y) and breast cancer (MCF-7) cells respectively. The data reveals the absence of any antiamyloidogenic activity of Sb on γ- Syn fibrillation at the concentrations of Sb used in the study. A weak binding interaction in the range of ~10mM, along with differential cytotoxicity for MCF-7 and SH-SY5Y cells is further established. The results demonstrate that although γ- Syn fibrillation is not inhibited in the presence of Sb, the fibrillation pathway is still modulated by Sb to form species that imparts altered cytotoxicity. The observations thus suggest that the mode of action of polyphenols or such small molecule modulators are not completely universal and possibly are governed by the specific protein-ligand interactions that regulate the propensity of the fibrillation pathway to become inhibited or more accelerated under the effect of such modulators. This in turn demands a need for detailed in-depth investigations on the effects of polyphenols on various classes of amyloid forming - pathogenic proteins before being used as therapeutics. 2. Results 2.1 Effect of Silibinin on the fibrillation kinetics of γ-Syn 2.1.1 Thioflavin T assay The fibrillation

kinetics of γ-Syn studied in the presence of increasing concentration of Sb (5 – 50 μM) by ThT assay showed no decrease in the ThT fluorescence in the presence of Sb as otherwise observed for the other two polyphenols, EGCG and quercetin (chapter 3.1 and 3.2 respectively). In the presence of 25 and 35 μM of Sb, although the final ThT fluorescence was found to be reduced, the decrease in the ThT fluorescence was not concentration – dependent and the overall kinetics remained unaffected in the presence of all the concentration of Sb. This suggests an absence of γ-Syn inhibition by Sb in the concentration range between 5-50 μM. Figure 1. Fibrillation kinetics of γ -Syn in the presence of increasing concentration of Silibinin by Thioflavin T assay. Monomeric γ -Syn was incubated in the presence of increasing concentration of silibinin (5- 50μM) under fibrillating conditions and the ThT fluorescence was recorded at regular interval of time. The overlapping ThT spectra in the presence of Sb show absence of fibrillation inhibition by Sb. The error bars represent the ±SD (n=3). 2. 1.2 Transmission Electron Microscopy of γ -Syn fibrils formed in the presence of Silibinin The morphology of γ-Syn fibrils formed in the absence and presence of Sb was further studied by TEM analysis. The untreated γ-Syn formed dense network of mature fibrils as also observed earlier. In the presence of increasing concentration of Sb (20 and 30μM), similar networks of mature fibrils were observed, indicating absence of fibrillation inhibition by Sb as also observed in ThT assay. At 50 μM Sb, although mature fibrils were observed, the morphology of the fibrils appeared different than the mature thick fibrils and they were found to be thin and disintegrated, lacking intricate fibrillar network. This suggest that although the fibrillar yield is not significantly reduced in the presence of even 50 μM of Sb, the change in the fibrillar morphology suggest a possible inhibition at concentrations higher than 50 μM, making it a weak modulator of γ-Syn fibrillation. Figure 2. Morphology of γ -Syn fibrils formed in the presence of Silibinin visualized by transmission electron microscope. TEM images of γ-Syn fibrils formed upon saturation (end of fibrillation) in the absence of Sb (A, B) and in the presence of 20μM (C, D), 30 μM (E, F) and 50 μM (G, H) Sb respectively. Scale bar: 100nm. 2.2 Size-exclusion chromatography of γ-Syn species formed in the presence of Silibinin In order to investigate as how Sb modulate the γ-Syn population in the absence of fibrillation inhibition, size-exclusion chromatography of γ-Syn species formed during fibrillation in the presence of Sb was carried out. The SEC profile of the soluble fraction of γ-Syn species formed in the presence of Sb during fibrillation showed a time-dependent depletion of both the oligomeric and monomeric species of γ-Syn with increased heterogeneity. This suggest that majority of monomeric γ-Syn is converted into insoluble fibrils which are removed during centrifugation leaving only trace of soluble γ-Syn species present in the population. Monomer Oligomer Figure 3. Size-exclusion chromatography of γ-Syn species formed in the presence and absence of Silibinin. The SEC profile of γ-Syn species formed in the presence of Sb at regular time-intervals during fibrillation. 2.3 Effect of Silibinin on the structure of γ -Syn under both native and fibrillation conditions The effect of Sb on the structure of γ -Syn both under native and fibrillating conditions was monitored by far-UV CD analysis and ANS binding assay. 2.3.1 Far-UV CD analysis of γ-Syn in the presence of Sb The far-UV CD spectra of γ-Syn in the absence and presence of Sb both under native and fibrillating conditions is shown in Figure 4A and B respectively. Under native conditions, in the presence of Sb an increase in the negative ellipticity at 200 nm is observed indicating the unfolding of the residual structure of γ-Syn by Sb. During fibrillation at 24 and 48h, an increase in the negative ellipticity at ~218 nm was observed both in the presence and absence of γ-Syn, indicating the formation of characteristic β-sheet structure. The negative ellipticity at ~218 nm was increased in the presence of Sb as compared to the untreated γ-Syn, further indicating an increased β-sheet forming propensity in the presence of Sb. A) B) Figure 4. Far-UV CD spectra of γ -Syn in the presence of Silibinin both native and fibrillating conditions. (A- B) The far-UV CD of γ-Syn in the presence and absence of Sb both under native and fibrillating conditions respectively were monitored at 25 °C using a cuvette of 1mm path length. A) Far-UV CD spectra of γ-Syn (0. 3 mg /ml) dissolved 20 mM phosphate buffer, pH-7.4 conditions in the presence of increasing concentration of Sb (30 and 50μM), monitored under native conditions. B) Far- UV CD spectra of γ-Syn (0 .3 mg/ml) in the presence of increasing concentrations of Sb (30 and 50μM) monitored at time- intervals of 24h (left panel) and 48h (right panel) during fibrillation showing a shift in the negative ellipticity from 200 nm to ~ 218 nm both in the absence and presence of Sb, depicting the formation of characteristic β- sheet conformation. 2.3.2 ANS binding assay The effect of Sb on the exposed surface hydrophobicity of γ-Syn was assessed by ANS binding assay both under native and fibrillating conditions. Binding of ANS to γ-Syn under native conditions both in the absence and presence of Sb showed overlapping spectra with an emission at ~520 nm (Figure 5A). At 24h of fibrillation (Figure 5B, left panel) an increase in the ANS intensity with a characteristic blue-shift

at ~ 480 nm was observed in the untreated γ -Syn. In the presence of Sb, compared to the untreated γ -Syn an increase in the ANS intensity with the similar blue - shift emission was seen. The increase in the ANS intensity was found to decrease with an increasing concentration of Sb with the ANS spectrum in the presence of 50 μM Sb overlapping with the spectrum of untreated γ-Syn. At the maturation stage of fibrillation (48h), the ANS intensity of untreated γ-Syn was further increased which was found to decrease in the presence of Sb in a concentration-dependent manner (Figure 5B, right panel). Interestingly, in the presence of 50 μM Sb, although the emission intensity was reduced, the spectrum was further blue-shifted to ~456 nm. The results indicate an overall increase in the surface hydrophobicity of γ-Syn in the presence of Sb and altered fibrillar surface properties. A) Figure Continued… B) Figure 5. ANS binding analysis of γ -Syn in the absence and presence of Silibinin. A) ANS spectra of γ -Syn in the presence of increasing concentration of Sb (5-40μM) under native conditions showing overlapping ANS spectra. B) ANS binding to γ -Syn in the presence of Sb (10, 30 and 50μM) under fibrillating conditions (24h and 48h) showing characteristic blue-shifted emission (black arrows) at 480 nm. 2.4 Binding interaction between γ-Syn and Silibinin The binding interaction between Sb and γ-Syn was further studied by fluorescence quenching, van't- Hoff plot and isothermal titration calorimetry. 2.4.1 Effect of Sb on intrinsic tyrosine fluorescence of γ-Synuclein The effect of Sb on the intrinsic tyrosine fluorescence in γ-Syn was studied by monitoring the changes in the tyrosine fluorescence upon continuous titration of γ-Syn with an increasing concentration of Sb carried out at different temperatures. As shown in Figure 6A, titration of γ-Syn with an increasing concentration of Sb showed a concentration-dependent decrease in the ThT fluorescence, indicating quenching of tyrosine fluorescence and interaction between Sb and γ-Syn. Titration of γ-Syn with an increasing concentration of Sb was accompanied by a red-shift in the emission spectra of tyrosine (Figure 6A (i) and (ii)) around 358 nm, indicating the shift of tyrosine to a more polar environment in the presence of Sb. Using the Stern-Volmer quenching plot the bimolecular quenching constant (kq) was calculated to be more than the diffusion-controlled value (>1010M-1s-1) indicating a static quenching mechanism and thus complex formation between γ-Syn and Sb (Figure 6A (iii)). The binding affinity (Ka) between γ-Syn and Sb was estimated by using the modified Stern-Volmer equation (Figure 6A (iv)). Sb was found to bind to γ-Syn with a weak binding interaction with a dissociation constant in the range of ~10 mM, suggesting the role weak non-covalent interactions between Sb and γ-Syn. The binding interaction between Sb and γ-Syn were also studied at different temperatures (15, 25 and 45°C) and the plots giving their bimolecular quenching constant (kq) as well as association constant (Ka) are shown in Figure 6 B to D respectively. The binding parameters estimated at different temperatures from the Stern-Volmer plot is summarized in Table I. The binding affinity was found to decrease with an increasing temperature indicating the role of non-covalent interactions between Sb binding to γ-Syn. A) (i) (ii) (iii) (iv) Figure continued… B) C) Figure continued… D) Figure 6. Intrinsic tyrosine fluorescence of γ-Syn in the presence of increasing concentration of Silibinin. A) (i) Steady-state fluorescence showing quenching of intrinsic tyrosine fluorescence of γ- Syn (0.3mg/ml) continuously titrated with an increasing concentration of Sb (2-30μM) at 37°C with a red-shift in the emission (black arrows), (ii) Plot of emission maxima of tyrosine (λmax) with respect to increasing concentration of Sb show a concentration –dependent shift in the emission wavelength with a red-shifted emission. (iii) Stern-Volmer plot of F0/F vs [Q] (Sb concentration) giving the value of 'bimolecular quenching constant' (kq) and (iv) Modified Stern-Volmer plot of log (F0-F)/F against log[Q] giving the binding affinity or association constant (Ka). B to D) (left panel) Plot of F0/F vs [Q] and (right panel) plot of log (F0-F)/F against log [Q] at 15, 25 and 45°C respectively. Table I. Binding Parameters calculated from Stern- Volmer Plot Temp. (K) kq× 1013M-1s-1 Ka × 104 M -1 n ΔG° (kJmol-1) ΔH° (kJmol-1) ΔS° (JK-1mol-1) 288.15 1.20 2.81 0.9~ 1 -24.6 298.15 1.75 2.39 0.8~ 1 -24.8 -19.1 19.28 310.15 1.16 1.8 0.9~ 1 -25 318.15 1.19 1.3 0.8 ~ 1 -25.2 2.4.2 Mode of binding interaction by using van't-Hoff plot An insight into the binding mode between γ-Syn and Sb was gained by estimating the free energy of binding (ΔG°), enthalpy (ΔH°) and entropy (ΔS°) by analyzing the temperature dependence of the binding constants using van't-Hoff equation and the binding constants obtained for γ-Syn and Sb from the modified Stern-Volmer plot were used for the analysis. The binding parameters of the γ-Syn-Sb complex at four different temperatures obtained by van't –Hoff plot is shown in Figure 7. The negative enthalpy (ΔH° = -19.1kJ mol-1) and a small positive entropy (ΔS° = 19.28 JK-1mol-1) indicate that binding of Sb to γ-Syn is a spontaneous reaction driven by electrostatic interactions. The negative free energy is contributed by a large negative enthalpy further suggesting role of van der Waals and hydrogen bonding interaction between Sb and γ-Syn. Figure 7. van't-Hoff plot showing the temperature

dependence of the binding constants. The data is fitted to a least-square regression line (black line). 2.4.3 Isothermal titration calorimetry of γ-Syn binding to Silibinin The thermodynamic parameters of Sb binding to γ-Syn were further characterized by ITC analysis. The ITC binding isotherm as shown in Figure 8, a sequential binding of γ-Syn to Sb with a negative cooperativity (K2 < K1) and a moderate to weak binding interaction between Sb and γ-Syn. The negative enthalpy with negligible entropy indicates an enthalpically driven reaction and the role of non-covalent interactions between Sb and γ-Syn. Figure 8. Isothermal titration calorimetry of silibinin binding to γ-Syn. The reaction was carried out at 37 °C with γ-Syn and Silibinin ratio of 1:20. Upper panel: A raw data plot of heat flow against time for titration of Sb into γ-Syn and lower panel: Plot of normalized heat released as a function of ligand concentration for the titration. The blue solid line shows the two-site sequential -fit for the obtained data. Table II. Thermodynamic parameters of Silibinin binding to γ-Synuclein Thermodynamic parameters Values K1 (M-1) 5.72 x 105 ± 9.8 x 104 K2 (M-1) 1.03 x 103± 0.001 ΔH1 (kcal/mol) -3.20 ± 0.03 ΔH2 (kcal/mol) -7.85 ± 0.004 ΔS1 (cal/mol/deg) 15.6 ΔS2 (cal/mol/deg) -12.6 2.5 Cytotoxic effects of Quercetin generated γ-Synuclein species studied by MTT assay In the absence of fibrillation inhibition by Sb, it was important to investigate if the nature of the γ -Syn fibrils formed in the presence of Sb were different from the untreated fibrils of γ- Syn and if even in the absence of inhibition, the γ-Syn fibrillation pathway was modulated by Sb. The MTT assay was carried out on both MCF-7 and SH-SY5Y cells to investigate the cytotoxic effects of γ -Syn species formed in the absence and presence of Sb. 2.5.1 MTT assay on MCF-7 cells The cytotoxic effects of γ-Syn species formed at different intervals (0, 24 and 48h) during fibrillation in the presence of Sb are shown in Figure 9. At 0h and 48h of fibrillation, the viability of MCF-7 cells in the presence of Sb was found to decrease with an increasing concentration of Sb. The γ-Syn species formed in the presence of 50 μM Sb were found to reduce the viability by almost 50 % and ~20% with respect to untreated cells and only γ-Syn treated cells respectively. Contrastingly, at 24h of fibrillation, the viability was significantly increased in the presence of γ-Syn species formed in the presence of 50 μM Sb. This suggests that the γ-Syn species (monomers and fibrils) formed in the presence of Sb are overall toxic to MCF-7 cells and the increased viability in the presence of 50 μM Sb at 24h indicate the modulation of oligomeric species of γ-Syn. MCF-7 Figure 9. MTT assay showing cytotoxic effects of γ -Syn species formed in the absence and presence of Silibinin on MCF-7 cells. At 0h of fibrillation, MTT assay show a concentration-dependent increase in cytotoxicity in the presence of Sb (***p < 0.0004, with respect 125 to untreated cells). At 24h, a significant increase in the viability in the presence of 50μM Sb is seen (****p < 0.0001, with respect to untreated cells). At 48h of fibrillation, a significant reduction in cell viability with an increasing concentration of Sb is seen (****p < 0.0001, compared to untreated cells). The statistical analysis was done using one-way ANOVA. The error bar represents ±SD (n=5). 2.5.2 MTT assay on SH-SY5Y cells The effects of γ-Syn species on the viability of SH- SY5Y cells are shown in Figure 10. The 25–35-induced toxicity in SH-SY5Y cells", Acta Pharmacologica Sinica, 2/2008">viability of SH-SY5Y cells at 0h remained unaffected in the presence of Sb treated γ-Syn species. While the viability was marginally reduced in the presence of Sb treated γ-Syn fibrils at 48 h of fibrillation, the viability at all the concentrations of Sb for 24h species was significantly increased that rescued the cells from complete toxicity, indicating variable effects of Sb on different species of γ-Syn. SHSY-5Y Figure 10. MTT assay showing cytotoxic effects of γ -Syn species formed in the absence and presence of Silibinin on SH-SY5Y cells. At 0h of fibrillation, the viability of cells in the presence of Sb treated cells remains unaffected. MTT assay show an increased viability in the presence of Sb treated γ-Syn species at 24h of fibrillation (****p < 0.0001, with respect to untreated cells). At 48h of fibrillation, the viability was marginally affected in the presence of Sb irrespective of Sb concentration (*p < 0.05, compared to untreated cells). The statistical analysis was done using one- way ANOVA. The error bar represents ±SD (n=5). 3. Discussion The medicinal and therapeutic properties of silibinin have been widely established for various liver diseases as well as increasingly for neurodegenerative diseases and cancer. Although Sb has been reported to inhibit fibrillation of some amyloid forming proteins such as Aβ-peptide (Yin et al., 2011), polygalacturonase (Chinisaz et al., 2014) and hIAPP (Cheng et al., 2012; Young et al., 2013), the direct effect of Sb on fibrillation pathways of many other amyloid- forming proteins, such as Synucleins is unavailable. This study investigates the anti-amyloidogenic effects of Sb on the γ-Syn fibrillation pathway and observes an absence of any fibrillation inhibition by Sb. In a previous report, Sb was found to inhibit fibrillation at a higher concentration range between 50 – 250 μM, with best inhibitory concentration of ~200 μM (Chinisaz et al., 2014), a much higher concentration than that used in this study. This suggests that Sb affects the fibrillation pathways only when present at a molar excess than the fibril

forming protein thus indicating Sb to be a weak small-molecule modulator as compared to other polyphenols like EGCG which bring complete suppression even at sub-stoichiometric concentrations (Bieschke et al., 2010) and as observed in chapter 3.1. The change in the fibrillar morphology of γ -Syn in the presence of 50 μM Sb and reduction in the overall fibrillar yield, as observed by TEM (Figure 2) gives rise to the possibility of inhibition of γ-Syn fibrillation pathway by Sb at a concentration higher than that used in the study (> 50 μM) A sub-stoichiometric concentration of Sb was used (5 – 50 μM) in order to compare the anti- amyloidogenic activities of the three polyphenols (EGCG, quercetin and Sb) used in the present study. Investigation on the effects of Sb on the γ-Syn structure reveal a characteristic gain in the β-sheet structure indicating fibril formation and thus absence of inhibition (Figure 4). The ANS binding assay suggest that the fibrils formed in the presence of Sb have altered surface hydrophobicity (Figure 5) which possibly in turn gives rise to altered fibril morphology (Figure 2). The decrease in the ANS intensity with an increasing concentration of Sb at 48h of fibrillation could possibly occur due to the inaccessibility of ANS to its binding sites on the ordered fibrillar structures also observed previously (Bolognesi et al., 2010), and demonstrated in this study by a pronounced blue-shifted emission of ANS at ~456 nm in the presence of 50μM Sb. The mode of binding interaction between Sb and γ-Syn as studied by fluorescence quenching, van't – Hoff plot and ITC analysis (Figure 6, 7 and 8 respectively) establish a weak binding affinity with an association constant (ka) of ~104M-1. Binding of Sb to γ-Syn increases the polarity around tyrosine which is clearly demonstrated by the red-shift emission at an increasing concentration of Sb, an effect also observed for Sb binding to human serum albumin reported previously (Maiti et al., 2008). Sb forms a weak binding complex with γ- Syn and the decrease in the binding affinity with an increasing temperature further establishes the role of van de Waals and hydrogen bonding interactions between Sb and γ-Syn. The oligomeric and protofibrillar species of amyloid- forming proteins are although increasingly being evidenced to be more toxic than the mature fibrils (Caughey & Lansbury Jr, 2003), the ability of mature fibrils to impart toxicity under the effects of small molecule modulators cannot be ruled out. As revealed by MTT assay, the viability of MCF-7 cells was significantly reduced in the presence of Sb treated monomers as well as the mature fibrils (Figure 9), while the viability of SH-SY5Y cells remain unaffected with a marginal increase in the viability in the presence Sb generated fibrillar species, again demonstrating differential toxicity as observed for EGCG and quercetin (Sections). Interestingly, the protective effect of Sb generated γ-Syn oligomers formed at the 24h of fibrillation on both the MCF-7 and SH- SY5Y cells suggest that Sb modulates the oligomeric species of γ-Syn that render them less toxic. The variable effects of Sb generated species on both the MCF-7 and SH-SY5Y cells indicate species specific interaction of Sb with γ-Syn that govern the toxic characteristics of these species and possibly involve a complex mechanism that needs to be investigated for better understanding. Chapter 3: Conclusion CONCLUSION Chapter 4 Effect of Polyols on the Structure and Aggregation of γ-Synuclein This chapter is adapted from: 1. Background Among the protective osmolytes, the stabilizing effects of polyol osmolytes (polyhydric alcohols) on the structure, stability and aggregation of globular proteins have been widely established (Gerlsma, 1968; Xie & Timasheff, 1997; Kaushik & Bhat, 1998; Mishra et al., 2005; Tiwari & Bhat, 2006; Vagenende et al., 2009; Khan et al., 2017). The polyols have been reported to impart protective effects by increasing thermal stability (Back et al., 1979; J. C. Lee & Timasheff, 1981) as well as by increasing the surface tension of the aqueous solutions thus facilitating protein folding (Kaushik & Bhat, 1998; Tiwari & Bhat, 2006). A linear relationship between the increasing hydroxyl groups (-OH group) in the polyols contributing to the excluded volume effect with the increasing thermal stability, (Gerlsma, 1968; Fujita et al., 1982) increasing surface tension and thus increased protein stability (Kaushik & Bhat, 1998; Tiwari & Bhat, 2006) has also been established previously. Additionally, the polyols have also been demonstrated to induce a native-like structure from the denatured state by process of cooperative folding (Devaraneni et al., 2012) and also inhibit aggregation as well as promote refolding of a highly aggregation prone protein, citrate synthase (Mishra et al., 2005). While the effects of osmolytes on the folding and aggregation of globular proteins is well established, the understanding of the osmolyte-mediated regulation of intrinsically disordered proteins with respect to their aggregation and fibrillation is not very clear. In this study the effect of the series of polyols comprising ethylene glycol, glycerol, erythritol, xylitol and sorbitol with an increment of single hydroxyl groups from 2 to 6 respectively, on the structure and aggregation of γ-Syn is investigated. The physicochemical properties of these polyols in the aqueous solution and the experimental transfer free energies of the amino acid chains and the peptide backbone have also been estimated based on the values reported previously. The study observes varying effects of polyols on γ-Syn aggregation ranging from no effect

to aggregation as well as suppression depending on the polyol concentration. The experimental evidences suggest that the polyols affect γ-Syn nucleation and reduces overall fibrillation, however unlike in the case of globular proteins, a perfectly linear relationship between the increasing –OH group in the polyols and their effects on structure and aggregation has not been evident. Together, the study suggests that the effect of polyol osmolytes on the stability and aggregation of IDP is much complex than their effect of the globular proteins. It is further proposed that the modulatory effects of polyols on IDPs are largely governed by the balance between the favourable solvent – side chain and unfavourable peptide backbone-solvent interaction. The chemical structure of the polyols used in the study is shown below: Ethylene glycol Glycerol Erythritol Xylitol Sorbitol 2. Results 2.1 Effect of polyols on the fibrillation kinetics of γ-Syn 2.1.1 Thioflavin T assay The effect of polyol series with an increment of single hydroxyl groups from 2 to 6 in ethylene glycol (EG), glycerol, erythritol, xylitol and sorbitol respectively on the fibrillation kinetics of γ-Syn was monitored using ThT assay. γ-Syn was incubated in the presence of an increasing concentration of polyols and the ThT fluorescence was recorded at regular intervals as a function of time. As shown in Figure 1A, in the presence of increasing concentration of EG (0.5 – 7.5M), the ThT fluorescence increases initially at an intermediate concentrations and diminishes at a concentration > 4.5M. The change in the ThT fluorescence with respect to increasing concentration of EG is depicted in the Figure 1A (right panel), where suppression of fibrillation is observed at a higher concentration of EG. In the presence of an increasing concentration of glycerol (0. 5 – 4.5M), a concentration – dependent decrease 132 in the ThT fluorescence was observed indicating suppression of fibrillation (Figure 1B). While no noticeable difference in the ThT fluorescence in the presence of erythritol (0.5 – 2.5M) and xylitol (0.5 – 3M) was observed (Figure 1C and D respectively), the ThT fluorescence was significantly reduced in the presence of increasing concentration of sorbitol (0.5 – 2M) thus indicating suppression of fibrillation by sorbitol (Figure 1E). As shown in Figure 1F, the ThT fluorescence measured at an equimolar concentration of polyols (2M) showed a reduced ThT fluorescence in the presence of only glycerol and sorbitol, while the effects of other polyols were observed to only marginally to negligibly affect the fibrillation pathway of γ-Syn. This suggests that among the polyols, glycerol and sorbitol inhibits γ-Syn fibrillation. A) B) C) D) Figure Continued… E) F) Figure 1. Fibrillation kinetics of γ -Syn in presence of increasing concentrations of polyols by Thioflavin T assay. The changes in the ThT fluorescence with :(left and right) an increasing time of fibrillation and increasing concentration of polyols (A to E: EG, glycerol, erythritol, xylitol and sorbitol) respectively is shown. F) The relative ThT fluorescence at equimolar concentration (2M) of polyols. The ThT was excited at 445 nm and the emission maximum was monitored at 480 nm with an excitation and emission slit width of 5 nm. The error bars show ±SD (n=3). 2.1.2 Kinetic parameters of γ-Syn fibrillation in the presence of polyols In order to further understand the effect of polyols on the fibrillation pathway of γ-Syn, the kinetic parameters of fibrillation, i.e. the lag time (tlag) and apparent rate of fibrillation (kapp) was estimated using the equation described previously (Ban et al., 2003). Due to the absence of sigmoidal aggregation curve and poor fit quality, the effect of EG on the kinetic parameters of γ-Syn fibrillation could not be estimated. As shown in Figure 2A, a concentration- dependent increase in the tlag and a simultaneous decrease in the kapp were observed in the presence of an increasing concentration of glycerol. This suggests that glycerol suppresses γ-Syn fibrillation by inhibiting γ-Syn nucleation and retarding fibril polymerization. In the presence of erythritol (Figure 2B), an increase in the lag time with an increasing erythritol concentration was observed. The apparent rate of fibrillation (kapp) although showed an overall increase in the trend, a direct dependence to the increasing erythritol concentration was not established. The increase in the lag time in the presence of erythritol also suggest the retardation of nucleation but the faster rate of fibrillation on the contrary suggests faster fibril polymerization, indicating a dual effect of erythritol on γ-Syn fibrillation. As shown in Figure 2C, an inverse relationship between the lag time and rate of fibrillation was observed in the presence of xylitol, as also observed in the case of glycerol. The increased lag time and reduced rate of fibrillation in the presence of xylitol also suggest stabilization of the natively unfolded monomer of γ-Syn that retards nucleation as well as stabilization of the protofibrillar species of the pathway that reduces the rate of fibrillation. Interestingly, as opposed to the observation made in the ThT fluorescence data that demonstrates suppression of γ-Syn fibrillation by sorbitol (Figure 1E), the kinetic parameters showed an initial increase in the lag time at lower concentrations which further decreased with an increasing sorbitol concentration (>0.5M), demonstrating sorbitol mediated faster nucleation of γ-Syn monomers at higher concentrations. Also, a concentration dependent increase in the rate of fibrillation (kapp) in the presence of sorbitol was observed, suggesting

accelerated polymerization (Figure 2D). Figure 2E, shows the comparison between the relative lag times of γ-Syn fibrillation at equimolar concentration (2M) of the polyols. The data demonstrated an inverse relationship between the increasing –OH groups in the polyols and the lag time of fibrillation, where the lag time of fibrillation was observed to decrease with an increasing –OH groups. This suggests that polyols with higher number of –OH groups exclude strongly from the protein vicinity and facilitate γ-Syn nucleation, required for fibrillation. A) B) C) D) E) Figure 2. The kinetic parameters of γ-Syn fibrillation. The relationship between the lag time (tlag) and an apparent rate of fibrillation (kapp) of γ-Syn fibrillation in the presence of increasing concentration of polyols (A to D: glycerol, erythritol, xylitol and sorbitol respectively) is shown. E) The bar graph showing the comparison between the lag times of fibrillation in presence of equimolar concentration (2M) of polyols. An increased lag time in the presence of glycerol and erythritol (****p < 0. 0001 and **p<0. 005 with respect to control in presence of glycerol and erythritol, respectively) is seen. In the presence of xylitol, with respect to control, no significant difference in the lag time was observed and in the presence of sorbitol, the lag time was marginally, yet significantly reduced (*p< 0.05). The statistical analysis for the control and the polyol treated samples were analyzed using unpaired t-test. The data further show significant reduction in the lag time of fibrillation with the increasing –OH group in the presence of 2M polyols (####p< 0.0001, analyzed by one-way ANOVA). The error bars show ±SD (n=3). 2.1.3 Light scattering by γ-Synuclein species formed during fibrillation in presence of polyols: The effect of polyols on the aggregation propensity of γ-Syn was also validated by Rayleigh light scattering. γ -Syn was incubated in the presence of an increasing concentration of polyols and the light scattering was monitored at regular intervals during fibrillation. As shown in Figure 3, an overall reduction in the scattering intensity in the presence of all the polyols were observed, indicating an overall reduced fibrillation as well as aggregation in the presence of polyols. In the presence of EG and glycerol (Figure 3A and B respectively) an early increase in the scattering intensity indicates the formation of amorphous aggregates in the earlier stages of the fibrillation pathway. The delayed increase in the scattering intensity 138 in the presence of xylitol indicates slowed aggregation as also validated by the increased lag time and reduced rate of fibrillation (Figure 2C). The significant decrease in the scattering intensity in the presence of sorbitol (Figure 3E) further validates the reduced fibrillation as observed by reduced overall fluorescence of ThT (Figure 1E). A) B) C) D) Figure Continued… E) Figure 18. Light scattering by γ-Syn species formed in the presence and absence of polyols during fibrillation. The change in the scattering intensity with respect to the increasing concentration of polyols (A to E: EG, glycerol, erythritol, xylitol and sorbitol, respectively was monitored at regular time interval (0h, 4h, 8h, 12h, 24h, 30h and 48h) during fibrillation. 2.1.4 Morphology of the γ-Syn fibrils formed in the presence of polyols visualized by transmission electron microscopy (TEM): The morphology of the γ -Syn fibrils formed in the presence of lower and higher concentrations of polyols were analyzed by TEM studies. As shown in Figure 4, the overall fibrillar yield in the presence of all the polyols was found to be reduced as compared to the fibrils formed by the untreated γ-Syn. In the presence of high concentration of ethylene glycol (7M), a significant disappearance of the mature fibrils along with the presence of disintegrated small structures was observed corresponding to the reduced ThT fluorescence observed in Figure 1A. In the presence of glycerol and erythritol, along with reduced fibrillar yields, amorphous aggregates were also seen adhering to the fibrillar surface. In the presence of xylitol and sorbitol short and broken fibrils were also observed. Thus the TEM images were in accordance with the overall reduced scattering observed in the presence of polyols (Figure 3). Figure 4. Morphology of γ -Syn fibrils formed in the presence of polyols visualized by transmission electron microscopy .TEM images of γ -Syn fibrils formed upon saturation in the (top to bottom) absence of polyols and in the presence of increasing concentration of EG, glycerol, erythritol, xylitol and sorbitol. (Red arrow) show the formation of amorphous aggregates sticking on fibrillar surface and (black arrows) depict the formation of shorter fibrils in presence of xylitol and sorbitol. A scale bar of 100 nm is shown. 2.2 Effect of polyols on the structure of γ -Syn both under native and fibrillation conditions The effect of polyols on the secondary structure of γ -Syn both under native and fibrillation conditions was also investigated by using far-UV circular dichroism (CD) spectroscopy and ANS binding assay. 2.2.1 Far-UV CD spectroscopy 2.2.1.1 Under native conditions: In order to investigate the effects of polyols on the natively unfolded conformation of γ-Syn under non-fibrillating conditions, the far-UV CD spectra of γ -Syn in the absence and presence of increasing concentration of polyols were recorded (Figure 5A). The untreated γ-Syn showed a large negative ellipticity at ~200 nm and a small value at ~222 nm, characteristic of natively unfolded proteins. In the presence of EG, a concentration

dependent increase in the negative ellipticity at 200 nm as well as 222 nm was observed indicating a partial unfolding of the residual structure of γ-Syn. While no such concentration dependence is observed in the presence of glycerol, with increasing –OH groups in the polyols, the natively unfolded conformation of γ-Syn was found to be stabilized at all concentrations of polyols. In the presence of erythritol a dual effect was observed where at lower concentration, the negative ellipticity at 200 nm was found to increase which further decreased reaching close to that of the untreated γ-Syn, indicating the stabilization of the natively unfolded conformation of γ-Syn at higher concentrations of erythritol. Thus a linear relationship between the increasing –OH groups in the polyols with the increased stabilization of natively unfolded conformation of γ-Syn was established. 2.2.1.2 Under fibrillation conditions: The effect of polyols on the structural transitions of γ-Syn occurred during aggregation both in the absence and presence of polyols was further investigated by incubating γ-Syn in the presence of equimolar concentration of polyols (2M) and recording the far-UV CD spectra at regular intervals during fibrillation (0, 8, 24 and 48h). As shown in Figure 5B, except in the presence of EG, an increased α-helical propensity with a two characteristic minima at ~208 nm and ~222 nm during the exponential phase (24h) of γ-Syn fibrillation was observed. In the presence of EG, a structural transition from a natively unfolded conformation to a characteristic β-sheet structure with a negative ellipticity at ~218 nm was observed. Erythritol and xylitol were observed to retain the α-helicity even at the saturation stage of fibrillation (48h). It is also noteworthy, that the α-helical propensity induced in presence of polyols is retained by the intermediate polyols in the series, i.e. glycerol, erythritol and xylitol even at a saturation stage whereas both the polyols with 2 and 6 –OH groups, (EG and sorbitol, respectively) result in the formation of a predominant β-sheet structure upon saturation. The combined far-UV CD spectra of γ -Syn in the presence of equimolar concentration of polyols at 24h of fibrillation (Figure 5C) clearly demonstrate an increased α-helical tendency with an increasing –OH group in the polyols. A) Figure Continued… B) Figure Continued… C) Figure 5. Structural characterization of γ-Syn in presence of polyols by far-UV circular dichroism spectroscopy. The far-UV CD of γ-Syn in the presence and absence of polyols both under native and fibrillating conditions respectively were monitored at 25 °C using a cuvette of 1mm path length. A) Far-UV CD spectra of γ-Syn (0.5 mg /ml) dissolved 20 mM phosphate buffer, pH-7.4 conditions in the presence of increasing concentration of polyols monitored under native conditions. B) Far-UV CD spectra of γ-Syn (0 .3 mg/ml) in presence of increasing concentrations of polyols monitored at time- intervals of 0h, 8h, 24h and 48h during fibrillation. C) Combined far-UV CD spectra at 24h of fibrillation taken from panel B (EG to Sorbitol) comparing the differences between the secondary structure propensities of γ -Syn in the presence of polyols (2M). 2.2.2 ANS binding assay The effect of polyols on the extent of exposed hydrophobic surface area in γ -Syn was assessed by ANS binding assay. The ANS fluorescence spectra of monomeric γ -Syn in the absence and presence of 2M polyols nearly overlapped with each other, with an emission around 505 ± 0.5 nm (Figure 6A). Under fibrillating condition (24h), an increase in the ANS intensity with an increasing hydroxyl groups (OH) in the polyols was observed with the blue- shifted emission maxima at ~480 nm (Figure 6B and C) with the exception of sorbitol. The ANS emission in the presence of sorbitol although was further blue-shifted, the ANS intensity was much reduced in the presence of sorbitol. The diminished ANS fluorescence in the presence of sorbitol could possibly be due to the sorbitol mediated compaction of γ-Syn leading to the burial of the sites required for ANS binding. Except sorbitol, overall these results demonstrate that the extent of exposed surface hydrophobicity on γ-Syn increases with the increasing –OH group in the polyols, thus establishing a role of stronger preferential exclusion in polyols with higher number of –OH groups. A) B) C) Figure 6. ANS binding to γ-Syn in presence of EGCG shows an overall low surface hydrophobicity. A) Emission spectra of ANS binding to γ-Syn under native conditions in the presence of 2M polyols. B) ANS binding to aggregating species of γ-Syn formed after 24h of fibrillation in the presence of polyols showing an increase in the ANS intensity with increasing –OH groups in polyols with a characteristic blue-shifted emission (solid arrow) at ~480 nm. A larger blue- shift is observed in the presence of EG (dashed arrow). C) Plot of ANS binding fluorescence intensity of γ-Syn at 480 nm in 2M polyols. 2.3 The transfer free energy value of γ-Syn from water to polyols In order to gain an insight into the mechanism of varied effects of polyols on the fibrillation pathway of γ-Syn as observed in this study, the contribution by the amino acid side chains in γ-Syn to its stability and aggregation in the presence of polyols was investigated by estimating the free energy of transfer of γ-Syn from water into the 1M glycerol and 1M sorbitol, based on the amino acid composition of γ-Syn. The transfer free energies of free amino acids from water to 1M glycerol and 1M sorbitol were taken from the previously estimated values by

Bolen and co-workers (Auton & Bolen, 2004, 2005; Auton et al., 2008). The amino acid side chain values were calculated by subtracting the glycine values from those of the given free energy transfer values of amino acids. As shown in the Table I, the free energy of transfer to 1M sorbitol (3.9 kcal/mol) is more unfavourable than in 1M glycerol (3.2 kcal/mol), which demonstrates the role of a stronger preferential exclusion of sorbitol than glycerol. The calculations based on the amino acid compositions further suggest that the amino acid composition of γ-Syn as well as other IDP largely govern the modulatory effects of polyols other than only the preferential exclusion effect. Table I. Transfer free energies (cal/mol) of γ-Synuclein from water to 1M Glycerol and 1M Sorbitol calculated from its amino acid composition data. Amino Acid side chain No. of Residues 1M Glycerola (ΔG°tran) Total residue value (ΔG°tran) 1M Sorbitola (ΔG°tran) Total residue value (ΔG°tran) Nonpolar Ala Phe Leu Ile Val Pro Met Polar Gly Ser Thr Gln Asn Acidic Asp Glu Basic His Lys Arg 16 2 1 2 22 2 2 10 10 10 6 4 3 19 - 15 2 7.76 59.8 -34.4 38.2 -1.4 -60.6 13.9 0 6.3 17.5 -2.8 51.6 52.1 63.4 - -34 -30.7 124.16 119.6 -34.4 76.4 -30.8 -121.2 27.8 0 63 175 -16.8 206.4 156.3 1204.6 - -510 -61.4 18.02 36.6 53.4 55 40 -24 21.7 0 -3.9 20.7 -18.6 -20.5 -76 -63.1 - -21.6 -18.9 288.32 73.2 53.4 110 880 -48 43.4 0 -39 207 -111.6 -82 -228 -1198.9 - -324 -37.8 Backbone 126 15b 1890 35 b 4410 Total (ΔG° transfer) 3268.6 3996 a. The side chain free energy transfer values from water to 1M glycerol and 1M sorbitol calculated by using values described by Auton et. al (Auton et al., 2008). b. Peptide backbone contribution to free energy of transfer from water to 1M glycerol and 1M sorbitol described from supplementary ref. (Auton & Bolen, 2004) and (Auton & Bolen, 2004, 2005), respectively. 3. Discussion Studies on the effect of polyols on the structure and aggregation of intrinsically disordered proteins, which are otherwise known to stabilize the folded or native state of globular proteins (Mishra et al., 2005; Tiwari & Bhat, 2006; Vagenende et al., 2009; Devaraneni et al., 2012), is critical to answer a question as to how does a cell simultaneously regulate the balance between the globular and intrinsically disordered proteins under conditions of stress and preserve the physiological function of the proteins involved? In this study the effect of a series of polyols on the structure and aggregation of γ-Syn is investigated and the relationship between the increasing number of –OH groups in polyols with enhanced protein stability and aggregation/fibrillation is examined. The ThT fluorescence data, monitored in the presence of polyols (Figure 1), reveal a varied effect on the fibrillation pathway of γ-Syn ranging from promoting aggregation to suppression or having a negligible effect, unlike reported for globular proteins previously (Mishra et al., 2005).The kinetic parameters (Figure 2), i.e. the lag time (tlag) and apparent rate of γ-Syn fibrillation (kapp), estimated from the ThT assay (Figure 1), reveal that polyols act on the initial stages of γ-Syn fibrillation and a decrease in the lag time with increasing number of -OH groups in polyols is seen, except for ethylene glycol (EG) (Figure 1A) where no lag time was observable (Figure 2E). Ethylene glycol shows a dual effect on γ-Syn fibrillation which is dependent on its concentration where the fibrillation is promoted at lower concentrations but is almost completely suppressed at higher concentration (>4.5M) (Figure 1A). Such a concentration mediated suppression of fibrillation by EG can be attributed to the increasing viscosity of the polyol (Munishkina et al., 2004; Kumar, 2009; Theillet et al., 2014) that possibly restricts the diffusion of protein molecules that inhibits protein-protein association and give rise to partially polymerized or reduced fibrils as seen in electron micrographs (Figure 4) and thus suppresses γ-Syn aggregation. EG has earlier been observed to affect the folding kinetics of the protein CI2 depending on its concentration, wherein an inverse relationship between the concentration of EG and rate of folding of the protein was observed. This effect has been related it to the concentration-dependent changes in the viscosity of EG (Silow & Oliveberg, 2003). Light scattering studies show an overall reduced scattering by γ-Syn species in the presence of high concentration of EG (Figure 3A). Unlike complete suppression observed in the ThT assay, an increase in the scattering intensity was observed in the presence of higher concentration of EG, which indicate the formation of amorphous aggregates that do not bind to ThT thus giving reduced fluorescence intensity in the ThT assay. However, the masking of ThT binding sites on γ-Syn fibrils at high concentration of polyols leading to reduced fluorescence intensity in ThT assay (Figure 1A) also could not be ruled out. Glycerol, known to be the smallest protein stabilizer among osmolytes (Vagenende et al., 2009) suppresses γ-Syn fibrillation in a concentration dependent manner that prolongs nucleation as well as retards the apparent rate of fibrillation (kapp) thus preventing oligomerization and γ-Syn polymerization (Figure 1B, 2A and 3B). The TEM images further reveal an overall reduction in the fibrillar yield along with the formation of amorphous aggregates, adhering to the fibrillar surface, in the presence of glycerol. The effect of glycerol observed on γ-Syn fibrillation could be explained by the 'solvophobic effect' of glycerol (Tiwari & Bhat, 2006) where it may favour the

interaction between water molecules and protein surfaces, inhibiting the unfolding of the residual structure present in γ-Syn (Uversky et al., 2002; Marsh et al., 2006). The inhibition of γ-Syn fibrillation in the presence of glycerol could be explained by its preferential interaction with the exposed hydrophobic patches on the protein, possibly the NAC domain in γ-Syn (George, 2001), that stabilizes the aggregation-prone intermediates, thus imparting a dual effect based on the nature of the protein and the physicochemical properties of glycerol (Tiwari & Bhat, 2006; Vagenende et al., 2009). As opposed to the inhibition of γ-Syn fibrillation in the presence of glycerol is observed in this study, glycerol has been previously reported to promote fibrillation of α- Synuclein (Munishkina et al., 2004) protein while both the α - and γ-Syn belong to the same family of synuclein proteins (George, 2001). The contrasting effect of a polyol on the two members of the same family of proteins highlights the complexity of the effect of osmolytes toward the stability of IDPs. The early rise in the scattering intensity followed by an early saturation (Figure 3B) in the presence of higher concentrations of glycerol could also be explained by the dual effect of glycerol where it possibly favours the collapse of the unfolded structure of γ-Syn at initial stages of fibrillation and lead to the formation of amorphous aggregates that do not participate in γ-Syn fibrillation. The next polyols in the series, erythritol and xylitol lead to no significant change in the overall ThT fluorescence. The kinetic parameters of γ-Syn fibrillation reduced light scattering intensity and appearance of short fibrils in the TEM studies (Figure 2C, 3D and 4 respectively) in the presence of xylitol clearly indicates retarded fibril elongation and delayed nucleation. Thus, xylitol affects the fibrillation pathway of γ-Syn by acting on both the initial and the intermediate stages of fibrillation, as also seen in the presence of glycerol. Sorbitol, a polyol with six –OH groups, reported to impart stability to globular proteins predominantly by preferential exclusion (Tiwari & Bhat, 2006) suppresses overall γ- Syn fibrillation and aggregation with increasing concentration (Figure 1E and 3E). Interestingly, the kinetic parameters of γ-Syn fibrillation show a concentration dependent decrease in the lag time (tlag) and a simultaneous increase in the rate of fibrillation (kapp) (Figure 2D) which suggest that at lower concentrations, sorbitol being a predominantly hydrophilic solvent relative to the other polyols used (Hydrophobicity index being sorbitolformation of a molten-globule like state in γ-Syn leading to compaction, that in turn promotes early nucleation and polymerization. Free energy of transfer of amino acid side chains and the peptide backbone from water to various osmolytes including glycerol and sorbitol, evaluated by Bolen and co-workers, result in the net free energy of transfer of γ-Syn (based on its amino acid composition) from water to 1M glycerol and 1M sorbitol of 3.27 kcal/mol and 3.99 kcal/mol, respectively (Table I). This 152 suggests that free energy transfer of γ-Syn in sorbitol is much more unfavourable than in glycerol, which is in accordance with the reduced lag time observed in the presence of sorbitol relative to glycerol. The data in the table suggest varying free energies of transfer contributions by the polar, nonpolar and charged side chains in the presence of polyols used. It is noteworthy that except EG and sorbitol, all other polyols with respect to control, lead to an increase in lag time of γ-Syn fibrillation, despite their preferential-exclusion property, whereas polymeric crowders like Ficoll and dextran are reported to reduce the lag time of α- Syn aggregation and promote fibrillation (Munishkina et al., 2004). These findings demonstrate that the balance between the preferential interaction of the polyol osmolytes with the polar and charged side chains and preferential exclusion due to unfavourable interaction with the peptide-backbone as well as with the non-polar side chains is significant in governing the stability of IDPs in the presence of polyol osmolytes. Thus, it is established that in the case of IDPs, the stabilizing /destabilizing effect of osmolytes, and hence, their effect on fibrillation and aggregation would be governed by the strength of protein-solvent interactions and solute-solvent interactions which could vary from one IDP to another. The TEM studies in the presence of polyols show clumping of fibrils and an overall reduction in the fibrillar yield without altering the fibrillar morphology, an observation commonly reported in the presence of other osmolytes previously (Munishkina et al., 2004; Seeliger et al., 2013; Choudhary et al., 2015). Also, with increasing –OH group in the series that is, from erythritol to sorbitol, much shorter fibrillar species are formed which possibly arises due to macromolecular crowding (Latshaw et al., 2014). The far-UV CD and ANS binding studies reveal a relationship between increasing –OH group in polyols with increasing stability (Figure 5A and 6A) where the natively unfolded conformation of γ-Syn is maintained almost linearly with the increasing –OH groups in the polyols. The far-UV CD under fibrillation conditions shows that polyols with the increasing –Oh groups delay the early structural transitions to β-sheet structures during fibrillation and induces the formation of an α-helical intermediate during the exponential stage of fibrillation which is marked by an increase in negative ellipticity with two minima at ~208 nm and ~222 nm (Figure 5B). Osmolytes have

also been previously reported to predominantly induce an α-helical conformation in IDPs (Uversky, 2009; Levine et al., 2015) and regulate the IDPs by shuffling the different protein conformations of IDPs rather than giving rise to fundamentally new structures (Levine et al., 2015). 4. Conclusion In conclusion, the study suggests that fine balancing of general preferential exclusion effect of polyols based dominantly on the peptide backbone repulsion, weak and non-specific interaction with side chains of IDPs and the physico-chemical nature of the solution especially at higher concentration of polyols is expected to regulate and govern the formation of different conformational states of IDPs. The various conformational states of an IDP that arises in the presence of polyols could either be prone to aggregation/ fibril formation or could lead to the stability of the monomeric form, leading to suppression of fibrillation. Overall, the effect of polyol osmolytes on the conformation, stability, aggregation and fibril formation of an IDP like γ-Syn seems to be much more complex than observed for their effect on globular protein stability and aggregation. The findings suggest that under stress in cellular systems, the effect of polyol osmolyte on IDPs would vary depending on the physicochemical properties of polyols, amino acid side chain composition of IDP as well as active concentration of polyol in the protein vicinity. This necessitates the role of natural selection in fine tuning the osmolyte production at optimal concentrations and orchestrating the balance between the stability of globular proteins as well as different naturally selected conformational states of IDPs to enable the cellular systems to combat stress. Chapter 1: Introduction Chapter3 .1: Effect of EGCG Chapter3.2: Effect of Quercetin Chapter3.2: Effect of Quercetin Chapter 3. 3: Effect of Silibinin Chapter 3.3: Effect of Silibinin Chapter 3. 3: Effect of Silibinin Chapter 3. 3: Effect of Silibinin Chapter 3.3: Effect of Silibinin Chapter 3. 3: Effect of Silibinin Chapter 3. 3: Effect of Silibinin Chapter 3.3: Effect of Silibinin Chapter 3. 3: Effect of Silibinin Chapter 3. 3: Effect of Silibinin Chapter 3.3: Effect of Silibinin Chapter 3. 3: Effect of Silibinin Chapter 3. 3: Effect of Silibinin Chapter 3.3: Effect of Silibinin Chapter 3. 3: Effect of Silibinin Chapter 3. 3: Effect of Silibinin Chapter 3.3: Effect of Silibinin Chapter 3. 3: Effect of Silibinin Chapter4: Effect of Polyols Chapter4: Effect of Polyols Chapter4: Effect of Polyols Chapter4: Effect of Polyols Chapter4: Effect of Polyols Chapter4: Effect of Polyols Chapter4: Effect of Polyols Chapter4: Effect of Polyols Chapter4: Effect of Polyols Chapter4: Effect of Polyols Chapter4: Effect of Polyols Chapter4: Effect of Polyols Chapter4: Effect of Polyols Chapter4: Effect of Polyols Chapter4: Effect of Polyols Chapter4: Effect of

Polyols Chapter4: Effect of Polyols Chapter4: Effect of Polyols Chapter4: Effect of Polyols Chapter4: Effect of Polyols Chapter4: Effect of Polyols Chapter4: Effect of Polyols Chapter4: Effect of Polyols 3 6 10 11 12 13 17 18 20 22 23 24 25 26 27 28 29 30 31 34 35 37 39 40 42 43 45 46 47 48 49 50 51 52 53 54 55 56 57 58 59 60 61 62 63 64 65 66 67 68 69 74 75 76 77 78 79 80 81 83 84 86 87 88 89 90 92 93 95 96 97 98 99 100 101 102 103 104 105 108 109 110 112 113 114 115 116 117 118 119 120 121 122 123 124 126 127 128 129 130 131 133 134 135 136 137 139 140 141 142 143 144 145 146 147 148 149 150 151 153 154 155